9-1-2021

EXTRACELLULAR POLYMERIC SUBSTANCES IN OXYGENIC PHOTOGRANULES: INVESTIGATION OF THEIR ROLE IN PHOTOGRANULATION IN A HYDROSTATIC ENVIRONMENT

Wenye Camilla Kuo-Dahab
University of Massachusetts Amherst

EXTRACELLULAR POLYMERIC SUBSTANCES IN OXYGENIC PHOTOGRANULES: INVESTIGATION OF THEIR ROLE IN PHOTOGRANULATION IN A HYDROSTATIC ENVIRONMENT

Wenye Camilla Kuo-Dahab

EXTRACELLULAR POLYMERIC SUBSTANCES IN OXYGENIC PHOTOGRANULES: INVESTIGATION OF THEIR ROLE IN PHOTOGRANULATION IN A HYDROSTATIC ENVIRONMENT

A Dissertation Presented

by

WENYE CAMILLA KUO-DAHAB

Submitted to the Graduate School of the
University of Massachusetts Amherst in partial fulfillment
of the requirements for the degree of

DOCTOR OF PHILOSOPHY

September 2021

Department of Civil and Environmental Engineering

EXTRACELLULAR POLYMERIC SUBSTANCES IN OXYGENIC PHOTOGRANULES: INVESTIGATION OF THEIR ROLE IN PHOTOGRANULATION IN A HYDROSTATIC ENVIRONMENT

A Dissertation Presented

by

WENYE CAMILLA KUO-DAHAB

Approved as to style and content by:

DocuSigned by:
01D6091B23DA416...
Caityln S. Butler, Chair

DocuSigned by:
EE1A80204C744B8...
Kristen M. DeAngelis, Member

DocuSigned by:
David Reckhow
12FF31E86CAC438...
David A. Reckhow, Member

DocuSigned by:
John E. Tobiason
E74AD5B712444E7...
John E. Tobiason, Department Head
Department of Civil and Environmental Engineering

DEDICATION

To my loving child and husband, Ayrton Zoltán Kuo-Dahab and Amine Dahab

“Ich denke sowieso mit dem Knie”-Joseph Beuy

ACKNOWLEDGMENTS

Foremost, I would like to extend my sincerest gratitude to my academic advisor, Caitlyn Butler, for her unwavering support and guidance throughout my time as a graduate student. Dr. Butler has given me a priceless opportunity to study and grow both professionally and personally and beyond what I could have possibly imagined, and for that, I am humbled and grateful.

I would also like to thank my esteemed committee members, Kristen DeAngelis and David Reckhow for all their guidance and advice in the past few years. My meetings with Dr. DeAngelis and Dr. Reckhow, a lot of the times, are what I needed to push me forward. I feel especially lucky to have met Dr. DeAngelis who is one of the smartest and kindest people I have ever met. Thank you for sitting down and making time to have those tough talks with me. Dr. Reckhow, thank you for your unconditional support and advice. I truly appreciate the patience of my committee chair and members as I have tried to overcome academic and personal challenges as I transitioned through my Ph.D. studies. A big thank you to all my committee members for reading, editing and providing feedback on my dissertation.

Thank you to Dr. Chul Park, this work on oxygenic photogranules would have not been possible without your support and guidance.

Thank you to Dr. Hélène Carrere, Dr. Jérôme Hamelin, Dr. Kim Milferstedt, and Marjolaine Hamelin and your assistance during my time in France. I am so very lucky to have had their support during my challenging time in France.

To Sherrie Webb-Yagodzinski, the greatest lab manager to ever walk the earth. None of this lab work would have been completed without you.

Being a part of the EWRE group has been one of the greatest joys since arriving in Massachusetts. I went to work every day with colleagues who have become lifelong friends. To my wonderful friends and colleagues, Ahmed, Arianne, Cynthia, Joann, Kristie, Meng, Rassil, Scott and Xuyen, you have made my years in Amherst wonderful. A special thanks to the undergrads, especially Ana, Brian, and Mason.

Thank you to Jodi Ozdarski and the other admin staff that have helped guide me through the graduate school process.

To my mentors specifically, David Duest, Dr. George Sprouse, and Dr. Timothy LaPara, I am honored that they have been able to mentor and guide me all of these years in the industry.

To my family, for their unwavering support throughout the years, their patience in listening to my ordeals and challenges, and despite it all, their infinite love. My family is a strong source of support and encouragement, and I feel extremely fortunate to have them all in my life.

To my friends, past and present, each of you have played an integral role in the person I am today, and I could not have come this far without your love and support.

To my husband and partner, Amine. There are no words to describe how grateful and blessed I am to be your partner in life. Thank you for your undivided love, support and your belief in our dreams. I’m not sure how far I would have made it without you as we are the same person now. Your ambition, attitude and grit are my guiding beacons every day.

To my child, Lulu, you are my heart.

ABSTRACT

EXTRACELLULAR POLYMERIC SUBSTANCES IN OXYGENIC PHOTOGRANULES: INVESTIGATION OF THEIR ROLE IN PHOTOGRANULATION IN A HYDROSTATIC ENVIRONMENT

SEPTEMBER 2021

WENYE CAMILLA KUO-DAHAB, B.S., UNIVERSITY OF MINNESOTA AT TWIN CITIES

Ph.D., UNIVERSITY OF MASSACHUSETTS AMHERST

Directed by: Dr. Caitlyn S. Butler

The purpose of this dissertation was to assess the critical role of extracellular polymeric substances (EPS) in the photogranulation of activated sludge, in a hydrostatic environment.

The first section evaluates the fate and dynamics of different fractions of EPS in sludge-based photogranulation under hydrostatic conditions. The study shows that during the transformation of activated sludge into a photogranular biomass, sludge's base-extractable proteins selectively degrade. Strong correlations between base-extracted proteins and the growth of chlorophyll a and chlorophyll a/b ratio suggest that the bioavailability of this organic nitrogen is linked with selection and enrichment of filamentous cyanobacteria under hydrostatic conditions. The results of soluble and sonication-extractable EPS and microscopy also show that the growth of filamentous cyanobacteria required large amounts of polysaccharide-based EPS for their motility and maintenance. With findings on the progression of photogranulation, the fate and dynamics of EPS, and microscopy on microstructures associated with EPS, potential mechanisms of photogranulation occurring under hydrostatic conditions are discussed.

The second section evaluates and shows that multiple EPS extraction methods are required in order to characterize EPS during the transformation of activated sludge into a photogranule in a hydrostatic environment. The present study reveals why cyanobacteria are selected and how different fractions of EPS and their recycle leads to photogranulation in hydrostatic conditions. Despite differences in sludge inoculum, EPS extraction using five different methods, centrifugation, cation exchange resin (CER), base, sonication, and heat, show that trends are significantly similar, statistically, between two sludge sources (Amherst and Hadley). The results presented above show that different EPS extraction methods are required to capture different fractions of EPS with respect to protein, polysaccharide, and humic acid composition and organic carbon and nitrogen content. EPS extraction methods for polysaccharides was found to be the most biased, followed by humic acids, then proteins. This suggests that different methods target different EPS fractions (more associated with polysaccharides), but may share overlap between the methods (proteins and humic acids). All methods had statistically significant moderate to strong correlations with one or more constituents, chlorophylls, N-species, and select cations and anions, which have been previously established as strong indicators of successful granule formation. These results suggest that different EPS fractions are linked to multiple processes during hydrostatic photogranulation, including the enrichment of filamentous cyanobacteria, nitrogen metabolism and recycle of organic nitrogen, assimilation and biofilm incorporation of ammonium (NH_4^+-N), and biofilm structure, further suggesting that the role of EPS is a complex process with multiple courses of action.

The final section focuses on the addition and role of cations for the enhancement of activated sludge photogranulation in a hydrostatic environment. This study observed that the addition of monovalent (sodium-Na^{+}) and divalent cations (Calcium-Ca^{2+} and Magnesium- Mg^{2+}), at specific concentrations 10-40 meq/L, leads to a higher percentage of total and spherical granules, in comparison to light control (no cation amendment) and dark control cultivations. Based on crude EPS, ammonium sulfate precipitation, and sulfate polyacrylamide gel electrophoresis (SDS-PAGE) results, Light+Ca^{2+} treatments show greater recovery of CER protein after ASP, and different recovery patterns in comparison to light and dark control, suggesting that more hydrophobic protein is available. This further infers that the addition of Ca^{2+} may influence the hydrophobicity of EPS proteins during hydrostatic photogranulation. After ASP, SDS-PAGE was applied and banding pattern across the treatments showed same the EPS protein on a molecular level which did not change with the addition of Ca^{2+} (in comparison to control). This may further imply that enhancement is more likely due to Ca^{2+} cation bridging, versus changes on a molecular level influenced by the microbial community.

TABLE OF CONTENTS

LIST OF TABLES

LIST OF FIGURES

CHAPTER 1

INTRODUCTION

1.1 Introduction

Population and economic growth have driven rapid rise in demand for water resources. About 36% of the world's population or over 2.4 billion people live-in water-scare regions and lack access to an improved sanitation system many of them in developing countries, where the incentive to invest in advanced wastewater treatment is low (WHO/UNICEF, 2015). This has significant implications for public health, environmental sustainability, and social equity. The United Nations (UN) Member States have shared a blueprint for peace and prosperity for people and the planet, for now and the future. At the heart of this plan are the 17 Sustainable Development Goals (SDGs) which are a call for action by all countries with strategies that improve health and education, reduce inequality, and contribute to economic growth. The SDG targets for water include improving water quality, implementing integrated water resource management, achieving water use efficiency across sectors, reducing the number of people suffering from water scarcity, and restoring water-related ecosystems. In order for countries to achieve the SDGs, governments will need to significantly increase levels of wastewater treatment in these regions.

Developed countries rely on the activated sludge process to treat wastewater, a 100-year-old technology. Although this approach is effective for organic matter removal, the process is very energy intensive- the shortcoming is aeration to dissolve O_2 gas into wastewater, which accounts for about 50-60% of energy used at wastewater treatment plants (WWTPs). Additionally, it has become more challenging to meet today's increasingly stringent effluent requirements including enhanced removal of nitrogen (N)

and phosphorus (P). The energy demands for current wastewater treatment is approximately 75 billion kilowatt hours per year or about 3% of total energy consumed in the United States (US), while mechanical aeration accounts for 25-60% of total plant energy use (United States Environmental Protection Agency, 2010)

Additionally, a new paradigm shift at multiple levels aims to advance sanitation services (i.e., wastewater treatment) toward a circular economy. Here, wastewater is considered a valuable resource rather than a liability by fostering resource reuse and recovery ensuring sustainable wastewater management, and has become a central focus of the UN and Member States. Energy, potable water, fertilizers, and nutrients can be extracted or recovered from wastewater- and used to help achieve SDGs. One of the key advantages of adopting circular economy principles in the processing of wastewater is that resource recovery and reuse can transform sanitation from a costly service to one that is self-sustaining and adds value to the economy. Indeed, if financial returns can cover operation and maintenance costs partially or fully, improved wastewater management offers a double value proposition. Therefore, processes that reduce energy consumption, meet enhanced removal standards, and can be adopted worldwide in a circular economy are desperately needed.

To respond to these challenges, the research presented here in this document advances the Oxygenic Photogranule (OPG) process that was developed previously (Abouhend et al., 2018; Milferstedt et al., 2017; Park & Dolan, 2015; Stauch-White et al., 2017). The OPG process is based on microbial symbiosis of microalgae and bacteria for self-aeration and produces bioenergetic feedstock by wastewater treatment, closing the wastewater treatment loop and contributing to a sustainable, circular economy. In this process, phototrophs produce O_2 in-situ and bacteria use this O_2 to degrade organic matter. As a result, wastewater treatment could be accomplished without mechanical aeration, while potentially producing useful bioenergy feedstock (Park et al., 2011; Ji et

al., 2018; Tiron et al., 2015; Zhang et al., 2021). Furthermore, symbiotic growth of phototrophic and chemotrophic microorganisms leads to the removal of nitrogen (N) and phosphorous (P) through the combinations of symbiotic metabolisms and assimilation. The diverse metabolic capacity in these granules could therefore achieve nutrient removal without adding an external source of organic C in anaerobic or anoxic reactions (Park et al., 2011; Ji et al., 2018; Tiron et al., 2015; Zhang et al., 2021).

The discovery of OPGs began with the unexpected finding that microalgae (i.e., cyanobacteria) and other heterotrophic bacteria in activated sludge, form spherical shaped biomass in “hydrostatic” environments (Figure 1.1) (Abouhend et al., 2018; Milferstedt et al., 2017; Chul Park & Dolan, 2015; Stauch-White et al., 2017).

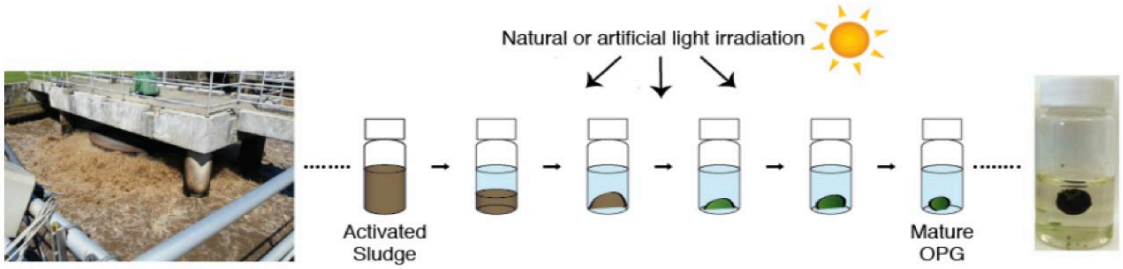

Figure 1.1: Formation of Oxygenic Photogranules Under Static Conditions

We applied this naturally occurring phenomenon to wastewater treatment and found that OPGs also manifest in turbulently mixed reactor environments with flow-through of wastewater, lending to the treatment of wastewater without aeration (Figure 1.2) (Abouhend et al., 2018).

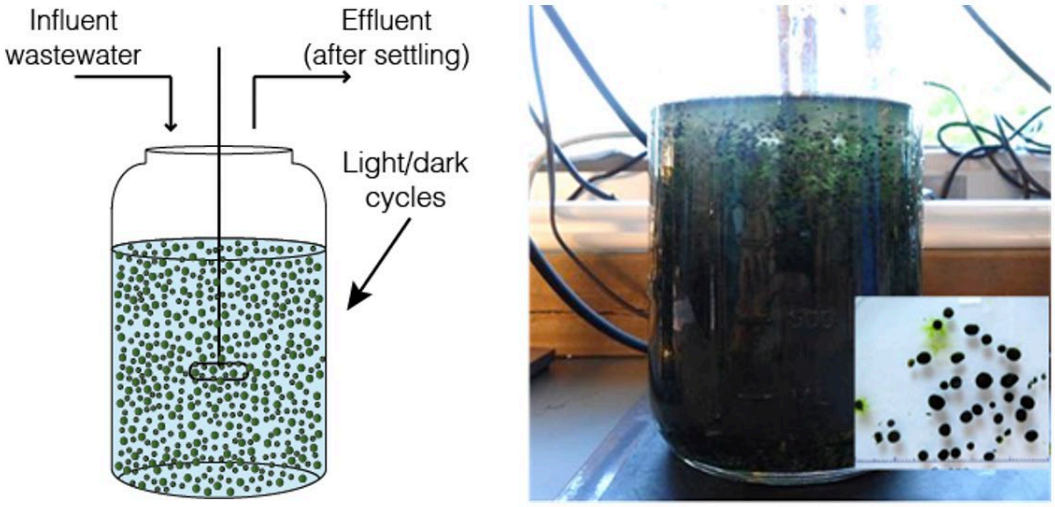

Figure 1.2: OPG Reactor Treating Wastewater with Photo of OPG Biomass Formed During Reactor Operation

In addition to energy savings due to autonomous aeration, dense, granular OPGs also enable effective biomass separation compared to activated sludge flocs, which can further reduce operational costs and capital investment. It is hypothesized that due to the photoautotrophic assimilation of CO_2, the system recovers both solar energy and chemical energy in wastewater in the form of easily harvestable biofeedstock – despite the traditional view about wastewater, wastewater itself presents a renewable energy; in the U.S. alone, the recovery of chemical energy in wastewater could generate 50-100 billion kWh per year, equivalent to energy from burning 90-180 million barrels of oil each year. Overall, the OPG process shows the potential to substantially reduce costs for wastewater treatment and generate enough energy to turn WWTPs into energy positive green infrastructure.

However, though this process holds promise for advancing wastewater treatment toward more sustainable practices, research gaps exist in the path toward developing this process as a full-scale treatment system. A particular channel is cultivation of seed biomass to populate large scale operation. We know OPG granulation is repeatable but

not consistently reproducible. This means that there are key biophysical phenomena that are not yet understood to generate the desirable biomass in a consistent way. Currently, very few studies have examined the formation of photogranules. Motivated by the direct need for promoting the OPG system and with it improving conventional wastewater treatment systems, the purpose of this dissertation is to advance our understanding of photogranulation in a hydrostatic environment to better understand the network of exocellular polymeric substance that stabilize OPG structure – the granular biofilm structure that makes them uniquely suited to host the diverse microbial communities that facilitate energy-efficient, advanced wastewater treatment. It is well known that EPS production support commensalisms and redox gradient that allow diverse community to coexist at the microscale. But the evolution of the EPS in the formation of oxygenic photogranule is largely absent from existing literature. Here, I seek to begin to understand the general trends in EPS development in OPG formation, understand the characteristic groups of EPS through different methods of isolation, and how these groups change with key chemical signatures that have been documented through EPS formation. Following a literature review in Chapter 2, the work presented has been divided into three separate sections with the following objectives:

1) To investigate the fate and dynamics of EPS during photogranulation on activated sludge in hydrostatic conditions (Chapter 3),
2) To characterize different EPS fractions with multiple EPS extraction and isolation protocols and build corollaries with key feature and biochemical trends in hydrostatic photogranulation of activated sludge (Chapter 4), and
3) Through improved characterization of EPS fractions, understand if OPG structure can be enhanced in a hydrostatic environment, and the stability of OPG final structure, through cation addition to bridge EPS (Chapter 5).

The collective work pertains to the role of EPS during hydrostatic photogranulation for the formation of photogranules. Through better understanding of the EPS components of the OPG biofilm, OPG stability and performance in reactor operation can be improved and, in turn, improve pollutant removal and energy efficient wastewater treatment with the OPG process. As we further understand dynamics and reproducibility that govern the hydrostatic photogranulation process, more resilient OPG systems can be designed and scaled to advance this technology towards implementation.

CHAPTER 2

REVIEW OF RELEVANT LITERATURE

2.1 Overview of Biological WWTP

Conventional aerobic biological wastewater treatment process, also known as the conventional activated sludge (CAS) process, is the most widely and commonly applied biological treatment technology (Encyclopedia of Ecology, 2008). CAS was first developed in the late nineteenth century and applied at full-scale in 1913 by Arden and Lockett in Manchester, United Kingdom. In the CAS process, oxygen is supplied via surface aeration or immersed air-bubble diffusers. Oxygen is transferred to the bulk liquid by ways of a liquid/air interface. Within the bulk liquid, suspended bacterial biomass (activated sludge) grows by utilizing organic matter as substrate through a series of chemical oxidation and reduction reactions, from the influent wastewater.

In advanced activated sludge systems, like biological nutrient removal (BNR), nitrogen (N) and phosphorus (P) are removed simultaneously by different bacterial groups. N is removed via nitrification/denitrification pathways. Nitrification is the oxidation of ammonia into nitrite and nitrite into nitrate. The first conversion is performed by a group of bacteria known as Nitrosomonas. The second step is done by a group of bacteria known as Nitrobacter. Nitrifying organisms are autotrophic organisms that use inorganic carbon (CO_2) as their carbon (C) source. The second part of nitrogen removal is denitrification, in which nitrite or nitrate is used as the electron acceptor for the oxidation of organic C which is subsequently converted to N gas. This process takes place under anoxic conditions. P is either removed by chemical precipitation or biologically as part of the BNR process. The biological BNR P removal process involves changing conditions between anaerobic and aerobic conditions. During the anaerobic

period substrates like acetate are taken up by the cell and stored as poly-β-hydroxybutyrate (PHB) while hydrolysis of intracellular stored polyphosphate (poly-P) to orthophosphate is released into the bulk liquid. Glycogen is converted to the reducing equivalents necessary to convert acetate to PHB which is stored during the aerobic period. In the aerobic or anoxic phase, PHB is used as substrate for cell growth, polyphosphate synthesis and glycogen formation, without the presence of an external substrate (Rittman & McCarty, 2001).

In CAS and BNR systems, microorganisms are usually present in the form of flocs. Sludge flocs are composed of organic matter, inorganic cations and anions, and other pollutants from the influent wastewater (Frølund et al., 1996; Higgins & Novak, 1997a,1997b; Park & Helm, 2008; Park et al., 2008a, 2008b; Park and Novak, 2007, 2009). Further, the organic matter within the floc is separated into microorganisms and extracellular polymeric substances (EPS; Andreadakis, 1993; Durmaz, 2001; Frølund et al., 1995, 1996; Guo et al., 2016; Higgins & Novak, 1997a,1997b; Park & Helm, 2008; Park et al., 2008a, 2008b; Park and Novak, 2007, 2009; Steiner et al., 1976; Ye et al., 2011). Activated sludge flocs are formed by direct interactions between cells, EPS and other organic and inorganic matter in the floc or aggregate defined as cell-to- aggregate interactions. Many of these direct interactions are a result from EPS that is produced in response to physiochemical changes by microorganisms (Hermansson, 1999).

2.2 Aerobic and Anaerobic Granular Technologies

Up-flow anaerobic sludge blanket (UASB) systems, aerobic granular sludge (AGS), and anaerobic ammonium-oxidizing bacteria (ANAMMOX) systems are granular processes. UASB and AGS have been adopted, mostly in Europe, for secondary wastewater treatment while ANAMMOX is typically used as sidestream treatment of

nutrient-rich streams (i.e., centrate and filtrate from processes like dewatering). In these systems, microorganisms are present in the form of granules. Granules are dense, spherical bioaggregates that can be formed in both aerobic and anaerobic environments (Adav et al., 2008; Beun et al., 1999; Ding et al., 2015; McSwain et al., 2005; Zhang et al., 2007; Zhu et al., 2015). The rigidity and structure of granules gives them several advantages in comparison to flocs, including higher resistance to shear stress, protective role for bacteria inside the granule against toxic compounds in the bulk liquid, facilitation of solid-liquid separation, and enhancement of biomass retention by preventing washout (Ding et al., 2015; Sheng et al., 2010). These advantages have increased the demand for the use of granules in the wastewater treatment industry.

In UASB systems, methanogenic archaea and bacteria biodegrade organics anaerobically and produce biogas. The complexity of the waste (substrate) being treated, controls the composition of the bacterial communities residing in UASB systems, and have been found to include fermentative organisms, fatty acid-oxidizing bacteria (syntrophs), acetogenic bacteria and methanogens (Briones & Raskin, 2003; Rittman & McCarty, 2001; Schink, 1992, 1997). It has been proposed that anaerobic granules are structured by concentric layers of biofilm possessing different trophic groups of microorganisms (Harmsen et al., 1996; Lens et al., 1993; Liu et al., 2003; Zheng et al., 2006). UASB systems have been widely adopted around the world treating multiple types of wastewaters (Sharma & Khan, 2008).

AGS systems are used for simultaneous aerobic degradation of organics, and removal of N and P under aerobic and anoxic conditions in one sequencing batch reactor (SBR; De Kreuk et al., 2010; Liu & Tay, 2004). Anaerobic ammonium-oxidizing bacteria (ANAMMOX) can also be found in some AGS systems (Gao et al., 2011). According to Gao et al. (2011), aerobic heterotrophic bacteria, ANAMMOX bacteria, and facultative anaerobic bacteria are the three groups of microbial communities that form

AGS. These three communities are distributed throughout the granule based on their specific niche (i.e., aerobic bacteria are located on the outside and exposed to oxygen). AGS is a novel wastewater treatment process in comparison to CAS and BNR. It consumes less energy, withstands variable organic loading rates and toxic compounds, and facilitates solid-liquid separation (De Kreuk et al., 2010).

Currently, AGS has potential to replace CAS and BNR systems. However, even though granular processes have demonstrated technological advantages the mechanism of sludge granulation is still unclear. It is hard to design effective operational strategies due to limited knowledge of the granulation mechanism. Thus, the AGS system currently has limited engineering application (Adav et al., 2008; Beun et al., 1999; De Kreuk et al., 2010; Liu et al., 2010; Seviour et al., 2009; Tay et al., 2001).

2.3 Microalgae Technologies

Cyanobacteria and green algae, or defined more broadly as microalgae, have been investigated since the early 1950's due to their rapid growth rate and ability to sequester atmospheric or waste CO_2 from coal-fired power plants (Sheehan et al., 1998). Today, microalgae sit at the nexus of wastewater treatment, energy recovery, and energy production. Microalgae perform photosynthetic oxygenation and use light as their source of energy producing oxygen as a byproduct from photosynthesis (Oswald et al., 1952. Microalgae can grow in nutrient-rich wastewaters using N and P for cell synthesis thus removing and reducing nutrient loads into receiving water bodies (Rittman & McCarty, 2001). Multiple microalgae-based wastewater treatment processes have been developed and applied in the last decade (Oswald et al., 1952). Oswald et al. (1952) reported the use of a microalgae-bacterial symbiosis in open oxidation ponds or lagoons for the removal of organic matter from sewage. Oswald et al. showed that microalgae

provide oxygen to bacteria through photosynthetic oxygenation, and bacteria supply microalgae with inorganic C from carbon dioxide (CO_2), N and other nutrients from the degradation of sewage. Moreover, microalgae can be cultivated to produce biomass for a wide range of applications, including biofuel production. Unlike other terrestrial biofuel stocks (i.e., corn, soy, sugarcane and wheat), production of microalgae does not have the same economic and environmental constraints as crop production (Strum & Lamer, 2011).

A serious bottleneck to microalgae-based wastewater treatment processes and cultivation of microalgae for biofuel production is the harvesting of biomass (Pittman et al., 2011; de Godos et al., 2011). Harvesting biomass alone increases the production costs by 20-30% (Barros et al., 2017; Grima et al., 2003). This is due to the microscopic sizes of microalgae (0.5-30 μm; Benemann, 1977; Grima et al., 2003) limiting the harvesting efficiency by low biomass concentration (0.2 – 2.5 g/L). Harvesting requires the removal of large volumes of water to concentrate or dewater microalgal biomass, forming a slurry that consists of 1-15% total solids concentration (Mata et al., 2010). Centrifugation is also a proven technology and effective for harvesting, however, its high capital and operational costs make this solution infeasible when the harvested biomass is used for low-value applications. Usual separation techniques applied in wastewater such as conventional sedimentation have low harvesting efficiencies in the case of microalgal biomass (60-70%) and require the addition of coagulants (i.e., alum, lime or polyelectrolytes) and/or biomass recycling to stimulate bioflocculation (Benemann, 1977; Branyikova et al., 2018). On the other hand, filamentous cyanobacteria, with sizes of about 200 μm, can reduce the harvesting problem because they may be harvested more easily by filtration. In addition, some filamentous cyanobacteria form aggregates and can be harvested by conventional sedimentation or by flotation (De La Noüe & Bassères, 1989; Hori et al., 2002; Tiron et al., 2017).

2.3.1 Microalgae-bacterial Flocs

Researchers have been focused on investigating floccular and granular forms of microalgae-bacterial aggregates in order to avoid the physical (i.e., footprint, dewatering) and economic costs associated with harvesting microalgae from traditional processes like open lagoons and ponds (Grima et al., 2003). Gutzeit et al. (2005) developed microalgae-bacterial flocs similar to activated sludge floc, that were quickly settleable. Flocs ranged in size from 400-800 μm and mostly contained *Chlorella vulgaris* a unicellular green alga. Gutzeit et al. operated batch and continuous flow reactors at both lab and pilot-scale. Continuous flow stirred tank reactors (CFSTR) had a hydraulic retention time (HRT) of 2-3 days, sludge age of 20-25 days, reactor depth of 0.3-0.5 m and a biomass TSS of 1000-1500 mg/L. In the CFSTR, they showed an 88-93% removal in chemical oxygen demand (COD) and dissolved organic carbon (DOC), total nitrogen removal of 15%, and phosphorus removal of 53%.

2.3.2 Microalgae Granules

Tiron et al. (2015) first reported granular activated algae (GAA) for the treatment of low-strength wastewater in sequencing batch reactors (SBR). Tiron et al. (2017) showed that GAA were cultivated through the process of photogranulation. GAA starts in a batch reactor with the addition of *Chlorella* sp. to activated sludge to form activated algae flocs. From literature it is unclear whether activated algae flocs are then left in batch reactors and the granulation process takes place in the batch reactor or if activated algae flocs are used to inoculate an SBR and the granulation process takes place in the SBR. GAA were found to have an optimum size range of 700-1,500 μm and mostly contained unicellular and filamentous microalgae, *Chlorella* sp. and *Phormidium* sp., respectively. In the SBR, Tiron et al. (2015) showed an 86-98% removal of COD and

11-85% removal of phosphorous. The transformation rate of ammonium (NH^{4+}) to nitrate (NO^{3-}) was found to increase with an increase in oxygen (O_2) percentage. A high microalgae recovery efficiency or settleability was found ranging between 99.85 to 99.99% with a settling velocity of 19±3.6 m/h. Recently, de Godos et al. (2014) reported that settling velocity of 0.28-0.42 m/h was achieved for cyanobacterial-bacterial flocs in a photobioreactor. This suggests that GAA are highly efficient at settling. Arcila and Buitron (2016) reported the use of microalgae-bacteria aggregates in a high-rate algal pond (HRAP). These aggregates consisted of both flocs and granules, ranging in size from 0.3- 1 cm and contained mostly unicellular (*Scenedesmus* sp.), filamentous green algae (*Stigeoclonium*), and diatoms (*Navicula* and *Nitzschia*). The HRAP had an HRT of 2-10 days, and showed a 92% removal of COD, 85% removal of NH_4^+-N and 30% removal of phosphate (PO_4^{3-}-P). At an HRT of 6 days, the settling velocity was 8.3±0.8 m/h with 92.7% recovery efficiency, while at 10 days settling velocity was 1.4±0.2 m/h with a 98.3% recovery efficiency.

Ji et al. (2020) reported on a self-sustaining synergetic microalgal-bacterial granular sludge process towards energy-efficient and environmentally sustainable municipal wastewater treatment. The authors developed a self-sustaining synergetic microalgal-bacterial granular sludge process. The results showed that the microalgal-bacterial granular sludge process was capable of removing 92.69%, 96.84% and 87.16% of influent organics, ammonia and phosphorus under non-aeration conditions over a short time of 6 hours. The effluent could meet the increasingly stringent discharge standards in many countries worldwide. A tight synergetic interrelationship effect between microalgae and bacteria in granules was essential for such excellent process performance. The stoichiometric and functional genes analyses further revealed that most of organic matter and nutrients were removed through microalgal and bacterial assimilations. Moreover, it was found that there existed a desirable distribution of

functional species of microalgae and bacteria in microalgal-bacterial granules, which appeared to be essential for the self-sustaining synergetic reactions and stability of microalgal bacterial granules. Consequently, this work may offer a promising engineering alternative with potential to achieve energy-efficient and environmentally sustainable municipal wastewater treatment.

2.3.3 Oxygenic Photogranules

The oxygenic photogranule (OPG) process is a new granular technology with the potential to replace the conventional activated sludge system (CAS) (Figure 2.1). Milferstedt et al. (2017) and Abouhend et al. (2018) first presented oxygenic photogranules (OPGs). In OPG systems, microorganisms are also present in the form of granules (like AGS and UASB systems) (Figure 2.2). The OPG is a hybrid composed of microalgae and bacteria. In contrast to AGS and UASB granules that only form under hydrodynamic conditions, OPG are formed under both static and turbulently mixed conditions. In the OPG process, cyanobacteria and microalgae perform oxygenic photosynthesis to produce energy and oxygen as a byproduct. It has been proposed that heterotrophic bacteria then use the oxygen to degrade organic matter (Abouhend et al., 2018; Milferstedt et al., 2017). Since oxygen is produced in situ there is no need for external aeration and chemical and solar energy from the wastewater are potentially recovered in the form of value-added bio-feedstock.

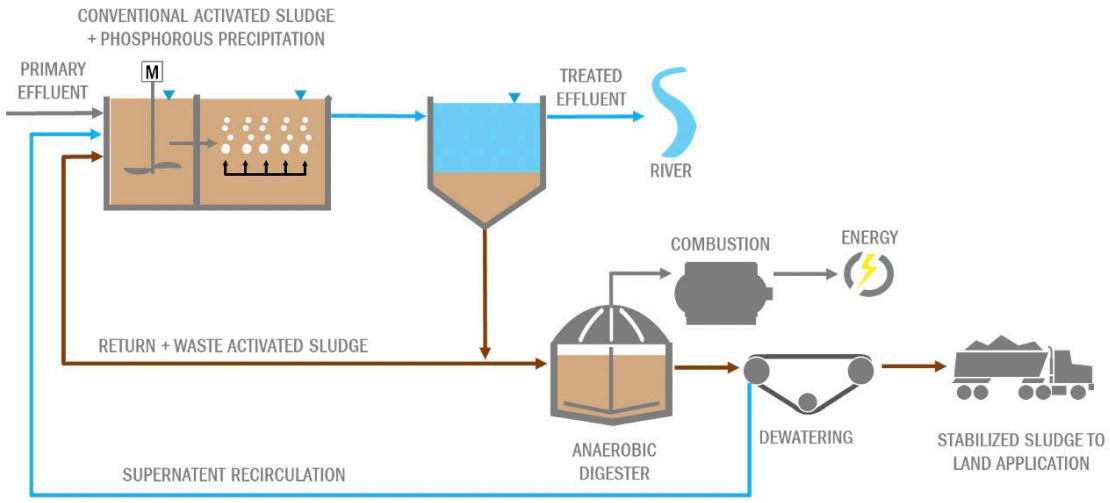

Figure 2.1: Process Scheme of Conventional Activated Sludge (CAS) System. Upstream unit processes identical for both processes (screening, grit removal, primary settling) are omitted from the figure for clarity. Line colors correspond to liquid phase (blue) and sludge (brown).

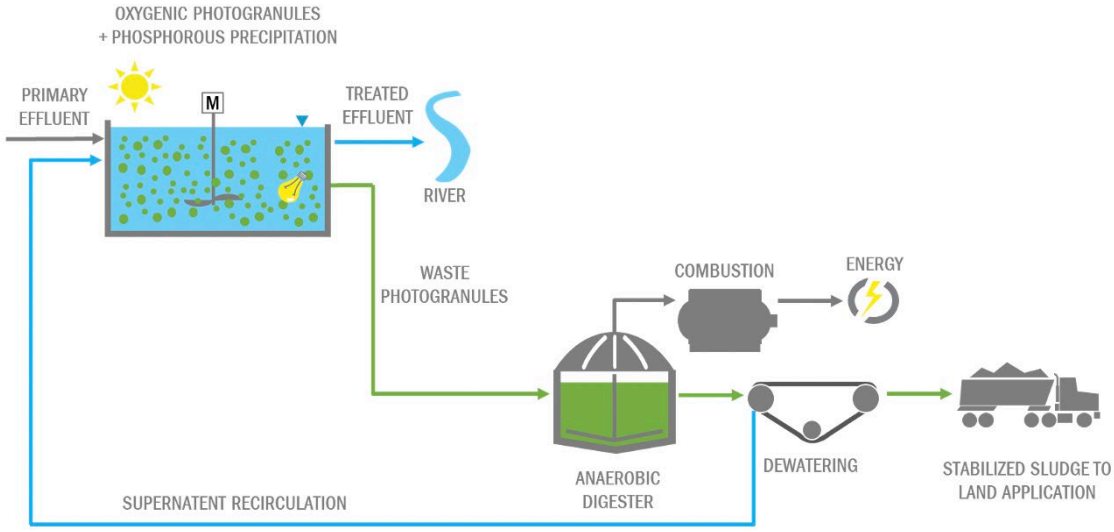

Figure 2.2: Process Scheme of Oxygenic Photogranule (OPG) System. Upstream unit processes identical for both processes (screening, grit removal, primary settling) are omitted from the figure for clarity. Line colors correspond to liquid phase (blue) and photogranules (green).

OPGs are also microalgae-bacterial granules which range in size from 100-4,500 μm and are composed of both motile, filamentous cyanobacteria, *Oscillatoriales* and microalga *Acutodesmus obliquus* embedded in and surrounded by a matrix of extracellular polymeric substances (EPS).

Milferstedt et al. (2017) showed that photogranulation can occur with or without the presence of hydrodynamic selection pressures. Authors revealed that the OPG they formed in both conditions (static and hydrodynamic). Thus, this is different from AGS or UASB granules which are typically created under hydrodynamic conditions without a source of light (Tay et al., 2001). Milferstedt et al. also reported that both hydrostatic and hydrodynamically formed granules share many of the same attributes, including a dense outer layer of motile filamentous cyanobacteria and an inner section composed of bacterial and other micro algal aggregates. The abundance of bacterial sequences in OPG were found to be significantly less than the average maximum abundances of cyanobacterial sequences. Further, this study showed that the bacterial sequences in OPG were significantly different than bacterial sequences in activated sludge inoculum at the start of OPG cultivation. The two most commonly found sequences were associated with genera *Sediminibacterium* and *Lysobacter.* The majority of cyanobacterial sequences in OPG were associated with *Oscillatoriales* and *Microcoleus*. Most algal sequences detected in OPG were associated with *Acutodesmus* but in much lower numbers in comparison to cyanobacterial sequences. Authors also reported that OPG shared similar microbial composition and structure to naturally formed cryoconite granules and microbial mats. Further, Milferstedt et al. reported that an increase in EPS polysaccharide to protein (PS/PN) ratio occurs during photogranulation suggesting that EPS PS are produced by filamentous cyanobacteria contributed to the formation and stability of OPG.

Concurrently, Stauch-White et al. (2017) investigated the role of dissolved inorganic nitrogen (DIN) in the successful formation of hydrostatic OPG. This study proposed that the availability of DIN, particularly ammonium (NH_4^+-N) is the key to successful hydrostatic photogranulation and hypothesized that the decrease in NH_4^+-N may be due to assimilation by cyanobacteria. This study suggested the N may have an

important role in the formation of hydrostatic OPG. The study also reported that successful cultivations showed an increase in the relative abundance of cyanobacterial 16s rRNA gene (*CYAN*). The successful community had a greater relative abundance (46%) of operation taxonomic units (OTUs) associated with genera *Oscillatoria* and *Geitlernema* than the unsuccessful community (27%), supporting that filamentous cyanobacterium are essential for successful OPG formation, and further supporting results reported by Milferstedt et al. (2017).

Abouhend (2018) operated an OPG SBR with an HRT of 0.75 days and an SRT of 21-42 days. Abouhend et al. showed a 77-86% COD removal with a total COD less than 30 mg/L in the effluent, and 28-71% N removal over an operation period of 150 days.

Most recently, Ansari et al. (2019) reported the effects of seeding density on OPG SBR with hydrostatically formed OPG. During the study, three SBR were seeded with a different number (or density) of hydrostatic OPG which was approximately 600, 900, and 1100 mg/L for R1, R2, and R3, respectively. Overall results from this study showed that different seeding densities resulted in significantly different granulation rates and physicochemical characteristics of the biomass, including EPS proteins and polysaccharides, hydrophobicity and biomass settleability. Authors found that R2 produced OPG with optimum compactness, spherical structure and increased hydrophobicity along with highest biomass yield and EPS PN, PS and lipid concentrations. Authors also showed that a negative correlation was found between relative hydrophobicity and sludge volume index suggesting that a decrease in both EPS PN and relative hydrophobicity caused a deterioration in settleability of the biomass. The study also showed an increase in EPS PS/PN ratio similar to Milferstedt et al. (2017).

Abouhend et al. (2020) presented the changes in granular morphology and phototrophic community in reactor photogranules. The authors reported that as

photogranules grew larger, filamentous cyanobacteria became enriched while other phototrophic microbes became significantly less abundant. Photogranules greater than 3 mm showed the development of a layered structure in which filamentous cyanobacteria created concentric layers that enclosed other phototrophic and heterotrophic microorganisms. Authors observed that the growth of photogranules significantly impacted the production of oxygen, a key element for OPG wastewater treatment. Seven size classes were used to classify photogranules. Photogranules in the 0.5−1 mm size group showed the highest specific oxygen production rate (SOPR), 21.9 ± 1.3 mg O_2/g VSS-h, approximately 75% greater than the SOPR of mixed photogranular biomass. Additionally, the authors discussed engineering the OPG process based on photogranule size, promoting the stability of the granular process and enhancing efficiency for self-aerating wastewater treatment.

Gikonyo et al. (2021) presented the hydrodynamic granulation of oxygenic photogranules. Authors report that OPGs, granular assemblages of phototrophic and chemotrophic microbes, offer a promising biotechnology for wastewater treatment with self-aerating potential. Currently, the seed OPG is produced under hydrostatic conditions with activated-sludge inoculum. They investigated the development of OPGs under hydrodynamic conditions employing batches with different light, shear, and inoculum conditions. The results demonstrated hydrodynamic granulation of OPGs from activated sludge, presenting opportunities for rapid (less than 8 days) and bulk development. From the matrix of conditions investigated, they found that granulation occurs only with some combinations of different magnitudes of these input energies. For example, ×4 dilute inoculum combined with low light supported granulation under the different shear conditions utilized. However, ×4 dilution inoculum with high light and high shear did not support granulation. This observed disparity in applied conditions suggests that OPG granulation ensues only with favorable interaction of variable induced energy pressures

coupled with biological response selecting for spheroidal aggregates. Multi-regression analysis on temporal changes in the ratio of sludge volume index for 5 min to 30 min settling, a metric for granulation, confirmed the intercorrelation of these energy inputs on OPG granulation. Authors suggest that this granulation scheme, dependent on goldilocks interaction of selection pressures, can potentially be extended to other granules applied in wastewater treatment.

2.3.4 Modeling of Photogranules

Ouazaite et al. (2020) presented an experimental and modeling approach to quantify phototrophic O_2 production, heterotrophic O_2 consumption, and O_2 diffusion in filamentous photogranules. Authors used planar optodes for the acquisition of spatio-temporal oxygen distributions combined with two-dimensional mathematical modeling. Light penetration into the photogranule was the factor controlling photogranule activities. The spatial distribution of heterotrophs and phototrophs had less impact. The photosynthetic response of filaments to light was detectable within seconds, emphasizing the need to analyze dynamics of light exposure of individual photogranules in photobioreactors. Authors believe that studying other recurring photogranule morphologies will eventually enable the description of photogranule-based processes as the interplay of interacting photogranule populations.

Tenore et al. (2021) presented a mathematical model which describes both the genesis and growth of oxygenic photogranules (OPGs) and the related treatment process. The photogranule is modelled as a free boundary domain with radial symmetry, which evolves over time as a result of microbial growth, attachment and detachment processes. A system of hyperbolic and parabolic partial differential equations (PDEs) have been considered to model the advective transport and growth of sessile biomass

and the diffusive transport and conversion of soluble substrates. The reactor is modelled as a sequencing batch reactor (SBR), through a system of first order impulsive ordinary differential equations (IDEs). Phototrophic biomass has been considered for the first time in granular biofilms, and cyanobacteria and microalgae are taken into account separately, to model their differences in growth rate and light harvesting and utilization. To describe the key role of cyanobacteria in the formation process of photogranules, the attachment velocity of all suspended microbial species has been modelled as a function of the cyanobacteria concentration in suspended form. The model takes into account the main biological aspects and processes involved in OBGs based systems: heterotrophic and photoautotrophic activities of cyanobacteria and microalgae, metabolic activity of heterotrophic and nitrifying bacteria, microbial decay, EPS secretion, diffusion and conversion of soluble substrates (inorganic and organic carbon, ammonia, nitrate and oxygen), symbiotic and competitive interactions between the different microbial species, day-night cycle, light diffusion and attenuation across the granular biofilm and photoinhibition phenomena. The model has been integrated numerically, investigating the evolution and microbial composition of photogranules and the treatment efficiency of the OPGs-based system. The results show the consistency of the model and confirm the purifying effectiveness of the OPGs technology, by analyzing the effects of the wastewater influent composition and light conditions on the process.

2.4 Naturally Occurring Granules and Mats

There are several examples of microbial granules that are also produced in nature. One example is the cryoconite granules which are spherical bioaggregates found in melt holes on the surface of glacial ice around the world (Hodson et al., 2010; Langford et al., 2014; Takeuchi et al., 2001, 2010). Cryoconite granules from different

geographic origins were found to share similar physical characteristics and microbial composition- a layered structure of filamentous cyanobacteria and EPS that encase biomass composed of organic matter, and other phototrophic and heterotrophic microorganisms. Cryoconite granules typically range from 0.3 to 4 mm in diameter (Takeuchi et al., 2010). These granules are located on the sediment of the hole above which a layer of water is present. Except during the melting period during summer, the hole is presumed to provide a stagnant environment with a covering of ice, like a vial cap. Interestingly, in cryoconite granules, it has been reported that EPS PS may control the formation of these aggregates (Hodson et al., 2010; Stibal et al., 2006). The other feature shared between OPGs and cryoconite granules is a strong filamentous cyanobacterial community. In contrast to granules formed in bioprocesses, cryoconite granules are found under conditions that defy the typical hydrodynamic environment where aerobic and anaerobic granules are found.

Another example is the kefir granule. Two types of kefir granules exist, milk and sugary kefir granules. Both types of granules are small, white, cauliflower-shaped bioaggregates which are composed of EPS, various bacterial, mainly lactobacilli and acetobacteria, and yeast species used in milk fermentation (Hsieh et al., 2012). Hsieh et al. (2012) found that bacterial strains in the granules were significantly affected by the fermentation substrate used. In addition, milk kefir granule EPS is composed of kefrin, a complex heteropolysaccharide, while sugary kefir granule EPS mostly consisted of dextran. The diameter of these granules ranges from 1 to 5 mm. The main mechanism of their aggregation is the formation of EPS slime that is composed of polysaccharides. The EPS slime connects the individual microorganisms together in an EPS matrix (Hsieh et al., 2012).

Last, in microbial mats the combination of cyanobacterial filaments and EPS matrix are thought to be the major constituents that form and maintain the mat structure

(de los Ríos et al., 2004). Generally, the first step for the formation of layered microbial mats is cyanobacterial colonization (Rossi & De Philippis, 2015). EPS has six main roles in microbial mats: adhesion, structure, protection against a-biotic stress, bio-weathering processes, for gliding motility, and as nutrient storage (Rossi & De Philippis, 2015). Similar to a closed vial, microbial mats are closed systems maintained by phototrophic microorganisms who use light for photosynthesis (Stal, 1995; Stuart et al., 2015. Thus, microbial mats may be a good model system for OPGs regarding their environment, layered structure, EPS composition, and community of cyanobacteria.

However, the question remains, why do some aggregates form spherical shapes while mats remain as flat, layered sheets? The static conditions and similarities between natural granules, mats and OPGs may hold the key to answer that question. One example is from a study by Castenholz (1968) where he first reported the natural aggregation of filamentous cyanobacteria, *Oscillatoria terebriformis*, isolated from a microbial mat. Castenholz observed that in nature, in flowing water *Oscillatoria* formed mats, however in the stationary Petri dish in the laboratory *Oscillatoria* showed motile responses by forming a single dense, spherical mass. With agitation, the spherical mass dispersed initially, but aggregated after a few minutes. Thus, when taken from a hydrodynamic environment and placed in a static, controlled environment with light, a spherical mass persisted.

2.5 Extracellular Polymeric Substances (EPS)

2.5.1 Definition of EPS

Extracellular polymeric substances (EPS) is a heterogeneous mixture of material that is organic and inorganic. EPS are major components of microbial bioaggregates

(also commonly known as biofilms)- flocs, mats, granules. EPS are produced by archaeal, bacterial, and eukaryotic microorganisms (Dignac et al., 1998; Flemming et al., 2007; Frølund et al., 1996; Higgins & Novak, 1997a, 1997b; Liu & Fang, 2002; Wingender et al., 1999). EPS are located directly on or outside of the cell surface and are generally characterized with respect to their association with cell surface. This also makes it difficult to truly define EPS as it is based on numerous environmental parameters such as microorganisms, substrate, pH, ion availability, organic and inorganic matter.

The key components of activated sludge EPS are protein, polysaccharides, and humic substances. Significant amounts of uronic acids, nucleic acids, and inorganic cations and anions are also present. The EPS matrix in activated sludge can vary in the composition of these components and can be affected by multiple factors including influent wastewater characteristics, growth conditions, bioreactor parameters and operation, extraction method and analysis (Wingender et al., 1999; Nielsen & Jahn, 1999). Earlier studies have shown that polysaccharides are the most abundant EPS components in activated sludge (Brown & Lester, 1980; Morgan et al., 1990). In contrast, multiple studies have shown that the quantity of EPS proteins is two of three times higher than polysaccharides in activated sludge (Comte et al., 2006; Dignac et al., 1998; Frølund et al., 1996; Higgins & Novak, 1997a, 1997b; Liu & Fang, 2002; Nielsen et al., 1996; Urbain et al., 1992; Wingender et al., 1999). Studies have also reported the presence of glycoproteins that are present in activated sludge EPS (Goodwin & Forster, 1985; Horan & Eccles, 1999; Jorand et al., 1998). Glycoproteins function as receptors and are present on cell surfaces (Wu, 2003). They are also known to exhibit acidic and hydrophobic properties (Jorand et al., 1995). Park and Novak (2009) reported the presence of glycoprotein specific lectins in hydrophobic regions of activated sludge EPS.

The study also showed that lectin-mediated bacterial aggregation is one mechanism for activated sludge bioflocculation.

EPS can be subdivided into two forms, soluble EPS (soluble macromolecules, colloids, and slimes) and bound or biomass-associated EPS (sheaths, capsular polymers, condensed gels, loosely bound polymers, and attached organic material) (Wingender et al., 1999). As of late, researchers have reported further subdividing bound EPS into tightly bound (TB) or loosely bound (LB) fractions. TB-EPS may include sheaths, capsular polymers (Seviour et al., 2012) while LB-EPS can include gels and amorphous structure-like EPS (McSwain et al., 2005).

2.5.2 EPS Extraction Methods

Multiple methods have been applied to study and extract EPS from a variety of substances, including but not limited to pure cultures, mixed cultures, activated sludge floc, mats, and granules (Adav et al., 2008; Adav & Lee, 2008; Basuvaraj et al., 2015; Brown & Lester, 1980; Caudan et al., 2014; Comte et al., 2006 d'Abzac et al., 2010a, 2020b; Frølund et al., 1995, 1996; Gong et al., 2009; Guo et al., 2016; 1996; Jahn & Nielsen, 1995; Jorand et al., 1995, 1998; Klock et al., 2007; Kuo-Dahab et al., 2018; Liu & Fang, 2002; Li & Yang, 2007; McSwain et al., 2005; Monique et al., 2008; Nacher et al., 2013; Ni et al., 2009; Park et al., 2008a, 2008b; Park & Novak, 2007, 2009; Seviour et al., 2012; Sheng & Yu, 2006; Takahashi et al., 2009; Toyofuku et al., 2012; Weber et al., 2007; Zhang et al., 1999). Table 2.1 presents different physical and chemical extractions methods, and a combination of methods used sequentially for a variety of systems. Multiple researchers have shown that no universal method exists that extracts for all EPS and typically a combination of methods is required to study the complete EPS matrix (Novak & Higgins, 1997a, 1997b; Park & Novak, 2007, 2009; Park et al., 2008a,

2008b). Multiple physiochemical interactions occur in the EPX matrix and include repulsive forces, electrostatic attractive forces, ionic attractive forces, hydrogen bonding, and van der Waals interactions (Flemming et al., 2010). Extraction methods need to have enough potency to break these interactions but gentle enough to avoid cell lysis and intracellular contamination (Nielsen & Jahn, 1999).

Physical methods apply shear to extract EPS and include centrifugation, homogenization, mixing, shaking, sonication, and thermal treatments (i.e., dry heat or steam). Centrifugation is a separation process that uses centrifugal force to promote settling of particles in a solid-liquid mixture. The settling or sedimentation of particles in a liquid results from the difference in density between the solids and particles and liquid and is achieved using a centrifugal force that is greater than the gravitational force. Based on differences in their mass, particles, like proteins, can be separated out from solution by centrifugation. Mechanical homogenizers use liquid shear to cause disruptions breaking interactions in EPS. Mixing and shaking can be in various forms and can include mortar and pestles, manually shaking and stirring, and pumping to create shear and cause disruptions. An ultrasonic homogenizer of sonication applies sound energy to agitate particles. Ultrasonic waves are used to create pressure variations and cavitation in a mixture, transforming sound waves into mechanical energy by the growth and collapse of bubbles. Thermal treatments include both dry heat like (i.e., oven), steam heat (i.e., autoclave), and boiling.

Chemical methods use the addition of a variety of chemicals to break EPS interactions and linkages in the EPS matrix (Table 2.1). Chemical extraction methods include, but are not limited to, alkaline or base treatment, cation exchange resin (CER), EDTA, ethanol, formamide, formaldehyde, and glutaraldehyde. Of these treatment methods, base and CER treatment are most commonly used for activated sludge, aerobic and anaerobic granules. Alkaline or base extraction increases the pH to greater

than 9 which causes ionization of charged groups like carboxylic groups in biopolymers (Nielsen & Jahn, 1999). At high pH covalent bonds are also broken and uronic acids are degraded (Zayas, 1996). Park and Novak (2007, 2008) used base treatment at pH 10.5 to selectively extract aluminum (Al^{3+}) -bound EPS from activated sludge, based on the solubility of Al^{3+} (Park et al., 2007; Park et al., 2008a, 2008b) In addition, this study also found that base extraction also releases iron ($Fe^{2+/3+}$) from sludge and extracts $Fe^{2+/3+}$-bound EPS. During anaerobic digestion, Fe^{3+} is reduced to soluble Fe^{2+} releasing any EPS that is bound with $Fe^{2+/3}$. Similar to base extraction, CER is known to select and extract for EPS bound with divalent cations, Ca^{2+} and Mg^{2+} (Higgins & Novak, 1997a, 1997b; Park & Novak, 2007). Divalent cations cross-link negatively charged sites on EPS, binding to microbial cell surfaces and more EPS. Higgins and Novak (1997a, 1997b) and Park and Novak (2007) proposed that these cations were mostly associated with EPS proteins versus polysaccharides suggesting proteins are the dominant force in bioflocculation of activated sludge.

2.5.3 Cyanobacterial EPS

Polysaccharides synthesized by filamentous and unicellular cyanobacteria can vary greatly in composition based on the glycosidic bond between different monosaccharides (Delattre et al., 2016; Pereira et al., 2015). The diverse array of polysaccharides each have different chemical and physical properties (Periera et al., 2015). The physiological functions of polysaccharides show a great deal of variety and depend on the structure and form of each polysaccharide. Polysaccharides are both excreted as EPS and provide carbon and energy reserves for many cells (Stuart et al., 2015). In cyanobacteria polysaccharides synthesis and export are well described by Pereira et al. (2015). Briefly, monosaccharides are converted into activated nucleotide

sugars in the cytoplasm. Next, nucleotide sugars are pieced together by glycosyltransferases (key enzymes) and moved to carrier molecules in the plasma membrane. Last, one of three and/or a combination of the three pathways is used to form polymer chains, fits the chains together, and transfers them out of the cell. These three pathways are the Wzy, ABC transporter, and Synthase-dependent pathways (Pereira et al., 2015). Recently, Pereira et al. also identified genes encoding the PN that are related to the three pathways used for moving the polymer chains out of the cell.

The monosaccharide composition of cyanobacterial EPS has been well studied (Delattre et al., 2016; Di Pippo et al., 2013). Polysaccharides produced by cyanobacteria are mainly composed of glucose, galactose, and xylose, even though other monosaccharides such as mannose, fucose, and rhamnose, ribose, arabinose, fructose, galacturonic acid, and glucuronic acid are present (Delattre et al., 2016; Di Pippo et al., 2013). In 1987, Tease and Walker first reported the change in bound EPS (sheath) polysaccharide composition from cyanobacterium *Gloethece* when exposed to different nitrogen sources. In 1998, Hoiczyk found that in filamentous cyanobacterium, *Phormidium uncinatum,* monosaccharide composition varied between soluble and bound EPS. The composition for soluble (slime) EPS was found to be <5% arabinose and rhamnose, 12% xylose, 18% galactose and 60% glucose. In contrast, the study found bound (sheath) EPS to be composed of 3% rhamnose, 9% fuccose, 10% galactose, 11% arabinose, 33% xylose, and 34% glucose.

Multiple species of unicellular and filamentous cyanobacteria are known to produce polysaccahride- based EPS (Hoiczyk, 1998; Mota et al., 2013; Otero & Vincenzini, 2004; Pereira et al., 2015). Cyanobacteria are known to have distinct cell surfaces formed by structures that are involved in the secretion of EPS (Hoiczyk, 2000). Cyanobacterial EPS can be subdivided into slime, tubes and sheaths. These are all associated with the cell surface but differ in thickness and consistency (De Philippis &

Vincenzini, 1998; Rossi & De Philippis, 2015). Slime is a mucilaginous substance that is loosely dispersed around the cell. Sheaths and tubes are generally thicker and more tightly bound around the cell. Cyanobacterial EPS is mostly composed of heteropolysaccharides which make them an attractive source for polymers in industrial applications (Rossi & De Philippis, 2015). Like other EPS-producing microorganisms, the type and abundance of cyanobacterial EPS produced are also based on several factors including environmental conditions.

Synthesis of EPS in cyanobacteria relies on culture conditions and is believed to be a part of their response to different types of stress (i.e., UV light intensity, salt stress, nutrient stress, etc.; Stal, 1995; De Phillippis et al., 1996; De Phillippis & Vincenzini, 1998; Otero & Vincenzini, 2004; Trabelsi et al., 2008; Wingender et al. 1999). The synthesis of EPS was observed to be enhanced by nitrogen limitation in *Cyanothece* and *Anabaena* sp. (De Philippis & Vincenzini, 1998; Moreno et al., 1998). Various nitrogen sources have also been shown to affect EPS production in cyanobacteria. Lupi et al. (1994) showed that different concentration levels of EPS were produced depending on whether the nitrogen source was nitrate ammonium, or urea. Ozturk and Aslim (2010) showed that under salt stress, cyanobacteria *Synechocystis* sp. both increased EPS production and varied EPS composition. Filamentous cyanobacteria also produce EPS for gliding motility. In new cultures of *Phormidium* sp., gliding motility and slime EPS were both present. In old cultures (6-7 weeks), under nutrient stress, cyanobacteria produced sheaths which in turn inhibit motility (Hoiczyk, 1998). Cyanobacteria were also found to vary sheath composition depending on nitrogen source availability (Tease & Walker, 1987). Hoiczyk (1998) observed that motility was not seen in ensheathed *phormidium* sp. filaments. Cyanobacteria with this capability range from unicellular (*Synechocystis* sp. PCC 6803) to filamentous (*Nostoc punctiforme*; Wilde & Mullineaux, 2015).

In addition to EPS production, in times of stress cyanobacteria have the ability to recycle and utilize organic carbon for survival (Herrero et al., 2001; Stuart et al., 2015). Stuart et al. (2015) found that cyanobacteria degrade and incorporate extracellular-derived carbon from its own soluble EPS. Also, the authors confirmed that cyanobacterial enzymes in mats and biofilms are capable of extracellular protein degradation, and α- and β-glucan hydrolysis.

2.5.5 Role of EPS in Granulation and Aggregation

EPS plays a major role in the formation/aggregation, protection, and architecture of microbial aggregates (Liu et al., 2004; Limoli et al., 2015). The polysaccharide to protein interaction, hydrogen bonding, and ionic interactions within the EPS matrix also interact with the environment. The entire EPS matrix has an effect on the structural and physiochemical properties of bioaggregates. Some of these properties are surface charge, dewaterability, structural stability, settleability, flocculation, and rheology (Adav et al., 2008; Liu et al., 2003; Park et al., 2006; Park & Novak, 2007; Seviour et al., 2009; Ye et al., 2011). In addition, EPS can also undergo enzymatic degradation to simpler molecules to become available for bacterial utilization in their metabolism (Frølund et al., 1995).

Cations have been shown to have a significant effect on the bulk properties of activated sludge. Novak and co-workers (Higgins & Novak, 1997a, 1997b; Novak & Haugen, 1981), showed that for both lab-scale and full-scale wastewater treatment systems, sludge settling, and dewatering properties could be improved by the addition of cations to the influent wastewater. In each case, settling properties were improved with the addition of calcium (Ca^{2+}) or magnesium (Mg^{2+}). Batch addition of cations to activated sludge also showed improvement in the sludge settling characteristics (Higgins

& Novak, 1997a). Zita and Hermansson (1994) described the role of cations in floc formation in terms of the Derjaugin, Landau, Verwey and Overbeek (DLVO) theory. Using this theory, the presence of cations reduces the separation distance between negatively charged bacteria promoting flocculation. They found that both monovalent and divalent cations had the same capacity to enhance flocculation and no ion exchange was observed. In contrast to this model, Higgins and Novak (1997a) proposed that cations were involved in flocculation through ionic bridging. In this case, the negatively charged sites of extracellular polymeric substances (EPS) are bridged by cations. Higgins and Novak (1997a) also maintained that according to the DLVO theory, settling and dewatering should be improved with sodium (Na^+) at any concentration. This was experimentally shown not to be the case. The cationic bridging model was also proposed by Kakii et al. (1985) and Eriksson and Alm (1991) who found the removal of calcium from sludge with a chelating agent (ethylenediaminetetraacetic acid (EDTA)), resulted in reduced settling and dewatering characteristics. Cousin and Ganczarczyk (1999) investigated the effect of Ca^{2+} on specific floc properties such as size and density. It was found that the addition of calcium (> 4 meq/L) resulted in an increase in floc size and a decrease in porosity. A minimum addition of 4 meq/L was thought to be necessary to overcome the ion exchange between competing ions, such as Na^+. The increase in floc size was then speculated to be due to the formation of Ca^{2+} bridges among microbial aggregates and particles. Biggs et al., 2001 investigated the effect of Ca^{2+} on activated sludge flocculation dynamics using a unique experimental technique. The technique allowed online analysis of the size of activated sludge flocs during flocculation. Activated sludge samples were firstly sonicated for 3 minutes at 50W and then stirred at 100 rpm. The floc size was subsequently measured on-line using a Malvern Mastersizer/E. For concentrations of Ca^{2+} less than 4 meq/L no significant increase in final floc size was observed even though an increase in the initial rate of change of floc size could be seen.

Addition of Ca^{2+} greater than 4 meq/L resulted in an increase in floc size. Results from this investigation support the theory that cations are involved in flocculation through cationic bridging, and will be used in ongoing investigations to model the flocculation process.

Caudan et al. (2014) reported that alpha (1-4) glucans and proteins play role in aerobic granulation, and proteins were found to be distributed throughout aerobic granules. Caudan et al. suggested that granule cohesion depends partially on Ca^{2+} linkages with anionic proteins in EDTA extracted EPS. The EPS protein pool was found to contain two major fractions, one group corresponding to low molecular mass proteins (~1.6 kDa) and one group corresponding to high molecular mass proteins (~200 kDa).

Granulation is the development of a dense, spherical mass from the aggregation of microorganisms, and organic and inorganic matter. EPS is believed to facilitate and improve granulation in addition to the physiochemical and structural roles EPS play within the aggregate (Adav et al., 2008; Liu et al., 2004; McSwain et al., 2005; Seviour et al., 2009). The anionic nature of EPS gives it its ability to be used as a cohesive construction material.

Currently, granules used in biological wastewater treatment and energy recovery processes are generated in hydrodynamic conditions. Anaerobic granular sludge was first found in up-flow anaerobic sludge blanket (UASB) reactors in the 1980s (Lettinga et al., 1980). In 1997, Morgenroth et al. used an up-flow aerobic sequencing batch reactor to develop aerobic granular sludge. Hydraulic shear force and settling time are prevalent in these types of systems and have been known to be essential for the formation of granules (Tay et al., 2001). In addition, granulation is influenced by other factors, such as organic loading rate, dissolved oxygen, starvation periods, temperature, the presence of divalent cations, and quorum sensing molecules (Gao et al., 2011; Tan et al., 2014.

There are multiple theories for the mechanisms of granulation, i.e., Liu and Tay (2002) and Zhou et al. (2014), and EPS has a significant role in each theory. Whether cell- to-cell adhesion or aggregation, it is suggested in literature that EPS components (polysaccharides and proteins) have a significant effect and role in granulation. In 1999, Beun et al. first proposed a mechanism based on short settling time. Authors believed that filamentous fungal pellets were a substratum for bacterial growth. With time, pellets disintegrated under hydraulic shear force and bacterial colonies remained due to the short settling time (Beun et al., 1999). Then, Tay et al. (2001) found that the combination of higher hydraulic shear stress and shorter settling times stimulated PS production in aerobic granules. Authors also found that an increase in PS changes the surface properties of microorganisms and induces granulation. An increase in PS/PN ratio was observed with granulation, however this remains controversial as PS/PN ratio is dependent on many aspects of operation. Table 2.1 was modified from Ding et al. (2015) to summarize EPS composition in different systems. In 2002, Liu and Tay proposed the first four-step process that has been the norm for granulation: 1) motility to initiate cell-to-cell contact, 2) initial attractive forces to stabilize aggregates, 3) production of EPS to adhere cells to larger aggregates and 4) hydrodynamic shear force that shapes a stable granule structure. In this four-step process, EPS can potentially play a significant role in steps one through three.

In 2014, Zhou et al. proposed the first granulation mechanism without microbial selection pressure as a requirement for granulation. The mechanism includes the following four-steps: 1) growth of young granules and aggregation (due to collision and EPS), 2) increased granule growth due to attachment of floc to granules, 3) mature granule formation by self-aggregation, and 4) detachment of biomass and re-aggregation to form new granules. In contrast to the Liu and Tay (2002) theory, the authors found that granulation was a result of random aggregation during steady state

operation. Further, Zhou et al. claimed that microbial selection pressure is not a factor for granulation since no change was found in microbial communities.

In both mechanisms, EPS polysaccharides and proteins are thought to play major roles in granulation. However, mechanisms are not the only topics that remain controversial. The fate and dynamics of EPS (composition and PS/PN ratio) are also debatable. McSwain et al. (2005) and other authors observed that PS covered the outer layer of aerobic granules while proteins remained in an inner core (Adav et al., 2008; Adav & Lee, 2008). In contrast to Tay et al. (2001), these authors found that PS/PN ratio decreases for aerobic granules- Table 2.1. While Cauden et al. (2014) found that proteins are not only in the core of the granule but are distributed throughout, while polysaccharides are arranged in a layer only around microorganisms. The authors showed that the most crucial biomolecules are α (1-4) glucans and anionic proteins that act as the main force for granule cohesion. Authors also found that divalent cations play a major role in the aggregation mechanism, like cation bridging in activated sludge floc. In a more detailed analysis Seviour et al., 2012 found that EPS polysaccharides consist of more than one polysaccharide that create a gel-like structure in granules, coined Granulen and Alginate-Like Exopolysacchardides (ALE). On the other hand, some studies have also found that proteins favored the formation of aerobic granules and enhance granule electronegativity and surface hydrophobicity (Cauden et al., 2014; Laspidou & Rittmann, 2002; McSwain et al., 2005; Zhang et al., 2007). Multiple studies have reported varying PS/PN ratios (Table 2.1). Thus, it makes it difficult to draw a conclusion about the role of EPS composition in granulation and it remains a controversial topic.

2.6 Ca^{2+} Addition in Aerobic Granules

Ca^{+2} addition is shown to enhance granulation in aerobic granules. Multiple researchers have studied the effects of divalent cations/metals, such as Ca^{2+} and Mg^{2+}, in the granulation of aerobic granules. Jiang et al. (2012) in their investigations, used wastewater containing 100 mg/L of Ca^{2+} and reported that the time to cultivate metal fed granules was considerably decreased to 16 days compared with 32 days without adding Ca^{2+}. The settleability and EPS of Ca^{2+} catalyzed aerobic granules were higher than the sludge without metal augmentation. A similar study was also conducted by Liu et al. (2010) using Mg^{2+} as the bivalent metal, and a positive correlation between Mg^{2+} addition and the time to achieve granulation was observed, but the effect was slightly slower than that from Ca^{2+} addition. Both of these publications assumed that the positive charge of divalent metals neutralized the overall negative charge on the surface of the microbial biomass and EPS molecules and thus helped to enhance the granulation process, but these studies did not provide any experimental evidence of this phenomenon occurring. Liu et al., in the comparison of Ca^{2+} and Mg^{2+} addition to granules, stated that the better performance of Ca^{2+} over Mg^{2+} during the granulation process was because the former (because of its positive charge) acted as a bridge to make cross-linked structures for the union of negatively charged organic components of sludges, and the latter failed to do so. However, the problem is that Mg^{2+} is also a positively charged metal, and contradicts the hypothesis questioning, why granulation with Mg^{2+} addition didn't follow a similar structure during the granulation process. Similarly, contradictory findings had been reported for EPS produced by using different divalent metals during the sludge granulation process. EPS mainly consists of proteins and polysaccharides and is responsible for developing various properties of aerobic granules by changing the surface characteristics due to the presence of active functional

groups, such as hydroxyl, carboxyl and amide, on their molecules. In another study, Sajjd and Kim (2015) operated three aerobic granular sludge SBR reactors were run for 60 days; R-1 functioned as a control reactor, whereas R-2 and R-3 were operated by dosing 25 mg/L of Ca^{2+} and Mg^{2+}, respectively, and the other operating conditions were similar in all of the SBRs. The granulation rate, particle size and sludge settleability were rapidly increased by Ca^{2+} addition, whereas the sludge dewaterability was significantly enhanced by Mg^{2+} augmentation. During the investigations, R-1, R-2 and R-3 had 1.31, 2.98- and 1.58-times higher quantities of polysaccharides, whereas proteins were 1.28, 1.74 and 2.41 times, respectively, more abundant than seed sludge. The divalent metals profoundly changed the composition of EPS, but their total contents were almost similar. XPS and FTIR results showed that Ca^{2+} bonded strongly with hydroxyl groups of polysaccharides due to there being less steric hindrance than proteins, and Mg^{2+} preferably bonded with amide groups of proteins and found no such hindrance due to its smaller size and thus changed the composition of EPS, which eventually altered the granular sludge characteristics.

2.7 Sodium dodecyl sulfate polyacrylamide gel electrophoresis (SDS-PAGE)

Sodium dodecyl sulfate polyacrylamide gel electrophoresis (SDS-PAGE) has been utilized for more specific size-based separation and analysis of EPS proteins in biological systems. Park et al. (2008a) and Park et al. (2008b) showed the one application of SDS-PAGE to wastewater systems, specifically activated sludge and digested sludge. Park et al. extracted EPS proteins by different cation associated extraction methods. EPS protein was subsequently fractionated by ammonium sulfate precipitation (ASP) and subjected to SDS-PAGE. The results showed that each extraction method led to a unique SDS-PAGE protein profile. The study also showed

that CER extracts for EPS proteins that are bound to Ca^{2+} and Mg^{2+}, base extracts for aluminum (Al^{3+})-bound EPS proteins, and sulfide extracts for iron ($Fe^{2+/3+}$)-bound EPS. Park et al. also identified ten proteins ranging in molecular mass (~21-66 kDa) using proteomics analysis. The study reported that some common proteins were extracted by all the methods; base and sulfide proteins shared some similarity suggesting that base can target both Al^{3+} and $Fe^{2+/3+}$-bound EPS. Zhu et al. (2015) compared the SDS-PAGE profile of activated sludge flocs, aerobic and anaerobic granular sludge EPS. The authors found that EPS proteins bound with Ca^{2+} and Mg^{2+}, reduce the surface charge by forming linkages between EPS and cells promoting adhesion and formation of granules. Zhu et al. also showed that high molecular mass proteins (~66-97 kDa) were favored during sludge granulation. Authors suggested that high molecular mass proteins offer more binding sites and interaction points with divalent cations and EPS promoting granulation. These studies show that SDS-PAGE is a useful tool to characterize EPS proteins that are present during photogranulation. Further, studies suggest that different molecular mass proteins may have different roles during photogranulation, and multiple extraction methods may identify different proteins in EPS pools. A better understanding of the dynamics and fate of EPS proteins during photogranulation is crucial for improving our understanding of photogranulation. Presently, there is no literature that characterizes EPS proteins composition using different extraction methods on a molecular level during hydrostatic photogranulation.

2.8 Ca^{2+} and Cyanobacteria

In cyanobacteria, research has suggested that Ca^{2+} is a signaling molecule and is modulated by EPS. The prevalence of Ca^{2+}-binding proteins identified by Vilhauer et al. (2014) and the known role of Ca^{2+} in cyanobacterial phenotypic state suggest that the

control of Ca^{2+} levels is modulated to some degree by EPS. The diversity of proteins and metabolites found indicate that the extracellular matrix outside the cyanobacterial cell is an important contributor to cell fate decisions. The authors proposed that minor changes in extracellular protein sequences can dramatically influence phenotypic outputs and these proteins are essentially the determinants of community organization.

Table 2.1 Physical and Chemical Extraction Methods for Defined Systems

Reference	Year	Extraction Method	Extraction Details	Type of system (i.e., pure culture, biofilm)
Brown and Lester	1980	High-speed centrifugation	33,000 x g, 10 min, 4°C	*K. aerogenes* flocs
Brown and Lester	1980	Ultrasonication	18 W, 10 min	*K. aerogenes* flocs
Brown and Lester	1980	Ultrasonication + High-speed centrifugation	33,000 x g, 10 min, 4°C 18 W, 10 min	*K. aerogenes* flocs
Brown and Lester	1980	Thermal treatment	steam autoclave, 10 min	*K. aerogenes* flocs
Brown and Lester	1980	Alkaline treatment	2 M NaOH, 5 hr, 20°C	*K. aerogenes* flocs
Brown and Lester	1980	EDTA	2% EDTA, 3 hr, 4°C	*K. aerogenes* flocs
Frølund et al.	1995	Centrifugation	2,000 x g, 15 min, 4°C	Activated sludge flocs
Frølund et al.	1995	CER	600 rpm, 0-8 hr, 4°C	Activated sludge flocs
Jahn and Nielsen	1995	Centrifugation	12,000 x g, 10 min, 4°C	Biofilm and bacterial cultures
Jahn and Nielsen	1995	CER	stirring, 1 hr, 4°C	Biofilm and bacterial cultures
Jahn and Nielsen	1995	Sonication	11 W, 30 sec.	Biofilm and bacterial cultures
Frølund et al.	1996	Centrifugation	2,000 x g, 15 min, 4°C	Activated sludge flocs
		CER	100-1100 rpm, 0.5-17 hr, 4°C	
Frølund et al.	1996	NaOH	pH>11, 1 hr	Activated sludge flocs
Frølund et al.	1996	Thermal treatment	Heating, 1 hr, 80°C	Activated sludge flocs
Liu and Fang	2002	EDTA	2% EDTA, 3 hr, 4°C	Activated sludge flocs
Liu and Fang	2002	CER	600 rpm, 1 hr, 4°C	Activated sludge flocs

Liu and Fang	2002	Formaldehyde	36.5% formaldehyde, 1 hr, 4°C	Activated sludge flocs
Liu and Fang	2002	Formaldehyde	36.5% formaldehyde, 1 hr, 4°C + NaOH 1M, 3 hr, 4°C	Activated sludge flocs
Liu and Fang	2002	Formaldehyde	60 W, 2.5 min	Activated sludge flocs
		Sonication	1N NaOH, 3 hr, 4°C	
Comte et al.	2006	Centrifugation	4,000 x g, 20 min, 4°C	Activated sludge flocs
Comte et al.	2006	EDTA	2%, 3 hr, 4°C	Activated sludge flocs
Comte et al.	2006	Formaldehyde	36.5% formaldehyde, 1 hr, 4°C + NaOH 1M, 3 hr, 4°C	Activated sludge flocs
Comte et al.	2006	Glutaraldehyde	10% glutaraldehyde, 12 hr, 4°C	Activated sludge flocs
Comte et al.	2006	Sonication	40W, 2 min	Activated sludge flocs
Comte et al.	2006	CER	600 rpm, 1 hr, 4°C	Activated sludge flocs
Comte et al.	2006	Sonication	40W, 2 min	Activated sludge flocs
		CER	600 rpm, 1 hr, 4°C	
Comte et al.	2006	Heating	1 bar, 10 min, 80°C	Activated sludge flocs
Comte et al.	2006	Ultracentrifugation x2	20,000 x g, 20 min, 10,000 x g, 15 min, 4°C	Activated sludge flocs
Park and Novak	2007	Centrifugation	600 x g, 10 min, 4°C	Activated sludge flocs
		Alkaline treatment	1N NaOH, pH>10.5, 3 hr, 4°C	
Park and Novak	2007	Centrifugation	600 x g, 10 min, 4°C	Activated sludge flocs
		CER	600 rpm, 1 hr, 4°C	

Park and Novak	2007	Centrifugation	600 x g, 10 min, 4°C	Activated sludge flocs
		Sulfide	(Na2S·9H2O solution (pH ~7.5)	
Klock et al.	2007	Centrifugation	NaCl 10%, 15 min, 40°C 4,000 x g, 15 min, x3	cyanobacterial mat
Klock et al.	2007	Centrifugation	NaCl 10% + EDTA 4 mM, 15 min, 40°C, 15 min 4,000 x g, 15 min, x3	cyanobacterial mat
Klock et al.	2007	Centrifugation	40% artificial seawater, 15 min, 40°C, 15 min 4,000 x g, 15 min, x3	cyanobacterial mat
Klock et al.	2007	Centrifugation	10% artificial seawater + EDTA 4mM, 15 min, 40°C, 15 min 4,000 x g, 15 min, x4	cyanobacterial mat
Klock et al.	2007	Centrifugation	NaCl 10% + EDTA 4 mM, 15 min, 40°C, 15 min 4,000 x g, 15 min, x3	cyanobacterial mat
Klock et al.	2007	Centrifugation	10% artificial seawater + EDTA 4 mM, 15 min, 40°C, 15 min 4,000 x g, 15 min, x4	cyanobacterial mat
Klock et al.	2007	Centrifugation	NaCl 10% + EDTA 4 mM, 15 min, 40°C, 15 min 8,220 x g, 10 min, x3	cyanobacterial mat
Klock et al.	2007	Centrifugation	NaCl 10%, 15 min, 40°C, 15 min 8,220 x g, 15 min, x4	cyanobacterial mat
Adav and Lee	2008	Thermal treatment	80°C, 30 min	Aerobic granules
Adav and Lee	2008	Formaldehyde	36.5% formaldehyde, 1 hr, 4°C	Aerobic granules
		Alkaline treatment	1N NaOH, 3 hr, 4°C	

		Centrifugation	10,000 x g, 20 min, 4°C	
Adav and Lee	2008	Sonication	120 W, 5 min	Aerobic granules
		Formaldehyde	36.5% formaldehyde, 1 hr, 4°C	
		Alkaline treatment	1N NaOH, 3 hr, 4°C	
		Centrifugation	10,000 x g, 20 min, 4°C	
Adav and Lee	2008	Formaldehyde	36.5% formaldehyde, 1 hr, 4°C	Aerobic granules
		Alkaline treatment	1N NaOH, 3 hr, 4°C	
		Sonication	120 W, 5 min	
		Centrifugation	10,000 x g, 20 min, 4°C	
Adav and Lee	2008	Formamide	0.06 mL formamide, 1 hr, 4°C	Aerobic granules
		Alkaline treatment	1N NaOH, 3 hr, 4°C	
		Centrifugation	10,000 x g, 20 min, 4°C	
Adav and Lee	2008	Sonication	120 W, 5 min	Aerobic granules
		Formamide	0.06 mL formamide, 1 hr, 4°C	
		Alkaline treatment	1N NaOH, 3 hr, 4°C	
		Centrifugation	10,000 x g, 20 min, 4°C	
Adav and Lee	2008	Formamide	0.06 mL formamide, 1 hr, 4°C	Aerobic granules
		Alkaline treatment	1N NaOH, 3 hr, 4°C	
		Sonication	120 W, 5 min	
		Centrifugation	10,000 x g, 20 min, 4°C	
Gong et al.	2009	Formaldehyde	0.22%, 2 hr, 4°C	*Salmonella pullorum* SA 1685 culture
		Lyophilization	Freeze, 15 min, -80°C --> 60 mTorr, 6 hr, -60°C	

Gong et al.	2009	Formaldehyde	0.22%, 2 hr, 4°C	*Salmonella pullorum* SA 1685 culture
		Ethanol	Cold ethanol, overnight, 4°C	
Gong et al.	2009	Sonication	3.5 Hz, 20 sec.	*Salmonella pullorum* SA 1685 culture
D'Abzac et al.	2010	Centrifugation	20,000 x g, 20 min, 4°C	Anaerobic granules
D'Abzac et al.	2010	Sonication	37 W, 1 min	Anaerobic granules
D'Abzac et al.	2010	Sonication	37 W, 1 min	Anaerobic granules
		CER	600 rpm, 1 hr, 4°C	
D'Abzac et al.	2010	CER	600 rpm, 1 hr, 4°C	Anaerobic granules
D'Abzac et al.	2010	Thermal treatment	Heating, 10 min, 80°C	Anaerobic granules
D'Abzac et al.	2010	Formaldehyde	36.5% formaldehyde, 1 hr, 4°C	Anaerobic granules
		Thermal treatment	Heating, 10 min, 80°C	
D'Abzac et al.	2010	Formaldehyde	36.5% formaldehyde, 1 hr, 4°C	Anaerobic granules
		Alkaline treatment	1N NaOH,3 hr, 4°C	
D'Abzac et al.	2010	Centrifugation	20,000 x g, 20 min, 4°C	Anaerobic granules
		Ethanol	96% Cold ethanol, overnight, 4°C	
Nacher et al.	2013	Centrifugation	5,000 x g, 1.5 min, swing-bucket rotor, 4°C 12,000 x g, 10 min, fixed-angle rotor, 4°C 5,000 x g, 15 min, swing-bucket rotor, 4°C	Mixed-culture biomass
Nacher at al.	2013	Sonication	50 J/mL	Mixed-culture biomass
		Formamide	100% formamide 6µL/mL, 1 hr, 4°C	
Nacher et al.	2013	Alkaline treatment	1M NaOH, pH>11, 1 hr, 300 rpm, 4°C	Mixed-culture biomass
Nacher et al.	2013	Acid treatment	95-97% H2SO4, 1 hr, 300 rpm, 4°C	Mixed-culture biomass
Nacher et al.	2013	CER	300 rpm, 1 hr, 4°C	Mixed-culture biomass

Nacher et al.	2013	Triton	0.5% Triton, 300 rpm,1 hr, 4°C	Mixed-culture biomass
Zhu et al.	2015	Homogenization	1 min	Activated sludge flocs, aerobic granules, anaerobic granules
		Centrifugation	6000 rpm, 10 min	
		Thermal treatment	Heating, 45 min, 80°C	
		Centrifugation	20,000 rpm, 20 min	
Hou et al.	2015	Centrifugation	4,000 x g, 10 min, 4°C	Anammox sludge
		CER	200 rpm, 3 hr, 4°C	
		Centrifugation	9,000 x g, 20 min, 4°C	

CHAPTER 3

INVESTIGATION OF THE FATE AND DYNAMICS OF EXTRACELLULAR POLYMERIC SUBSTANCES (EPS) DURING SLUDGE-BASED PHOTOGRANULATION UNDER HYDROSTATIC CONDITIONS

See Appendix A.

Wenye Camilla Kuo-Dahab,†,‡ Kristie Stauch-White,† Caitlyn S. Butler,†Gitau J. Gikonyo,† Blanca Carbajal-González,§ Anastasia Ivanova,∥Sona Dolan,†,⊥ and Chul Park†

†Department of Civil and Environmental Engineering, University of Massachusetts, Amherst, Massachusetts 01003 United States

‡Brown and Caldwell; One Tech Drive, Andover, Massachusetts 01810, United States

§Science Center Microscopy Facility, Mount Holyoke College, South Hadley, Massachusetts 01075, United States

∥Department of Biology, University of Massachusetts, Amherst, Massachusetts 01003, United States

Submitted to Environmental Science & Technology: June 4, 2018

Accepted: August 28, 2018

Published: August 28, 2018, Environmental Science & Technology, 52, 10462-10471

CHAPTER 4

RELATIONS BETWEEN EXTRACELLULAR POLYMERIC SUBSTANCES (EPS) PROTOCOLS AND HYDROSTATIC PHOTOGRANULATION OF ACTIVATED SLUDGE- COMPARISON OF FIVE EPS EXTRACTION METHODS

4.1 Introduction

New advancements in wastewater treatment are in demand due to a rapid growth in human population and the need to incorporate sustainability into society. The two main drivers of these developments are general process improvements and the collection and recycling of resources as society moves to circular versus linear economies (Flores et al., 2018; Guest et al., 2009). The main limitations of conventional biological treatment or the activated sludge process are the land requirements for gravity-based separation of flocculant activated sludge biomass from treated water, high aeration requirements to drive the biochemical reactions needed to facilitate biodegradation and organic matter removal, and the large capital investment costs. Additionally, activated sludge treatment, has not fundamentally changed over the past 100 years. Anaerobic processes at resource recovery facilities are utilized for digestion of excess activated sludge, but only a fraction of energy potential of wastewater is recovered (Rittmann and McCarty et al., 2001).

In the last decade, another form of sludge, aerobic granules, have been engineered to replace flocculant activated sludge biomass to treat wastewater. The spherical form of these granules is advantageous because it improves the efficiency of gravity-based separation and reduces the area and cost requirements for the process. However, these technologies still require aeration to drive the biochemical reactions needed to removal organic matter, nitrogen and/or phosphorous.

Recently, a new granular process, oxygenic photogranule (OPG), was introduced where the need for aeration is eliminated making it an attractive alternative for wastewater treatment (Abouhend et al., 2018; Milferstedt et al., 2017; Park & Dolan, 2015). The OPG process is a light-driven, biological wastewater treatment process operated as a sequencing batch reactor (SBR) without aeration (Abouhend et al., 2018). The OPG is a microbial granular biofilm that consists of microorganisms that organize into highly structured spherical form that can remove biodegradable organic matter, nitrogen (N), and phosphorous (P) (Abouhend et al., 2018). A common approach to start-up new processes is the addition of previously grown microbial biomass as a starter culture (Abouhend et al., 2018; Ansari et al., 2019). The starter culture has to-date primarily been grown hydrostatically (Abouhend et al., 2018; Kuo-Dahab et al., 2018; Milferstedt et al., 2017). Hydrostatically-grown OPG used to inoculate the reactors are cultivated in small (20mL), hydrostatic batch vials through the phenomenon coined hydrostatic photogranulation (Milferstedt et al., 2017). Photogranulation occurs when activated sludge inoculum is placed under a source of light in a hydrostatic environment over a period of time (Kuo-Dahab et al., 2018; Milferstedt et al., 2017). Hydrostatically cultivated OPGs have spherical or sphere like-structure in which layers of filamentous cyanobacteria surround microbes in an extracellular polymeric matrix (Kuo-Dahab et al., 2018; Milferstedt et al., 2017).

Recently, the photogranulation mechanism of OPGs in hydrostatic conditions was proposed by Milferstedt et al. (2017) and Kuo-Dahab et al. (2018). Milferstedt et al. (2017) reported that enrichment of motile, filamentous cyanobacteria from activated sludge inoculum plays a key role in the photogranulation mechanism. Motile, filamentous cyanobacteria are known to produce high molecular weight extracellular polymeric substances (EPS) composed of polysaccharides (De Philippis & Vincenzini, 1998; Hoiczyk, 1998). In general, EPS are mainly the high-molecular-weight secretions from

microorganisms, and the products of cellular lysis and hydrolysis of macromolecules. In addition, some organic matters from wastewater can also be adsorbed to the EPS matrix (Liu & Fang, 2002; Nielsen & Jahn, 1999). EPS are generally characterized with respect to their association with the microbial cell surfaces- these forms can be subdivided into bound EPS (sheaths, capsular polymers, condensed gels, loosely bound polymers, and attached organic materials) and soluble EPS (soluble macromolecules, colloids, and slimes; Laspidou & Rittmann, 2002; Nielsen & Jahn, 1999). Bound EPS are closely bound with cells, while soluble EPS are weakly bound with cells or dissolved into the solution. Proteins and polysaccharides are usually found to be the major components of EPS. Humic substances may also be a key component of the EPS in sludge in biological wastewater treatment reactors, accounting for approximately 20% of the total amount (Frølund et al., 1995, 1996). In addition, lipids, nucleic acids, uronic acids and some inorganic components have also been found in EPS from various matrices (D'Abzac et al., 2010a, 2010b; Dignac et al., 1998; Frølund et al., 1996). Their fractions in EPS depended strongly upon the extraction methods and the sludge origins.

Milferstedt et al. (2017) and Kuo-Dahab et al. (2018) show that an increase in total EPS polysaccharide to protein (PS/PN) ratio is associated with photogranulation under hydrostatic conditions. Kuo-Dahab et al. and Stauch-White et al. (2017) reported that an initial nitrogen limiting period during the start of the cultivation and the recycle of organic nitrogen (N), which is base-extractable fraction of EPS, by phototrophic microorganisms are components that lead to photogranulation under hydrostatic conditions. Kuo-Dahab et al. show that both degradation and generation of EPS are involved in and are critical for hydrostatic photogranulation.

Literature on activated sludge and process granules (i.e., aerobic and anaerobic granules) show that the quantification and quality of EPS characteristics and the amounts of extracted EPS can vary widely as a function of the biomass attributes and

initial conditions (i.e., form [floccular or granular], sludge origin and microbial community). To date, there is no single, universal method to extract EPS from biological flocs and granules to better infer the role of EPS in these granular biofilms (i.e., activated sludge, aerobic granules, anaerobic granules, OPGs) (Nielsen & Jahn, 1999; Novak & Haugen (1981); Park & Novak, 2007). Additionally, a combination of methods is shown to improve the characterization of the total EPS in activated sludge flocs or granules, as shown by Park and Novak (2007). Park et al. (2008a) and (2008b) showed an application of molecular tool SDS-PAGE to wastewater systems, specifically activated sludge and digested sludge. Park et al. extracted EPS proteins by different cation associated extraction methods. EPS proteins were subsequently fractionated by ammonium sulfate precipitation (ASP) and subjected to SDS-PAGE. The results showed that each extraction method led to a unique SDS-PAGE protein profile. The study also showed that cation exchange resin (CER) extracts for EPS proteins that are bound to Ca^{2+} and $Mg^{2+,}$ base extracts for aluminum (Al^{3+})-bound EPS proteins, and sulfide extracts for iron ($Fe^{2+/3+}$)-bound EPS (Park et al., 2008b). This study shows that multiple methods are needed to fully extract and characterize all the available fractions of EPS.

Kuo-Dahab et al. (2018) and Milferstedt et al. (2017) have both shown significant physical and biochemical changes that arise during photogranulation. For example, one observable change is the morphology of the biomass. Using microscopy and genomic tools, authors observed significant biomass changes as the microbial community became dominated by motile, filamentous cyanobacteria. In nature, motile, filamentous cyanobacteria are known produce copious amounts of soluble EPS (i.e., slime tubes) and bound EPS that is more rigid in the form of sheaths (Hoiczyk & Baumeister, 1995,1997; Hoiczyk, 1998). It is thought that slime tubes are produced for motility or during active periods while sheaths are produced in aging cultures as a means of protection and are permanently attached to the cell surface (De Philippis & Vincenzini,

1998; Hoiczyk, 1998). Hoiczyk (1998) extracted the soluble EPS fraction with centrifugation and mild heat while bound EPS in the form of sheaths were extracted with centrifugation, sonication and heat treatment. Hoiczyk analysis revealed that bound EPS fraction or sheaths are composed of various types of polysaccharides that are highly resistant to chemical degradation, showing that multiple physical extraction may be needed to extract and distinguish soluble and bound EPS fractions from cyanobacteria in OPGs (Hoiczyk, 1998). Because of the sheath's protective abilities and resistance to chemical degradation, physical extraction methods may be more effective at extracting bound EPS fraction from the cyanobacteria's cell surface. Thus, both chemical and/or physical extraction methods may be effective for extracting soluble and bound EPS fractions in biomass that contain cyanobacterial EPS.

To date, no studies have fully characterized or shown the dynamics of different EPS fractions during hydrostatic photogranulation, using multiple comprehensive physical and chemical extraction methods. The evolution of EPS is tied both to the structure of OPG and is needed to understand the cycling of carbon (C) and nitrogen (N) during the formation of hydrostatic photogranules. The aim of the present investigation is two-fold: first, to determine if multiple extraction methods are needed to fully characterize EPS fractions, and second, further describe the dynamics between EPS, C and N, during hydrostatic photogranulation for OPG formation. To achieve the aims of this study, we assessed four physical and/or chemical bound EPS extraction methods, CER, alkaline (base) treatment, sonication, and heat treatment, following the temporal progression of photogranulation. The composite assessment of soluble and bound EPS polysaccharides, proteins and humic acids from the different extraction methods are analyzed in correlation with chlorophyll and nutrients data during different phases of photogranulation. The outcome of this study is expected to elucidate the dynamics of different EPS fractions and their role in successful hydrostatic photogranulation. These

results will ultimately be beneficial for optimization of hydrostatic photogranulation and subsequently the OPG process for wastewater treatment.

4.2 Materials and Methods

4.2.1 Source of Activated Sludge and Cultivation of OPGs

The extraction methods were tested on activated sludge inoculum, and during the temporal progression of photogranulation of activated sludge to OPGs in January 2016. Activated sludge was sampled directly from the aeration tank of Amherst and Hadley wastewater treatment plant (WWTP). As secondary treatment process, Amherst WWTP utilizes biological nutrient removal with a solids retention time (SRT) of 10-15 days and domestic wastewater as their influent source. Hadley WWTP operates a conventional activated sludge process to remove organic matter with nitrification at a 10-day SRT with mostly residential, commercial, and agricultural influent sources. The main characteristics of the sludge and the WWTP is described in subsequent sections and presented in Table 1. OPGs were cultivated following the procedure of Milferstedt et al. (2017) and Kuo-Dahab et al. (2018). After activated sludge was sampled, 10mL of well-mixed aliquots were pipetted into 20mL scintillation vials and capped immediately after returning to the lab, resulting in 420 individual vials for each sludge set (Figure 4.1). Additional activated sludge was used for day 0 chemical analysis and t=0 represents initial conditions of the experiment and water quality for the activated sludge sets. Vials were kept in hydrostatic conditions, illuminated under broadband LED lights (that were equally distributed) at approximately 10 klux, 24 hr. per day at 18°C. Sampling was performed at day 0, 2, 4, 6, 9, 12, 16, 20, 24, and 28. At day 28, the cultivation was considered complete, and a final sample collection was performed. To determine the

success of granulation (100% of vials at the end of cultivation yielded a granule), a shake test was performed on remaining vials (n=20) by using three firm shakes by hand then observing the vial contents. When a granule remained intact with little or no cloud of particles in the bulk liquid, the granulation was determined to be a success.

Figure 4.1: Oxygenic Photogranules Cultivated in a Hydrostatic Environment. Top shelf is Hadley sludge, bottom shelf is Amherst sludge.

4.2.2 Microscopy

The development of granules was observed by using a transmitted light (EVOS FL Color AMEFC 4300) and scanning electron microscope (SEM; FEI Quanta 200). Images by light microscopy were obtained periodically to check granule development during different phases. Literature was used for identification of microorganisms in the samples. SEM samples were also collected on day 28 and a typical biological sample preparation by the way of fixation and dehydration following the procedure presented in Milferstedt et al. (2017). The samples were then critically point-dried using a Tousimis SAMDRI 780B critical point dryer following vendor instructions or tertiary butanol-dried

as described by Baskin et al. (2014). After drying samples were mounted on aluminum stubs, sputter-coated with gold using a Polaron E5100 sputter coater and imaged using an SEM operated at 15 kV and a spot size of 3.5 µm

4.2.3 Analytical Procedures

Phototrophic microorganisms can be indirectly quantified by extracting and measuring the concentration of chlorophyll in the biomass. Green algae contain both chlorophyll *a* and *b*. Cyanobacteria, on the other hand, only contain chlorophyll *a* and accessory pigment proteins known as phycobilins. Chlorophyll *a/b* ratio can be used as a surrogate to represent cyanobacterial growth.

Solids content, total suspended solids (TSS) and volatile suspended solids (VSS), and chemical oxygen demand (COD) were measured at each sampling date using triplicate samples, all according to APHA standard engineering methods (APHA, 1998).

Dissolved organic carbon (DOC) and dissolved total nitrogen (DTN) using a Shimadzu TN/DOC analyzer (Shimadzu TOC-VCPH with TNM-1, Shimadzu North America, SSI Inc., Columbia, MD, USA).

Dissolved constituents in the bulk liquid: dissolved nitrogen species, nitrate (NO_3^--N), nitrite (NO_2^--N), and ammonium (NH_4^+-N), and divalent and monovalent anions, phosphate (PO_4^{3-}), sulfate (SO_4^{2-}), and cations, sodium (Na^+), potassium (K^+), calcium (Ca^{2+}), and magnesium (Mg^{2+}), were measured using a Metrohm 850 Professional Ion Chromatograph (IC) (Metrohm Inc., Switzerland) with a Metrosep A Supp 5-250 anion column and Metrosep C 2-250 cation column.

4.2.4 EPS Extraction and Chemical Analysis

EPS was extracted and characterized after centrifugation and homogenization by four extraction methods: the use of cation-exchange resin (CER), alkaline or base treatment (NaOH), particle agitation by sonication, and heat treatment. A general pathway of the four extraction methods is presented in Figure 4.2.

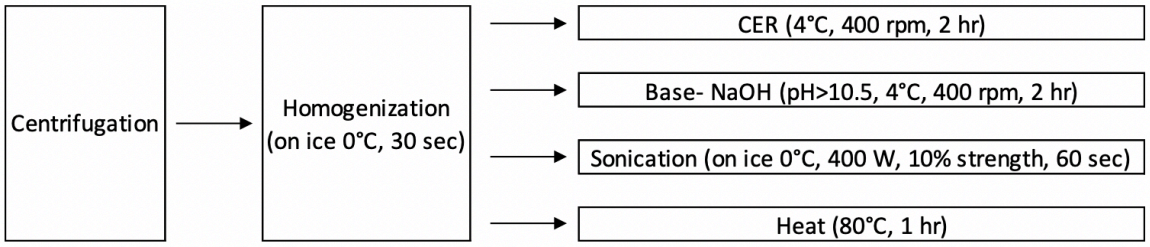

Figure 4.2: General Pathway of Four Extraction Methods for Biomass-Bound EPS. EPS was extracted and characterized after centrifugation and homogenization by four extraction methods: The use of cation-exchange resin (CER), alkaline or base treatment (NAOH), particle agitation by sonication, and heat treatment

4.2.4.1 Sample Pretreatment

Each sample vial initially contained 10 mL of activated sludge (which later became one OPG). The cultivation initially contained 420 individual vial samples. At each sample point, samples were collected and destructively sampled in triplicates or three 10 mL samples and individually processed as three separate samples. Each individual 10 mL sample was transferred from scintillation vial to a sterile 50mL centrifuge tube and centrifuged at 4°C and 12,000 rpm for 20 min. The supernatant was collected and filtered through 0.45 μm cellulose filters to determine the chemical composition of the liquid phase of the vial contents also known as soluble EPS fraction. The pellets were resuspended in phosphate buffer solution (10 mM NaCl, 1.2 mM KH_2PO_4, and 6 mM Na_2HPO_4) to a total volume of 20 mL in the same 50mL centrifuge tubes. Phosphate buffer was prepared according to Frølund et al. (1996), the

conductivity of the buffer was made to be the same as the conductivity found for the activated sludge inoculum at a pH of 7.2 (Frølund et al., 1995, 1996; Nielsen et al., 1996). Each replicate was homogenized individually (500 W IKA T18 ULTRA-TURRAX) for 30 sec. After sample pre-treatment, samples were equally divided and each of the four extraction approaches were applied to each triplicate set, as described in the next sections.

4.2.4.2 Cation-Exchange Resin Extraction

EPS extraction using Dowex 50x8, Na^+ Form, cation exchange resin (CER)(DOWEX) was performed with as 70g CER/g VS of CER ratio according to the method of Frølund et al. (Frølund et al., 1995, 1996; Nielsen et al., 1996). Resin was pre-washed in phosphate buffer (10 mM NaCl, 1.2 mM KH_2PO_4, and 6 mM Na_2HPO_4; pH 7.2). For each individual sample, 50 mL centrifuge tubes were used with 20 mL sample to provide adequate mixing. 70g/g VS of CER was weighed and added to each centrifuge tube based on initial VS concentration of the sample. The samples were mixed at 400 rpm on a shaker table for 2 hr in the dark at 4°C. A Milli-q water with CER and phosphate buffer (10 mM NaCl, 1.2 mM KH_2PO_4, and 6 mM Na_2HPO_4; pH 7.2) was also tested at the start of the study as a blank control.

4.2.4.3 Sodium Hydroxide (NaOH) Extraction

Homogenized samples (suspended in 20 mL phosphate buffer; 10 mM NaCl, 1.2 mM KH_2PO_4, and 6 mM Na_2HPO_4; pH 7.2) were adjusted to a pH 11 by using 1 M NaOH and mixed at 400 rpm for 2 hours in the dark at 4°C (Wang, 2013). A vial with only phosphate buffer adjusted to pH 11 with NaOH was also measured as a blank control.

4.2.4.4 Sonication Extraction

After homogenization, each individual 10 mL sample (suspended in 20 mL phosphate buffer; 10 mM NaCl, 1.2 mM KH_2PO_4, and 6 mM Na_2HPO_4; pH 7.2) was placed on ice and a 400 W sonic dismembrator (Fisher Scientific model 500) was used at 10% strength for 1 min at 20 kHz. This delivered an ultrasonic dose of approximately 4.1 W-min/mL, following the calculation shown by Muller (Muller, 2006).

4.2.4.5 Heat Extraction

After homogenization, each individual 10 mL sample (suspended in 20 mL phosphate buffer; 10 mM NaCl, 1.2 mM KH_2PO_4, and 6 mM Na_2HPO_4; pH 7.2) was heated at 80°C for 1 hour in closed glass vials in an oven (Fisher Scientific).

4.2.4.6 EPS Characterization

After each extraction method, each sample was centrifuged at 4°C at 12,000 rpm for 20 min. Afterward, EPS supernatant was stored at -20°C in aliquots until chemical analyses were performed. DOC and DTN were measured using the same procedure as the liquid phase. Proteins, humic acids and polysaccharides were measured according to modified Lowry and DuBois methods, respectively (Dubois et al., 1956; Frølund et al., 1995, 1996; Lowry et al., 1951). Bovine albumin serum, HA and glucose were used as standards for proteins, humic acids and polysaccharides, respectively.

4.2.5 Contribution of Organic C and N from Biomolecules

The following equations below are used, for each extraction method, to calculate the contribution of organic C and N from polysaccharides, proteins, and humic acids to

the overall organic C and N fractions. Based on the chemical formula for glucose ($C_6H_{12}O_6$), BSA, humic acids it is assumed that 40% of the molecular weight of polysaccharide (PS) is C, 54% of the molecular weight of protein (PN) is C, and 48% of the molecular weight of humic acids (HA) is C, where $DOC_{PS+PN+HA}$ and $BOC_{PS+PN+HA}$ are shown in Equation 1.

Equation 1:

$$DOC\ and\ BOC_{PS+PN+HA} = 0.40 * EPS\ PS_{Conc.} + 0.54 * EPS\ PN_{Conc.} + 0.48 * EPS\ HA_{Conc.}$$

16% of the molecular weight of proteins is N and 3% of the molecular weight of humic acids is N, where DON_{PN+HA} and/or BON_{PN+HA} are shown in Equation 2.

Equation 2:

$$DON\ and\ BON_{PN+HA} = 0.16 * EPS\ PN_{Conc.} + 0.03 * EPS\ HA_{Conc.}$$

4.2.6 Statistical Analysis

Correlation analysis was performed in R (R Core Team, 2021) using R studio (RStudio Team, 2021) interface to compute correlations and significance between two variables. Each variable is the average for the values collected in triplicate (from triplicate vials). The correlation analysis was done for every variable over the course of photogranulation and explored during different phases of photogranulation. The "PerformanceAnalytics" package (Peterson & Carl, 2020) was used to investigate the dependence between two variables at the same time and presented in a correlation matrix. Pearson correlation coefficient is presented which measures the linear dependence between two variables. Each correlation matrix plot shows the distribution of each variable along the diagonal. On the bottom section of the diagonal, the bivariate scatter plots with a fitted line are displayed. On the top section of the diagonal, the value of the Pearson correlation coefficient plus the significance level as stars. Each

significance level is associated to a symbol: p-values (0.001, 0.01, 0.05, 0.1, 1) correspond to symbols (“***”, “**”, “*”, “.”, " “).

4.3 Results

In order to validate the consideration of EPS and the methods with which they were extracted, OPG photogranulation in a hydrostatic environment is characterized and defined with respect to sludge biomass characteristics, for both sludge source sets (Amherst and Hadley), soluble constituents in the bulk liquid, and previous literature. Initial correlation analysis of dissolved components in the bulk liquid allows for the interpretation of EPS analysis in a closed, batch environment over the cultivation period.

4.3.1 Initial Characteristics and Variability of Activated Sludge Inoculum

Initial characteristics of the activated sludge collected from two different WWTP are presented in Table 1. Briefly, after activated sludge was collected 10mL of sludge was pipetted into 20mL scintillation vials resulting in a cultivation set of 420 vials for each sludge, Amherst and Hadley (details described in the methods section). Both WWTP have an open basin with mechanical aeration. Initial solids concentration of Amherst and Hadley sludge inoculum is 1387±55 mg/L and 3390±40 mg/L total suspended solids (TSS), respectively. Hadley sludge solids concentration is approximately 2.5 times the concentration of Amherst sludge. The total organic matter can be quantified by measuring the volatile suspended solids (VSS); the organic fraction for Amherst and Hadley sludge inoculum is 80% or 1113±40 mg/L and 82% or 2793±59 mg/L VSS, respectively. The VSS concentration remained relatively constant during the cultivation period with an approximate overall change of ±10% for both sludge sources (data not shown). Assuming the chemical formula of a mixed culture ($C_5H_7O_2N$, carbon (C)

represents about 53.5% and nitrogen (N) represents about 12.4% of the molecular weight. Biomass organic C and N can be estimated from VSS, yielding an initial estimate of the concentration of organic C (Amherst: 595 mg/L and Hadley: 1,496 mg/L) and organic N (Amherst: 138 mg/L and Hadley: 346 mg/L; Rittman & McCarty, 2001). Initial dissolved organic carbon (DOC) and dissolved total nitrogen (DTN) content are found to be 9.7±2.4 mg/L and 0.7±0.1 mg/L for Amherst, and 18.2±2.2 mg/L and 1.9±0.3 mg/L for Hadley, respectively. Dissolved inorganic nitrogen (DIN) was found to be 96% of DTN or 15.9±0.6 mg/L for Amherst, and 95% of DTN or 8.8±0.3 mg/L for Hadley. This data shows that Hadley sludge cultivation set had higher concentration of organic biomass, and higher organic C and N in the bulk liquid during the start of the cultivation, in comparison to Amherst.

Table 4.1 Initial Characteristics of Activated Sludge Inoculum

		Amherst Activated Sludge		**Hadley Activated Sludge**	
Parameter	Units	Value	SD	Value	SD
Biological Process	-	Biological nutrient removal	-	Conventional activated sludge	-
Basin Configuration	-	Open	-	Open	-
Aeration Type	-	Mechanical	-	Mechanical	-
Influent Sources	-	Residential and Umass	-	Residential and commercial	-
SRT	days	10-15	-	10	-
TSS	mg/L	1387	55	3390	40
VSS	mg/L	1113	40	2793	59
VSS/TSS	%	80.2	4.0	82.4	2.0
DOC	mg/L	9.7	0	18.2	0.2
DTN	mg/L-N	16.7	1	9.4	0.3
DON	mg/L-N	0.7	0.6	1.9	0.3
DIN	mg/L-N	15.9	0	8.9	0.1
Chlorophyll *a*	mg/L	0.5	0.0	1.1	0.0
Chlorophyll *b*	mg/L	0.3	0.0	0.4	0.0
Chlorophyll *a/b*	mg/L/mg/L	1.7	0.1	2.7	0.2

4.3.2 Phototrophic Growth During the Phases of Photogranulation

Temporal progression with the phases of photogranulation (Figure 4.3), I) sludge compaction, II) phototrophic bloom, III) main granulation, and IV) maturation, were first

reported by Kuo-Dahab et al. (2018). Chlorophyll *a* and *b* concentration and *a/b* ratio across those four phases of growth are consistent with previous studies (Figure 4.4; Milferstedt et al., 2017; Kuo-Dahab et al., 2018). We defined different phases of photogranulation based on biomass morphology and chlorophyll concentration. Phase I is the sludge compaction period which occurs between day 0 and 3. During this phase sludge continues to settle and compacts. During the first phase, chlorophyll a is near the limit of detection day 0 with a concentration of 0.51 mg/L and 1.1 mg/L and yields a chlorophyll *a/b* ratio of 1.65 and 2.68, for Amherst and Hadley sludge, respectively. Phase II is the phototrophic bloom period which occurs between day 3 and 14. During this phase motile, filamentous cyanobacterium are enriched and morphological changes in the biomass color and form is observable. The biomass color changes from brown to green and the biomass begins to contract and shrink. Phase III is coined the main granulation period and occurs between day 14 and 21. During this phase morphological changes continue and a blue-green or dark green, spherical, or granular form emerges. A maximum chlorophyll *a* concentration of 11.4 mg/L at day and 12.6 mg/L at day 16, for Amherst and Hadley, respectively, is seen during this phase. During phase II and III chlorophyll *a/b* ratio increases exponentially plateauing at day 20 for Amherst and day 24 for Hadley. Phase IV is maturation. During this phase granules have matured, and the morphology of the biomass is completely spherical.

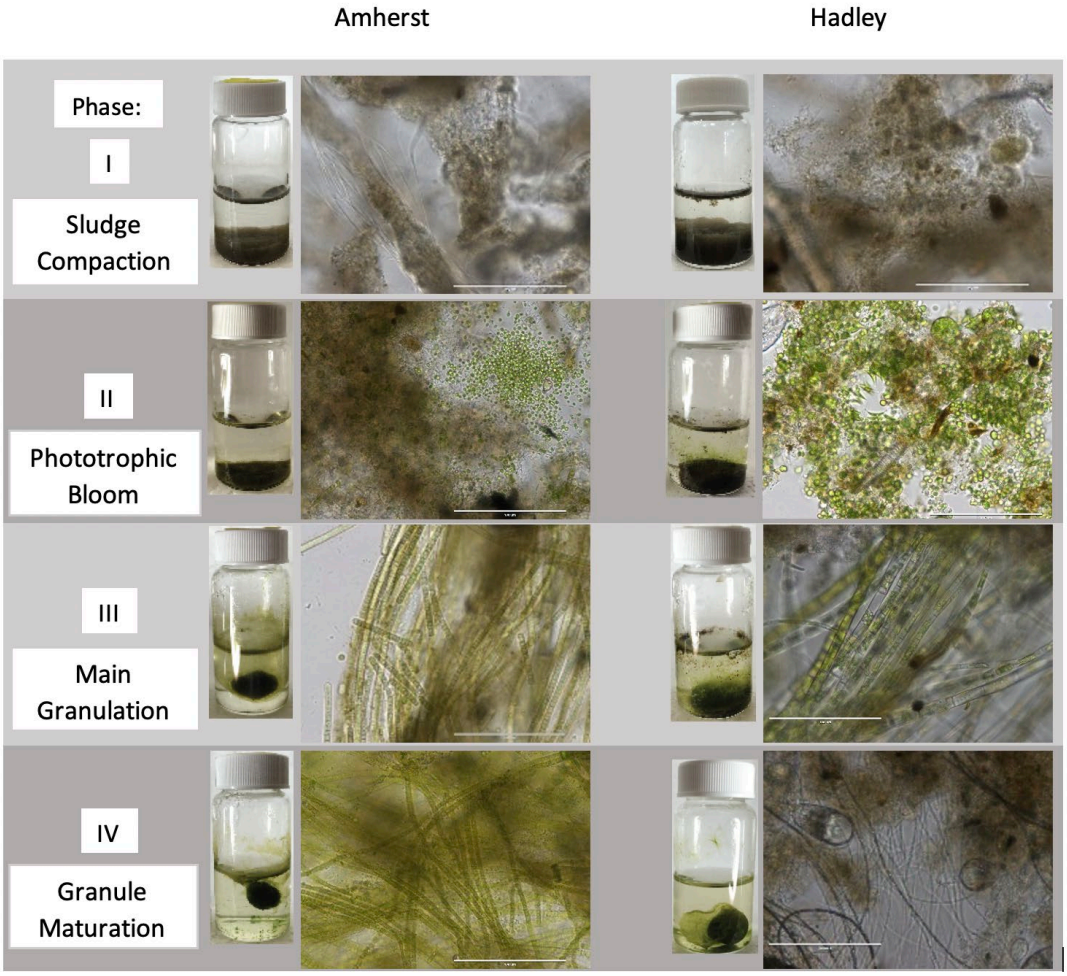

Figure 4.3: Temporal Progression of Photogranulation Under Hydrostatic Conditions. Activated sludge (10 ml) from the aeration basin of two wastewater treatment plants, Amherst and Hadley, transforms into a hydrostatic oxygenic photogranule when exposed to light in an unagitated environment, here a 20 ml scintillation vial with an outer diameter of 28mm and height of 61mm

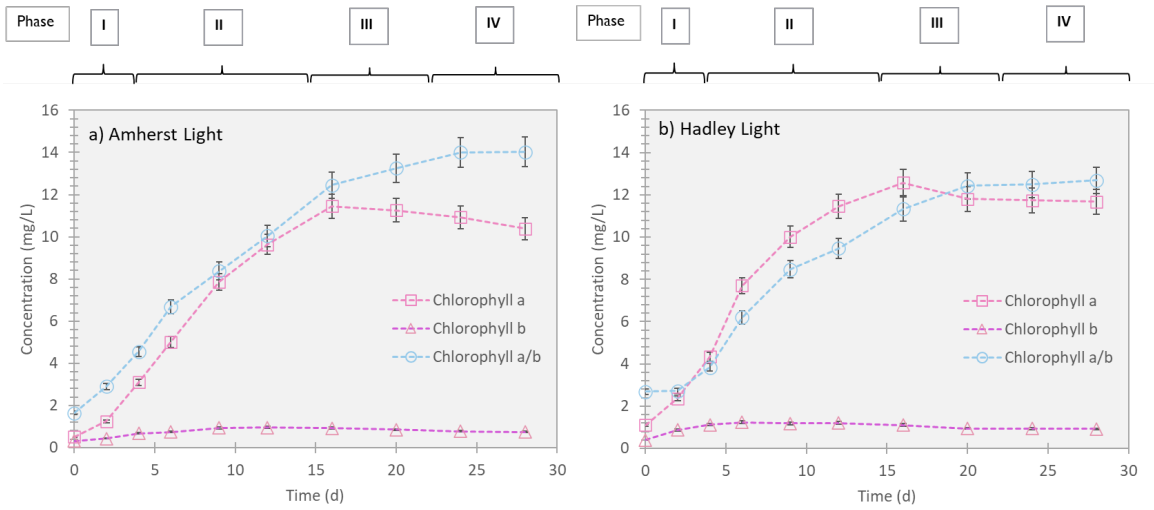

Figure 4.4: Chlorophyll Content During the Transformation of Activated Sludge During Photogranulation in a Hydrostatic Environment, for Two Sludge Sources Amherst and Hadley. Phases are labeled above as, Phase I: sludge compaction, Phase II: phototrophic bloom, Phase III: main granulation, and Phase IV: granule maturation. Concentration of *Chlorophyll a*, *b* and *a/b* ratio for Hadley sludge cultivation. Error bars represent standard deviation of three replicates for chlorophylls

Scanning electron microscopy (SEM) images are presented in Figure 4.5 of phase IV mature, hydrostatically formed photogranules. SEM of Amherst and Hadley photogranules are shown in upper and lower rows, respectively. (a) and (b) 21× and 17× magnification showing a cross-section of whole photogranules in Amherst and Hadley cultivation, respectively. Due to large size, both photogranules collapsed when sliced with a razor blade. (c) and (d) 524× and 416× magnification showing the inner portion of the biomass for Amherst and Hadley cultivation, respectively. The biomass is observed to be more floccular in nature, in comparison to the outer edge, and when sliced for imaging, portions of the inner biomass disassociated from the photogranule. (e) and (f) 340× and 385× showing the outer edge of the photogranules and magnification of EPS microstructures for Amherst and Hadley photogranules, respectively. An outer crust-like entanglement of cyanobacteria filaments is observed with multiple sheath and tube-like structures.

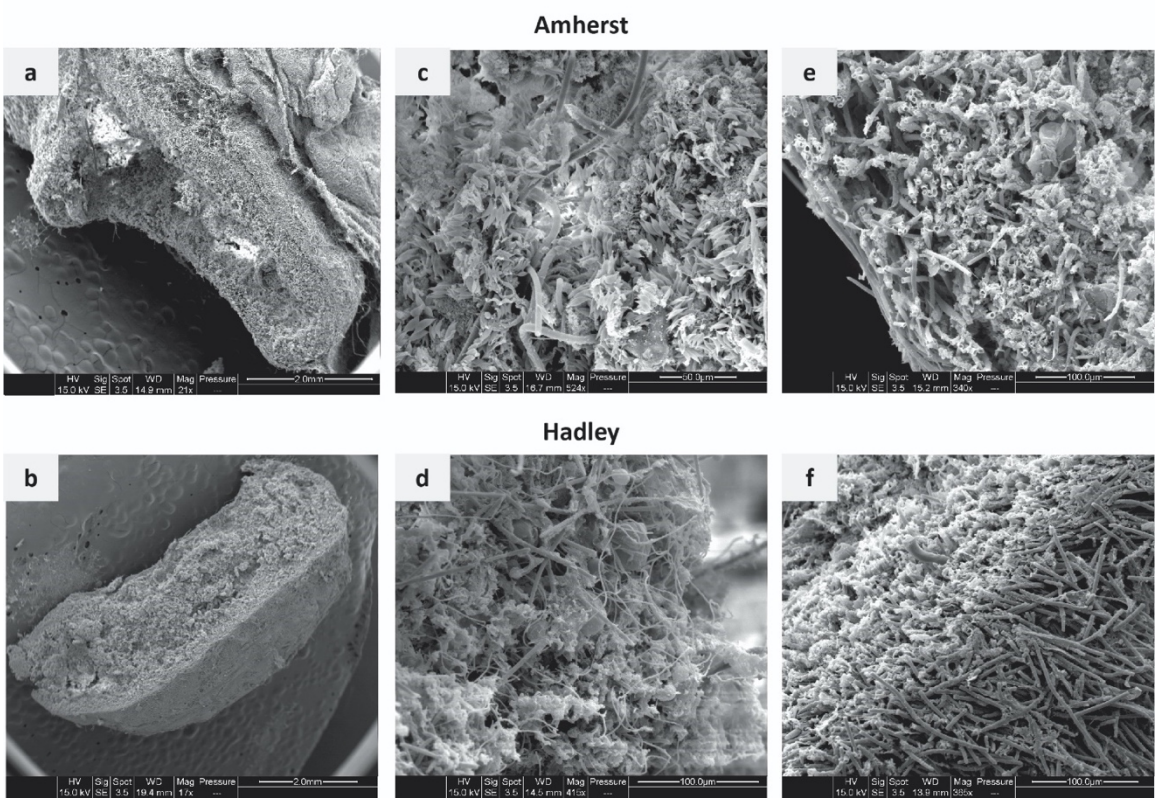

Figure 4.5: Scanning Electron Microscopy of Mature Hydrostatically Formed Photogranules. SEM of Amherst and Hadley photogranules are shown in upper and lower rows, respectively. (a) and (b) 21× and 17× magnification showing a cross-section of whole photogranules in Amherst and Hadley cultivation, respectively. Due to large size, both photogranules collapsed when sliced with a razor blade. (c) and (d) 524× and 416× magnification showing the inner portion of the biomass for Amherst and Hadley cultivation, respectively. (e) and (f) 340× and 385× showing the outer edge of the photogranules and magnification of tube microstructures Amherst and Hadley cultivation, respectively.

4.3.3 Dynamics of Dissolved Constituents in Bulk Liquid

Dissolved nitrogen species are quantified during hydrostatic photogranulation and concentrations are depicted in Figure 4.6. Dissolved total nitrogen (DTN), which is mainly composed of ammonium (NH_4^+-N) for day 0 Amherst and Hadley sludge sources, decreased significantly during the first 6 days of the cultivation. Previous studies have shown that the availability of dissolved inorganic nitrogen (DIN), particularly ammonium NH_4^+-N is correlated with successful granulation (Kuo-Dahab et al., 2018; Stauch-White

et al., 2017). Stauch-White et al. (2017) observed that NH_4^+-N remained high for the first two days of successful cultivations and was quickly depleted by day 4. In contrast to this study, they showed that NH_4^+-N depletion was followed by a corresponding increase in nitrate (NO_3^--N), with subsequent depletion by day 12, remaining low for the remainder of the cultivation. Here, we observe some decreases and increases in both NO_3^--N and nitrite (NO_2^--N), but both remain relatively low (<0.8 mg N/L) for both sludge sources during photogranulation. An increase in DON is observed in this study for both sludge sources that occurs from day 3 during the cultivation. DON trends shown here corroborate results reported by both Stauch-White et al. and Kuo-Dahab et al. (2018). Correlation analysis was performed and values between chlorophylls, N, and ions during hydrostatic cultivation of photogranules are presented in Figure 4.7 (Amherst sludge) and Figure 4.8 (Hadley sludge). Chlorophyll *a* and *a/b* ratio show moderate to strong correlations with DON (Amherst: r=0.90 and 0.95; Hadley: r= 0.78 and 0.91) and NH_4^+-N (Amherst: r=-0.83 and -0.80; Hadley: r=-0.88 and -0.83), suggesting the uptake of NH_4^+-N and subsequent release of DON is related to the enrichment of cyanobacteria and phototrophs. Generally, these progressive DON and DIN trends validate that cultivation was consistent with other studies and evaluation of the EPS components is translatable to other cultivation of OPGs.

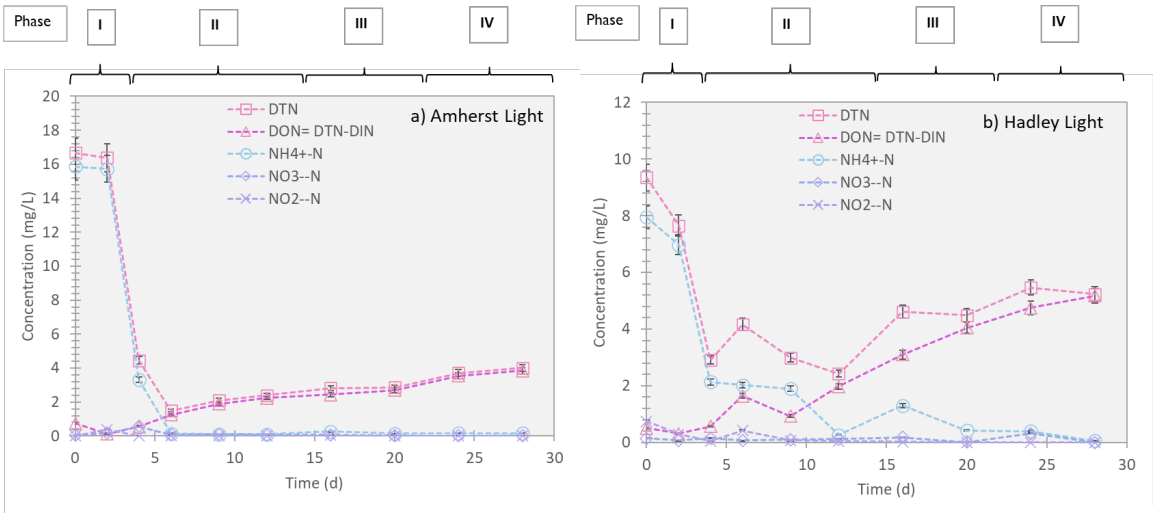

Figure 4.6: Nitrogen Species During the Transformation of Activated Sludge During Photogranulation in a Hydrostatic Environment, for Two Sludge Sources Amherst and Hadley. Phases are labeled above as, Phase I: sludge compaction, Phase II: phototrophic bloom, Phase II: main granulation, and Phase IV: granule maturation. Concentration of DTN, DON, NH_4^+-N, NO_3-N, and NO_2-N for both sludge sources during photogranulation. Error bars represent standard deviation of three replicates for nitrogen

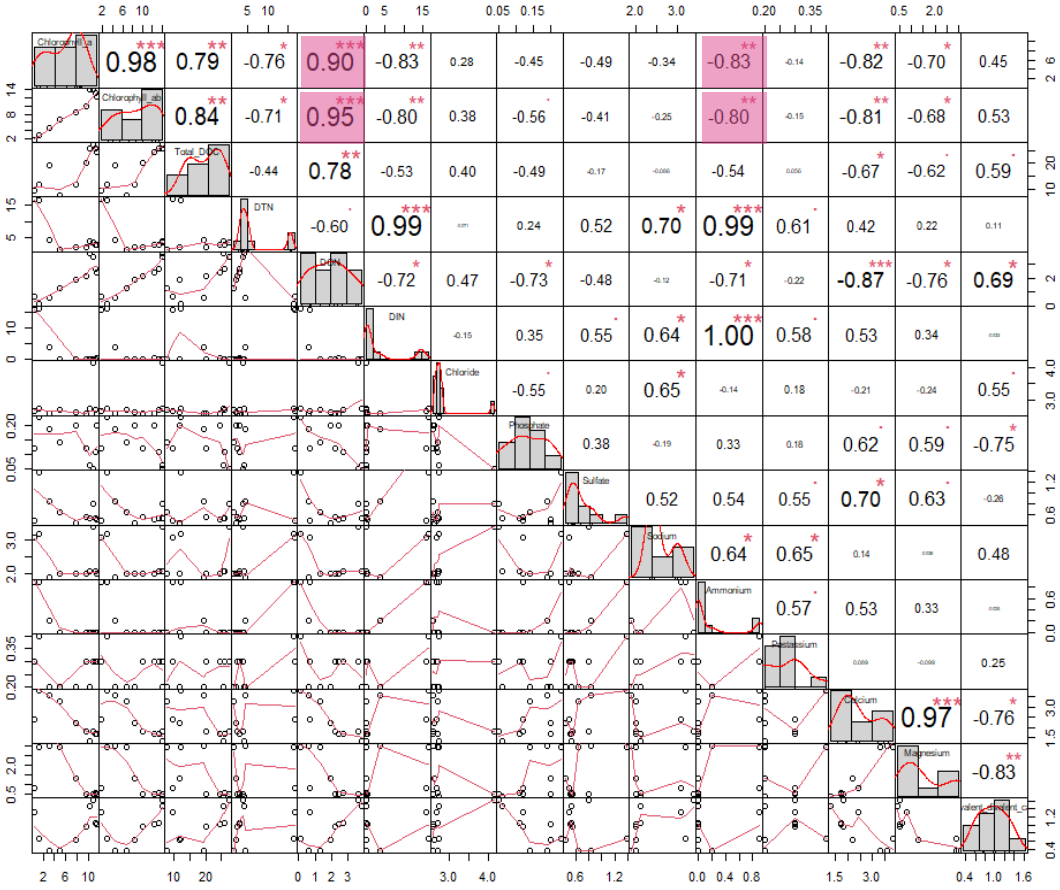

Figure 4.7: Correlation of chlorophylls, N-species, and ions for Amherst sludge. The distribution of each variable (chlorophyll a, chlorophyll a/b, DOC, DTN, DON, DIN, Cl^-, PO_4^{3-}, SO_4^{2-}, Na^+, NH_4^+-N, K^+, Ca^{2+}, Mg^{2+}, monovalent:diavalent cation ratio) for Amherst sludge is shown on the diagonal. On the bottom of the diagonal: The bivariate scatter plots with a fitted line are displayed. On the top of the diagonal: the value of the correlation plus the significance level as stars. Each significance level is associated to a symbol: p-values (0.001, 0.01, 0.05, 0.1, 1) <=> symbols ("*", "**", "*", ".", " "). Highlighted pink boxes are notable correlations.**

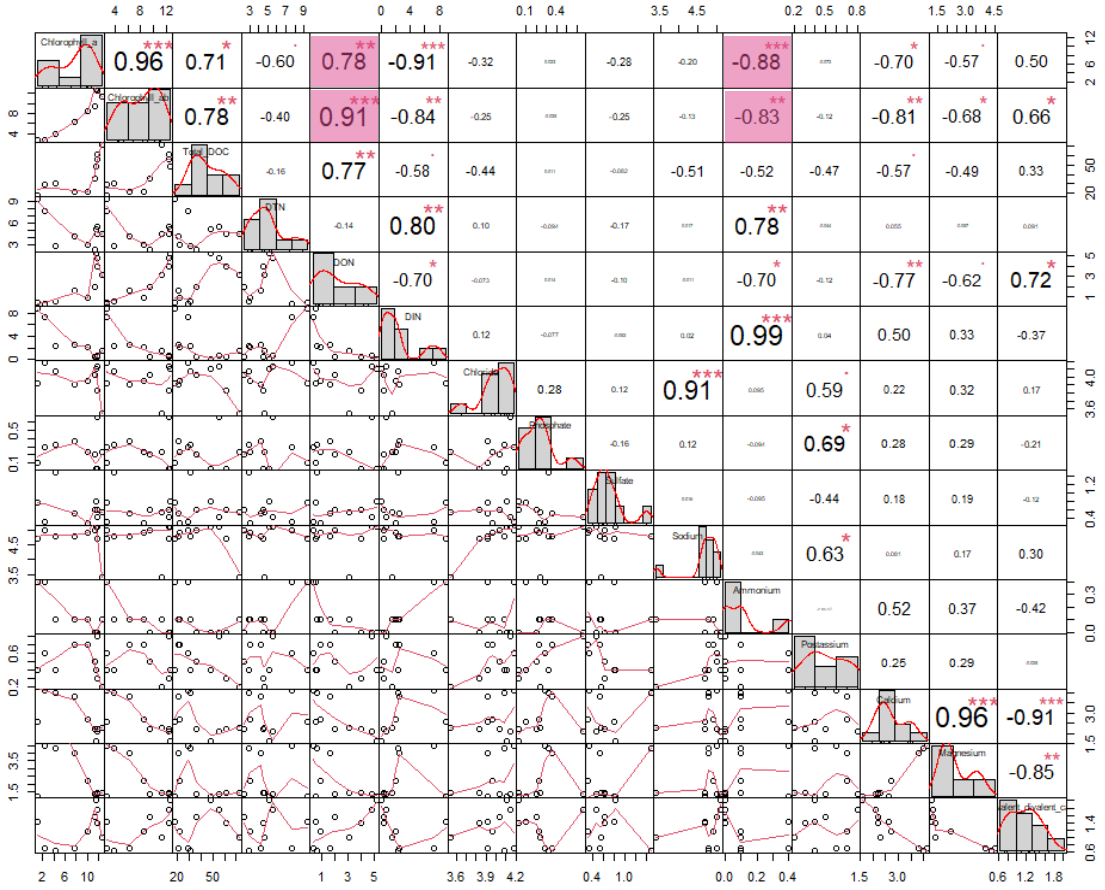

Figure 4.8: Correlation of chlorophylls, N-species, and ions for Hadley sludge. The distribution of each variable (chlorophyll a, chlorophyll a/b, DOC, DTN, DON, DIN, Cl^-, PO_4^{3-}, SO_4^{2-}, Na^+, NH_4^+-N, K^+, Ca^{2+}, Mg^{2+}, monovalent:diavalent cation ratio) for Hadley sludge is shown on the diagonal. On the bottom of the diagonal: The bivariate scatter plots with a fitted line are displayed. On the top of the diagonal: the value of the correlation plus the significance level as stars. Each significance level is associated to a symbol: p-values (0.001, 0.01, 0.05, 0.1, 1) <=> symbols ("*", "**", "*", ".", " "). Highlighted pink boxes are notable correlations.**

Divalent and monovalent anion, phosphate (PO_4^{3-}), sulfate (SO_4^{2-}) and cation, sodium (Na^+), potassium (K^+), calcium (Ca^{2+}), and magnesium (Mg^{2+}), concentrations in the bulk liquid are presented in Figure 4.9. during the cultivation for both sludge sources, Amherst and Hadley. Amherst and Hadley both show similar results for the duration of the cultivation. PO_4^{3-}, SO_4^{2-}, and K^+ all show similar trends with small releases and uptakes over the entire 28-day period between the two sludge sources. Calcium (Ca^{2+})

and Magnesium (Mg^{2+}) also show similar trends for both sludge sources, with large release during the first three days, followed by an uptake through day 12, then relatively unchanged until day 28 (Figure 4.10). Ca^{2+} shows a moderate to strong correlation (Amherst: r=-0.87; Hadley: r=-0.77) with DON suggesting that the availability of Ca^{2+} in the bulk liquid may be from the decay of organic matter from the activated sludge biomass (Figure 4.10). Additionally, Mg^{2+} only shows a moderate correlation with DON for Amherst (r=-0.76) and Hadley (r=-0.62) sludges (Figure 4.10). Ca^{2+} and Mg^{2+} also show significantly moderate to strong negative correlation with chlorophyll *a/b* for Amherst (Ca^{2+}: r=-0.81 and Mg^{2+}: r=-0.68) and Hadley (Ca^{2+}: r=-0.81 and Mg^{2+}: r=-0.68), suggesting that the release and uptake of these divalent cations from the bulk liquid is related to the enrichment of cyanobacteria.

The divalent cation bridging theory has been supported by findings from several studies that divalent, specially Ca^{2+} and Mg^{2+}, helps biofilm formation. Higgins and Novak (1997a) reported that when the sum of monovalent cation concentration (Na^{+}, NH_4^{+}-N, and K^{+}) divided by the sum of the divalent cations (Ca^{2+} and Mg^{2+}) was greater than 2, then there is a loss of biomass aggregation due to loss of biofilm EPS stability. The monovalent to divalent cation ratio is also depicted in Figure 4.9**.** Results here show ratio of monovalent to divalent cations is less than 2 during photogranulation and suggests that biofilm formation is promoted with no deterioration to the biomass.

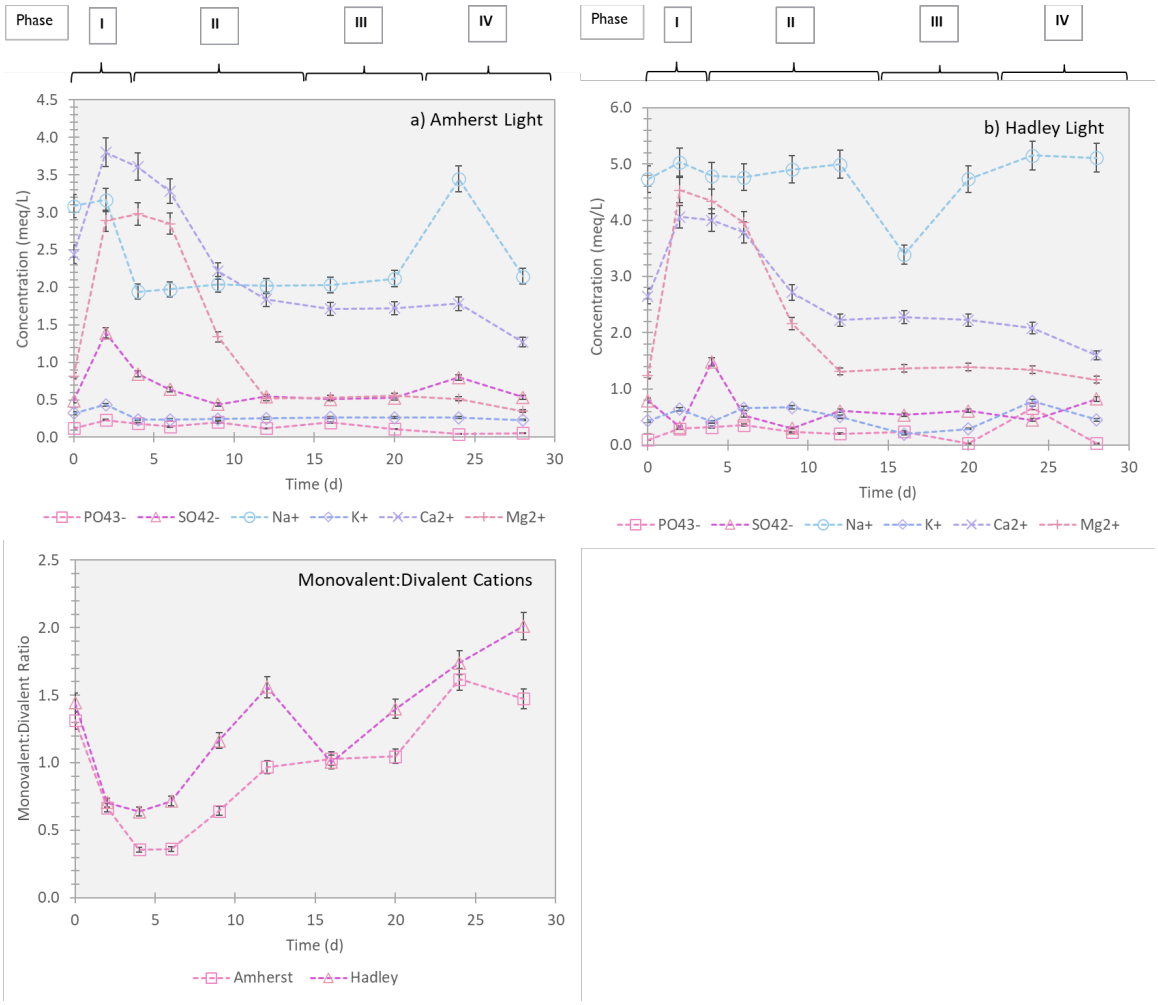

Figure 4.9: Anion and Cation Concentrations, and Monovalent to Divalent Cation Ratio During the Transformation of Activated Sludge in a Hydrostatic Environment, for Two Sludge Sources Amherst and Hadley. Phases are labeled above as, Phase I: sludge compaction, Phase II: phototrophic bloom, Phase II: main granulation, and Phase IV: granule maturation. Concentration of PO_4^{3-}, SO_4^{2-}, Na^+, K^+, Ca^{2+}, and Mg^{2+} for Hadley sludge cultivation. Error bars represent standard deviation of three replicates for anions and cations.

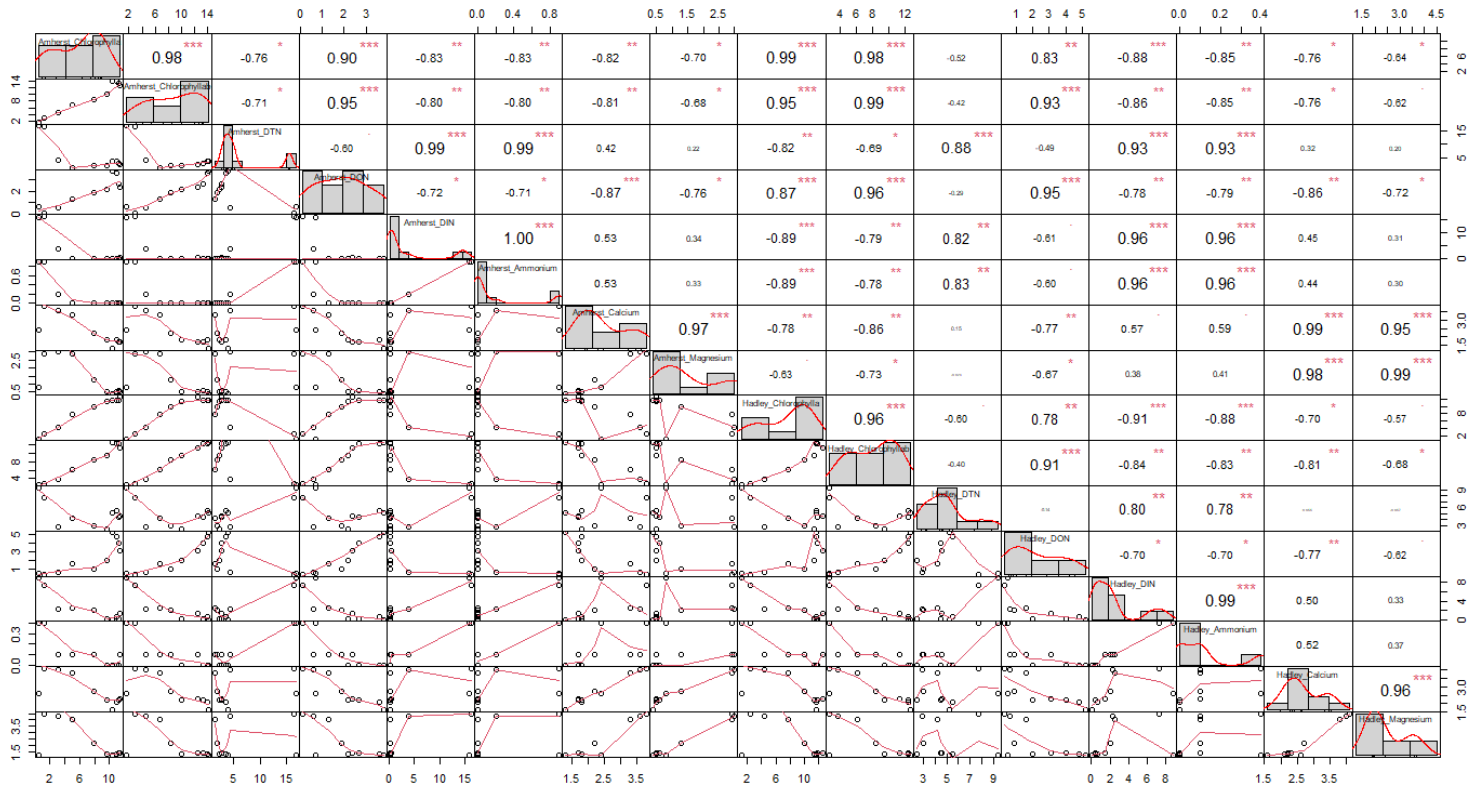

Figure 4.10: Correlation of chlorophylls, N-species, and ion for Amherst and Hadley sludge. The distribution of each variable, Amherst, and Hadley constituents (chlorophyll a, chlorophyll a/b ratio, DTN, DON, DIN, NH_4^+-N, Ca^{2+}, Mg^{2+}) is shown on the diagonal. On the bottom of the diagonal: The bivariate scatter plots with a fitted line are displayed. On the top of the diagonal: the value of the correlation plus the significance level as stars. Each significance level is associated to a symbol: p-values (0, 0.001, 0.01, 0.05, 0.1, 1) <=> symbols (“*”, “**”, “*”, “.”, " “). Highlighted values in pink are correlations between the same sludge sources.**

4.3.4 Fate and Dynamics of Different EPS Fractions and Different Sludge Sources During Hydrostatic Photogranulation

In general, EPS can be grouped into two main groups of EPS, soluble or biomass-bound (Nielsen & Jahn, 1999). Soluble EPS (soluble macromolecules, colloids, and slimes) are situated in the surrounding environment of the bacterial cells whereas bound EPS (sheaths, capsular polymers, condensed gels, etc.) can be tightly or loosely attached to the cell surface (Comte et al., 2006; Flemming et al., 2010; Nielsen & Jahn, 1999). Here, soluble and bound EPS are extracted using five different extraction methods: centrifugation for soluble EPS, and CER, base, sonication, and heat for bound EPS fractions. Figure 4.11 depicts (a) and (b) EPS proteins, (c) and (d) EPS polysaccharides, (e) and (f) EPS humic acids for Amherst and Hadley sludge sources, respectively. Each extraction method was evaluated by quantifying polysaccharides, proteins and humic acids using colorimetric assays. The results show similar trends, with respect to proteins, polysaccharides, and humic acids concentrations, across both sludge sources (Amherst and Hadley). However, the quantity of proteins, polysaccharides, and humic acids over the photogranulation period are strongly dependent on the extraction method and/or the trends varied between each EPS extraction method (i.e., centrifugation, base, CER, and sonication) during photogranulation (Figure 4.11) suggesting that each method is associated with a different EPS fraction. A comparative analysis was also performed to understand which extraction method correlated with key trends during granule development to validate the method as capturing relevant protein, polysaccharide, and humic acid concentrations to OPG development.

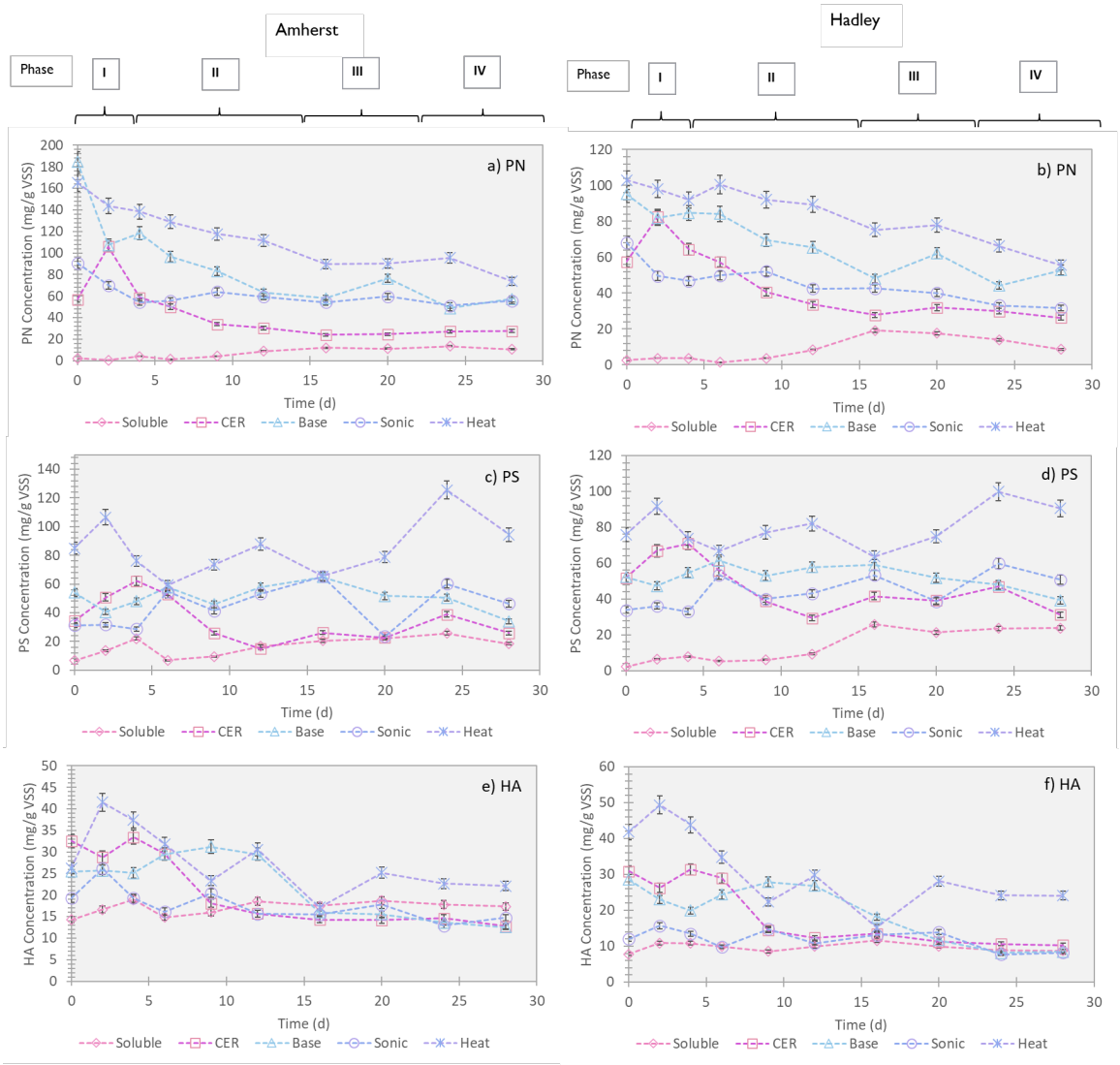

Figure 4.11: The Dynamics of Different Fractions of Soluble and Biomass-bound EPS During Hydrostatic Cultivation of Photogranules for Two Sludge Sources (Soluble Fraction in Supplementary Info). Biomass-bound components, (a) and (b) proteins (PN), (c) and (d) polysaccharides (PS), and (e) and (f) humic acids (HA) are depicted. Soluble EPS was collected using centrifugation. Biomass-bound EPS is extracted using four different procedures- CER, base, sonication, and heat. Phase of photogranulation is shown at the top of the figure and the duration of each phase is indicated by brackets. Concentration is shown in mg/L on the y-axis. For all figures, time is shown on the x-axis in days. Diamonds represent soluble EPS, squares represent CER-extractable EPS, triangles represent base-extractable fraction, circles represent sonic-extractable fraction, and stars represent heat-extractable fraction of EPS. Error bars represent the standard deviation of triplicate samples.

4.3.4.1 Similarities and Differences Between EPS Extraction Methods and Sludge Sources

Both sludge sources, Amherst and Hadley, show very similar results for each extraction method with respect to overall trend during photogranulation, but with different quantities for proteins, polysaccharides, and humic acids. Different quantities make sense, as initial TSS and VSS of Hadley sludge is much higher than Amherst sludge accounting for the higher EPS quantities observed for each EPS fraction. Concentrations normalized per g VSS for soluble and bound EPS proteins, polysaccharides and humic acids are presented in Figure 4.11.

General EPS protein trends are similar between both sludges, Figure 4.11a and Figure 4.11b, while there is a different magnitude for each method. A significantly strong positive correlation between the sludge sources is shown for each method for extracted proteins (soluble: r= 0.88; CER: r=0.95; base: r=0.91; sonication: r=0.82; heat: r=0.93) Figure 4.12. Soluble proteins increase 4.8x and 6.4x by day 16 for Amherst and Hadley sludge, respectively. Bound proteins show a decreasing trend over the course of photogranulation for all extraction methods, for both sludge sources. CER extracted protein shows an initial increase (Amherst: Δ= 49 mg/g VSS; Hadley: Δ= 25 mg/g VSS) during the first 2 days of the cultivation, but a small change of (Amherst: Δ= 1 mg/g VSS; Hadley: Δ= 6 mg/g VSS) during phase I for Amherst and Hadley sludge, respectively. This is followed by a decrease for the remainder of the cultivation with a net decrease of 29 mg/g VSS and 31 g/g VSS for Amherst and Hadley sludge, respectively. Base extractable proteins show an overall decrease of 127 mg/g VSS and 42 mg/g VSS for Amherst and Hadley sludge, respectively. Sonication extractable protein shows a decrease during phase I, then remaining relatively constant for Amherst sludge. Hadley sludge also shows a decrease during phase I and continues to decrease through day 28

or phase IV. Both sludge sources show a net decrease (Amherst: ∆= 35 mg/g VSS; Hadley: ∆= 36 mg/g VSS) over the course of photogranulation. Heat extraction also shows an overall decrease for both sludge sources (Amherst: ∆= 92 mg/g VSS; Hadley: ∆= 47 mg/g VSS). Heat extracts show the highest extracted concentrations followed by base, then sonication and CER which vacillate during the first 6 days of the cultivation but remain in that order until day 28.

Bound proteins also show significant moderate to strong positive correlation with soluble proteins for CER (Amherst: r=-0.79; Hadley: r=-0.70), base (Amherst: r=-0.67; Hadley: r=-0.-0.76), and heat (Amherst: r=-0.82; Hadley: r=-0.66) extracts, for both sludge sources Figure 4.12. For both sludge sources, no correlation is shown between soluble proteins and sonication extractable proteins. This suggests that while a portion of CER, base and heat extractable proteins are solubilized into the bulk liquid, sonication proteins are not and most likely assimilated by microorganisms as substrate or into the biofilm matrix.

Bound proteins extracted with different methods show strong positive correlation between most methods (Figure 4.12). Amherst shows significant moderate to strong relationships for all methods except CER vs. base (r=0.56) and CER vs. Sonication (0.40), while Hadley sludge shows significant moderate to strong relationships for all methods (Figure 4.12). This would suggest that protein composition is the least biased by the approach selection. Soluble and bound base and sonication extractable proteins are also consistent with trends observed by Kuo-Dahab et al. (2018).

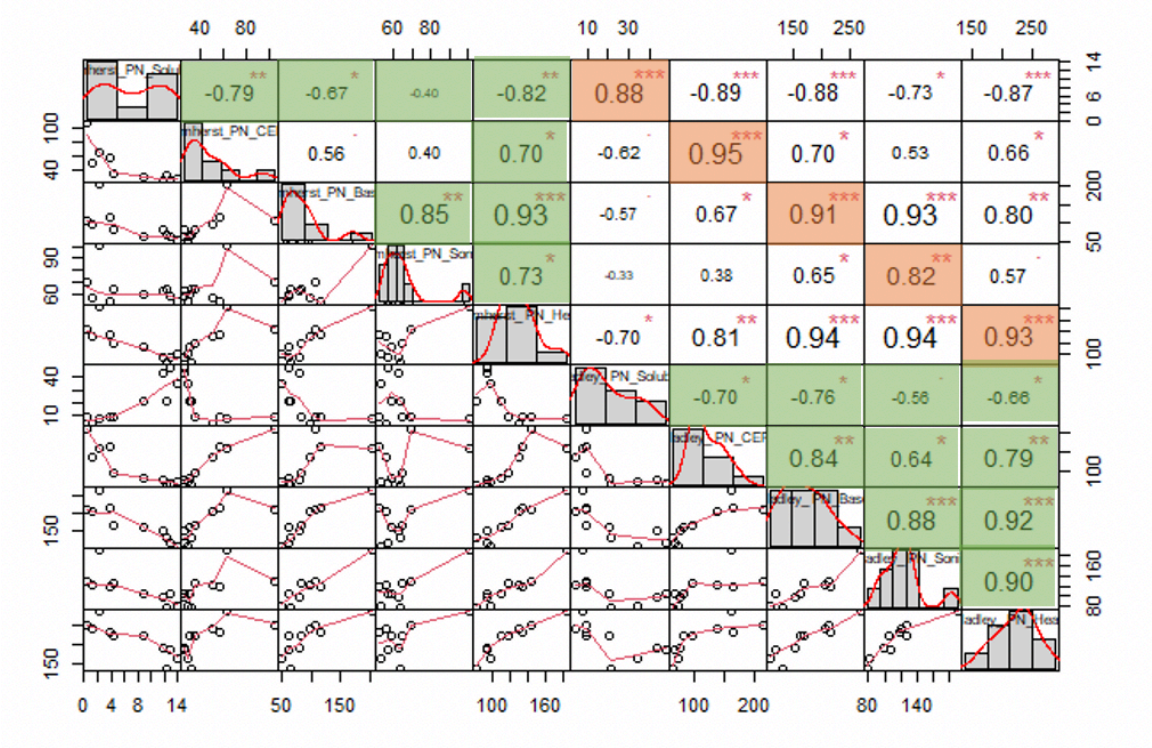

Figure 4.12: Correlation of EPS proteins between Amherst and Hadley sludge. The distribution of each variable, Amherst, and Hadley EPS proteins for each extraction method (soluble, CER, base, sonication, and heat), is shown on the diagonal. On the bottom of the diagonal: the bivariate scatter plots with a fitted line are displayed. On the top of the diagonal: the value of the correlation plus the significance level as stars. Each significance level is associated to a symbol: p-values (0.001, 0.01, 0.05, 0.1, 1) <=> symbols (“*”, “**”, “*”, “.”, " “). Highlighted values in orange are correlations between the same methods, but different sludge sources. Highlighted values in green are correlations between different methods but same sludge sources.**

Similar trends are observed across sludge (Figure 4.11c and Figure 4.11d) for extracted polysaccharides (soluble and bound), but polysaccharide concentration and trends vary by methods. Like proteins, a significantly strong positive correlation between the sludge sources is shown for each method for extracted polysaccharides (soluble: r= 0.84; CER: r=0.90; base: r=0.78; sonication: r=0.91; heat: r=0.95), Figure 4.13.

During phase I (Figure 4.11), soluble EPS polysaccharides increased by 15 mg/g VSS and 6 mg/g VSS for Amherst and Hadley sludges, respectively. At the start of phase II, both trends decreased slightly followed by further increase through the end of the cultivation by an overall net increase of 12 mg/g VSS and 22 mg/g VSS for Amherst

and Hadley sludges. CER extracted polysaccharides also show an increase during phase I by 28 mg/g VSS and 19 mg/g VSS, respectively for Amherst and Hadley sludges. During phase II there is a net decrease of 19 mg/g VSS and 22 mg/g VSS. CER shows slight changes through phase III and IV with a net increase of 11 mg/g VSS and 2 mg/g VSS by day 28 of the cultivation, for Amherst and Hadley sludges, respectively. Base extractable polysaccharides show some slight decreases and increases throughout the cultivation but ends with an overall net decrease of only 20 mg/g VSS and 13 mg/g VSS for Amherst and Hadley sludges, respectively at the end of phase IV. Sonication extracted polysaccharides follow similar trend to base extracted polysaccharides, but at lower concentrations for both sludge sources. Heat extraction shows an initial increase during phase I but very low overall net change (Amherst: Δ= 9 mg/g VSS; Hadley: Δ= 2 mg/g VSS), followed by a net increase during phase II (Amherst: Δ= 12 mg/g VSS; Hadley: Δ= 8 mg/g VSS), and overall net increase through phase III and IV (Amherst: Δ= 7 mg/g VSS; Hadley: Δ= 8 mg/g VSS).

Bound polysaccharides show no significant correlations between different extraction methods and soluble polysaccharides for both sludge sources, except Hadley sonication extractable polysaccharides (r=0.61), Figure 4.13. This suggests that polysaccharide-based EPS is not solubilized into the bulk liquid and any polysaccharides that are produced remain in the EPS matrix or are assimilated as substrate by microorganisms.

In contrast to proteins, bound polysaccharides extracted with different methods show weak correlation between each method (Figure 4.13), except for Hadley sludge, which shows a moderate negative correlation between base vs. heat (-0.66), but no other correlations. This would suggest that polysaccharide composition is probably the most biased by the approach selection and this is particularly important since cyanobacterial EPS is more polysaccharide based (Kuo-Dahab et al., 2018). This

suggests that different EPS extraction methods are necessary in order to characterize and define EPS during photogranulation.

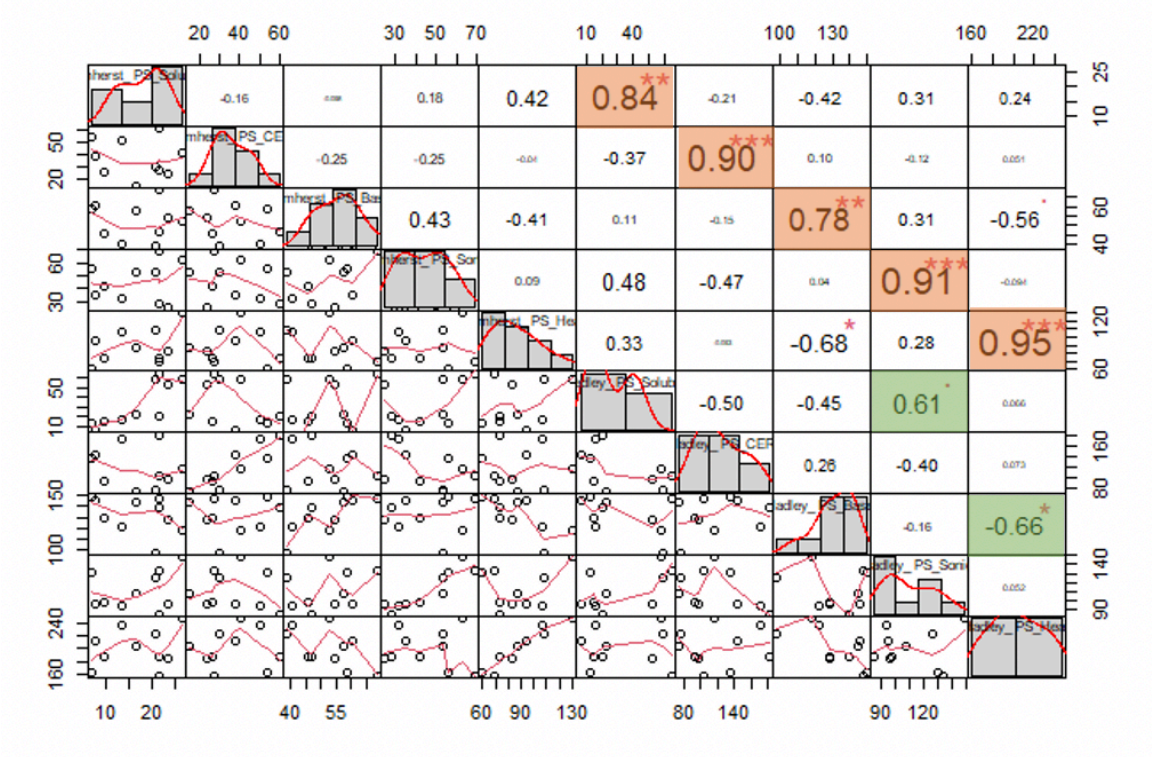

Figure 4.13: Correlation of EPS polysaccharides between Amherst and Hadley sludge. The distribution of each variable, Amherst, and Hadley EPS polysaccharides for each extraction method (soluble, CER, base, sonication, and heat), is shown on the diagonal. On the bottom of the diagonal: the bivariate scatter plots with a fitted line are displayed. On the top of the diagonal: the value of the correlation plus the significance level as stars. Each significance level is associated to a symbol: p-values (0.001, 0.01, 0.05, 0.1, 1) <=> symbols (“*”, “**”, “*”, “.”, " “). Highlighted values in orange are correlations between the same methods, but different sludge sources. Highlighted values in green are correlations between different methods but same sludge sources.**

Bound humic acids, show decreasing trends over the course of photogranulation for all methods, and both sludge sources. CER extracted humic acids show a large decrease through the midpoint of phase II (Amherst: Δ= 14 mg/g VSS; Hadley: Δ= 16 mg/g VSS), then remains relatively constant through the end of phase IV (Amherst: Δ= 5 mg/g VSS; Hadley: Δ= 4 mg/g VSS). Base extracted humic acids show small initial increases and decreases, but an overall decrease by phase II and IV (Amherst: Δ= 13

mg/g VSS; Hadley: ∆= 20 mg/g VSS). Sonication extractable humic acids also show small increases during phase I, but also decreases through phase IV for both sludge sources (Amherst: ∆= 5 mg/g VSS; Hadley: ∆= 4 mg/g VSS). Heat extracted humic acids show changes with the greatest magnitude with an increase during the first two days (Amherst: ∆= 15 mg/g VSS; Hadley: ∆= 8 mg/g VSS), followed by an overall decrease through phase IV (Amherst: ∆= 4 mg/g VSS; Hadley: ∆= 18 mg/g VSS).

In contrast to bound proteins, humic acids only show significant negative correlation with soluble proteins for CER (r=-0.66) and base (r=-0.79) extractable humic acids, and for Amherst sludge specifically, Figure 4.14. For all other extraction methods for Amherst (sonication and heat), and all methods for Hadley sludge, no correlation is shown between extraction methods and soluble humic acids. While a portion of CER and base extractable humic acids in Amherst sludge may have been solubilized into the bulk liquid, there seems to be an initial loss in humic acids and no corresponding increase in the bulk liquid concentration, which may suggest that humic acids are substrate when reduced C is limited in the initial phases of granulation.

Bound humic acids extracted with different methods show weak to moderate positive correlation between each method (Figure 4.14). Amherst shows significant weak to moderate correlation for CER vs base (r=0.56), CER vs heat (r=0.68), and sonication vs heat (0.59). Hadley shows significant moderate to strong correlation for CER vs base (r=0.62 and CER vs heat (r=0.85). This would suggest that humic acid composition is also less biased by the approach selection in comparison to the methods for polysaccharides, but more biased in comparison to proteins.

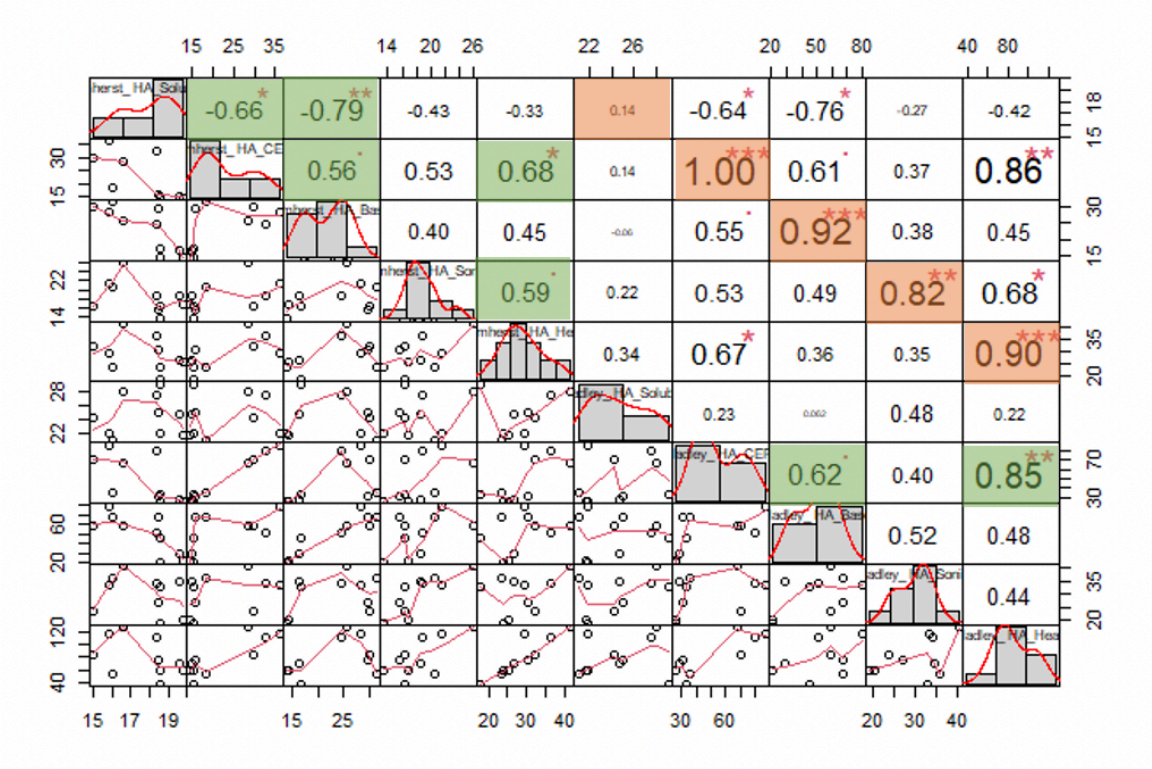

Figure 4.14: Correlation of EPS humic acids between Amherst and Hadley. The distribution of each variable, Amherst, and Hadley EPS humic acids for each extraction method (soluble, CER, base, sonication, and heat), is shown on the diagonal. On the bottom of the diagonal: the bivariate scatter plots with a fitted line are displayed. On the top of the diagonal: the value of the correlation plus the significance level as stars. Each significance level is associated to a symbol: p-values (0.001, 0.01, 0.05, 0.1, 1) <=> symbols (“*”, “**”, “*”, “.”, " “). Highlighted values in orange are correlations between the same methods, but different sludge sources. Highlighted values in green are correlations between different methods but same sludge sources.**

The results presented above show that different EPS extraction methods are required to capture different fractions of EPS with respect to protein, polysaccharide, and humic acid composition. EPS extraction methods for polysaccharides were found to be the most biased, followed by humic acids, then proteins. This suggests that different methods target different EPS fractions (more associated with polysaccharides), but may overlap between the methods (proteins and humic acids). Results also show that EPS extraction methods and trends are significantly similar, statistically, between two sludge sources (Amherst and Hadley).

4.3.4.2 Comparative Analysis of EPS Proteins, Polysaccharides, and Humic Acids with Key Trends During Granule Development

A comparative correlation analysis was performed in order to understand which EPS extraction methods correlate with key trends observed in granule development during hydrostatic photogranulation. The correlation analysis was performed between soluble and bound EPS proteins, polysaccharides and humic acids (for each extraction method) and dissolved constituents (chlorophyll, C, N-species, anions, and cations). The Pearson correlation, data distribution and corresponding p-values are presented in Figure 4.15 to Figure 4.20. Notable correlations between EPS extracts and constituents are highlighted- chlorophylls (pink), N-species (blue), anions and cations (purple).

4.3.4.3 EPS Proteins

All EPS extraction methods showed statistically significant moderate to strong correlations (Amherst: r= 0.56 - 0.94; Hadley: r= 0.78 to 0.95) between proteins and chlorophyll *a* and *a/b* ratio, for both sludge sources. Soluble proteins show a strong positive correlation while bound proteins all show negative correlations (Figure 4.15 and Figure 4.16).

Soluble proteins show a strong positive correlation with DON (Amherst: r=0.90; Hadley: r=0.72) while bound proteins show moderate to strong negative correlations (Amherst- CER: r= -0.82; base: r=-0.69; heat: r=-0.84, Hadley- CER: r =-0.81; base: r=-0.83; sonication: r=-0.78; heat: r=-0.92) except Amherst sonication extractable proteins (r=-0.38), for both sludge sources (Figure 4.15 and Figure 4.16).

All EPS extraction methods also have moderate to strong correlations (Amherst: r= 0.63 - 0.86; Hadley: r= 0.50 to 0.83) between proteins and NH_4^+-N. In contrast to

chlorophylls, Soluble proteins show a negative correlation while bound proteins show a positive correlation (Figure 4.15 and Figure 4.16).

Ca^{2+} and Mg^{2+} show negative correlation with soluble proteins (Amherst- Ca^{2+}: r=-0.85; Mg^{2+}: r=-0.79; Hadley- Ca^{2+}: r=-0.62; Mg^{2+}: r=-0.59). CER extractable proteins show a strong positive correlation with Ca^{2+} and Mg^{2+} (Amherst- Ca^{2+}: r=0.83; Mg^{2+}: r=0.72; Hadley- Ca^{2+}: r=0.87; Mg^{2+}: r=0.79) which corresponds to results in literature as CER targets EPS fractions that are bound with divalent cations (Park & Novak, 2007; Park et al., 2008a, 2008b). Heat extractable proteins also show a moderate positive correlation with Ca^{2+} but a weak correlation with Mg^{2+} (Amherst- Ca^{2+}: r=0.63; Mg^{2+}: r=0.46; Hadley- Ca^{2+}: r=0.67; Mg^{2+}: r=0.47).

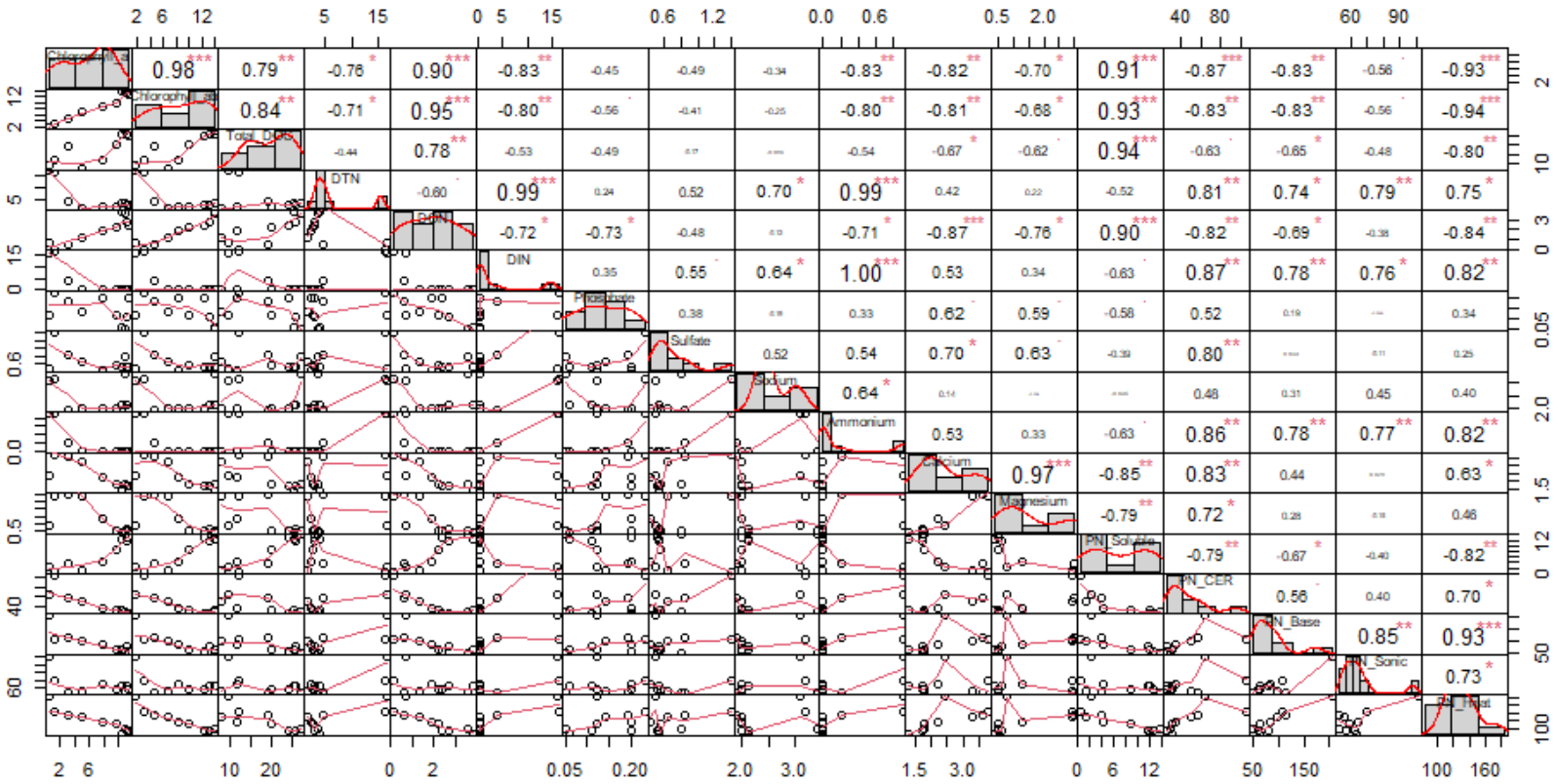

Figure 4.15: Correlation of chlorophylls, N-species, ions, and EPS proteins for Amherst sludge. The distribution of each variable for Amherst sludge (chlorophyll a, chlorophyll a/b ratio, total DOC, DTN, DON, DIN, PO_4^{3-}, SO_4^{2-}, Na^+, NH_4^+-N, Ca^{2+}, Mg^{2+}, soluble PN, CER PN, base PN, sonication PN, heat PN), is shown on the diagonal. On the bottom of the diagonal: the bivariate scatter plots with a fitted line are displayed. On the top of the diagonal: the value of the correlation plus the significance level as stars. Each significance level is associated to a symbol: p-values (0.001, 0.01, 0.05, 0.1, 1) <=> symbols ("*", "**", "*", ".", " ").**

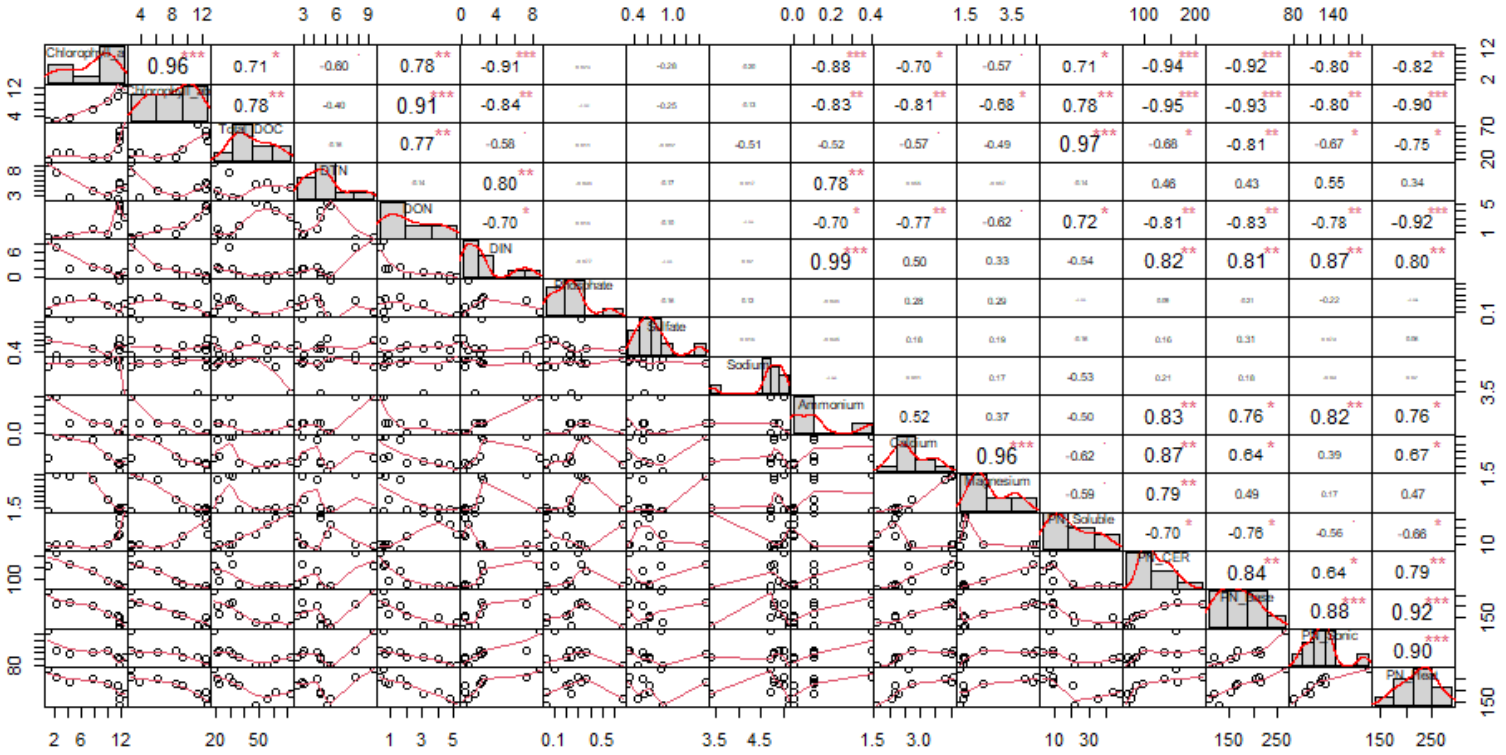

Figure 4.16: Correlation of chlorophylls, N-species, ions, and EPS proteins for Hadley sludge. The distribution of each variable for Hadley sludge (chlorophyll a, chlorophyll a/b ratio, total DOC, DTN, DON, DIN, PO_4^{3-}, SO_4^{2-}, Na^+, NH_4^+-N, Ca^{2+}, Mg^{2+}, soluble PN, CER PN, base PN, sonication PN, heat PN), is shown on the diagonal. On the bottom of the diagonal: the bivariate scatter plots with a fitted line are displayed. On the top of the diagonal: the value of the correlation plus the significance level as stars. Each significance level is associated to a symbol: p-values (0.001, 0.01, 0.05, 0.1, 1) <=> symbols ("*", "**", "*", ".", " ").**

4.3.4.4 EPS Polysaccharides

Soluble polysaccharides show a significant moderate positive correlation with chlorophyll *a* (Amherst: r=0.64; Hadley: r=0.75) and strong positive correlation with chlorophyll *a/b* ratio (Amherst: r=0.70; Hadley: r=0.86). Only CER extractable polysaccharides show a negative correlation with chlorophyll *a* (Amherst: r=-0.58; Hadley: r=-0.84) and chlorophyll *a/b* ratio (Amherst: r=0.68; Hadley: r=-0.82) (Figure 4.17 and Figure 4.18).

Soluble polysaccharides show some correlation with DON, with Hadley sludge having the strongest positive correlation (r=0.90) and Amherst having a moderate positive correlation (r=0.61). Bound CER polysaccharides show moderate negative correlations with DON (Amherst: r=-0.58; Hadley: r=-0.64), while sonication shows moderate positive correlation with DON (Amherst: r=0.55; Hadley: r=0.68) for both sludge sources. Hadley sludge also shows a moderate negative (r=-0.57) between base extractable polysaccharides and DON (Figure 4.17 and Figure 4.18).

NH_4^+-N only shows moderate correlation with soluble polysaccharides (r=-0.60) and CER extractable polysaccharides (r=0.66) for Hadley sludge, otherwise very weak insignificant correlations are seen for both sludges (Figure 4.17 and Figure 4.18).

Ca^{2+} and Mg^{2+} in the bulk liquid show a moderate negative correlation with soluble polysaccharides (r=-0.66) but only for Hadley sludge. CER extractable polysaccharides show a strong correlation with Ca^{2+} and Mg^{2+} (Amherst- Ca^{2+}: r=0.84; Mg^{2+}: r=0.84; Hadley- Ca^{2+}: r=0.86; Mg^{2+}: r=0.78) which corresponds to results observed for CER extractable proteins (Figure 4.17 and Figure 4.18).

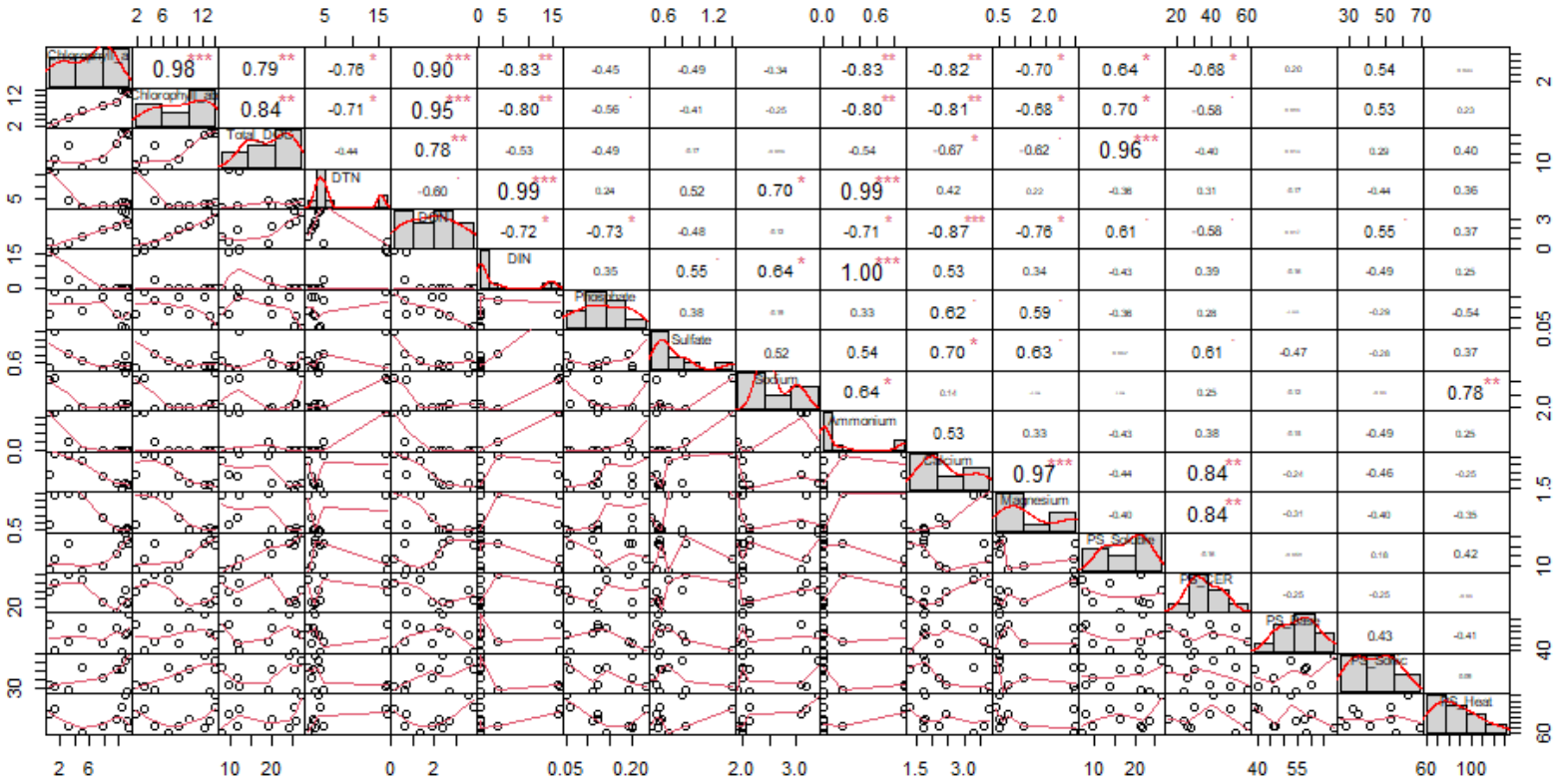

Figure 4.17: Correlation of chlorophylls, N-species, ions, and EPS polysaccharides for Amherst sludge. The distribution of each variable for Amherst sludge (chlorophyll a, chlorophyll a/b ratio, total DOC, DTN, DON, DIN, PO_4^{3-}, SO_4^{2-}, Na^+, NH_4^+-N, Ca^{2+}, Mg^{2+}, soluble PS, CER PS, base PS, sonication PS, heat PS), is shown on the diagonal. On the bottom of the diagonal: the bivariate scatter plots with a fitted line are displayed. On the top of the diagonal: the value of the correlation plus the significance level as stars. Each significance level is associated to a symbol: p-values (0.001, 0.01, 0.05, 0.1, 1) <=> symbols (“*”, “**”, “*”, “.”, " “).**

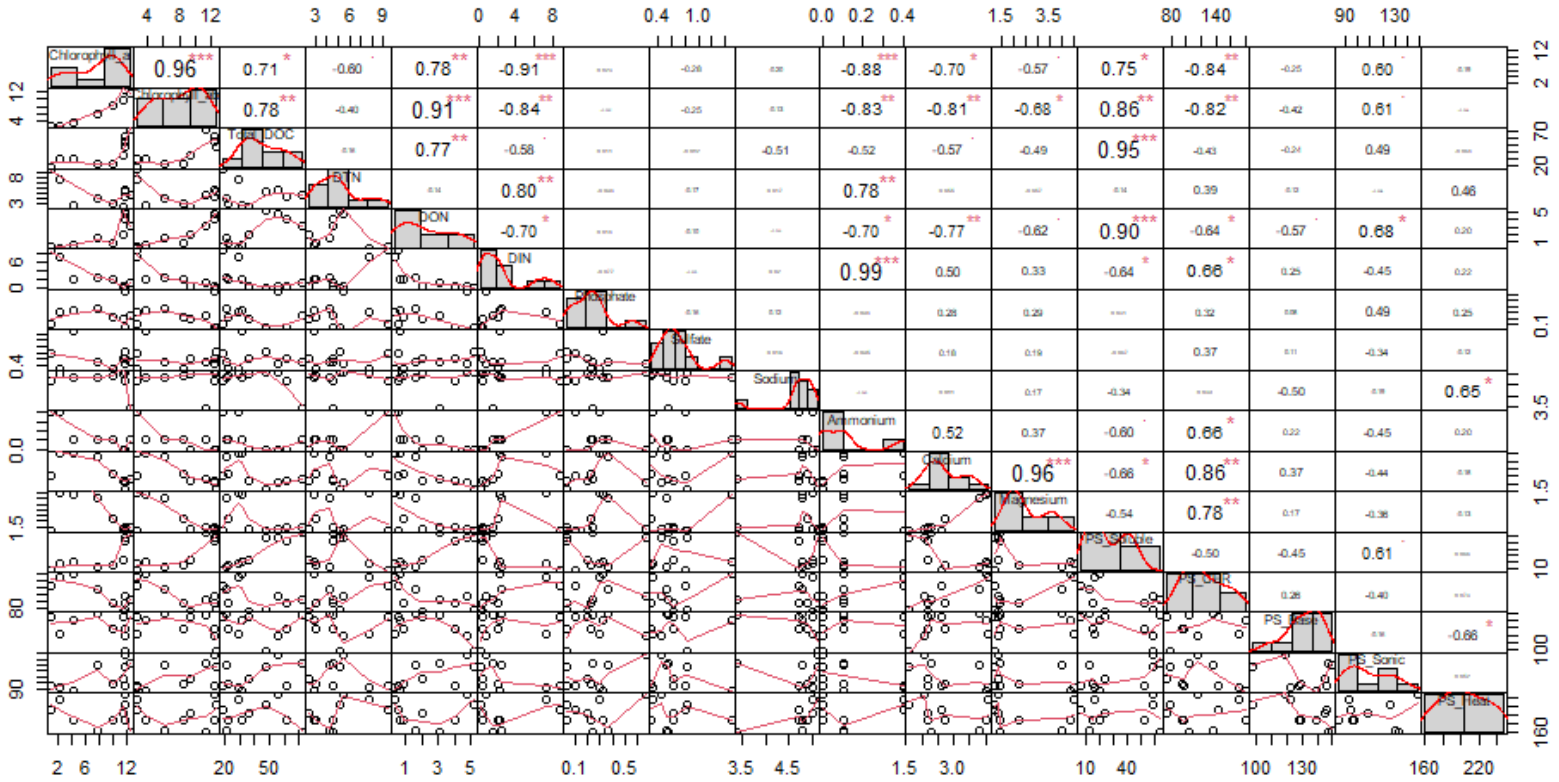

Figure 4.18: Correlation of chlorophylls, N-species, ions, and EPS polysaccharides for Hadley sludge. The distribution of each variable for Hadley sludge (chlorophyll a, chlorophyll a/b ratio, total DOC, DTN, DON, DIN, PO_4^{3-}, SO_4^{2-}, Na^+, NH_4^+-N, Ca^{2+}, Mg^{2+}, soluble PS, CER PS, base PS, sonication PS, heat PS), is shown on the diagonal. On the bottom of the diagonal: the bivariate scatter plots with a fitted line are displayed. On the top of the diagonal: the value of the correlation plus the significance level as stars. Each significance level is associated to a symbol: p-values (0.001, 0.01, 0.05, 0.1, 1) <=> symbols ("*", "**", "*", ".", " ").**

4.3.4.5 EPS Humic Acids

Amherst sludge, both soluble and bound EPS humic acids show strong correlations between humic acids and chlorophyll *a/b* ratio (soluble: r=0.73; CER: r= -0.93; base: r=-0.73; sonication: r=-0.72; heat: r=-0.72). While for Hadley sludge, only bound EPS humic acids show correlation with chlorophyll *a/b* ratio (CER: r=-0.94; base: r=-0.75; sonication: r=-0.55; heat: r=-0.89) (Figure 4.19 and Figure 4.20).

Only Amherst sludge soluble humic acids show a positive correlation with DON (r=0.66) while Hadley sludge shows no correlation. Bound proteins show moderate to strong negative correlations for both sludges and all extraction methods (Amherst- CER: r= -0.86; base: r=-0.70; sonication: r=-0.73; heat: r=-0.74, Hadley- CER: r =-0.78; base: r=-0.89; sonication: r=-0.69; heat: r=-0.69) (Figure 4.19 and Figure 4.20).

For Amherst sludge, CER (r=0.71), sonication (r=0.80), and heat (r=0.59) extractable humic acids show correlation with NH_4^+-N. For Hadley sludge, all methods, CER (r=0.74), base (r=0.62), sonication (r=0.60), and heat (r=0.74) show correlation with NH_4^+-N (Figure 4.19 and Figure 4.20).

For both sludge sources, CER (Amherst- Ca^{2+}: r=0.80; Mg^{2+}: r=0.70; Hadley- Ca^{2+}: r=0.77; Mg^{2+}: r=0.64). and heat (Amherst- Ca^{2+}: r=0.84; Mg^{2+}: r=0.79; Hadley- Ca^{2+}: r=0.71; Mg^{2+}: r=0.62). For Amherst sludge, sonication also shows a moderate correlation with only Ca^{2+} (r=0.57) (Figure 4.19 and Figure 4.20).

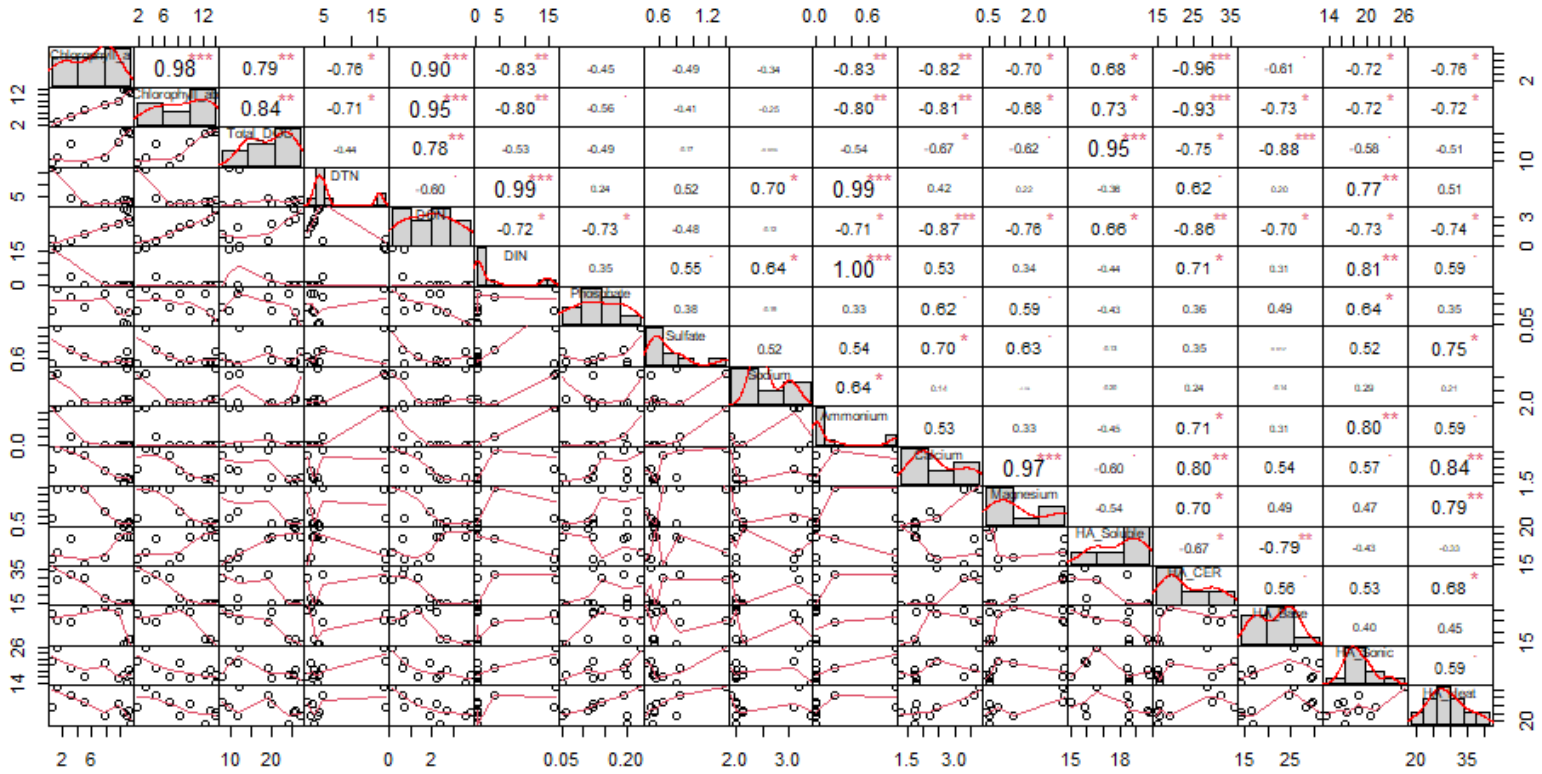

Figure 4.19: Correlation of chlorophylls, N-species, ions, and EPS humic acids for Amherst sludge. The distribution of each variable for Amherst sludge (chlorophyll a, chlorophyll a/b ratio, total DOC, DTN, DON, DIN, PO_4^{3-}, SO_4^{2-}, Na^+, NH_4^+-N, Ca^{2+}, Mg^{2+}, soluble HA, CER HA, base HA, sonication HA, heat HA), is shown on the diagonal. On the bottom of the diagonal: the bivariate scatter plots with a fitted line are displayed. On the top of the diagonal: the value of the correlation plus the significance level as stars. Each significance level is associated to a symbol: p-values (0.001, 0.01, 0.05, 0.1, 1) <=> symbols ("*", "**", "*", ".", " ").**

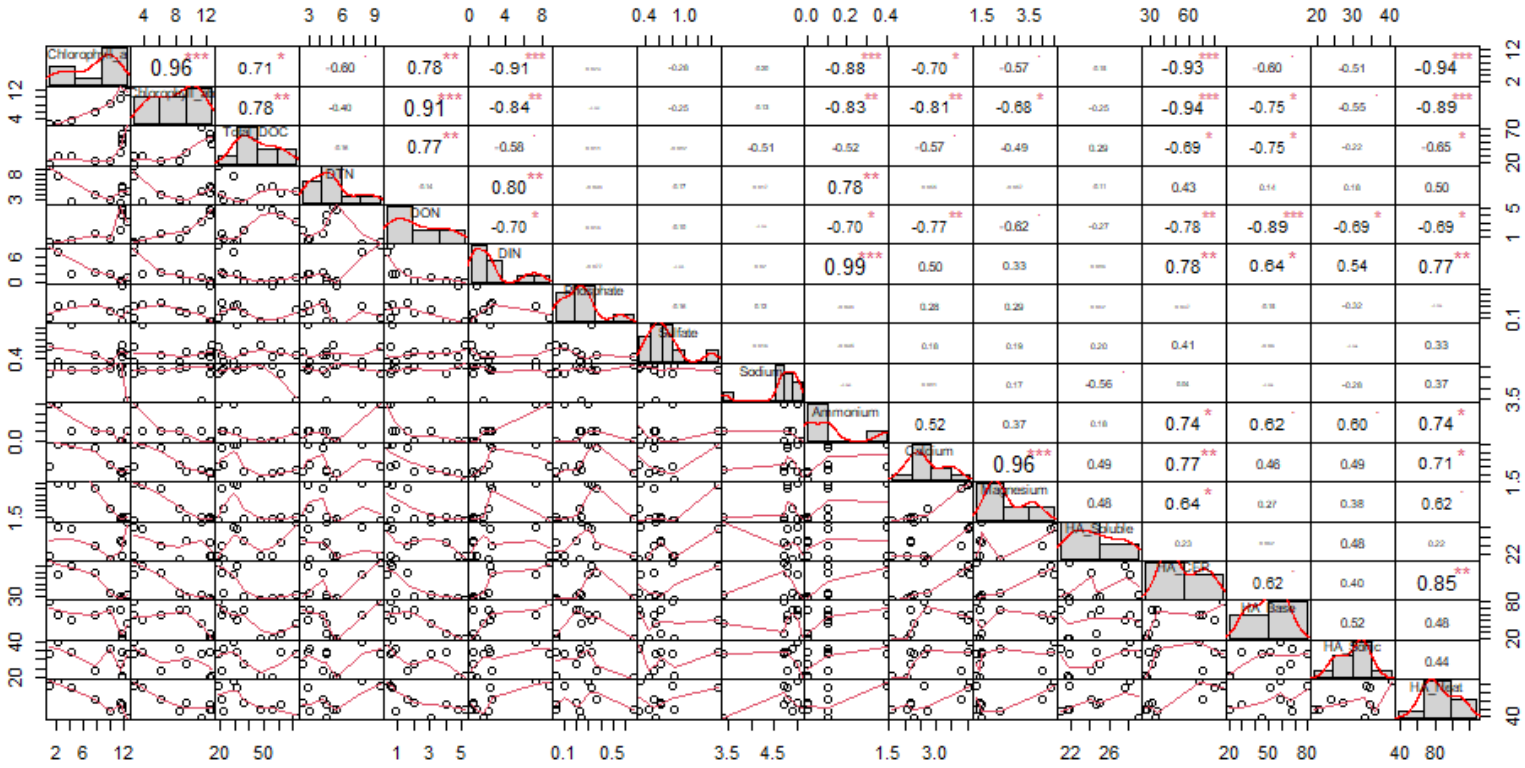

Figure 4.20: Correlation of chlorophylls, N-species, ions, and EPS proteins for Hadley sludge. The distribution of each variable for Hadley sludge (chlorophyll a, chlorophyll a/b ratio, total DOC, DTN, DON, DIN, PO_4^{3-}, SO_4^{2-}, Na^+, NH_4^+-N, Ca^{2+}, Mg^{2+}, soluble HA, CER HA, base HA, sonication HA, heat HA), is shown on the diagonal. On the bottom of the diagonal: the bivariate scatter plots with a fitted line are displayed. On the top of the diagonal: the value of the correlation plus the significance level as stars. Each significance level is associated to a symbol: p-values (0.001, 0.01, 0.05, 0.1, 1) <=> symbols ("*", "**", "*", ".", " ").**

All methods had some correlation with one or more constituents, chlorophylls, N-species, and select cations and anions, which have been previously established as strong indicators of successful granule formation (Kuo-Dahab et al., 2018; Milferstedt et al., 2017; Stauch-White et al., 2017). The results presented here show that different methods capture different fractions of EPS which align with the established key trends in photogranule development. Further, the comparative analysis results validate that EPS extraction methods capture relevant protein, polysaccharide and/or humic acid concentrations during photogranule development.

4.3.5 Changes in Organic Carbon (C) and Nitrogen (N) Among Different EPS Fractions During Photogranulation

To further characterize and analyze different EPS extraction methods, the content of organic C and N were determined in the soluble and bound EPS fractions for each extraction method. C and N in dissolved and bound fractions are defined as, dissolved organic carbon (DOC_{Total}), dissolved organic nitrogen (DON_{Total}), bound organic carbon (BOC_{Total}) and bound organic nitrogen (BON_{Total}) (Figure 4.21 and Figure 4.26).

4.3.5.1 Similarities and Differences Between EPS Extraction Methods Organic C and N Content and Sludge Sources

In accordance with above results for EPS proteins, polysaccharides and humic acids, significantly similar trends for each extraction method for organic C and N derived from proteins, polysaccharides and humic acids, were shown between the two sludges. Additionally, differences across the methods were observed with respect to organic C

and N content from proteins, polysaccharides and humic acids suggesting that EPS extraction methods target different fractions of the EPS matrix.

DOC_{Total} increases overall for both sludge sources with a net change of 10 mg C/L and 20 mg C/L, respectively, while BOC_{Total} decreases overall for all extraction methods during photogranulation Figure 4.20. DOC_{Total} and BOC_{Total} shows statistically strong positive correlation between the two sludge sources and all the EPS extraction methods (soluble: r=0.89; CER: r=0.96; base: r=0.87; sonication: r=0.83; heat: r=0.95), Figure 4.22. DOC and BOC proteins (soluble: r=0.88; CER: r=0.95; base: r=0.91; sonication: r=0.82; heat: r=0.93), polysaccharides(soluble: r=0.84; CER: r=0.90; base: r=0.78; sonication: r=0.91; heat: r=0.95), and humic acids (CER: r=1.00; base: r=0.92; sonication: r=0.82; heat: r=0.90) also show strong correlation between the two sludge sources, Amherst and Hadley, except Hadley DOC humic acids (r=0.12) (Figure 4.22 to Figure 4.25).

Different EPS extraction methods also capture different organic C content suggesting that the methods capture different fractions with respect to organic C content. For all extraction methods, BOC_{Total} decreases overall during photogranulation, but the composition of organic C from proteins, polysaccharides, and humic acids changes (Figure 4.21). The strongest and highest number of correlations are shown for DOC and BOC proteins between extraction methods (Amherst: n=8; Hadley: n=10), followed by DOC and BOC humic acid (Amherst: n= 5; Hadley: n=2) and last by DOC and BOC polysaccharides (Amherst: n=0; Hadley: n=1), which suggests that extraction methods for organic C and N derived from proteins show the least bias, followed by humic acids, then polysaccharides between methods. Correlations are presented in Figure 4.23, Figure 4.24, and Figure 4.25 for DOC and BOC proteins, polysaccharides, and humic acids, respectively. Values highlighted in pink represent correlations between methods for the sludge sources, blue highlight represents correlations that are different between

the methods for the two sludge sources, and purple highlight represents moderate to strong correlations between methods for the two sludge sources.

The composition of DOC_{Total} changes from mostly organic C derived from polysaccharides and humic acids to proteins in the bulk liquid for both sludge sources (Figure 4.21). The strongest correlations between soluble and bound organic C are CER (Amherst: r=-0.79; Hadley: r=-0.70), base (Amherst: r=-0.67; Hadley: r=-0.76) and heat (Amherst: r= -0.82; Hadley: r=-0.66) derived from proteins, suggesting that organic C in the bulk liquid is derived from bound proteins and available as substrate. Organic C derived from polysaccharides also shows an increase in the bulk liquid, however no or weak correlations are seen with all EPS extraction methods suggesting that this organic C is consumed or utilized in the biofilm versus dispersed into the bulk liquid.

Figure 4.21: Dynamics of C for Soluble and Biomass-bound Fractions During Hydrostatic Photogranulation for Two Sludge Sources- Amherst and Hadley. The panel on the left side show C concentrations in the Amherst sludge, while panel on the right side shows results for Hadley sludge. The figures are organized by EPS extraction method as follows: (a)-(b) soluble (centrifugation), (c)-(d) CER, (e)-(f) base, (g)-(h)sonication, and (i)-(j) heat-extractable fractions. Phase of photogranulation is shown at the top of the figure and the duration of each phase is indicated by brackets. Concentration is shown in mg/L on the y-axis for the line graphs for DOC and BOC Total. Histogram shows percentage of C in each extract for proteins, polysaccharides, and humic acids. For all figures, time is shown on the x-axis in days. Error bars represent the standard deviation of triplicate samples.

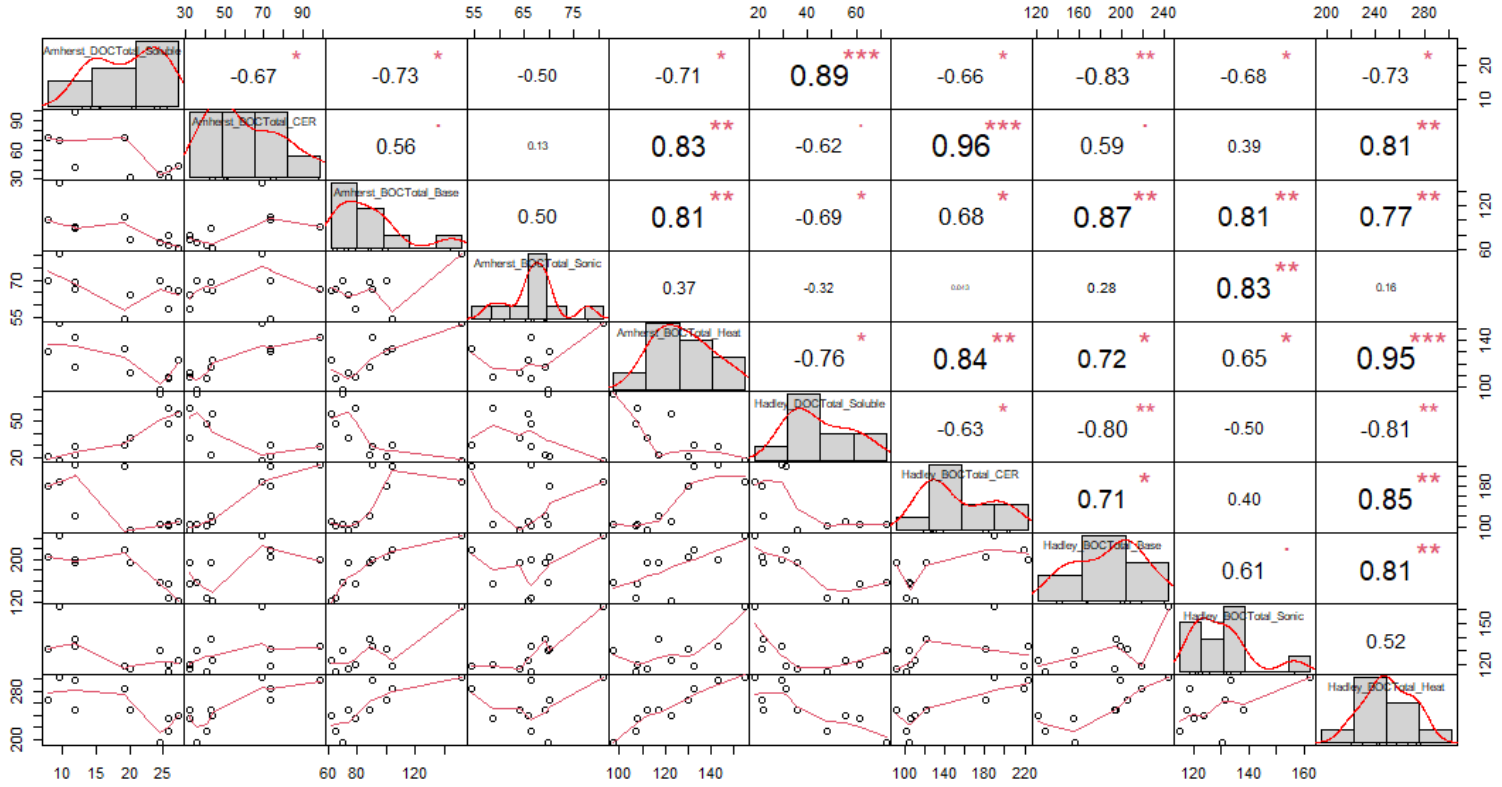

Figure 4.22: Correlation of dissolved and bound organic carbon between Amherst and Hadley sludge. The distribution of each variable for Amherst and Hadley sludge (Amherst soluble DOC_{total}, Amherst CER BOC_{total}, Amherst base BOC_{total}, Amherst sonication BOC_{total}, Amherst heat BOC_{total}, Hadley soluble DOC_{total}, Hadley CER BOC_{total}, Hadley base BOC_{total}, Hadley sonication BOC_{total}, and Hadley heat BOC_{total}), is shown on the diagonal. On the bottom of the diagonal: the bivariate scatter plots with a fitted line are displayed. On the top of the diagonal: the value of the correlation plus the significance level as stars. Each significance level is associated to a symbol: p-values (0.001, 0.01, 0.05, 0.1, 1) <=> symbols (“*”, “**”, “*”, “.”, " “).**

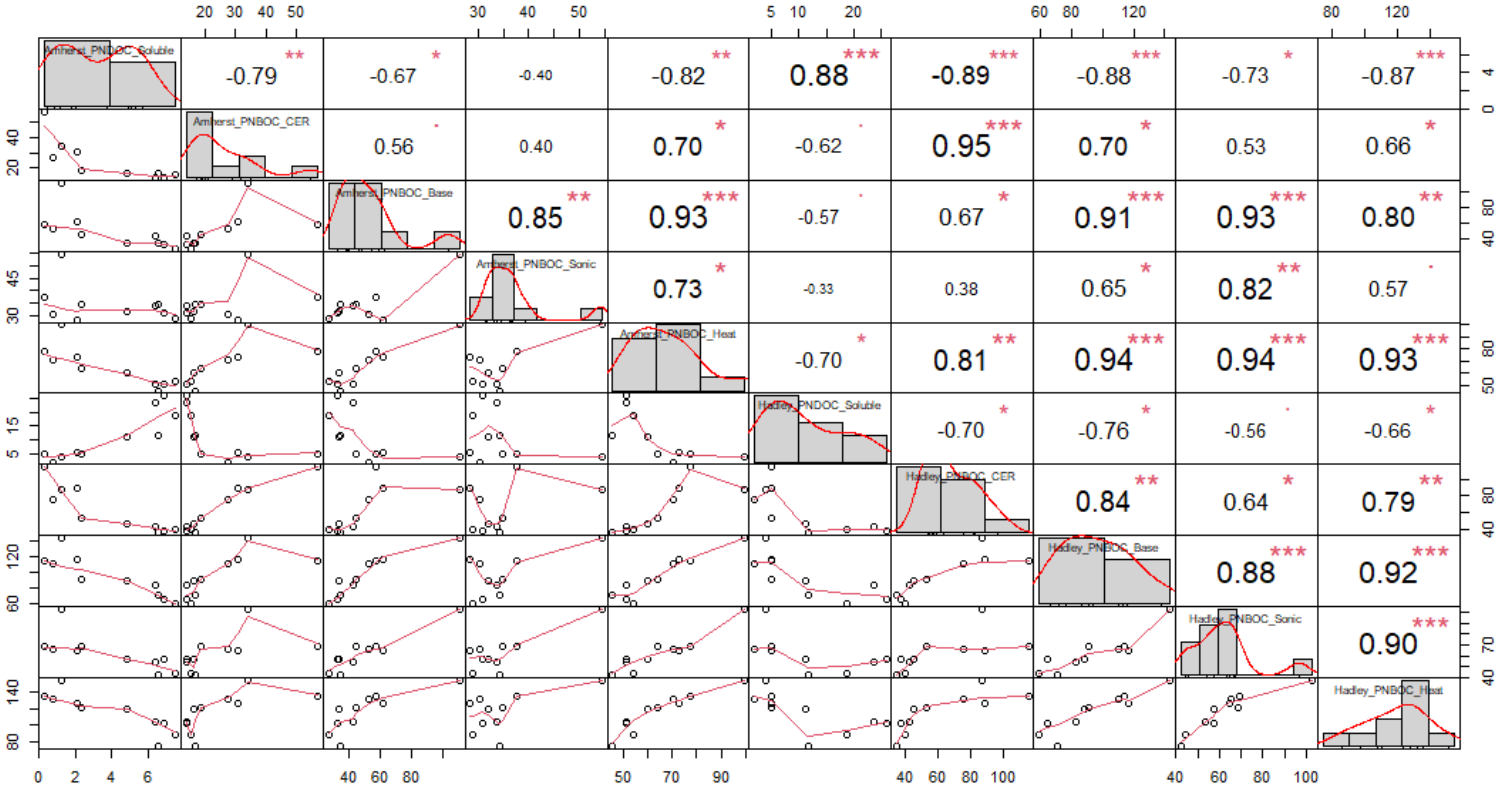

Figure 4.23: The correlation of EPS dissolved and bound organic carbon derived from proteins between Amherst and Hadley sludge. The distribution of each variable for Amherst and Hadley sludge (Amherst soluble DOC_{PN}, Amherst CER BOC_{PN}, Amherst base BOC_{PN}, Amherst sonication BOC_{PN}, Amherst heat BOC_{PN}, Hadley soluble DOC_{PN}, Hadley CER BOC_{PN}, Hadley base BOC_{PN}, Hadley sonication BOC_{PN}, and Hadley heat BOC_{PN}), is shown on the diagonal. On the bottom of the diagonal: the bivariate scatter plots with a fitted line are displayed. On the top of the diagonal: the value of the correlation plus the significance level as stars. Each significance level is associated to a symbol: p-values (0.001, 0.01, 0.05, 0.1, 1) <=> symbols (“*”, “**”, “*”, “.”, " “).**

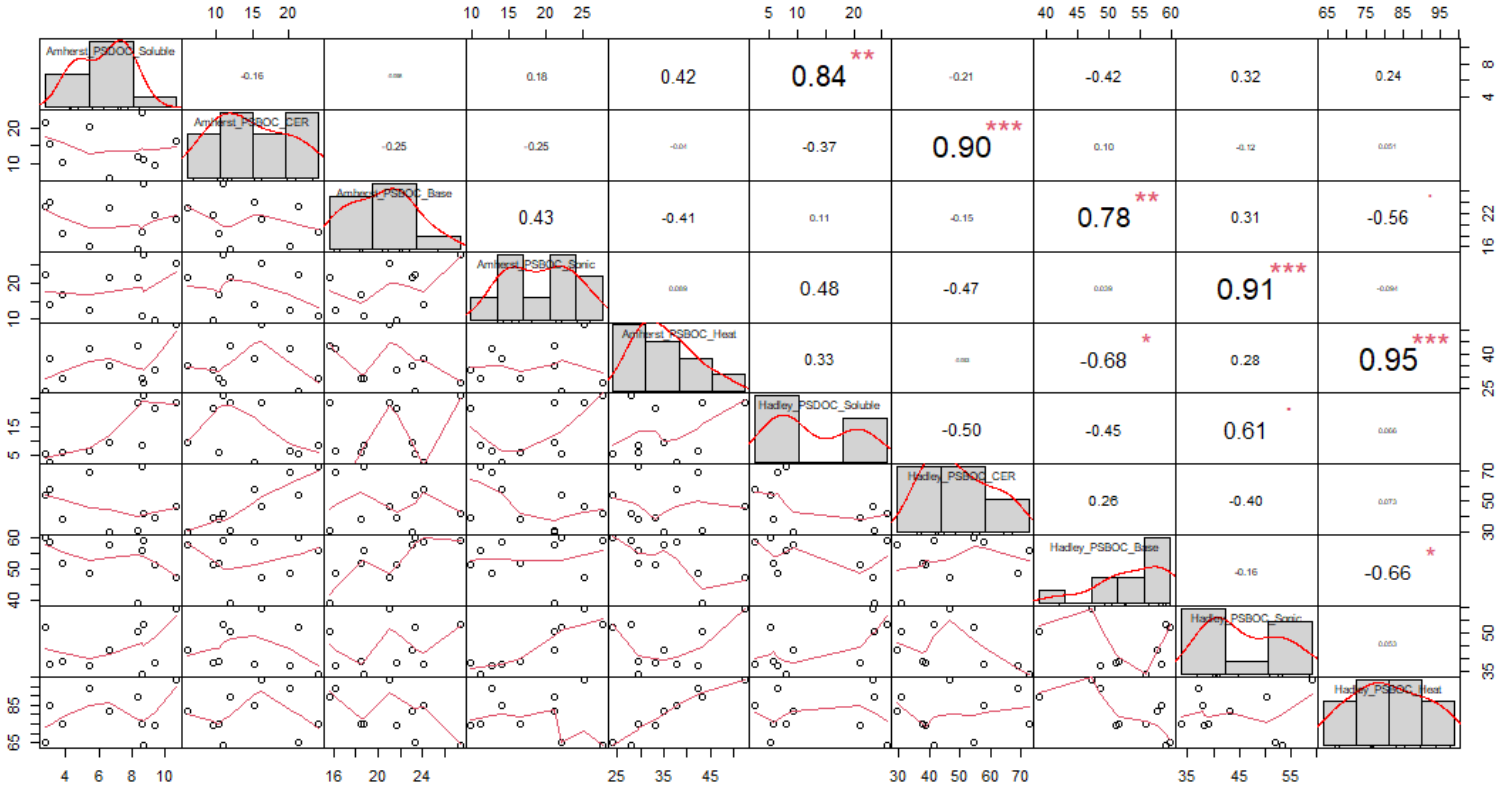

Figure 4.24: The correlation of EPS dissolved and bound organic carbon derived from polysaccharides between Amherst and Hadley sludge. The distribution of each variable for Amherst and Hadley sludge (Amherst soluble DOC_{PS}, Amherst CER BOC_{PS}, Amherst base BOC_{PS}, Amherst sonication BOC_{PS}, Amherst heat BOC_{PS}, Hadley soluble DOC_{PS}, Hadley CER BOC_{PS}, Hadley base BOC_{PS}, Hadley sonication BOC_{PS}, and Hadley heat BOC_{PS}), is shown on the diagonal. On the bottom of the diagonal: the bivariate scatter plots with a fitted line are displayed. On the top of the diagonal: the value of the correlation plus the significance level as stars. Each significance level is associated to a symbol: p-values (0.001, 0.01, 0.05, 0.1, 1) <=> symbols ("*", "**", "*", ".", " ").**

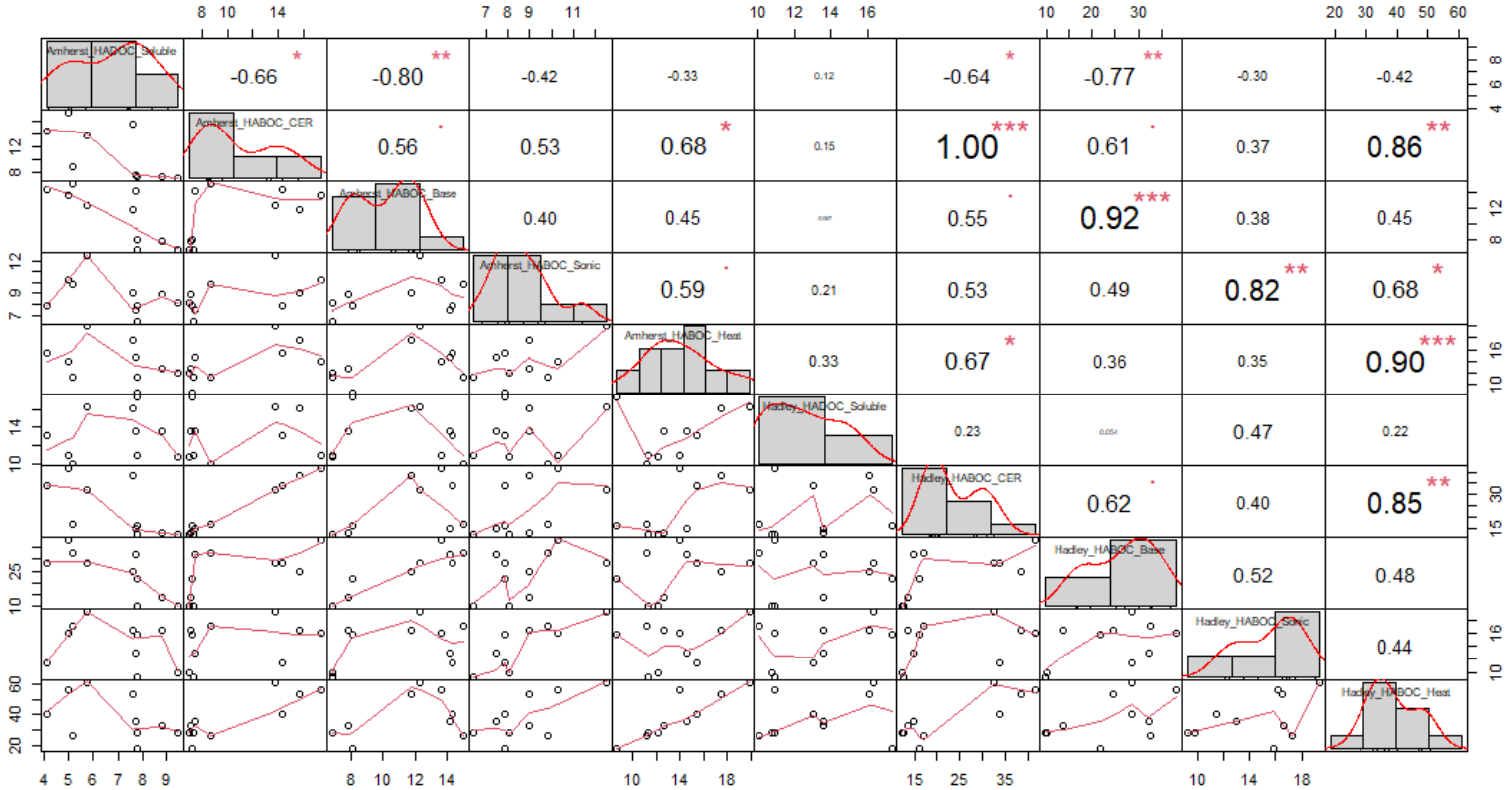

Figure 4.25: The correlation of EPS dissolved and bound organic carbon derived from humic acids between Amherst and Hadley sludge. The distribution of each variable for Amherst and Hadley sludge (Amherst soluble DOC_{HA}, Amherst CER BOC_{HA}, Amherst base BOC_{HA}, Amherst sonication BOC_{HA}, Amherst heat BOC_{HA}, Hadley soluble DOC_{HA}, Hadley CER BOC_{HA}, Hadley base BOC_{HA}, Hadley sonication BOC_{HA}, and Hadley heat BOC_{HA}), is shown on the diagonal. On the bottom of the diagonal: the bivariate scatter plots with a fitted line are displayed. On the top of the diagonal: the value of the correlation plus the significance level as stars. Each significance level is associated to a symbol: p-values (0.001, 0.01, 0.05, 0.1, 1) <=> symbols (“*”, “**”, “*”, “.”, " “).**

Similar to DOC, DON_{Total} for both Amherst and Hadley sludge sources increases overall for both sludge sources with a net change of 2 mg N/L and 2.4 mg N/L, respectively, Figure 4.26. Like DOC_{Total} and BOC, DON and BON_{Total} show strong correlation between the two sludge sources for all EPS extraction methods (soluble: r=0.86; CER: r=0.95; base: r=0.94; sonication: r=0.88; heat: r=0.91), Figure 27. DON and BON proteins (soluble: r=0.88; CER: r=0.95; base: r=0.91; sonication: r=0.82; heat: r=0.93) humic acids (CER: r=1.00; base: r=0.92; sonication: r=0.81; heat: r=0.90) also show strong correlation between the two sludge sources, Amherst and Hadley, except Hadley DOC humic acids (r=0.13) (Figure 4.28 to Figure 4.29).

Different EPS extraction methods also capture different organic N content, suggesting methods target different fractions. Like BOC, for all extraction methods, BON_{Total} decreases overall during photogranulation, but the composition of organic N between proteins and humic acids remains relatively constant (Figure 4.21) suggests proteins and humic acids are equally solubilized or utilized during photogranulation.

The strongest correlations are shown for DON and BON proteins (Amherst: n=8; Hadley: n=10) between extraction methods followed by DON and BON humic acids (Amherst: n=5; Hadley: n=2), which suggests that extraction methods for organic N derived from proteins show the least bias, then humic acids. Correlations are presented in Figure 4.28 and Figure 4.29 for DON and BON proteins and humic acids, respectively. Values highlighted in pink represent correlations between sludge sources, blue highlight represents correlations that are different between methods for the two sludge sources, and purple highlight represents moderate to strong correlations between methods for the two sludge sources.

The strongest correlations between soluble and bound organic N are CER (Amherst: r=-0.79; Hadley: r=-0.70), base (Amherst: r=-0.67; Hadley: r=-0.76) and heat (Amherst: r= -0.82; Hadley: r=-0.66) derived from proteins, suggesting that organic N in

the bulk liquid is derived from proteins and available as substrate. Amherst sludge BON humic acids also show moderate to strong correlation between soluble with CER (r=-0.66) and base (r=-0.81), while Hadley BON humic acids show no moderate or strong correlations with soluble DON. This suggests that organic N from humic acids in Amherst sets may be solubilized and contribute to DON.

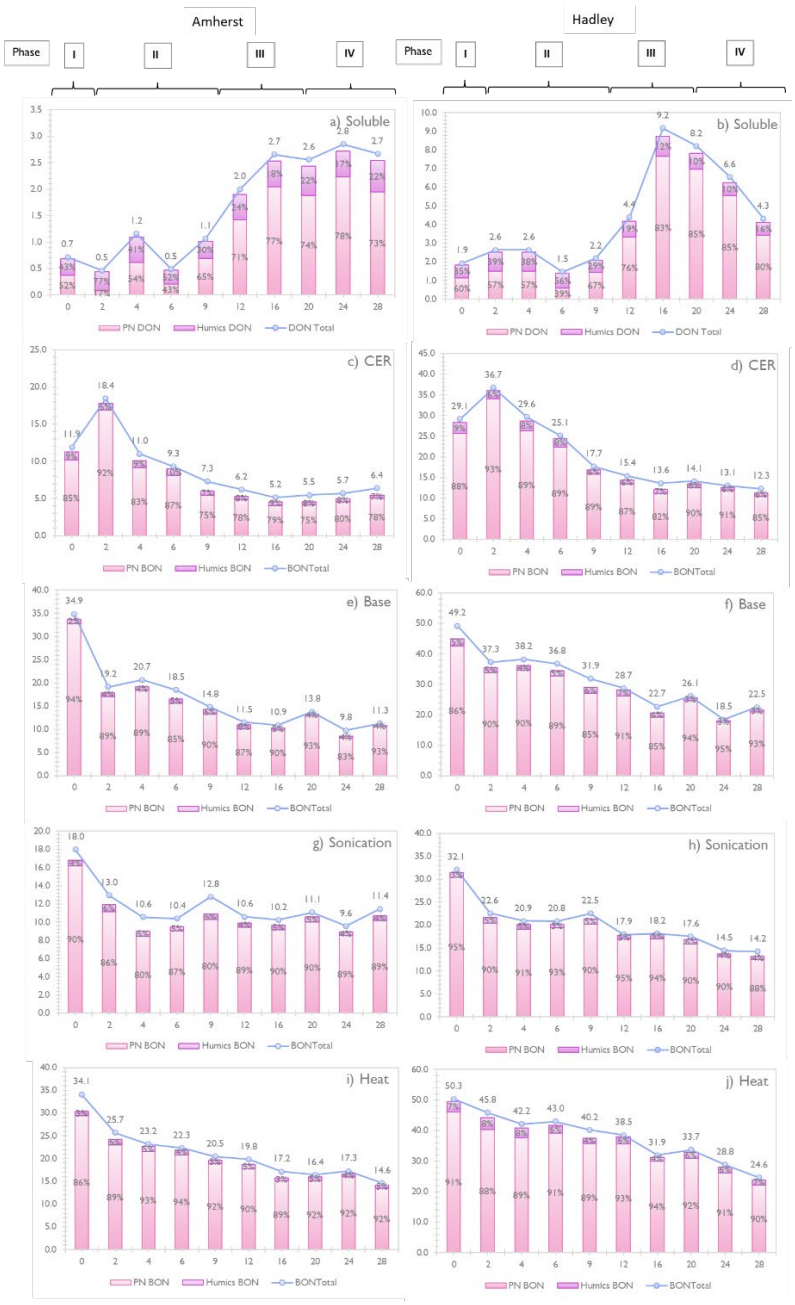

Figure 4.26: Dynamics of N for Soluble and Biomass-bound Fractions During Hydrostatic Photogranulation for Two Sludge Sources-Amherst and Hadley. The panel on the left side show N concentrations in the Amherst sludge, while panel on the right side shows results for Hadley sludge. The figures are organized by EPS extraction method as follows: (a)-(b) soluble (centrifugation), (c)-(d) CER, (e)-(f) base, (g)-(h)sonication, and (i)-(j) heat-extractable fractions. Phase of photogranulation is shown at the top of the figure and the duration of each phase is indicated by brackets. Concentration is shown in mg/L on the y-axis for the line graphs for DON and BON Total. Histogram shows percentage of N in each extract for proteins and humic acids. For all figures, time is shown on the x-axis in days. Error bars represent the standard deviation of triplicate samples.

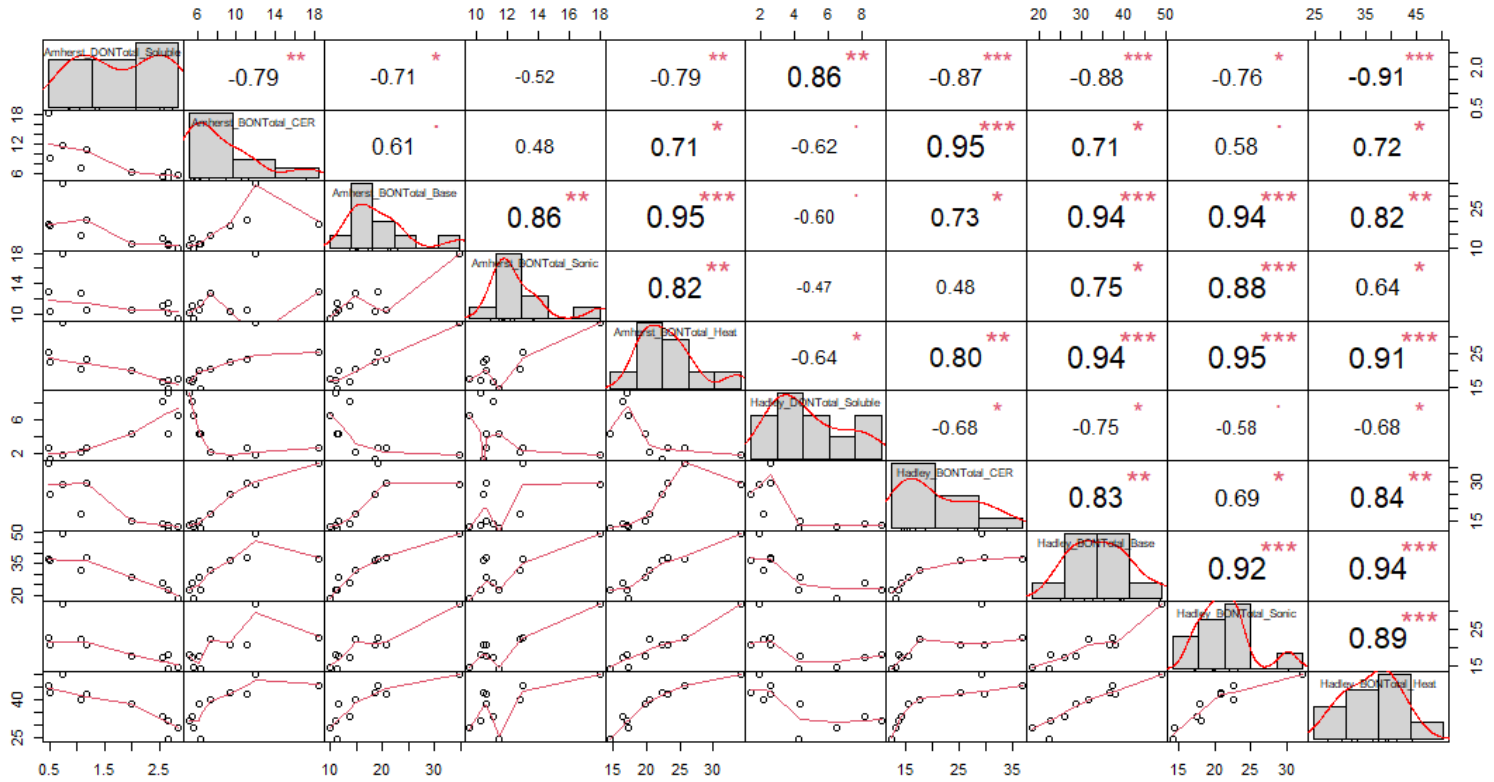

Figure 4.27: The correlation of EPS dissolved and bound organic nitrogen between Amherst and Hadley sludge. The distribution of each variable for Amherst and Hadley sludge (Amherst soluble DON_{TOTAL}, Amherst CER BON_{TOTAL}, Amherst base BON_{TOTAL}, Amherst sonication BON_{TOTAL}, Amherst heat BON_{TOTAL}, Hadley soluble DON_{TOTAL}, Hadley CER BON_{TOTAL}, Hadley base BON_{TOTAL}, Hadley sonication BON_{TOTAL}, and Hadley heat BON_{TOTAL}), is shown on the diagonal. On the bottom of the diagonal: the bivariate scatter plots with a fitted line are displayed. On the top of the diagonal: the value of the correlation plus the significance level as stars. Each significance level is associated to a symbol: p-values (0.001, 0.01, 0.05, 0.1, 1) <=> symbols (“*”, “**”, “*”, “.”, " “).**

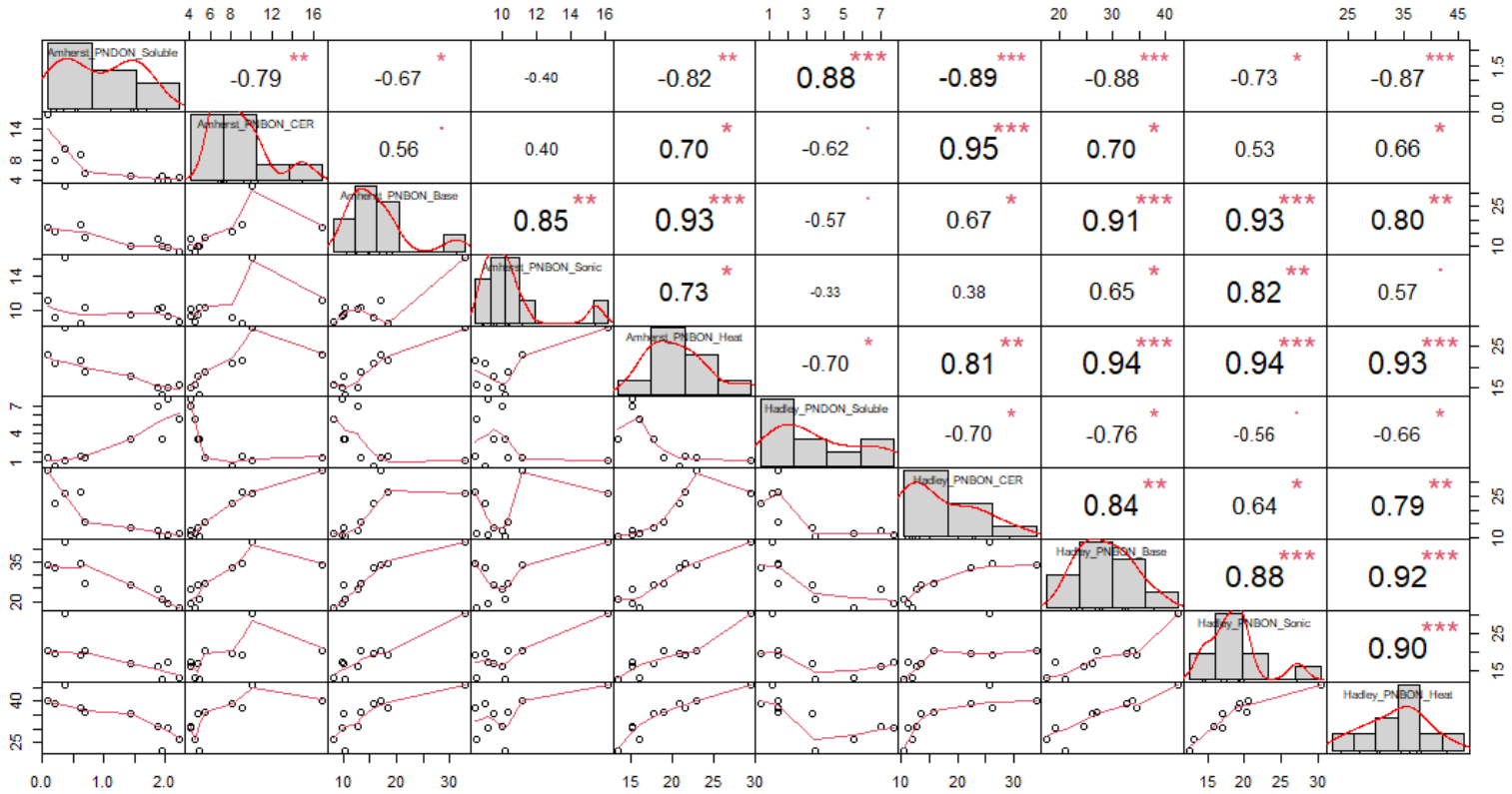

Figure 4.28: The correlation of EPS dissolved and bound organic nitrogen derived from proteins between Amherst and Hadley sludge. The distribution of each variable for Amherst and Hadley sludge (Amherst soluble DON_{PN}, Amherst CER BON_{PN}, Amherst base BON_{PN}, Amherst sonication BON_{PN}, Amherst heat BON_{PN}, Hadley soluble DON_{PN}, Hadley CER BON_{PN}, Hadley base BON_{PN}, Hadley sonication BON_{PN}, and Hadley heat BON_{PN}), is shown on the diagonal. On the bottom of the diagonal: the bivariate scatter plots with a fitted line are displayed. On the top of the diagonal: the value of the correlation plus the significance level as stars. Each significance level is associated to a symbol: p-values (0.001, 0.01, 0.05, 0.1, 1) <=> symbols (“*”, “**”, “*”, “.”, " “).**

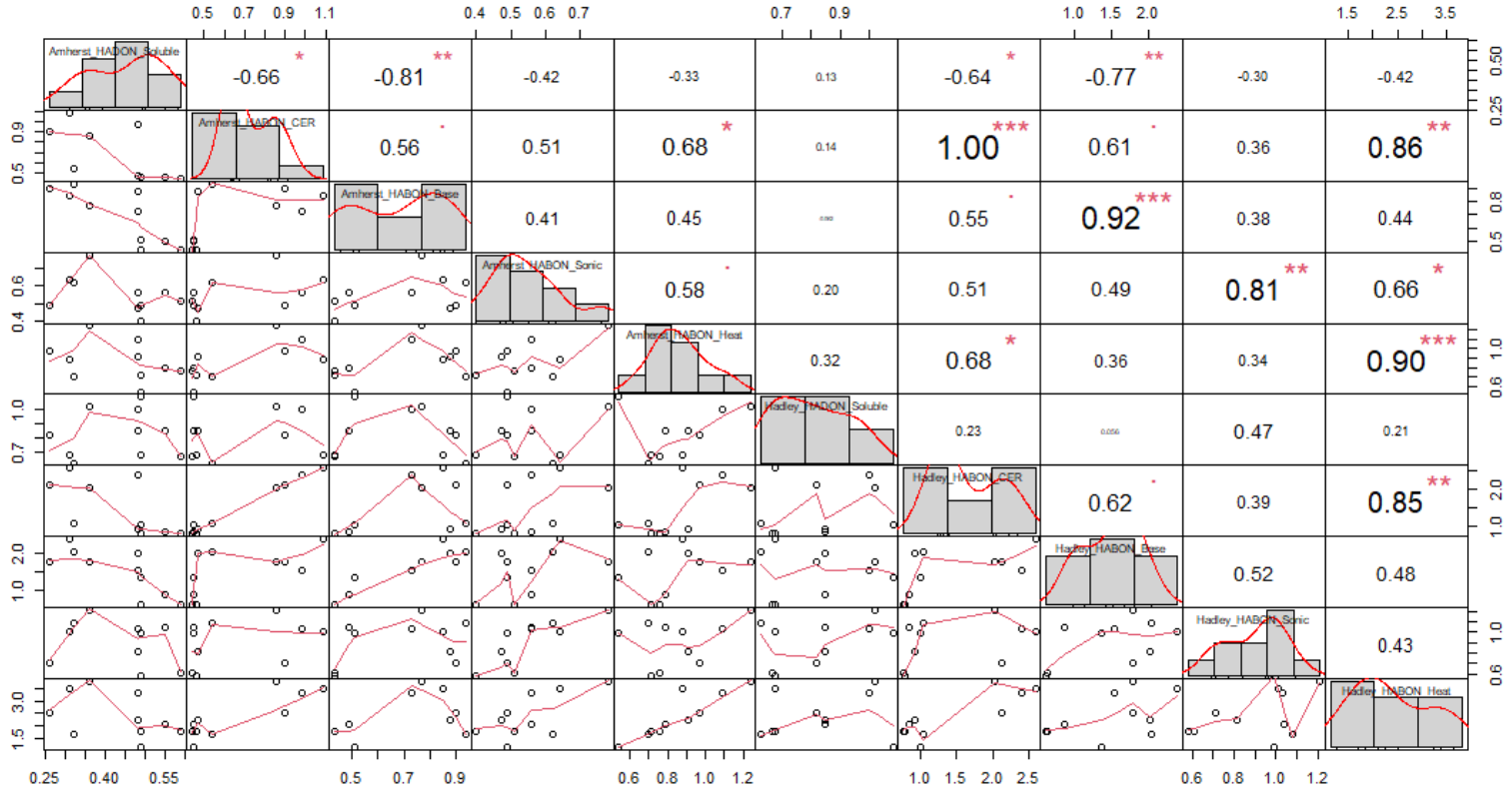

Figure 4.29: The correlation of EPS dissolved and bound organic nitrogen derived from humic acids between Amherst and Hadley sludge. The distribution of each variable for Amherst and Hadley sludge (Amherst soluble DON_{HA}, Amherst CER BON_{HA}, Amherst base BON_{HA}, Amherst sonication BON_{HA}, Amherst heat BON_{HA}, Hadley soluble DON_{HA}, Hadley CER BON_{HA}, Hadley base BON_{HA}, Hadley sonication BON_{HA}, and Hadley heat BON_{HA}), is shown on the diagonal. On the bottom of the diagonal: the bivariate scatter plots with a fitted line are displayed. On the top of the diagonal: the value of the correlation plus the significance level as stars. Each significance level is associated to a symbol: p-values (0.001, 0.01, 0.05, 0.1, 1) <=> symbols (“*”, “**”, “*”, “.”, " “).**

4.3.5.2 Comparative Analysis Between Dissolved and Organic C and N and Key Trends During Granule Development

Results presented in the previous section show that dissolved and bound organic C and N show statistically significant trends between the two sludge sources. Additionally, results show that the different extraction methods also show statistically different dissolved and bound organic C and N concentrations for each extract during photogranulation. Here, we present another comparative correlation analysis in order to understand how dissolved and bound organic C and N, for different extraction methods, correlates with key trends observed during hydrostatic photogranule development. The correlation analysis was performed between dissolved and bound organic C and N fractions and select dissolved constituents (chlorophyll, C, N-species, anions, and cations). The Pearson correlation, data distribution and corresponding p-values are presented in Figure 4.30 to Figure 4.39. Notable correlations between EPS extracts and constituents are highlighted- chlorophylls (pink), N-species (blue), anions and cations (purple) and also presented in Figure 4.40.

4.3.5.3 Dissolved and Bound Organic C

All DOC and BOC from proteins show significant correlation with chlorophylls (a and a/b ratio) for both sludge sources (Figure 4.30 and Figure 4.31). DOC from polysaccharides shows a moderate to strong correlation with chlorophylls, along with CER BOC for both sludge sources. Only Hadley sludge sonication BOC shows a significant moderate correlation with chlorophylls (Figure 4.32 and Figure 4.33). All dissolved and bound organic C from humic acids also show moderate to strong

correlation with chlorophylls, except DOC for Hadley sludge (Figure 4.34 and Figure 4.35).

Figure 4.40 summarizes moderate and strong correlations between DOC/BOC or DON/BON proteins polysaccharides and/or humic acids and the different extraction methods and both sludge sources. At least one method correlated with each constituent, chlorophylls, N-species, and select cations and anions, which have been previously established as indicators of successful granule formation (Kuo-Dahab et al., 2018; Milferstedt et al., 2017; Stauch-White et al., 2017). The results presented here show that different methods capture different dissolved and bound organic C quantities which align with the established key trends in photogranule development. Methods arranged from the highest number of correlations between dissolved and bound organic carbon with these constituents were CER (n=22), heat (n=14), soluble (n=10), base (n=7) and sonication (n=7). These results validate that EPS extraction methods capture relevant protein, polysaccharide and/or humic acid concentrations during photogranule development.

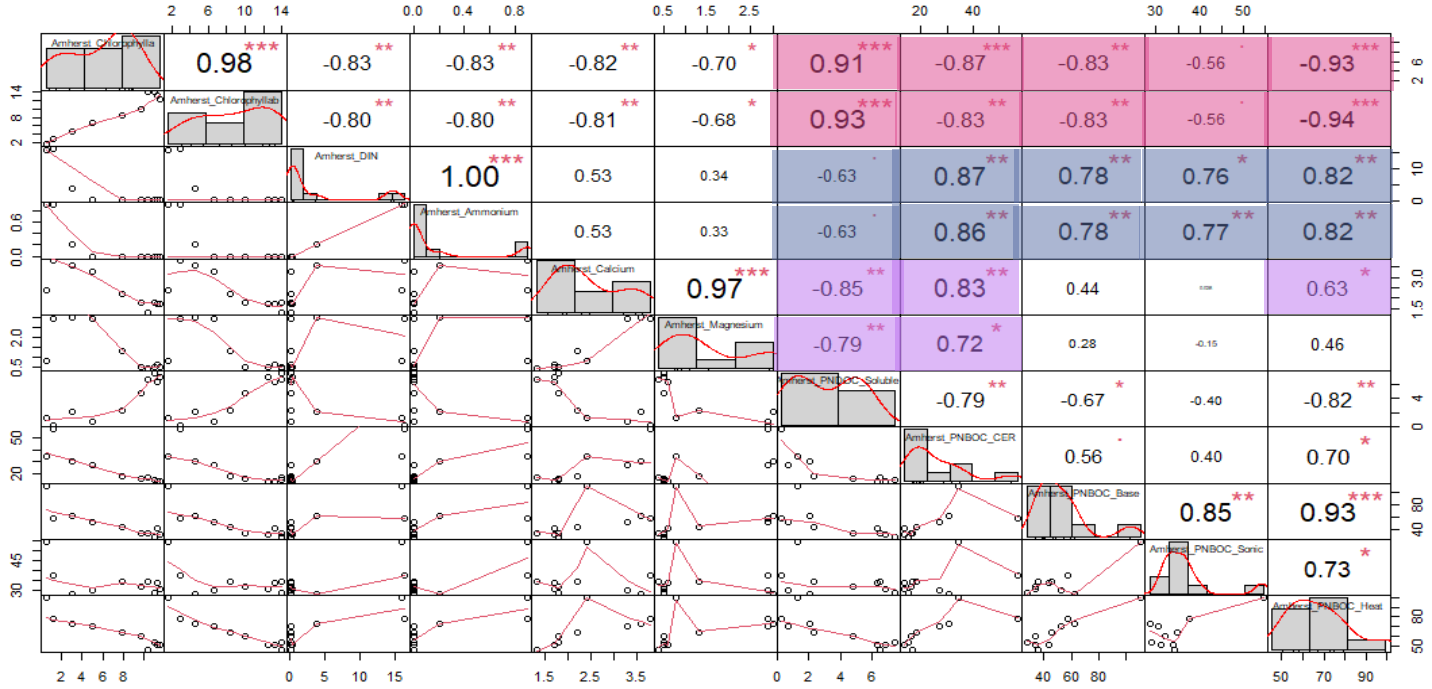

Figure 4.30: The correlation for chlorophylls, N-species, ions and organic carbon derived from proteins in Amherst sludge. The distribution of each variable for Amherst sludge (chlorophyll a, chlorophyll a/b ratio, DIN, NH_4^+-N, Ca^{2+}, Mg^{2+}, DOC_{PN}, CER BOC_{PN}, base BOC_{PN}, sonication BOC_{PN}, heat BOC_{PN}) is shown on the diagonal. On the bottom of the diagonal: the bivariate scatter plots with a fitted line are displayed. On the top of the diagonal: the value of the correlation plus the significance level as stars. Each significance level is associated to a symbol: p-values (0.001, 0.01, 0.05, 0.1, 1) <=> symbols ("*", "**", "*", ".", " "). Values highlighted in pink represent correlations for chlorophylls, values in blue represent correlations for DIN and NH_4^+-N, and values highlighted in purple represent correlations for Ca^{2+} and Mg^{2+}.**

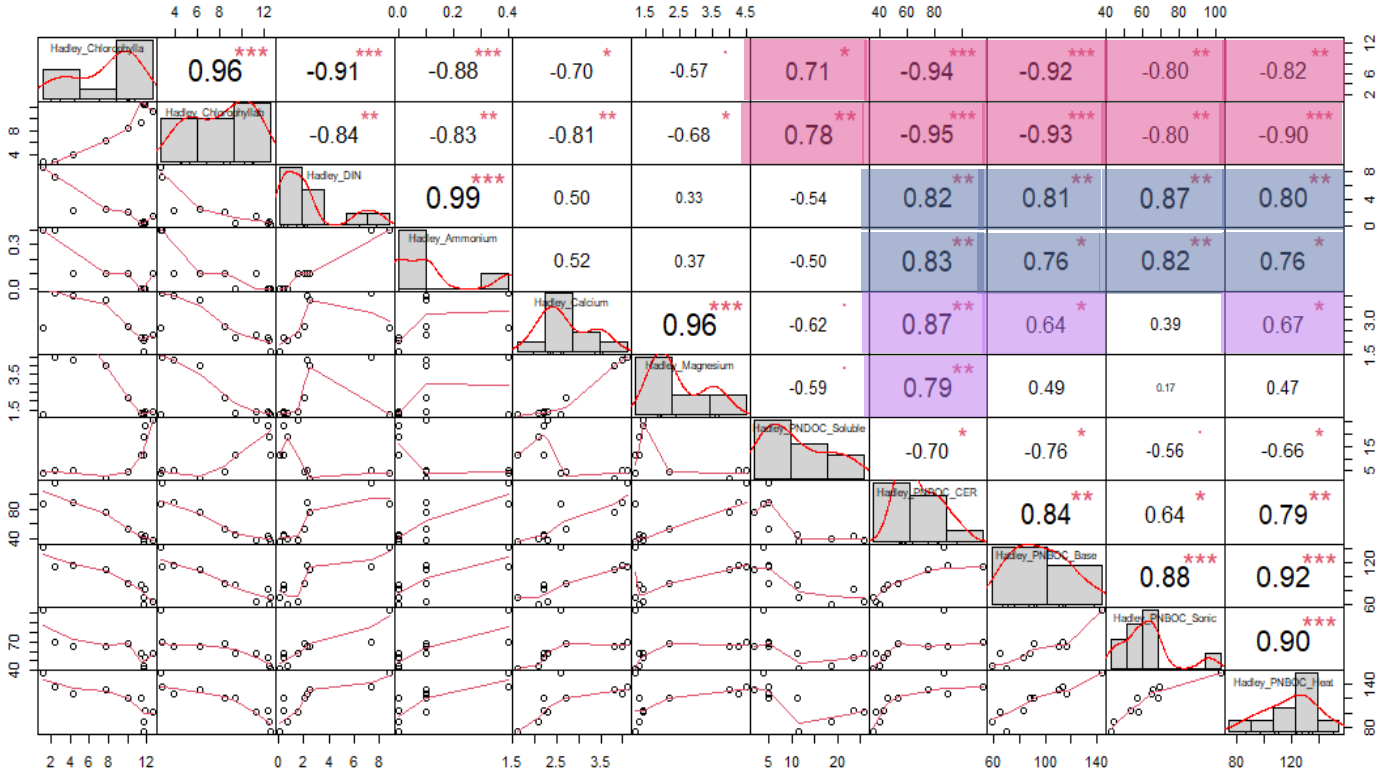

Figure 4.31: The correlation for chlorophylls, N-species, ions and organic carbon derived from proteins in Hadley sludge. The The distribution of each variable for Hadley sludge (chlorophyll a, chlorophyll a/b ratio, DIN, NH_4^+-N, Ca^{2+}, Mg^{2+}, DOC_{PN}, CER BOC_{PN}, base BOC_{PN}, sonication BOC_{PN}, heat BOC_{PN}) is shown on the diagonal. On the bottom of the diagonal: the bivariate scatter plots with a fitted line are displayed. On the top of the diagonal: the value of the correlation plus the significance level as stars. Each significance level is associated to a symbol: p-values (0.001, 0.01, 0.05, 0.1, 1) <=> symbols (“*”, “**”, “*”, “.”, " “). Values highlighted in pink represent correlations for chlorophylls, values in blue represent correlations for DIN and NH_4^+-N, and values highlighted in purple represent correlations for Ca^{2+} and Mg^{2+}.**

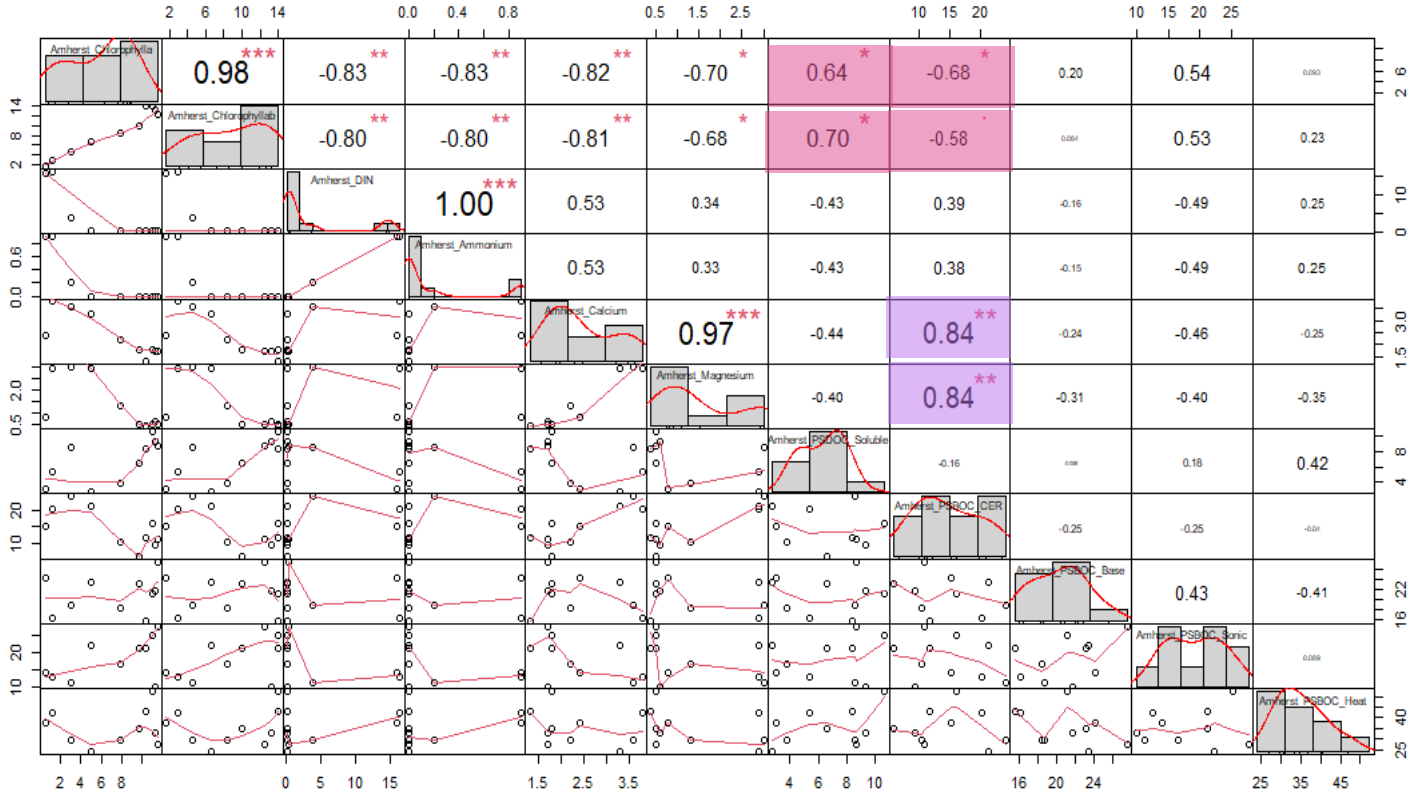

Figure 4.32: The correlation for chlorophylls, N-species, ions and organic carbon derived from polysaccharides in Amherst sludge. The distribution of each variable for Amherst sludge (chlorophyll a, chlorophyll a/b ratio, DIN, NH_4^+-N, Ca^{2+}, Mg^{2+}, DOC_{PS}, CER BOC_{PS}, base BOC_{PS}, sonication BOC_{PS}, heat BOC_{PS}) is shown on the diagonal. On the bottom of the diagonal: the bivariate scatter plots with a fitted line are displayed. On the top of the diagonal: the value of the correlation plus the significance level as stars. Each significance level is associated to a symbol: p-values (0.001, 0.01, 0.05, 0.1, 1) <=> symbols ("*", "**", "*", ".", " "). Values highlighted in pink represent correlations for chlorophylls, values in blue represent correlations for DIN and NH_4^+-N, and values highlighted in purple represent correlations for Ca^{2+} and Mg^{2+}.**

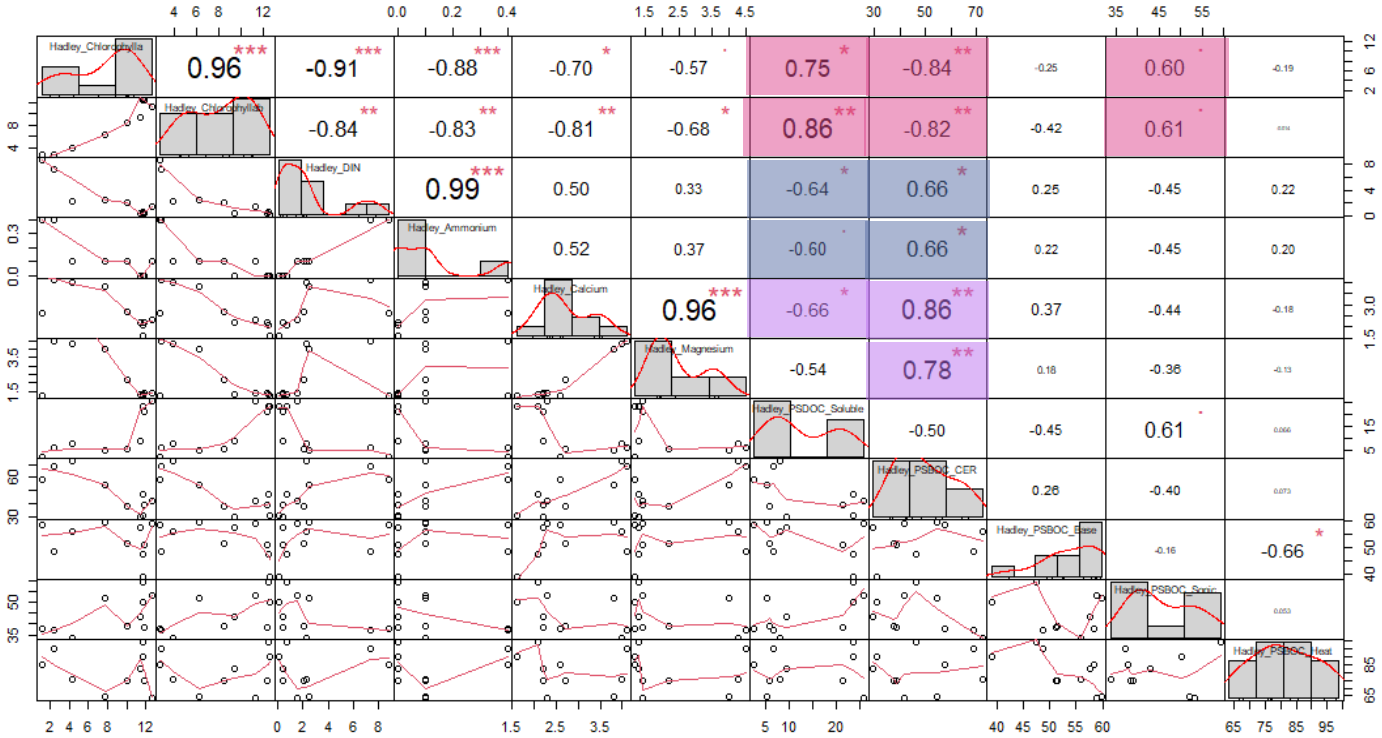

Figure 4.33: The correlation for chlorophylls, N-species, ions and organic carbon derived from polysaccharides in Hadley sludge. The distribution of each variable for Hadley sludge (chlorophyll a, chlorophyll a/b ratio, DIN, NH_4^+-N, Ca^{2+}, Mg^{2+}, DOC_{PS}, CER BOC_{PS}, base BOC_{PS}, sonication BOC_{PS}, heat BOC_{PS}) is shown on the diagonal. On the bottom of the diagonal: the bivariate scatter plots with a fitted line are displayed. On the top of the diagonal: the value of the correlation plus the significance level as stars. Each significance level is associated to a symbol: p-values (0.001, 0.01, 0.05, 0.1, 1) <=> symbols ("*", "**", "*", ".", " "). Values highlighted in pink represent correlations for chlorophylls, values in blue represent correlations for DIN and NH_4^+-N, and values highlighted in purple represent correlations for Ca^{2+} and Mg^{2+}.**

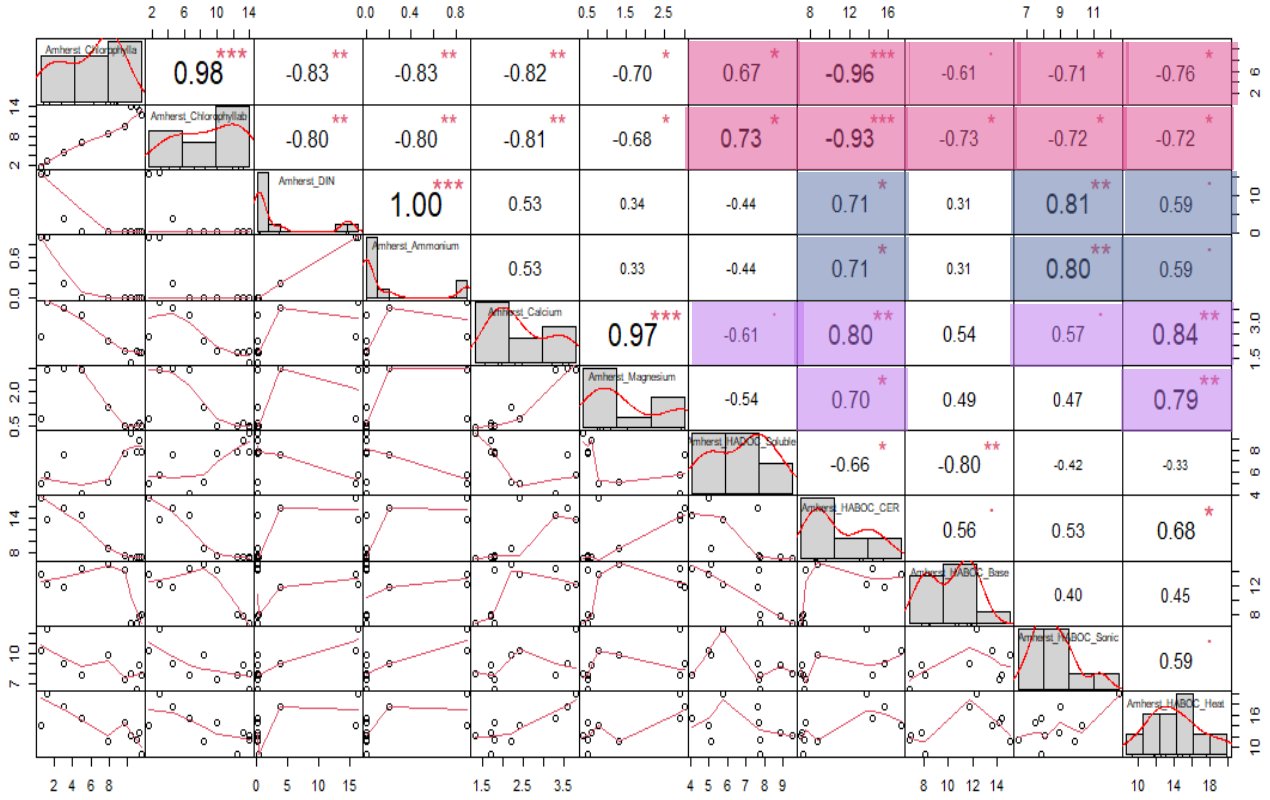

Figure 4.34: The correlation for chlorophylls, N-species, ions and organic carbon derived from humic acids in Amherst sludge. The distribution of each variable for Amherst sludge (chlorophyll a, chlorophyll a/b ratio, DIN, NH_4^+-N, Ca^{2+}, Mg^{2+}, DOC_{HA}, CER BOC_{HA}, base BOC_{HA}, sonication BOC_{HA}, heat BOC_{HA}) is shown on the diagonal. On the bottom of the diagonal: the bivariate scatter plots with a fitted line are displayed. On the top of the diagonal: the value of the correlation plus the significance level as stars. Each significance level is associated to a symbol: p-values (0.001, 0.01, 0.05, 0.1, 1) <=> symbols ("*", "**", "*", ".", " "). Values highlighted in pink represent correlations for chlorophylls, values in blue represent correlations for DIN and NH_4^+-N, and values highlighted in purple represent correlations for Ca^{2+} and Mg^{2+}.**

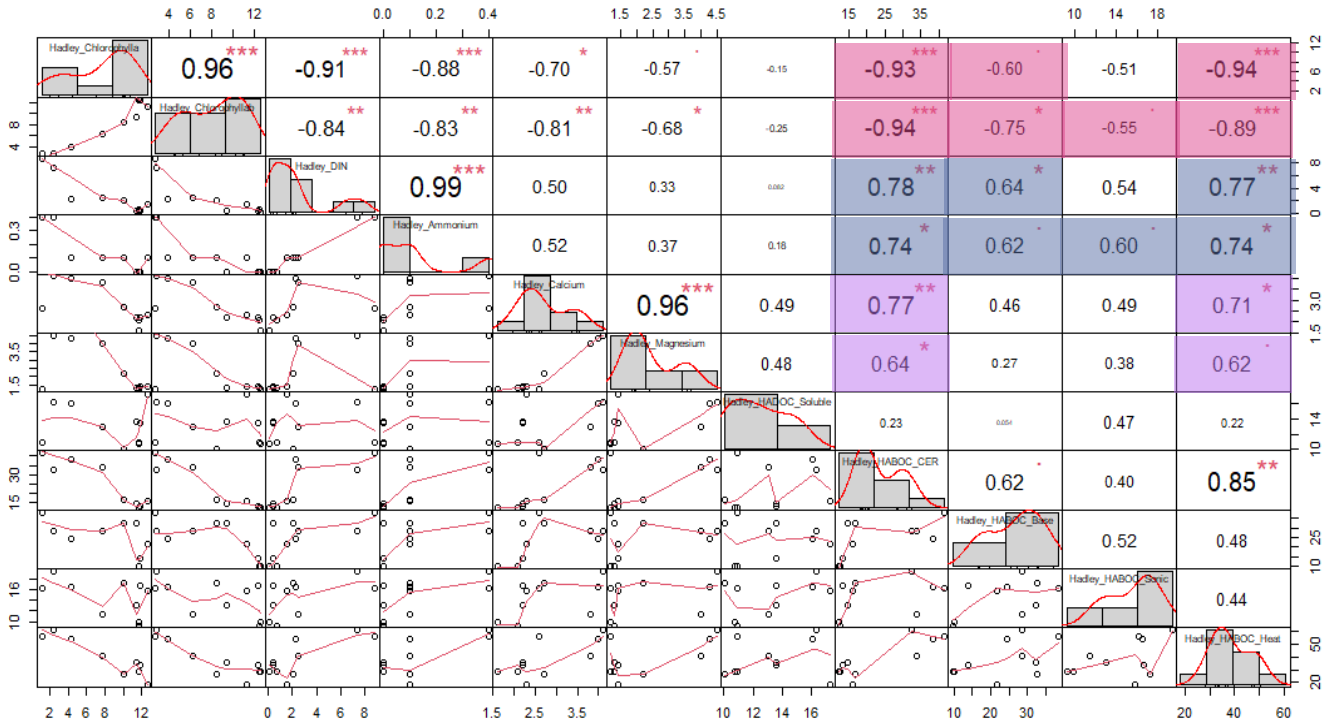

Figure 4.35: The correlation for chlorophylls, N-species, ions and organic carbon derived from humic acids in Amherst sludge. The distribution of each variable for Hadley sludge (chlorophyll a, chlorophyll a/b ratio, DIN, NH_4^+-N, Ca^{2+}, Mg^{2+}, DOC_{HA}, CER BOC_{HA}, base BOC_{HA}, sonication BOC_{HA}, heat BOC_{HA}) is shown on the diagonal. On the bottom of the diagonal: the bivariate scatter plots with a fitted line are displayed. On the top of the diagonal: the value of the correlation plus the significance level as stars. Each significance level is associated to a symbol: p-values (0.001, 0.01, 0.05, 0.1, 1) <=> symbols ("*", "**", "*", ".", " "). Values highlighted in pink represent correlations for chlorophylls, values in blue represent correlations for DIN and NH_4^+-N, and values highlighted in purple represent correlations for Ca^{2+} and Mg^{2+}.**

4.3.5.4 Dissolved and Bound Organic N

All DON and BON from proteins show significant correlation with chlorophylls (*a* and *a/b* ratio) for both sludge sources (Figure 4.36 and Figure 4.37). All dissolved and bound organic C from humic acids also show moderate to strong correlation with chlorophylls, except DON for Hadley sludge (Figure 4.38 and Figure 4.39).

Figure 4.40 summarizes moderate and strong correlations between DON/BON proteins and/or humic acids and the different extraction methods and both sludge sources. At least one method correlated with each constituent, chlorophylls, N-species, and select cations and anions, which have been previously established as indicators of successful granule formation (Kuo-Dahab et al., 2018; Milferstedt et al., 2017; Stauch-White et al., 2017). The results presented here show that different methods capture different dissolved and bound organic N quantities which align with the established key trends in photogranule development. Methods arranged from the highest number of correlations between dissolved and bound organic carbon with these constituents were CER (n=16), heat (n=14), sonication (n=8), base (n=7) and soluble (n=5). These results validate that EPS extraction methods capture relevant protein, polysaccharide and/or humic acid concentrations during photogranule development.

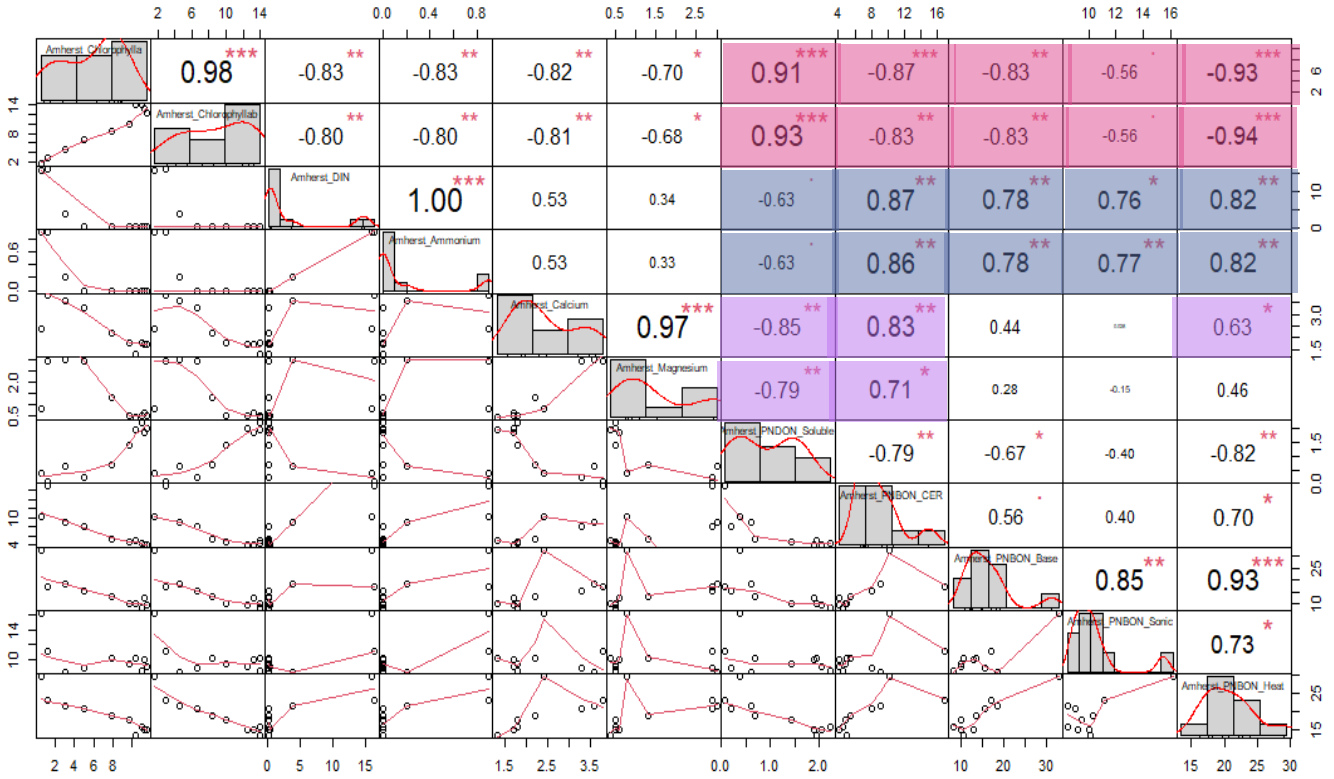

Figure 4.36: The correlation for chlorophylls, N-species, ions and organic nitrogen derived from proteins in Amherst sludge. The distribution of each variable for Amherst sludge (chlorophyll a, chlorophyll a/b ratio, DIN, NH_4^+-N, Ca^{2+}, Mg^{2+}, DON_{PN}, CER BON_{PN}, base BON_{PN}, sonication BON_{PN}, heat BON_{PN}) is shown on the diagonal. On the bottom of the diagonal: the bivariate scatter plots with a fitted line are displayed. On the top of the diagonal: the value of the correlation plus the significance level as stars. Each significance level is associated to a symbol: p-values (0.001, 0.01, 0.05, 0.1, 1) <=> symbols ("*", "**", "*", ".", " "). Values highlighted in pink represent correlations for chlorophylls, values in blue represent correlations for DIN and NH_4^+-N, and values highlighted in purple represent correlations for Ca^{2+} and Mg^{2+}.**

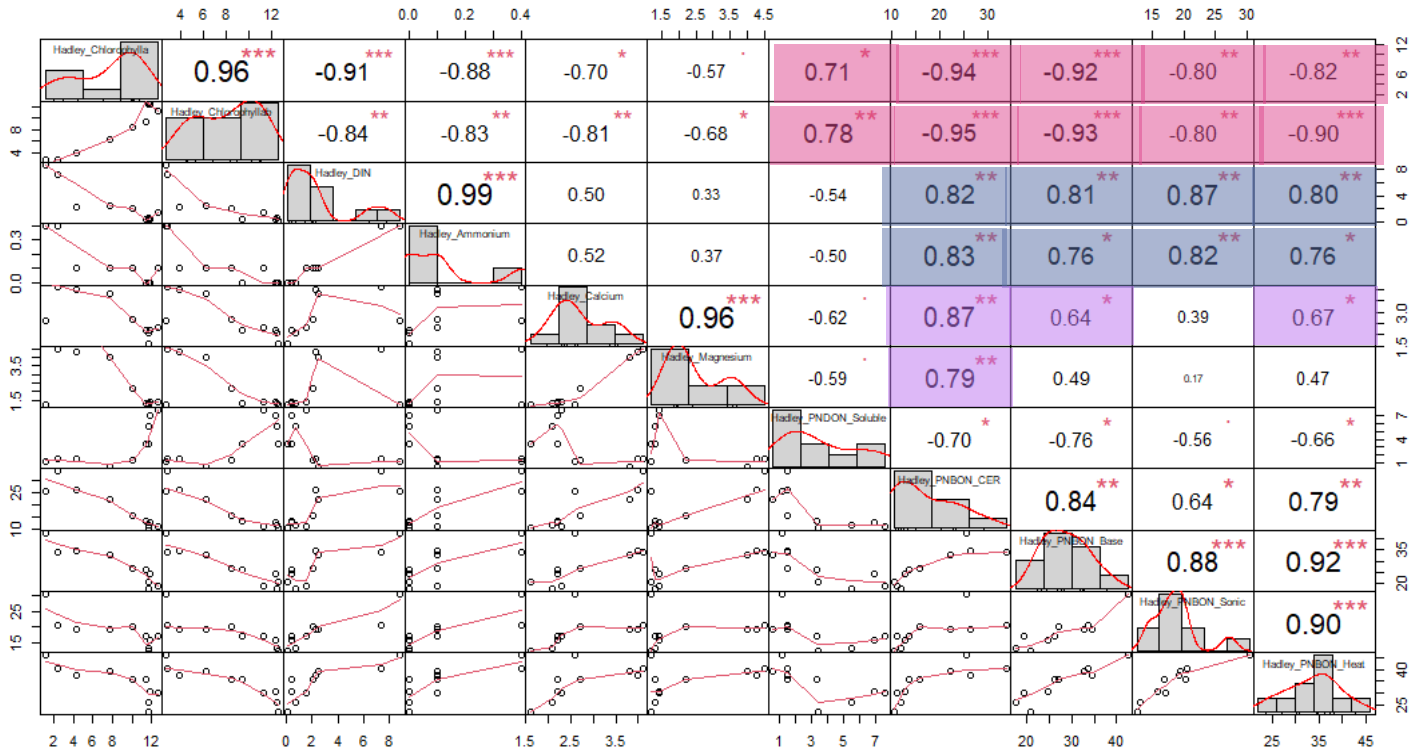

Figure 4.37: The correlation for chlorophylls, N-species, ions and organic nitrogen derived from proteins in Hadley sludge. The distribution of each variable for Hadley sludge (chlorophyll a, chlorophyll a/b ratio, DIN, NH_4^+-N, Ca^{2+}, Mg^{2+}, DON_{PN}, CER BON_{PN}, base BON_{PN}, sonication BON_{PN}, heat BON_{PN}) is shown on the diagonal. On the bottom of the diagonal: the bivariate scatter plots with a fitted line are displayed. On the top of the diagonal: the value of the correlation plus the significance level as stars. Each significance level is associated to a symbol: p-values (0.001, 0.01, 0.05, 0.1, 1) <=> symbols ("*", "**", "*", ".", " "). Values highlighted in pink represent correlations for chlorophylls, values in blue represent correlations for DIN and NH_4^+-N, and values highlighted in purple represent correlations for Ca^{2+} and Mg^{2+}.**

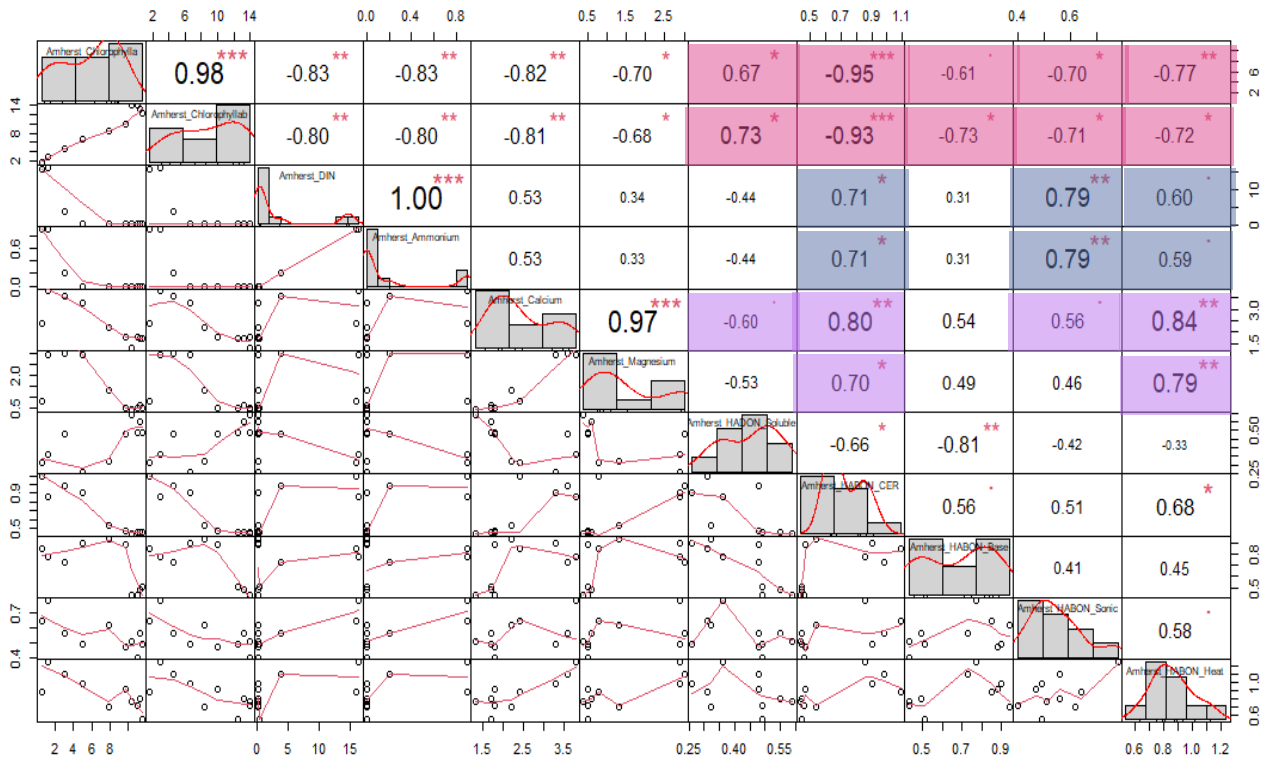

Figure 4.38: The correlation for chlorophylls, N-species, ions and organic nitrogen derived from humic acids in Amherst sludge. The distribution of each variable for Amherst sludge (chlorophyll a, chlorophyll a/b ratio, DIN, NH_4^+-N, Ca^{2+}, Mg^{2+}, DON_{HA}, CER BON_{HA}, base BON_{HA}, sonication BON_{HA}, heat BON_{HA}) is shown on the diagonal. On the bottom of the diagonal: the bivariate scatter plots with a fitted line are displayed. On the top of the diagonal: the value of the correlation plus the significance level as stars. Each significance level is associated to a symbol: p-values (0.001, 0.01, 0.05, 0.1, 1) <=> symbols (“*”, “**”, “*”, “.”, " “). Values highlighted in pink represent correlations for chlorophylls, values in blue represent correlations for DIN and NH_4^+-N, and values highlighted in purple represent correlations for Ca^{2+} and Mg^{2+}.**

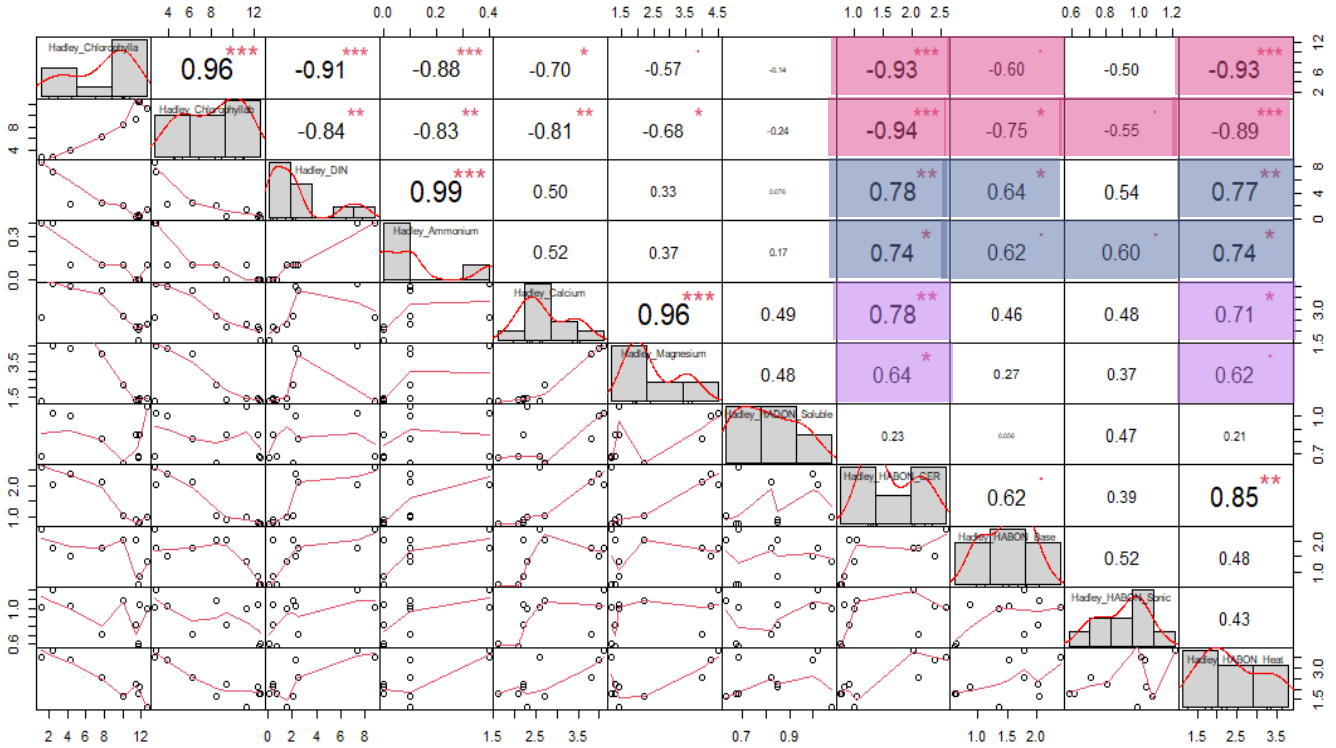

Figure 4.39: The correlation for chlorophylls, N-species, ions and organic nitrogen derived from humic acids in Hadley sludge. The distribution of each variable for Hadley sludge (chlorophyll a, chlorophyll a/b ratio, DIN, NH_4^+-N, Ca^{2+}, Mg^{2+}, DON_{HA}, CER BON_{HA}, base BON_{HA}, sonication BON_{HA}, heat BON_{HA}) is shown on the diagonal. On the bottom of the diagonal: the bivariate scatter plots with a fitted line are displayed. On the top of the diagonal: the value of the correlation plus the significance level as stars. Each significance level is associated to a symbol: p-values (0.001, 0.01, 0.05, 0.1, 1) <=> symbols (“*”, “**”, “*”, “.”, " “). Values highlighted in pink represent correlations for chlorophylls, values in blue represent correlations for DIN and NH_4^+-N, and values highlighted in purple represent correlations for Ca^{2+} and Mg^{2+}.**

			DIN		NH_4^+-N		Ca^{2+}		Mg^{2+}	
Amherst	DOC/BOC	Proteins	soluble	0.63	soluble	0.63	soluble	-0.85	soluble	-0.79
			CER	0.87	CER	0.86	CER	0.83	CER	0.72
			base	0.78	base	0.78	heat	0.63		
			sonic	0.76	sonic	0.77				
			heat	0.82	heat	0.82				
Hadley			CER	0.82	CER	0.83	soluble	-0.62	soluble	-0.59
			base	0.81	base	0.76	CER	0.87	CER	0.79
			sonic	0.87	sonic	0.82	base	0.64		
			heat	0.80	heat	0.76	heat	0.67		
Amherst		Polysaccharides					CER	0.84	CER	0.84
Hadley			soluble	-0.64	soluble	-0.60	soluble	-0.66	CER	0.78
			CER	0.66	CER	0.66	CER	0.86		
Amherst		Humic acids	CER	0.71	CER	0.71	soluble	-0.61	CER	0.70
			sonic	0.81	sonic	0.80	CER	0.80	heat	0.79
			heat	0.59	heat	0.59	sonic	0.57		
							heat	0.84		
Hadley			CER	0.78	CER	0.74	CER	0.77	CER	0.64
			base	0.64	base	0.62	heat	0.71	heat	0.62
			heat	0.77	sonic	0.60				
					heat	0.74				
Amherst	DON/BON	Proteins	soluble	-0.63	soluble	-0.63	soluble	-0.85	soluble	-0.79
			CER	0.87	CER	0.86	CER	0.83	CER	0.71
			base	0.78	base	0.78	heat	0.63		
			sonic	0.76	sonic	0.77				
			heat	0.82	heat	0.82				
Hadley			CER	0.82	CER	0.83	CER	0.87	CER	0.79
			base	0.81	base	0.76	base	0.64		
			sonic	0.87	sonic	0.82	heat	0.67		
			heat	0.8	heat	0.76				
Amherst		Humic acids	CER	0.71	CER	0.71	soluble	-0.60	CER	0.70
			sonic	0.79	sonic	0.79	CER	0.80	heat	0.79
			heat	0.60	heat	0.59	sonic	0.56		
							heat	0.84		
Hadley			CER	0.78	CER	0.74	CER	0.78	CER	0.64
			base	0.64	base	0.62	heat	0.71	heat	0.62
			heat	0.77	sonic	0.60				
					heat	0.74				

Figure 4.40: Summary of Notable Correlations Between Dissolved and Bound C and N Derived from Proteins, Polysaccharides and Humic Acids, and Different EPS Extraction Methods for Amherst and Hadley Sludge

4.4 Discussion

Granulation refers to the process by which the self-immobilization of microbes in biological wastewater treatment systems results in a compact, granule structure.

Currently, there is no single granulation mechanism model that can be applied across all granules, but several concepts have been reported that involve EPS, selection pressure (Hulshoff Pol et al.,1983; Liu & Tay, 2004); shear force (Liu & Tay, 2002); bridging by filamentous organisms (Beun et al., 1999; Wiegant et al., 1988); cell surface hydrophobicity (Ding et al., 2015; Gao et al., 2011; Kent et al., 2018; Sheng et al., 2010; Wang et al., 2018) concentric, layered organization of microorganisms (Lv et al., 2014; MacLeod et al., 1990; Sekiguchi et al., 1999; Tay et al., 2002; Vlaeminck et al., 2010). Each of these concepts involves EPS in one role or another.

EPS is not only thought to influence and mediate the formation of granules, but also suggests that EPS plays a role in the maintenance of the structure of granules. For example, Zhou et al. (2006) found that a slight overloading in upflow anaerobic sludge blanket (UASB) reactors would stimulate EPS production and shorten the period of granulation. Addition of exogenous EPS to anaerobic reactors with deteriorated granules would lead to a significant recuperation of operational performance of the reactors (Vivanco et al., 2006). In the aerobic sludge granulation process, the EPS content increased with cultivation time at the initial stage. All of these indicate the essential role of EPS in granulation.

Additionally, the composition and distribution of EPS influences the formation of granules. EPS can bind cells closely through ion bridging interactions, hydrophobic interactions, and polymer entanglement, which serves to enhance and promote the formation of granules. As no universal extraction method is available for the quantitative extraction of EPS from granules a method must be selected and optimized for each case, taking into consideration the sample characteristics. Several EPS extraction methods should be compared, and the most appropriate method selected (Sheng et al., 2010).

In order to fully understand hydrostatic granulation of oxygenic photogranules, first, we determined if multiple EPS extraction methods are needed to fully characterize EPS, and dynamics between EPS and key granulation trends were analyzed to infer OPG formation. Centrifugation was used to collect soluble EPS and four physical and/or chemical bound EPS extraction methods, CER, alkaline (base) treatment, sonication, and heat treatment, following the temporal progression of photogranulation using two different sludge sources. The composite assessment of soluble and bound EPS polysaccharides, proteins and humic acids from the different extraction methods were analyzed in correlation between the two sludges, the extraction methods themselves, and with chlorophyll and nutrients data during different phases of photogranulation.

4.4.1 Key Trends Observed Across Two Sludge Sources

Kuo-Dahab et al. (2018) first showed the use of multiple extraction methods, centrifugation, base and sonication, across two sludge sources to study the dynamics and fate of EPS during hydrostatic photogranulation. Despite the different origins and initial parameters of Amherst and Hadley activated sludge, photogranulation of both sludges in their study, showed four common phases and similar trends in chlorophylls, nitrogen, and soluble and bound EPS. Results in this study, corroborate findings in Kuo-Dahab et al. showing that both sludge sources have strong, statistically significant key trends with respect to chlorophyll *a* (r=0.99), chlorophyll *a/b* ratio (r=0.99), DTN (r=0.88), DON (r=0.95), DIN (r=0.96), NH_4^+-N (r=0.96), Ca^{2+} (0.99), and Mg^{2+} (0.99), during hydrostatic photogranulation (Figure 4.10). This shows that these trends are inherent in hydrostatic photogranulation.

Results for EPS extraction methods also show that protein (soluble: r= 0.88; CER: r=0.95; base: r=0.91; sonication: r=0.82; heat: r=0.93), polysaccharide (soluble: r=

0.84; CER: r=0.90; base: r=0.78; sonication: r=0.91; heat: r=0.95), and humic acid (soluble: r= 0.14); CER: r= 1.00; base: r=0.92 ; sonication: r=0.82: heat: r=0.90) trends are significantly similar between the two sludge sources Amherst and Hadley, except for soluble humic acids. This suggests that despite the differences in sludge source inoculum, these complex microbial biofilms share similar function with respect to EPS production and consumption during hydrostatic photogranulation, even though communities may contain different microorganisms and initial concentrations of constituents. Results also suggest that these EPS trends, like chlorophylls, nitrogen, and cations, may be essential for hydrostatic formation of photogranules.

4.4.2 Multiple EPS Extraction Methods to Capture Different Fractions of EPS

Results here show that different EPS extraction methods are required to capture different fractions of EPS, and the EPS extraction protocol used affects the quantity and composition of EPS extracted, with respect to protein, polysaccharide, and humic acids, during photogranulation. EPS extraction methods for polysaccharides were found to be the most biased, followed by humic acids, then proteins. This suggests that different methods target different EPS fractions, perhaps more associated with polysaccharides (as no correlations were found between methods based on polysaccharide content) but may overlap between the methods for protein and humic acids (as these methods showed high correlation between methods based on protein content). This is particularly important during photogranulation as cyanobacterial EPS is more polysaccharide based (Kuo-Dahab et al., 2018).

4.4.3 Comparative Analysis of Key Trends in Granule Development

The progressive chlorophyll *a*, *a/b* ratio, N-species, and cation and anion trends observed in this study validate that the cultivation was consistent with other studies (Kuo-Dahab et al., 2018; Milferstedt et al., 2017; Stauch-White et al., 2017), and evaluation of the EPS components is translatable across cultivation of OPGs. Multiple correlations between EPS extracts and chlorophylls, DON, DIN, NH_4^+-N, and anions/cations show that this closed system is composed of complex interactions that eventually produce a photogranule in a hydrostatic environment.

4.4.4 Chlorophylls

Activated sludge was initially collected from an open aeration basin, where light intensity is intermittent with turbulent mixing conditions. With the transition to a hydrostatic environment, with 24-hour light intensity, we observed an exponential increase in chlorophylls (*a* and *a/b* ratio) along with increases in soluble and bound EPS showing that these conditions are favorable for phototrophic microorganisms. The moderate to strong correlations between soluble proteins, polysaccharides, and humic acids (except Hadley soluble humic acids) suggests that the release or solubilization of these components into the bulk liquid is associated with phototrophic growth. Bound EPS also show moderate to strong negative correlations with chlorophylls, for both sludge sources: all EPS extraction methods for proteins and humic acids, and CER extracts for polysaccharides. First, this shows that there is a link between the dynamics of these bound fractions (production and consumption) and the enrichment of phototrophs. This may be due to either degradation of decay of the activated sludge biomass by phototrophs and/or the active production of “new” EPS by phototrophs.

Second, the extraction methods may select for different fraction of EPS associated with photographs during photogranulation.

4.4.5 Nitrogen Species

Stauch-White et al. (2017) first reported the correlation between successful photogranule cultivations and higher NH_4^+-N concentrations (>20 mg/L-N) in activated sludge inoculum. This study shows initial high NH_4^+-N bulk liquid concentrations for both sludge sources followed by an exponential uptake from the bulk liquid. NH_4^+-N also shows a strong negative correlation with chlorophylls suggesting that NH_4^+-N is assimilated by phototrophs.

By the end of phase I, both sludge sources show an NH_4^+-N concentration of <2 mg N/L. At the end of phase I, DON concentrations start to increase for both sludge sources. DON and NH_4^+-N show moderate negative correlation (Amherst: r=-0.71; Hadley: r=-0.70), while DON also shows moderate to strong positive correlation with chlorophylls (Amherst- chlorophyll a: r=0.90; chlorophyll a/b: r=0.95; Hadley- chlorophyll a: r=0.78; chlorophyll a/b: r=0.91). The strong correlations between chlorophylls, DON and NH_4^+-N suggest that the solubilization of DON and uptake of NH_4^+-N are linked to enrichment of phototrophs and their metabolism resulting in successful granule formation.

Here, we observe that all EPS extraction methods also have moderate to strong correlations (Amherst: r= 0.63 - 0.86; Hadley: r= 0.50 to 0.83) between proteins and NH_4^+-N. In contrast to chlorophylls, Soluble proteins show a negative correlation while bound proteins show a positive correlation (Figure 4.14 and Figure 4.15). Soluble proteins also show a strong positive correlation with DON (Amherst: r=0.90; Hadley: r=0.72) while bound proteins show moderate to strong negative correlations (Amherst-

CER: r= -0.82; base: r=-0.69; heat: r=-0.84, Hadley- CER: r =-0.81; base: r=-0.83; sonication: r=-0.78; heat: r=-0.92) except Amherst sonication extractable proteins (r=-0.38), for both sludge sources (Figure 4.14 and Figure 4.15).

NH_4^+-N only shows moderate correlation with soluble polysaccharides (r=-0.60) and CER extractable polysaccharides (r=0.66) for Hadley sludge, otherwise very weak insignificant correlations are seen for both sludges (Figure 4.16 and Figure 4.17). Soluble polysaccharides show some correlation with DON, with Hadley sludge having the strongest positive correlation (r=0.90) and Amherst having a moderate positive correlation (r=0.61). Bound CER polysaccharides show moderate negative correlations with DON (Amherst: r=-0.58; Hadley: r=-0.64), while sonication shows moderate positive correlation with DON (Amherst: r=0.55; Hadley: r=0.68) for both sludge sources. Hadley sludge also shows a moderate negative (r=-0.57) between base extractable polysaccharides and DON (Figure 4.16 and Figure 4.17).

For Amherst sludge, CER (r=0.71), sonication (r=0.80), and heat (r=0.59) extractable humic acids show correlation with NH_4^+-N. For Hadley sludge, all methods, CER (r=0.74), base (r=0.62), sonication (r=0.60), and heat (r=0.74) show correlation with NH_4^+-N (Figure 18 and Figure 19). Only Amherst sludge soluble humic acids show a positive correlation with DON (r=0.66) while Hadley sludge shows no correlation. Bound proteins show moderate to strong negative correlations for both sludges and all extraction methods (Amherst- CER: r= -0.86; base: r=-0.70; sonication: r=-0.73; heat: r=-0.74, Hadley- CER: r =-0.78; base: r=-0.89; sonication: r=-0.69; heat: r=-0.69) (Figure 4.18 and Figure 4.19).

The photogranulation mechanism has been explored in previous literature (Kuo-Dahab et al., 2018; Milferstedt et al., 2017; Stauch-White et al., 2017). Milferstedt et al. (2017) show that in hydrostatic cultivations, the initially provided activated sludge is the only major C source in this closed system, and biodegradation converts the sludge to

CO_2 which is then available for phototrophic growth. During photogranulation, they also observed an increase in chlorophyll *a* concentration with an overall unchanged biomass concentration and an increase in polysaccharide-based EPS. Here, chlorophyll content shows an increase in the amount of cyanobacteria during photogranulation, as microorganism community changes, results show that EPS composition and quantity also changes. Even though over the course of photogranulation polysaccharide concentration has a low net change, multiple dynamic changes are observed during photogranulation for each phase for polysaccharides in comparison to proteins and humic acids. Additionally, here we observe multiple correlations between DOC/BOC and DON/BON derived from EPS proteins, polysaccharides and humic acids using different extraction methods and chlorophylls, DIN, and NH_4^+-N (Figure 4.40). Dynamics of dissolved and bound organic C and N also show that these fractions are simultaneously increasing and decreasing, soluble organic C and N increase while bound organic C and N decrease during photogranulation. These results, first, suggest that different methods, target and extract different fractions of EPS, and second, recycle of organic C and N is most likely occurring during hydrostatic photogranulation through an uptake and degradation loop by phototrophic microorganisms.

Literature shows that cyanobacteria dictate the bioavailability of extracellular C in natural microbial mats (non-granular biofilms) through a balance of uptake and degradation. The turnover of EPS in some mats is 5-8% in 20-30min (Decho et al., 2005; Dupraz et al., 2009; Stuart et al., 2016). Stuart et al. (2015) showed that the extracellular matrix serves as a C store for microbial mat cyanobacteria. Their results provide evidence that the relationship of cyanobacteria (and other primary producers) with C in dynamic microbial communities is more complex than fluxes of only inorganic C. Authors also found that cyanobacteria, were degrading proteins, polysaccharides, and nucleic acids. Although it is likely that other bacteria also degrade extracellular organic matter,

they detected extracellular proteins assigned to Gammaproteobacteria, including several proteins involved in binding and uptake of sugars and amino acids. Authors confirmed that cyanobacteria were capable of extracellular protein degradation and alpha- and beta-glucan hydrolysis. They also identified 21 cyanobacterial extracellular proteins indicating there are commonly secreted proteins involved in protein and organic C metabolism, in cyanobacteria (Stuart et al., 2015). The degradative EPS proteins and links between degradation and assimilation that they identified confirm the important role of cyanobacterial organic C excretion and utilization in complex microbial communities.

The N cycle is composed of oxidation-reduction reactions, many of which are used in the energy metabolism of microbes. NH_4^+-N is incorporated into C-skeletons by phototrophic organisms in a process known as NH_4^+-N assimilation (Herrero et al., 2001). NH_4^+-N is the most reduced inorganic form of N available for assimilation, but normally, the N forms found in nature are oxidized forms, mainly nitrate (NO_3^--N), nitrite (NO_2^--N) and dinitrogen (N_2). In addition, certain ecosystems also contain other forms of N such as urea. In general, all these forms of N require their reduction to NH_4^+-N, a process that needs an energy expense. That is the reason why most of the phototrophic organisms prefer NH_4^+-N as a N source. In the absence of NH_4^+-N, they display different strategies to optimize N assimilation, by different regulatory systems that ensure N supply, and can harvest NH_4^+-N from amino acids (Muro-Pastor et al., 2003).

In addition to degradation, cyanobacteria are known to produce copious amounts of slime EPS for motility and sheath tubes during times of stress. SEM imaging of mature granules show the presence of multiple sheath tubes. The polysaccharide composition of slime versus sheath tubes also varies and thus could contribute to the changes in EPS polysaccharide quantities. Hoicyzk (1998, 2000) has shown that slime is composed of 34% glucose, 33% xylose, and less amounts of arabinose, galactose, fucose, and rhamnose, while sheath tubes are composed of 60% glucose, 18%

galactose and less of xylose, arabinose, and rhamnose. Additionally, the types of EPS produced by cyanobacteria varies and the different extraction methods used here may target these different types of EPS. Slime is more loosely present around the cell while sheath tubes are anchored to the cell surface. It is reasonable that different extraction methods are required to extract these different types of EPS. As low overall change in the quantity of polysaccharide-base EPS is observed during photogranulation, literature and results suggest that one type of EPS may be metabolized and assimilated or recycled for another type of EPS (i.e., slime for sheath tubes or vice versa).

It is also possible that other microorganisms in the biofilm are able to utilize EPS produced by other microorganisms besides just their own. Milferstedt et al. (2017) shows the presence of multiple different heterotrophic microorganisms in the community. Milferstedt et al. also shows that the community in photogranules changes over time to more specific community with less diversity. These microorganisms are also known to produce EPS and thus could be why dynamics in EPS composition and quantity are also observed. However, as the community is significantly composed of cyanobacteria and phototrophs, this would perhaps suggest that EPS dynamics is mainly due to these microorganisms.

4.4.6 Divalent Cations- Ca^{2+} and Mg^{2+}

The divalent cation bridging theory has been supported by findings from several studies that divalent, specially Ca^{2+} and Mg^{2+}, helps biofilm formation. Higgins and Novak (2002) reported that when the sum of monovalent cation concentration (Na^{+}, NH_4^{+}-N, and K^{+}) divided by the sum of the divalent cations (Ca^{2+} and Mg^{2+}) was greater than 2, then there is a loss of biomass aggregation due to loss of biofilm EPS stability. Results here show ratio of monovalent to divalent cations is less than 2 during

photogranulation and suggests that biofilm formation is promoted with no deterioration to the biomass and suggests that cations are assisting in granule formation. Positively charged cations, Ca^{2+} and Mg^{2+}, are known to stabilize negatively charged proteins in the biofilm structure. First, this may suggest CER and heat methods extract EPS fractions that are associated with biofilm structure. Second, these results infer that CER and heat extracts have an overlap in fractions extracted as we also observe significant correlation between heat extract and divalent cations.

4.5 Conclusion

The current study shows that multiple EPS extraction methods are required in order to characterize EPS during the transformation of activated sludge into a photogranule in a hydrostatic environment. While filamentous cyanobacteria, EPS and N are known to play key roles in photogranulation (Kuo-Dahab et al., 2018; Stauch-White et al., 2017), the present study reveals why cyanobacteria are selected and how different fractions of EPS and their recycle leads to photogranulation in hydrostatic conditions.

Despite differences in sludge inoculum, EPS trends using five different extraction methods, centrifugation, CER, base, sonication, and heat, show that trends are significantly similar, statistically, between two sludge sources (Amherst and Hadley). The results presented above show that different EPS extraction methods are required to capture different fractions of EPS with respect to protein, polysaccharide, and humic acid composition and organic C and N content. EPS extraction methods for polysaccharides was found to be the most biased, followed by humic acids, then proteins. This suggests that different methods target different EPS fractions (more associated with polysaccharides), but may share overlap between the methods (proteins and humic acids).

All methods had statistically significant moderate to strong correlations with one or more constituents, chlorophylls, N-species, and select cations and anions, which have been previously established as strong indicators of successful granule formation (Kuo-Dahab et al., 2018; Milferstedt et al., 2017; Stauch-White et al., 2017). Specifically, bound humic acids and no corresponding increase in the bulk liquid may suggest that humic acids are substrate when reduced carbon is limited in the initial phase of granulation These results suggest that different EPS fractions are linked to multiple processes during hydrostatic photogranulation, including the enrichment of filamentous cyanobacteria, nitrogen metabolism and recycle of organic C and N, assimilation and biofilm incorporation of NH_4^+-N, and biofilm structure, further suggesting that the role of EPS is a complex process with multiple courses of action. Thus, the evolution of EPS during photogranulation is tied to both the understanding of the photogranulation mechanism and to the OPG structure.

CHAPTER 5

INVESTIGATION ON THE ADDITION OF CATIONS FOR THE ENHANCEMENT OF ACTIVATED SLUDGE PHOTOGRANULATION IN A HYDROSTATIC ENVIRONMENT

5.1 Introduction

Recently, researchers have focused on the cultivation of granular forms of microalgae biomass in an attempt to avoid the physical challenges (large footprint) and associated economic costs of harvesting microalgae biomass from traditional processes (photobioreactors or open lagoons and ponds, etc.) (Molina Grima et al., 2003). Tiron et al. (2015, 2017) presented granular activated algae (GAA) to treat low-strength wastewater in a sequencing batch reactor (SBR). GAA are composed of unicellular and filamentous microalgae, *Chlorella* sp. and *Phormidium* sp., respectively, with an optimum range in size from 700-1,500μm (Tiron et al., 2015; Tiron et al., 2017). Recently, several authors presented oxygenic photogranules (OPG), also microalgae granules, which range in size from 100-4,500 μm (Abouhend et al., 2018; Ansari et al., 2019; Kuo-Dahab et al., 2018; Milferstedt et al., 2017; Park & Dolan, 2015; Stauch-White et al., 2017). OPG are composed of both motile, filamentous cyanobacteria, including cyanobacteria from the family *Oscillatoriales* and the microalga *Acutodesmus obliquus* embedded in and surrounded by a matrix of extracellular polymeric substances (EPS). Both types of microalgae granules have been studied for the treatment of domestic wastewater and biomass production (Abouhend et al., 2018; Milferstedt et al., 2017; O. Tiron et al., 2015; Olga Tiron et al., 2017).

Granular sludge is cultivated through the process of photogranulation, but with some differences. GAA starts with a sequencing batch reactor (SBR) and is inoculated with microalgae to form bacterial-algae flocs coined “activated algae” that develop

through the process of photogranulation into granules over time (numerous batches) (Tiron et al., 2015; Tiron et al., 2017). OPG are cultivated from activated sludge inoculum in individual glass vials in a hydrostatic environment over a period of approximately 25 to 42 days (Kuo-Dahab et al., 2018; Milferstedt et al., 2017; Chul Park & Dolan, 2015). A hydrostatic environment is void of mixing, while SBR systems are hydrodynamic. OPG SBR systems use hydrostatically cultivated OPGs to start-up the system, which subsequently produce new OPG biomass. During hydrostatic cultivation, it is not always guaranteed that all biomass in each vial will granulate fully during the long 25-to-42-day cultivation period. Therefore, it would be advantageous to enhance or expedite hydrostatic photogranulation for OPG reactor start-up and subsequent operation (Abouhend et al., 2018; Ansari et al., 2019; Milferstedt et al., 2017; Park & Dolan, 2015).

In OPGs, Milferstedt et al. observed an increase in EPS polysaccharide to protein (PS/PN) ratio during hydrostatic photogranulation. PS/PN ratio correlated with the enrichment of filamentous cyanobacteria, suggesting that an increase in EPS polysaccharides is linked to the emergence of cyanobacteria during photogranulation. Kuo-Dahab et al. (2018) also investigated the fate and dynamics of EPS during photogranulation of OPG under hydrostatic conditions. The authors found that multiple proteins and polysaccharides trends emerged when base and sonication EPS extraction methods were used. Chapter 4 shows that different EPS extraction methods target different fractions of EPS during photogranulation, revealing varying fates of EPS proteins, polysaccharides, and humic acids. Chapter 4 also shows that EPS extraction methods across two sludge sources are significantly similar with respect to EPS proteins, polysaccharides, and humic acids, and they’re respective organic C and N content. Authors also showed that multiple extraction methods are needed to fully characterize the total EPS pool. Kuo-Dahab et al. (2018) results show that base

extractable EPS proteins from sludge inoculum degrades and becomes the source of C and N for phototrophic growth. In addition, the authors found that the limitation of original dissolved inorganic nitrogen (DIN) and the release of organic N (e.g., proteinaceous EPS) is potentially advantageous to filamentous cyanobacteria, promoting photogranulation. This research shows that initial activated sludge inoculum, nutrients and EPS proteins from different fractions extracted by various methods have a significant role in promoting cyanobacterial growth and photogranulation.

Along with EPS proteins, multiple studies have also shown that cations play an essential role in the aggregation or bioflocculation of activated sludge, and the enhancement of granulation (Higgins & Novak, 1997a, 1997b; Park et al., 2006, 2008a, 2008b). Higgins and Novak (1997b) showed that divalent cations (Ca^{2+} and Mg^{2+}) bind extracellular proteins within activated sludge flocs, and is consistent with the ion-bridging model that was proposed by numerous researchers (Bruus et al., 1992; Novak & Haugan, 1980; Tezuka, 1969). The model proposed can be used to explain the relationship between EPS, cations, and settling and dewatering in activated sludge. Divalent cations bridge negatively charged sites on EPS, binding them to microbial surfaces and other EPS constituents. The binding of EPS constituents stabilizes the EPS matrix, which improves floc formation in addition to settling and clarification. The results from this study showed that high concentrations of monovalent cations displaced the divalent cations from within the floc and led to a decrease in the bound EPS protein content, which was associated with a deterioration in sludge settling properties. Cation concentrations mainly affected bound protein, not bound polysaccharide concentrations suggesting that proteins play an important role in bioflocculation and may be dominant in activated sludge.

SDS-PAGE is a molecular tool that can be used for the size-based separation and has been used to study activated sludge EPS proteins. Park et al. (2008a) and

(2008b) showed one application of SDS-PAGE to wastewater systems, specifically activated sludge and digested sludge. Park et al. extracted EPS proteins by different cation associated extraction methods. EPS protein was subsequently fractionated by ammonium sulfate precipitation (ASP) and subjected to SDS-PAGE. The results showed that each extraction method led to a unique SDS-PAGE protein profile. The study also shows that CER extracts for EPS protein that are bound to calcium (Ca^{2+}) and magnesium (Mg^{2+}), base extracts for aluminum (Al^{3+})-bound EPS protein, and sulfide extracts for iron ($Fe^{2+/3+}$)-bound EPS. Park et al. also identified ten proteins ranging in molecular mass (~21-66 kDa) using proteomics analysis. The study reported that some common proteins were extracted by all the methods; base and sulfide protein shared some similarity suggesting that base can target both Al^{3+} and $Fe^{2+/3+}$-bound EPS.

Caudan et al. (2014) reported that alpha (1-4) glucans and proteins play role in granulation and were found to be distributed throughout the granules. Caudan et al. suggested that granule cohesion depends partially on Ca^{2+} linkages with anionic proteins in EDTA extracted EPS. The EPS proteins pool was found to contain two major fractions, one group corresponding to low molecular mass proteins (~1.6 kDa) and one group corresponding to high molecular mass proteins (~200 kDa). Zhu et al. (2015) compared the SDS-PAGE profile of activated sludge flocs, aerobic and anaerobic granular sludge EPS. The authors found that EPS proteins bound with Ca^{2+} and Mg^{2+}, reduce the surface charge by forming linkages between EPS and cells promoting adhesion and formation of granules. Zhu et al. also showed that high molecular mass proteins (~66-97 kDa) were favored during sludge granulation. Authors suggested that high molecular mass proteins offer more binding sites and interaction points with divalent cations and EPS promoting granulation (Zhu et al., 2015). These studies show that SDS-PAGE is a useful tool to characterize EPS proteins that are present during photogranulation. Further, studies suggest that different molecular mass proteins may

have different roles in the various EPS extracted fractions, and that cations may play an important role in each of these fractions during photogranulation.

A better understanding of the dynamics and fate of cations and EPS fractions during photogranulation is crucial for improving our understanding of photogranulation phenomenon. Currently, there are no studies that investigate the role of cations during hydrostatic photogranulation of activated sludge. Additionally, there is no research that utilizes SDS-PAGE for more specific size-based separation and molecular analysis of EPS proteins in photogranules. The objective of this study is to determine how cation addition affects hydrostatic photogranulation. Here, activated sludge inoculum was collected from the aeration basin of a wastewater treatment plant and statically cultivated into OPG. Ca^{2+}, Mg^{2+}, Na^{+}, dextrose and EDTA were added as separate treatments. Chlorophyll, nutrients, and EPS dynamics were quantified over the course of photogranulation. EPS extracts were further subjected to ammonium sulfate precipitation (ASP) and subsequent SDS-PAGE profiling. SDS-PAGE banding pattern from different treatments (i.e., cation addition vs control) and EPS extractions is examined along with changes in chlorophylls and nutrients to determine the effect of treatments on photogranule development. The outcome of this study is expected to demonstrate the importance of cations and their effect on EPS dynamics during hydrostatic photogranulation, to enhance and expedite hydrostatic cultivation for OPG reactor operation and inform on OPG reactor performance.

5.2 Materials and Methods

5.2.1 Source of Activated Sludge for Cultivation of OPGs

Activated sludge was sampled directly from the aeration tank of Amherst and/or Hadley wastewater treatment plant (WWTP). The preliminary study used both Amherst and Hadley sludges as inoculum, and initial characteristics were not measured for the sludge sources. The In-depth study only used Hadley as a sludge source. As secondary treatment process, Amherst WWTP utilizes biological nutrient removal with a solids retention time (SRT) of 10-15 days and domestic wastewater as their influent source. Hadley WWTP operates a conventional activated sludge process to remove organic matter with nitrification at a 10-day SRT with mostly residential, commercial, and agricultural influent sources. The main characteristics of the sludge and the WWTP are described in subsequent sections and presented in Table 5.1.

Table 5.1 Initial Characteristics of Hadley Activated Sludge (t=0)

Hadley Activated Sludge Inoculum			
Parameter			
Biological Process		Conventional activated sludge	
Basin Configuration		Open	
Aeration Type		Mechanical	
Influent Sources		Residential and commercial	
SRT		10 d	
Parameter	Units	Value	SD
TSS	mg/L	2720	*123*
VSS	mg/L	2343	*112*
VSS/TSS	%	86.1	*2.0*
DOC	mg/L	19.8	*0.1*
DTN	mg/L-N	4.4	*0.1*
DON	mg/L-N	1.2	*0.01*
DIN	mg/L-N	3.2	*0.1*
Ca^{2+}	meq/L	1.9	*0.2*
Mg^{2+}	meq/L	2.4	*0.03*
pH	-	8.2	*0.2*
Chlorophyll *a*	mg/L	0.3	*0.1*
Chlorophyll *b*	mg/L	0.1	*0.01*
Chlorophyll *a/b*	mg/L/mg/L	3.3	*1.0*

OPGs were cultivated following the procedure of Milferstedt et al. (2017) and Kuo-Dahab et al. (2018). After activated sludge was sampled, 10mL of well-mixed aliquots were pipetted into 20mL scintillation vials and capped immediately after returning to the lab and set-up for cultivation.

5.2.2 Experimental Set-up for Chemical Addition Study in a Hydrostatic Environment

After returning to the lab, and before capping vials, chemical treatments, 10 meq/L, 20 meq/L, and 40 meq/L Mg^{2+}, 10 meq/L, 20 meq/L, and 40 meq/L Ca^{2+}, 10 meq/L, 20 meq/L, and 40 meq/L Na^{+}, 1mM dextrose, 5mM dextrose and 1mM EDTA (Figure 1) were added to individual vials containing 10mL of activated sludge from Amherst and Hadley sludge sources. The treatments were chosen based on literature

and to give a low, middle, and high concentration range. Two control treatments (one for each sludge) were also set-up for cultivation. Each treatment group was composed of 15 vial replicates for a total of 390 vials for the two sludge sources. Cations, Na^{+}, Ca^{2+} and Mg^{2+} were chosen for their role in the aggregation and bioflocculation of activated sludge. Ethylenediaminetetraacetic acid (EDTA), a chelating agent, was chosen because of its ability to remove Ca^{2+} from activated sludge. The cationic bridging model was proposed by Kakii et al. (1985) and Eriksson and Alm (1991) who observed reduced settling and dewatering characteristics when EDTA was added to activated sludge. Dextrose addition was chosen due to its ability to inhibit different microbial processes (i.e., sulfate reduction). Vials were kept in hydrostatic conditions, illuminated under broadband LED lights at approximately 10 kLux, 24 hours per day at 18°C. Vials were monitored over a period of 42 days and at the end of the study, each vial was characterized based on the morphology of the biomass. A "disc granule" is defined as biomass that remained intact after a shake test, but biomass was in the shape of an ellipse or ellipsoid. A "spherical granule" is defined as biomass that remained intact after a shake test, but biomass was in the shape of a sphere. Biomass that did not remain intact after the shake test is defined as "floccular biomass." To determine the success of granulation, a shake test was performed on the vials as described by Stauch-White et al. (2017). Briefly, three firm vertical shakes by hand are applied, then observing the vial contents. When the biomass remained intact with little to no cloud of visible particulates in the bulk liquid, granulation was determined to be successful. The chemical addition experiments were performed at two different time points, July and December to account for seasonal variation in activated sludge at both treatment plants. This study was performed prior to an in-depth progression and characterization study to determine more specific quantities for chemical addition for each treatment.

5.2.3 Experimental Set-up for Progression and Characterization Study with Chemical Addition in a Hydrostatic Environment

Hadley sludge was collected and after returning to the lab, chemical treatments, 20 meq/L Na^{+}, 40 meq/L Ca^{2+}, and 20 meq/L Al^{3+}, were added to individual vials as salts. Additionally, a light control or activated sludge with no chemical addition (a normal cultivation) and a dark control were included. A total of 240 vials for each sludge treatment and control sets were set-up (total of 1,200 vials). Additional activated sludge was used for day 0 chemical analysis and t=0 represents initial conditions of the experiment and water quality for the activated sludge sets. Only one sludge source was chosen for progression and characterization study based on results from Chapter 4, showing that two sludge sources show significantly similar trends during hydrostatic photogranulation. Vials were kept in hydrostatic conditions, illuminated under broadband LED lights at approximately 10 kLux, 24 hours. per day at 18°C. Sampling was performed at day 0, 3, 9, 27. At day 27, the cultivation was considered complete, and a final sample collection was performed. To determine the success of granulation (100% of vials at the end of cultivation yielded a granule), a shake test was performed on remaining vials (n=20) by using three firm shakes by hand then observing the vial contents. When a granule remained intact with little or no cloud of particles in the bulk liquid, the granulation was determined to be a success.

5.2.4 Analytical Procedures

Phototrophic microorganisms can be indirectly quantified by extracting and measuring the concentration of chlorophyll in the biomass. Green algae contain both chlorophyll *a* and *b*. Cyanobacteria, on the other hand, only contain chlorophyll *a* and

accessory pigment proteins known as phycobilins. Chlorophyll *a/b* ratio can be used as a surrogate to represent cyanobacterial growth.

Solids content, total suspended solids (TSS) and volatile suspended solids (VSS), and chemical oxygen demand (COD) were measured at each sampling date using triplicate samples, all according to APHA standard engineering methods (APHA, 1998).

Dissolved organic carbon (DOC) and dissolved total nitrogen (DTN) using a Shimadzu TN/DOC analyzer (Shimadzu TOC-VCPH with TNM-1, Shimadzu North America, SSI Inc., Columbia, MD, USA).

Dissolved constituents in the bulk liquid: dissolved nitrogen species, nitrate (NO_3^--N), nitrite (NO_2^--N), and ammonium (NH_4^+-N), and divalent and monovalent anions, phosphate (PO_4^{3-}), sulfate (SO_4^{2-}), and cations, sodium (Na^+), potassium (K^+), calcium (Ca^{2+}), and magnesium (Mg^{2+}), were measured using a Metrohm 850 Professional Ion Chromatograph (IC) (Metrohm Inc., Switzerland) with a Metrosep A Supp 5-250 anion column and Metrosep C 2-250 cation column.

5.2.5 Microscopy

The development of granules was observed by using a transmitted light (EVOS FL Color AMEFC 4300). Images by light microscopy were obtained periodically to check granule development during different phases. Literature was used for identification of microorganisms in the samples.

5.2.6 EPS Extraction and Chemical Analysis

All samples were pretreated by centrifugation and homogenization prior to EPS extraction. Bound crude EPS was extracted by three different extraction methods,

cation-exchange resin (CER), alkaline or base treatment (NaOH), and particle agitation by sonication. Base and sonication treatments followed the procedure of Kuo-Dahab et al. (2018) and Chapter 4 (8). Following extraction, crude extracts were centrifuged, filtered and characterized.

5.2.6.1 Sample Pretreatment

Each sample vial initially contained 10 mL of activated sludge (which later became one OPG). The cultivation initially contained 420 individual vial samples. At each sampling time point, samples were collected and destructively sampled in triplicates or three 10 mL samples and individually processed as three separate samples. Each individual 10 mL sample was transferred from scintillation vial to a sterile 50mL centrifuge tube and centrifuged at 4°C and 12,000 rpm for 20 min. The supernatant was collected and filtered through 0.45 µm cellulose filters to determine the chemical composition of the liquid phase of the vial contents also known as soluble EPS fraction. The pellets were resuspended in phosphate buffer solution (10 mM NaCl, 1.2 mM KH_2PO_4, and 6 mM Na_2HPO_4; pH 7.2) to a total volume of 20 mL in the same 50mL centrifuge tubes. Phosphate buffer was prepared according to Frølund et al. (1995, 1996), the conductivity of the buffer was made to be the same as the conductivity found for the activated sludge inoculum at a pH of 7.2 (Frølund et al., 1995, 1996). Each replicate was homogenized individually (500 W IKA T18 ULTRA-TURRAX) for 30 sec. After sample pre-treatment, samples were equally divided and each of the four extraction approaches were applied to each triplicate set, as described in the next sections.

5.2.6.2 Cation-Exchange Resin Extraction

EPS extraction using Dowex 50x8, Na+ Form, cation-exchange resin (DOWEX) was performed with a 0.5 g of VS-to-35 g of cation exchange resin ratio according to the method of Frølund et al. (1995,1996). Resin was pre-washed in phosphate buffer (10 mM NaCl, 1.2 mM KH_2PO_4, and 6 mM Na_2HPO_4; pH 7.2). For each individual sample, 50 mL centrifuge tubes were used with 20 mL sample to provide adequate mixing. 70g/g VS of CER was weighed and added to each centrifuge tube based on initial VS concentration of the sample. The samples were mixed at 400 rpm on a shaker table for 2 hr in the dark at 4°C. A Milli-q water with CER and phosphate buffer (10 mM NaCl, 1.2 mM KH_2PO_4, and 6 mM Na_2HPO_4; pH 7.2). was also tested at the start of the study as a blank control.

5.2.6.3 Sodium Hydroxide (NaOH) Extraction

Homogenized samples (suspended in 20 mL phosphate buffer; 10 mM NaCl, 1.2 mM KH_2PO_4, and 6 mM Na_2HPO_4; pH 7.2) were adjusted to a pH 10.5 by using 1 M NaOH and mixed at 400 rpm for 2 hours in the dark at 4°C (20). A blank vial with phosphate buffer adjusted to pH 10.5 with NaOH was also measured as a blank control.

5.2.6.4 Sonication Extraction

Homogenized samples (suspended in 20 mL phosphate buffer; 10 mM NaCl, 1.2 mM KH_2PO_4, and 6 mM Na_2HPO_4; pH 7.2) were placed on ice and a 400 W sonic dismembrator (Fisher Scientific model 500) was used at 10% strength for 1 min at 20 kHz. This delivered an ultrasonic dose of approximately 4.1 W-min/mL, following the calculation shown by Muller (2006).

5.2.6.5 EPS Characterization

After each extraction method, whole samples (20mL) were centrifuged at 4°C at 12,000 x g for 20 min and filtered by 0.45 µm cellulose filter. Afterward, EPS supernatant was stored at -20°C in aliquots until chemical analyses were performed. TOC and TN in EPS extracts were measured using the same procedure as the liquid phase. Proteins, polysaccharides, and humic acids were measured according to modified Lowry- and DuBois methods, respectively (Dubois et al., 1956; Frølund et al., 1995, 1996; Lowry et al., 1951). Bovine albumin serum, glucose and humic acids were used as standards.

5.2.7 Ammonium Sulfate Precipitation ($(NH_4)_2SO_4$)

Crude EPS extracts, from each method, were precipitated following the procedures of Park and Novak (2007), based on salting-out characteristics. EPS was precipitated by addition of ammonium sulfate ($(NH_4)_2SO_4$) (Park & Novak, 2007). $(NH_4)_2SO_4$ salt is often used as a protein precipitant due to its high solubility and ability to stabilize protein structure. At high salt concentrations or high ionic strength, proteins will precipitate out of solution. The solubility of proteins by ammonium sulfate is typically expressed as a function of the percent saturation. As more salt is added to the mixture, there is an increase in the surface tension of the water, thus increasing hydrophobic interactions between water and proteins. This ultimately leads to protein precipitation. In other words, with increasing ammonium sulfate concentrations, more hydrophilic proteins are precipitated. Samples were placed in 50 mL centrifuge tubes and solid $(NH_4)_2SO_4$ was added in one step to provide salt saturation levels of 90%. The precipitation was performed at 4℃ on a shaker table for at least 12 hours, usually overnight, until all solid $(NH_4)_2SO_4$ dissolved. The precipitate was recovered by centrifugation (20,000 x g, 20 min). The pellet was resuspended in 1.5 mL of PBS and

dialyzed for at least 24 h in the same PBS buffer with two changes of buffer at 4℃ on a shaker table. Samples were dialyzed using 6.8 kDa cellulose membrane dialysis tubing, excluding all samples smaller than 6.8 kDa.

5.2.8 Sodium Dodecyl Sulfate Polyacrylamide Gel Electrophoresis (SDS- PAGE)

Sodium dodecyl sulfate polyacrylamide gel electrophoresis (SDS-PAGE) was performed to investigate the EPS SDS-PAGE protein profile expressed during hydrostatic photogranulation of activated sludge for control and treated samples. SDS-PAGE is a technique that separates out proteins in a sample and yields valuable information on the similarity or dissimilarity of the sample. SDS-PAGE produces complex banding patterns of different molecular mass proteins, which is reproducible and can be considered a “fingerprint” of the sample that is investigated (Kersters & De Ley, 1975, 1980). The resulting protein profiles after SDS-PAGE can lead to a better understanding of the dynamics and diversity of microbial communities in the sample.

SDS- PAGE was performed according to the method of Laemmli (1970). Precast 4-12% Criterion™ Bis-Tris protein gels (12+2 well, 45 µL) were used for separations (Biorad, Hercules, CA). Protein concentration was measured in each sample using the modified Lowry procedure (1951) and samples were diluted with ultra-pure water in 2 mL centrifuge tubes. Samples were mixed with SDS-PAGE Biorad XT sample buffer (4-times) and Biorad XT reducing agent (20-times). The mixture was heated in a closed vial at 95℃ for 10 min, then the vial was opened for approximately 20 min to concentrate the samples down to 1.5 mL. Samples were briefly vortexed for 30 sec. then centrifuged at 22,000 x g for 1 min to remove debris, and the supernatant was loaded onto the SDS-PAGE gel. Protein concentration was quantified following modified Lowry method (Frølund et al., 1996) and a total mass of 8 µg of EPS protein was added to each well.

Precision Plus Protein™ dual color pre-stained protein standards were used for ladders (Biorad, Hercules, CA). Gels were run at 50 volts for 150 min then 70 volts for 75 min. for a total run time of 225 min. When electrophoresis was complete, the gel was washed with ultra-pure water and stained using the Pierce Silver Stain kit (Thermo Scientific, Waltham, MA).

5.2.9 Statistical Analysis

Correlation analysis was performed in R (R Core Team, 2021) using R studio (RStudio Team, 2021) interface to compute correlations and significance between two variables. Each variable is the average for the values collected in triplicate. The correlation analysis was done for every variable over the course of photogranulation and explored during different phases of photogranulation. The “PerformanceAnalytics” package (Peterson & Carl, 2020) was used to investigate the dependence between two variables at the same time and presented in a correlation matrix. Pearson correlation coefficient is presented which measures the linear dependence between two variables. Each correlation matrix plot shows the distribution of each variable along the diagonal. On the bottom section of the diagonal, the bivariate scatter plots with a fitted line are displayed. On the top section of the diagonal, the value of the Pearson correlation coefficient plus the significance level as stars. Each significance level is associated to a symbol: p-values (0.001, 0.01, 0.05, 0.1, 1) correspond to symbols (“***”, “**”, “*”, “.”, " “).

5.3 Results

5.3.1 Photogranulation with Chemical Addition Study in a Hydrostatic Environment

Activated sludge was collected from an open aeration basin from two different full-scale wastewater treatment plants (WWTP), Amherst and Hadley. This study investigated the effect of chemical addition in a hydrostatic environment on successful photogranulation. Briefly, vials were cultivated, according to procedure above, over a period of 42 days and each vial was characterized based on morphology of the biomass using a shake test to determine the success rate of granulation with chemical addition.

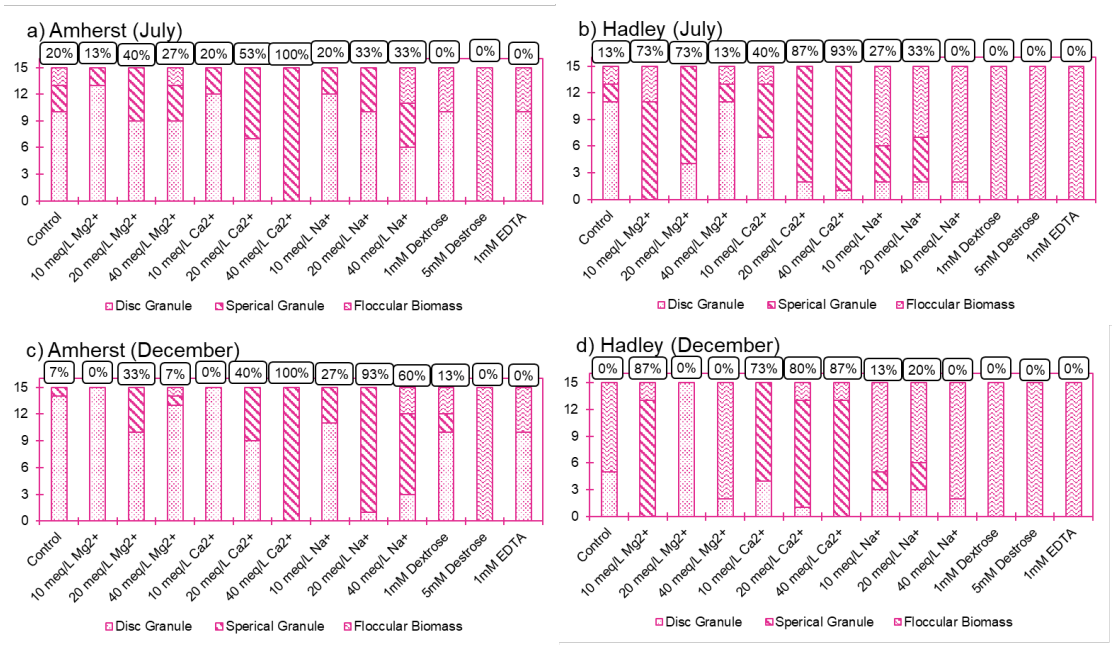

Figure 5.1: Photogranulation with Chemical Addition Study in a Hydrostatic Environment Final Granule Count. Panel a) Amherst sludge in July, b) Hadley sludge in July, c) Amherst sludge in December, and d) Hadley sludge in December. Control or treatment is indicated on the x-axis while sample number (n=15 total) or vial numbers is indicated on the y-axis. The dots indicate number of disc granules, the diagonal lines indicate the number of spherical granules, and the waved lines indicate number of vials with floccular biomass. The labels indicate the percent of successful spherical granules out of n=15 vials.

Results from the end of the study are presented in Figure 5.1. Both the success rate of granulation or total number of disc and spherical granules, and spherical success rate or total number of spherical granules only were calculated for each treatment. Percentages in graphs indicate the percentage of successful spherical granules out of n=15 samples or vials.

The addition of cations at most concentrations increased the percentage of total granules, except the EDTA and dextrose treatments, which had a percentage equal to or less than the control (Figure 5.1)

The addition of Mg^{2+} varied across sludge source and seasonality. For July, Mg^{2+} showed a high percentage of total granules (n>87%) for all three concentrations (10, 20, and 40 meq/L) for Amherst and Hadley (n>73%) sludge. Amherst and Hadley showed

relatively low percentage of spherical granules for all concentrations (<40%), except Hadley 10 and 20 meq/L (10 meq/L Mg^{2+}: n=73%; 20 meq/L Mg^{2+}: n=73%). For the December cultivation period, all concentrations (10, 20, and 40 meq/L) of Mg^{2+} increase total percentage of granules for Amherst (n>93%) but had low percentage of spherical granules (n<33%). For Hadley, 10 and 20 meq/L Mg^{2+} showed a high percentage of total granules (n>87%) with 40 meq/L showing low percentage (n=13%). Hadley 10 meq/L Mg^{2+} addition also showed a positive effect on percentage of spherical granules (n=87%), but no spherical granules appeared for 20 and 40 meq/L Mg^{2+}addition.

In contrast to Mg^{2+}, for the July sludge sets, the addition of 10, 20 and 40 meq/L Ca^{2+} increased the percentage of total granules for all concentrations for both sludges (n>87%). For both sludges, the percentage of spherical granules increased with higher Ca^{2+} concentrations (Amherst: 10 meq/L: n=20%; 20 meq/L: n=53%; 40 meq/L: n=100%; Hadley: 10 meq/L: n=40%; 20 meq/L: n=87%; 40 meq/L: n=93%). For December, similar results are also observed for all concentrations (10, 20 and 40 meq/L Ca^{2+}), with a high percentage of total granules (n>87%) for both sludge sources. The percentage of spherical granules increased with higher Ca^{2+} concentrations for both sludge sources (Amherst: 10 meq/L: n=0%; 20 meq/L: n= 40%; 40 meq/L: n=100%; Hadley: 10 meq/L: n=73%; 20 meq/L: n=80%; 40 meq/L: n=87%).

In comparison to controls which showed n=87% success rate for total granules, for both sludge sources in July. Percentage of spherical granules is n=20% and n=13% for Amherst and Hadley, respectively. For December, Amherst control granulated n=100% for total granules and with n=7% spherical granules, while Hadley control granulated at n=33% for total granules but no spherical granules. These results suggest that the divalent cation Ca^{2+} may have a stronger positive effect on photogranulation by producing spherical granules, versus Mg^{2+} addition, by increasing the total percentage of granules and spherical granules for any given cultivation (Figure 5.1). Additionally,

results also show that Mg^{2+} may have some positive effect as well on granulation with changes in season, but was not determined precisely during this study. Examples of final granules are presented in Figure 5.2.

The results presented in Figure 1 also suggest that monovalent cation Na^{+}, at lower concentrations, like 10 or 20 meq/L, may have a positive effect on the percentage of granules and spherical granules during photogranulation. During the July cultivation period, 10, 20, and 40 meq/L Na^{+} increased the percentage of granules in Amherst sludge (10 meq/L: n=100%; 20 meq/L: n=100%; 40 meq/L: n=73%), but low percentage of spherical granules for all concentrations (n<33%). Hadley showed no increase in total granules (n<47%) but did show increase in the total percentage of spherical granules for 10 meq/L (n=27%) and 20 meq/L (n=33%), in comparison to the light control. During the December cultivation, all Amherst Na^{+} show an increase in percentage of total granules (n>80%) and showing an increase in total spherical granules for 10 meq/L (n=27%), 20 meq/L (n=93%), and 40 meq/L (n=60%) in comparison to the control. In contrast, Hadley sludge only shows an increase in total granule percentage for 20 meq/L Na^{+} (n=40%) and total spherical granules for 10 meq/L Na^{+} (n=13%) and 20 meq/L Na^{+} (n=20%).

The addition of 1mM and 5mM dextrose and 1 mM EDTA was also tested (Figure 5.1). These chemical treatments and concentrations showed negative impacts on photogranulation. The negative impacts resulted in lower percent of total granules and spherical granules at the end of the cultivation period, in comparison to the control.

The results presented in Figure 5.1 suggest that the addition of cations (Na^{+}, Ca^{2+} and Mg^{2+}), at specific concentrations, leads to a higher percentage of spherical granules in comparison to control (no treatment) vials during hydrostatic cultivation. Na^{+} at 20 meq/L and Ca^{2+} at 40 meq/L show the highest percentage of spherical granules for monovalent and divalent cations, respectively, and were selected for the in-depth progression and characterization study.

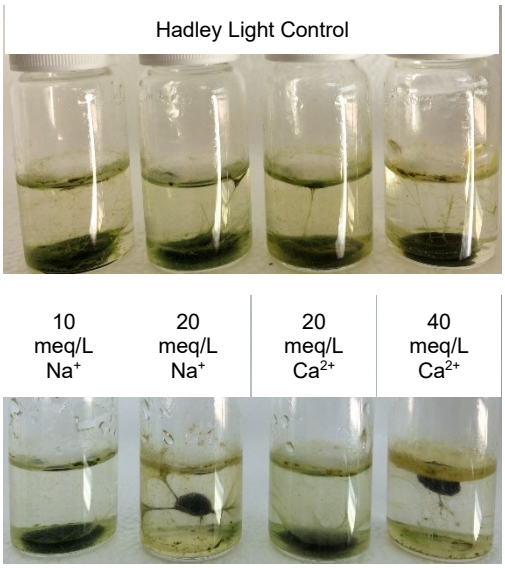

Figure 5.2: Example of Finale Granules from Chemical Addition Study

5.3.2 Progression and Characterization Study of Photogranulation in a Hydrostatic Environment

5.3.2.1 Background on Sludge Inoculum

A characterization study was completed to further examine the effect of monovalent and divalent cations during photogranulation. Based on the results from the addition study, one monovalent and one divalent cation were selected that showed a high percentage of spherical granules, the addition of Na^+ (20 meq/L) and Ca^{2+} (40 meq/L) was selected for the following in-depth characterization study. Ca^{2+} was chosen over Mg^{2+} due to the increase in both spherical and total granules for Amherst and Hadley sludge.

Activated sludge was collected from a single source, Hadley WWTP. Initial activated sludge inoculum solids content is 2720±123 mg/L TSS and 2343±112 mg/L VSS, with a VSS/TSS ratio of 86.1±2.0%. Dissolved nitrogen, DTN, DON, and DIN concentrations are 4.9±0.1, 1.7±0.0, and 3.2±0.1 mg/L-N, respectively. The initial pH of

the sludge was 8.2±0.2. Using microscopy (Figure 5.3) minimal number of microalgae were observed like previous literature (Kuo-Dahab et al., 2018; Milferstedt et al., 2017) and Chapter 3 and 4. This is supported by low initial chlorophyll a, b concentrations which are 0.3±0.1 and 0.1±0.0 mg/L, respectively.

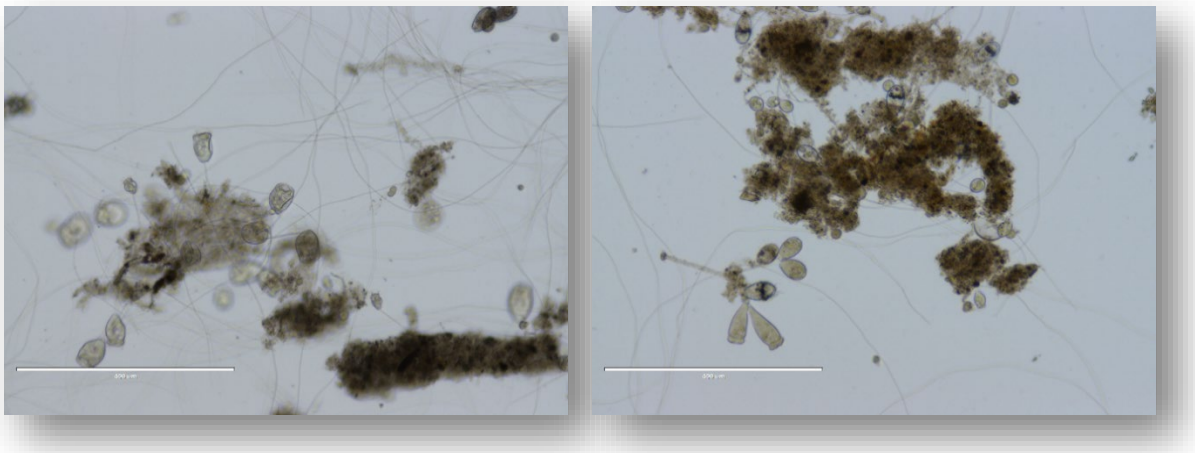

Figure 5.3: Hadley Sludge (t=0) Showing Minimal Numbers of Microalgae. Scalebars are set to 400µm

5.3.3 Final Granule Count

At the end of the cultivation period, 20 vials remained for each treatment in order to determine photogranulation succession. Using the aforementioned methodology, granulation was classified based on biomass morphology and a shake test. Results are presented in Table 5.2, including both the success rate of granulation or total number of disc and spherical granules, and spherical success rate or total number of spherical granules. The addition of 20 meq/L Na^+ and 40 meq/L Ca^{2+} had a positive effect on the total granule and spherical granule percentages in comparison to the control. The light+Na^+ treatment percentage of total granules was the same as the light control, however the treatment had a greater percentage of spherical granules in comparison to the control, 35% and 25%, respectively. The light+Ca^{2+} had both a higher percentage of

total granules, 100%, and spherical granules, 100%, in comparison to the light control with total granules of 90%, and spherical granules, 25%. These results suggest that Na^+ and Ca^{2+} addition has a positive effect on the total percentage of granules and spherical granules. However, results also indicate that Ca^{2+} may be more impactful in comparison to Na^+ based on final percentages.

Table 5.2 Final Granule Count for Hydrostatic Photogranulation with Three Different Treatments

		*Granule (Disc or spherical)					Spherical	Total Granules
Source	Treatment	Disc	Spherical	Floccular Biomass	Total "granules"	Total vials	Success Rate	Success Rate
Hadley	Light Control	13	5	2	18	20	25%	90%
	Light+Ca^{2+} (40 meq/L)	0	20	0	20	20	100%	100%
	Light+Na^+ (20 meq/L)	11	7	2	18	20	35%	90%
	Dark Control	0	0	20	0	20	0%	0%

5.3.3.1 Biomass Morphology, Chlorophyll, and Nitrogen Trends During Photogranulation

Chlorophylls and nitrogen species are presented in Figure 5.4 and Figure 5.6. Phases of photogranulation presented by Kuo-Dahab et al., 2018 were adopted for this study. Sludge compaction appeared at day 0 until day 3. During the first 3 days sludge biomass settled and became visibly more compact. Chlorophylls were detected in initial sludge inoculum for all treatments, but at low levels, in comparison to the proceeding days of the cultivation (Figure 5.4). Chlorophyll a was found to increase slightly during the first 3 days of granulation. All plants, algae and cyanobacteria that photosynthesize contain chlorophyll a pigment. Chlorophyll b pigment is present only in green algae and plants. Chlorophyll *a/b* ratio is used as an indicator for cyanobacterial growth as they only contain chlorophyll a pigment. Here, chlorophyll a/b increases significantly for the light+Ca^{2+} treatment, while the control and Na^+ treatment remain relatively low. The phototrophic bloom period typically occurs between day 3 and day 14 (Kuo-Dahab et al.,

2018; Chapter 4). The biomass initially floated to the top of the liquid in the vial between day 3 and 9, and the morphology of the biomass began to change with the appearance of motile, filamentous cyanobacteria for all light treatments, verified by light microscopy (videos not shown). This is observed with an increase in chlorophyll a until day 27 for all treatments, however only a significant increase in chlorophyll a/b ratio is shown for light+Ca^{2+} treatment.

Chlorophyll a show significant positive correlation (Figure 5.5) between the light control and light+Na^{+} (r=0.99; p-value=0.05) and light+Ca^{2+} (r=1.0; p-value=0.01). Chlorophyll a/b ratio show a positive insignificant correlation between the light control and light+Na^{+} (r=0.90; p-value=1.0) and light+Ca^{2+} (r=0.84; p-value=1.0). Green algae contain both chlorophyll *a* and *b*. Cyanobacteria, on the other hand, only contain chlorophyll *a* and accessory pigment proteins known as phycobilins. Chlorophyll *a/b* ratio can be used as a surrogate to represent cyanobacterial growth. These results suggest that cation addition may have an effect on cyanobacterial growth in both treatment conditions in comparison to the control. Additionally, Ca^{2+} addition may have greater effect as the chlorophyll a/b ratio was significantly higher than the light and dark control and the light+Na^{+} treatment.

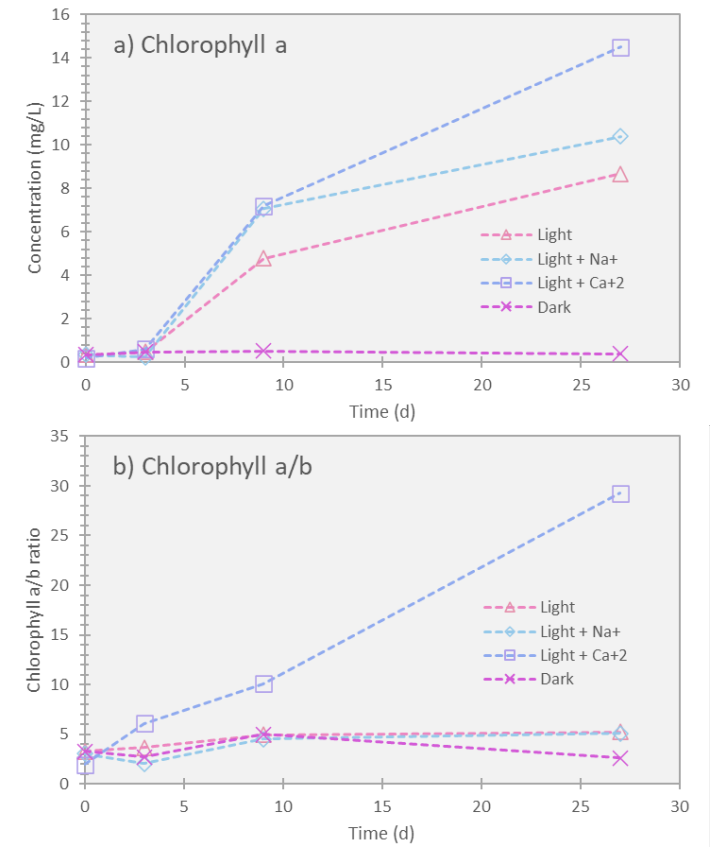

5.4: The Fate of a) Chlorophyll a and b) Chlorophyll a/b Ratio During Hydrostatic Cultivation of Photogranules for Light Control, Light with the Addition of Na+, Light with the Addition of Ca^{2+}, and Dark Control. Hydrostatically formed photogranules were formed from activated sludge inoculum. Error bars represent the standard deviation of triplicate vial samples.

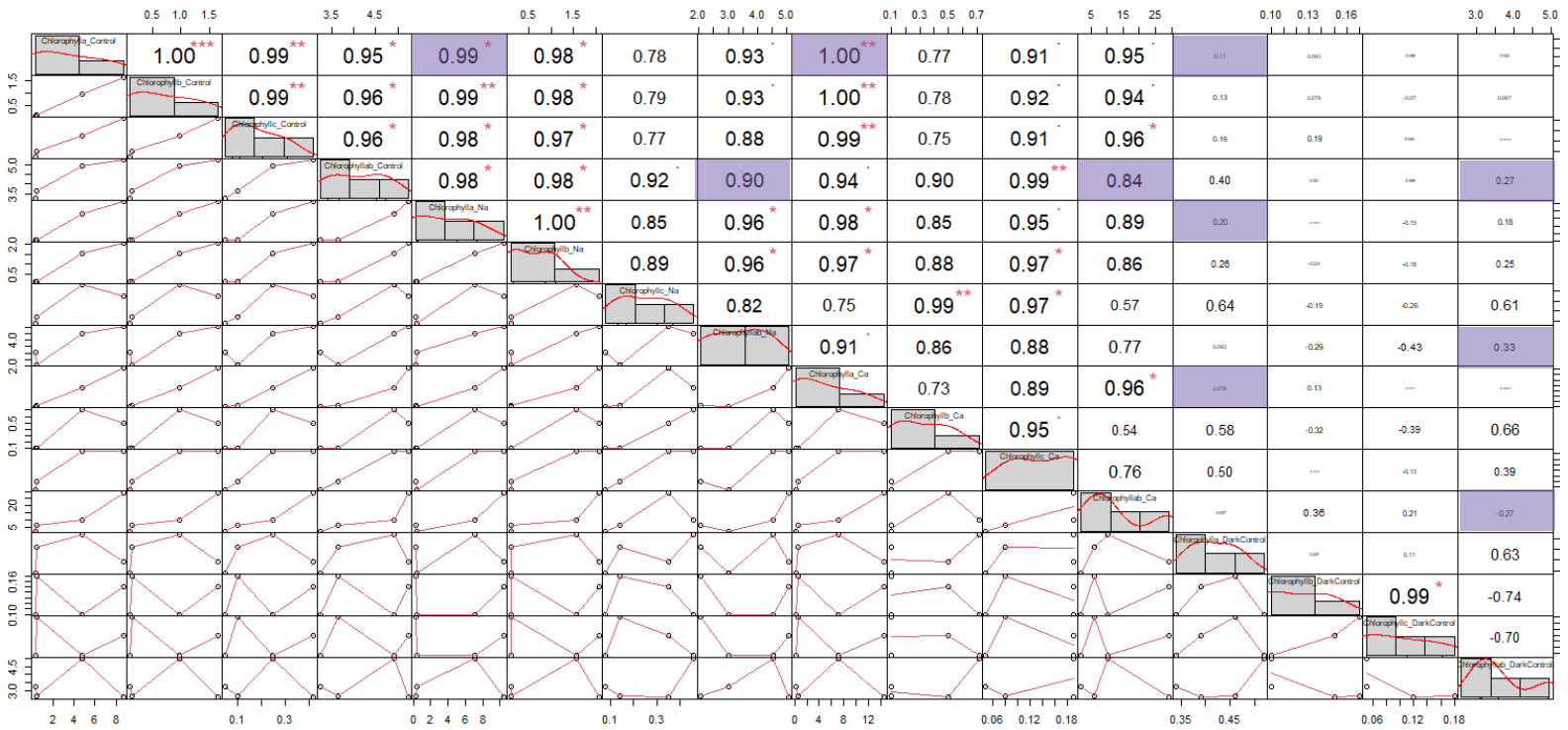

Figure 5.5: The correlation of chlorophylls between different treatments for Hadley sludge. The distribution of each variable (Chlorophyll a, chlorophyll b, chlorophyll c, and chlorophyll a/b ratio) for light control, light+Na^{+}, light+Ca^{2+} and dark control is shown on the diagonal. On the bottom of the diagonal: the bivariate scatter plots with a fitted line are displayed. On the top of the diagonal: the value of the correlation plus the significance level as stars. Each significance level is associated to a symbol: p-values (0.001, 0.01, 0.05, 0.1, 1) <=> symbols (“*”, “**”, “*”, “.”, " “).**

Along with changes in morphology and chlorophyll concentrations, changes in inorganic (DIN) nitrogen species and dissolved organic (DON) are also observed. Nitrate (NO_3^--N) and nitrite (NO_2^--N) (Figure 5.6) concentrations between the light control and the two treatments, light+Na^+, and light+Ca^{2+}, showed similar trends. Dark control showed different trends which makes sense as there is no oxygenic photosynthesis occurring and the closed environment should correspond to trends seen with batch anaerobic digestion without mixing. Similar to results shown in Chapter 4 and previous literature (Kuo-Dahab et al., 2018; Stauch-White et al., 2017), DIN or NO_2^--N and NO_3^--N are depleted immediately and remain low during photogranulation for all treatments. Light control and light+Na^+ addition show very similar trends for all N-species, while light+Ca^{2+} shows some differences with respect to magnitude of changes in concentrations.

Briefly, Ammonium (NH_4^+-N) shows an initial release into the bulk liquid during the first 3 days followed by an uptake between day 3 and 9. However, the initial NH_4^+-N release for light+Ca^{2+} treatment is lower than the release seen for the control and Na^+ treatments during the first 3 days. The initial release and uptake of NH_4^+-N occurs simultaneously with the enrichment of phototrophs as observed by an increase in chlorophyll *a* and *a/b* ratio. DON shows a slight release during the first 3 days for all treatments. A significant release of DON is observed for light and light+Na^+ treatments until day 9, which remains constant through day 27 (Figure 5.6). DON in the light+Ca^{2+} treatment is exponentially released into the bulk liquid through day 27. Dark control shows the most different trends with a large release of NH_4^+-N and a constant release of DON, commonly observed in anaerobic digestion. An increase in DON release can occur through intracellular and extracellular secretion of proteins, and other organic N decay.

These results show that Na^+ addition has little to no effect on N-species during photogranulation in comparison to the control, showing a significant positive linear Pearson correlation between light control and light+Na^+ DON (r=0.99) and NH_4^+-N (r=0.99) trends. Ca^{2+} addition may have an effect on DON and NH_4^+-N uptake and release from the bulk liquid during photogranulation, as the trends are different in comparison to the control. Light control and light+Ca^{2+} Pearson correlation for DON (r=0.84: p-value: 1.0) and NH_4^+-N (r=0.89; p-value: 1.0) are positively correlated but not significant.

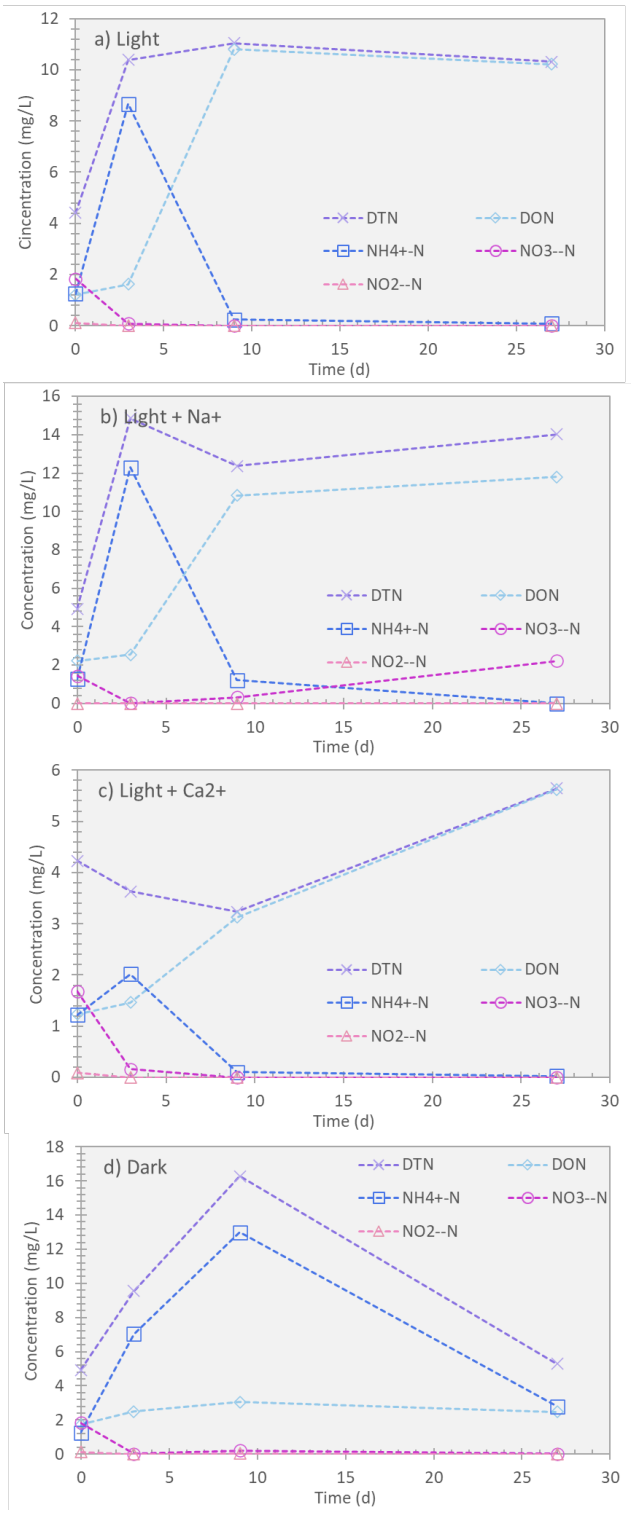

Figure 5.6: The Fate of Dissolved Nitrogen Species During Hydrostatic Cultivation of Photogranules for (a) Light Control, (b) Light with the Addition of Na^{+}, (c) Light with the Addition of Ca^{2+}, and (d) Dark Control. Hydrostatically formed photogranules were formed from activated sludge inoculum. Error bars represent the standard deviation of triplicate vial samples.

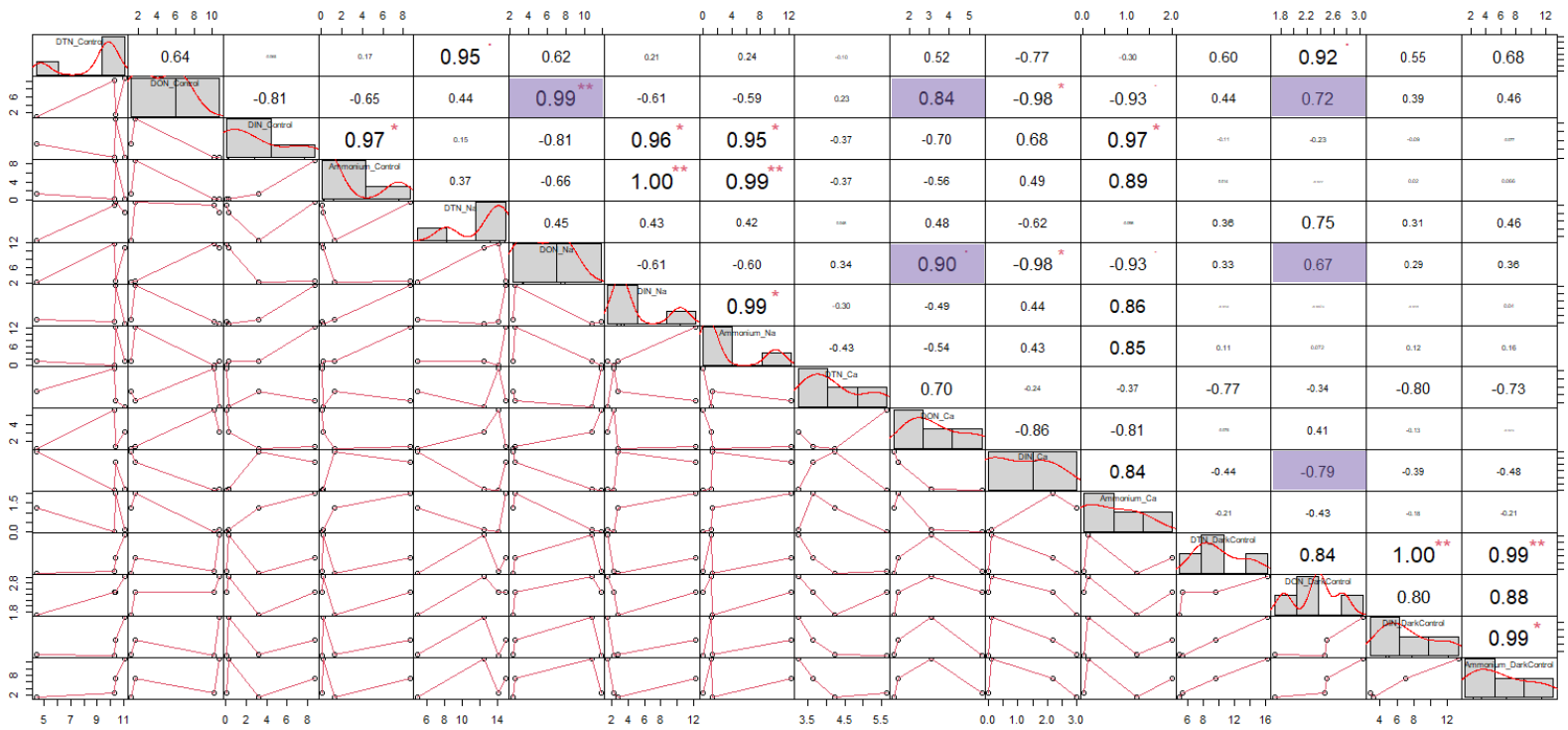

Figure 5.7: The correlation of N-species for different treatments for Hadley sludge. The distribution of each variable (DTN, DON, DIN, and NH_4^+-N) for light control, light+Na^+, light+Ca^{2+} and dark control is shown on the diagonal. On the bottom of the diagonal: the bivariate scatter plots with a fitted line are displayed. On the top of the diagonal: the value of the correlation plus the significance level as stars. Each significance level is associated to a symbol: p-values (0.001, 0.01, 0.05, 0.1, 1) <=> symbols (“*”, “**”, “*”, “.”, " “).**

5.3.4 Anions and Cations During Photogranulation

Anions, phosphate (PO_4^{3-}) and sulfate (SO_4^{2-}), and cations, potassium (K^+), sodium (Na^+), calcium (Ca^{2+}), and Magnesium (Mg^{2+}) concentrations during the photogranulation period are presented in Figure 5.8. Na^+ follows similar trend for all treatments remaining relatively constant for the duration of the cultivation (Figure 5.3), however Pearson correlation shows no significant correlation between the different treatments and light control. This suggests that the Na^+ addition may have some effect on photogranulation. K^+ trends are similar between light control and light+Na^+ treatment with an increase in concentration through day 9 followed by a decrease to day 27. In contrast, light+Ca^{2+} treatment K^+ decreases through day 9 followed by a slight increase at day 27 (Figure 5.8). Ca^{2+} shows varying trends between the different treatments, there are no significant correlations between the different treatments and light control (Figure 5.10). Briefly, light control shows an immediate release of Ca^{2+} into the bulk liquid by day 3, followed by a rapid uptake by day 9 and remaining constant at day 27. Light+Na^+ shows an overall release of Ca^{2+} into the bulk liquid by day 27 but at relatively low concentrations. Light+Ca^{2+} treatment shows a large release of Ca^{2+} by day 3, like light control, with a decrease to initial day 0 concentrations by day 27 (Figure 5.8). All treatments (except dark control) follow the same trend for Mg^{2+} with an initial release at day 3, followed by an uptake at day 9 and remaining constant at day 27 (Figure 5.8). Light control shows strong correlation with light+Na^+ treatment (r=0.99) and light + Ca^{2+} treatment (r=0.97), suggesting that the addition of cations had no effect on Mg^{2+} concentration in the bulk liquid. Mg^{2+} shows a similar trend to light control Ca^{2+} uptake during photogranulation (r=0.95). PO_4^{3-} also shows similar trends for the light and light+Na^+ treatment with an initial release followed by an uptake by day 9 and remaining at a low concentration by day 27 (Figure 5.8). Light+Ca^{2+} treatment shows an overall

uptake of PO_4^{3-} from day 0 through day 27. Light and light+Na^+ SO_4^{2-} trends are similar with an initial uptake, then a significant release at day 9, and an uptake again by day 27 (Figure 5.8). Light+Ca^{2+} treatment shows a different trend with an initial release at day 3, then an uptake through day 27 of SO_4^{2-}. These results suggest that since addition treatment (Na^+ and Ca^{2+}) are similar to light controls for some species in the bulk liquid, addition of cations may have not had an effect on PO_4^{3-}, Mg^{2+}, and SO_4^{2-} concentrations in the bulk liquid during photogranulation.

The ratio of monovalent to divalent cations was also determined for the different control (light and dark) and treatments (Na^+ and Ca^{2+}). Higgins and Novak (2002) reported that when the sum of monovalent cation concentration (Na^+, NH_4^+, and K^+) divided by the sum of the divalent cations (Ca^{2+} and Mg^{2+}) was greater than 2, then this could cause floc property deterioration. Results here show that without the addition of Ca^{2+}, ratio of monovalent to divalent cations is much greater than 2 (Figure 5.9).

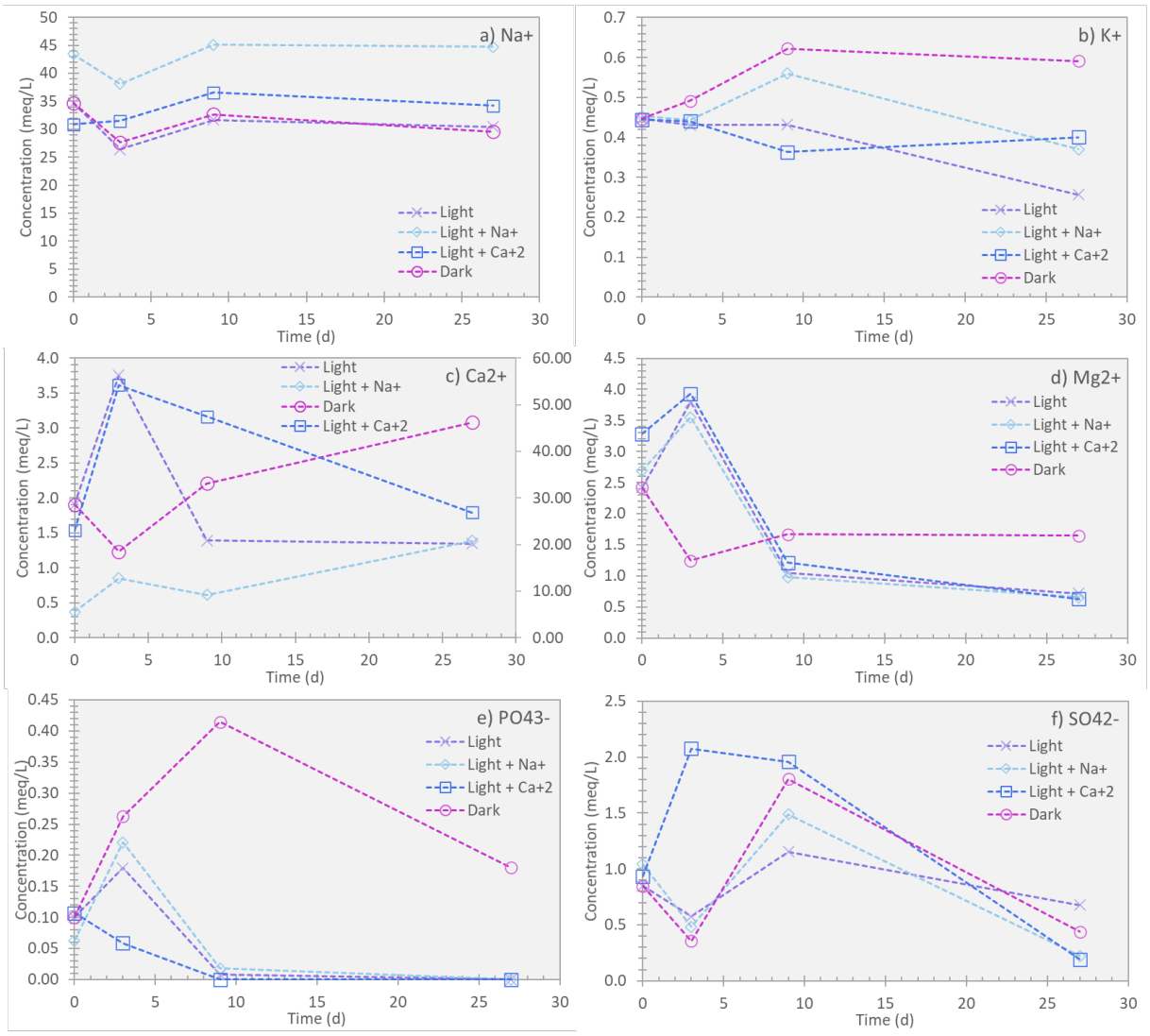

Figure 5.8: Changes in Anions and Cations in the Bulk Liquid During Hydrostatic Cultivation of Photogranules for Four Different Treatments- Light Control, Light with the Addition of $Na^{+,}$ light with the Addition of Ca^{2+} and Dark Control. Panel c) Ca^{2+} concentration is on the secondary axis.

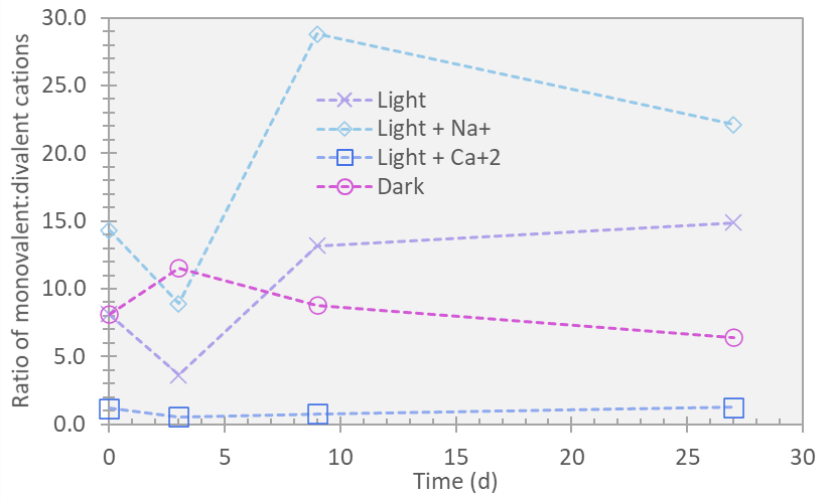

Figure 5.9: Ratio of Monovalent to Divalent Cations During Hydrostatic Photogranulation for Four Different Treatments- Light Control, Light with the Addition of Na^{+}, Light with the Addition of Ca^{2+} and Dark Control

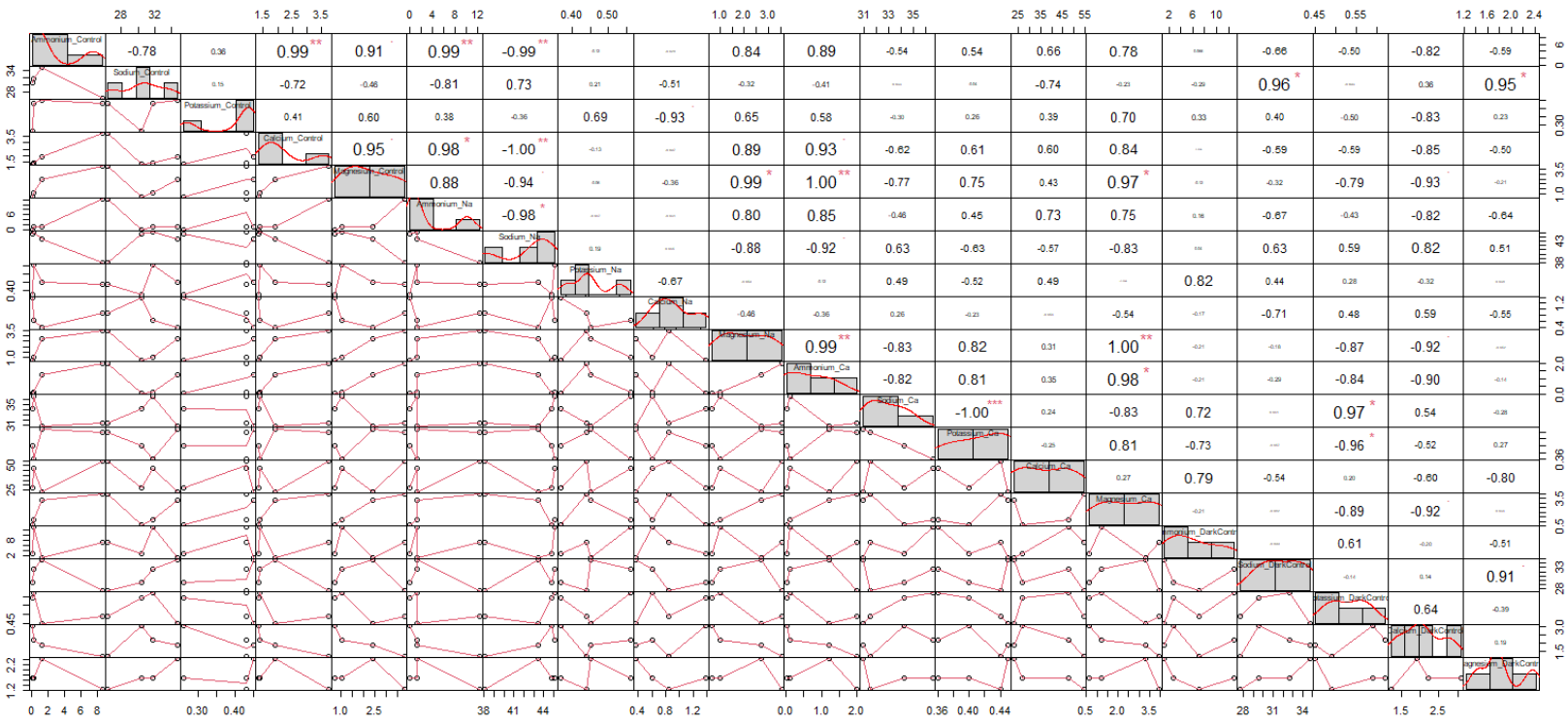

Figure 5.10: The correlation of ions between different treatments for Hadley sludge. The distribution of each variable (NH_4^+-N, Na^+, K^+, Ca^{2+}, and Mg^{2+}) for light control, light+Na^+, light+Ca^{2+} and dark control is shown on the diagonal. On the bottom of the diagonal: the bivariate scatter plots with a fitted line are displayed. On the top of the diagonal: the value of the correlation plus the significance level as stars. Each significance level is associated to a symbol: p-values (0.001, 0.01, 0.05, 0.1, 1) <=> symbols (“*”, “**”, “*”, “.”, " “).**

5.3.5 Dynamics of EPS During Progression of Photogranulation in Hydrostatic Conditions

5.3.5.1 Crude EPS During Photogranulation by Different Extraction Methods Across Cation Addition Treatments and Controls

Crude EPS (soluble and bound) proteins, polysaccharides and humic aids concentrations are presented in Figure 5.11, Figure 5.12, and Figure 5.13, respectively, during photogranulation for the three different treatments (light control, light+Na^{+}, and light+Ca^{2+}). Soluble EPS was collected using centrifugation and filtration while bound EPS was extracted using three different extraction methods, CER, base and sonication. Subsequently, each EPS extract was subject to SDS-PAGE analysis. The results for crude EPS corroborate findings by Kuo-Dahab et al., 2018 and results in Chapter 4, which shows that different EPS extraction methods led to unique protein factions.

Soluble EPS proteins showed similar trend during photogranulation across all the treatments and to the results presented in Chapter 4 and Kuo-Dahab et al. (2018) for light and dark controls. An increase in soluble proteins during day 3 to 9, with a slight decrease during the last days of photogranulation is observed (Figure 5.11). Bound EPS trends for the different extraction methods show the same trends as described in Kuo-Dahab et al. and Chapter 4 for light and dark controls. Bound EPS proteins show varying trends for the three different treatments and the three different extraction protocols. Light control base extractable proteins show high initial concentration with a 48% decrease during the first 3 days of cultivation. Base extractable proteins continue to decrease from day 3 to 27 with an overall decrease of 86% from the initial starting concentration. CER extractable proteins shows an initial 58% increase by day 3, followed by a 3% overall

decrease over the cultivation period. Sonication extractable proteins shows a consistent decrease of 75% overall over the cultivation period. Bound proteins for light+Na^+ treatment follows similar trends overall but with differences in percent of EPS that is extracted in comparison to the light control. Base extractable proteins has an initial 57% decrease during the first three days and an overall decrease of 71%. CER extractable proteins shows only a 19% initial increase but with a 35% decrease overall over the entire cultivation period. Sonication extractable proteins shows a consistent decrease of only 24% overall during the cultivation. In contrast, bound proteins for the light+Ca^{2+} treatment differs in comparison to the light and light+Na^+ treatment. Base extractable proteins has an initial decrease of only 4% until day 3 jumping up to a 54% decrease by day 9, and an overall decrease of 73% for the duration of the cultivation. CER extractable proteins shows an increase of 33% by day 3, remaining constant through day 9, and decreasing by an overall 32% from the initial concentration by day 27. Sonication extractable proteins shows a consistent decrease of 27% overall during photogranulation.

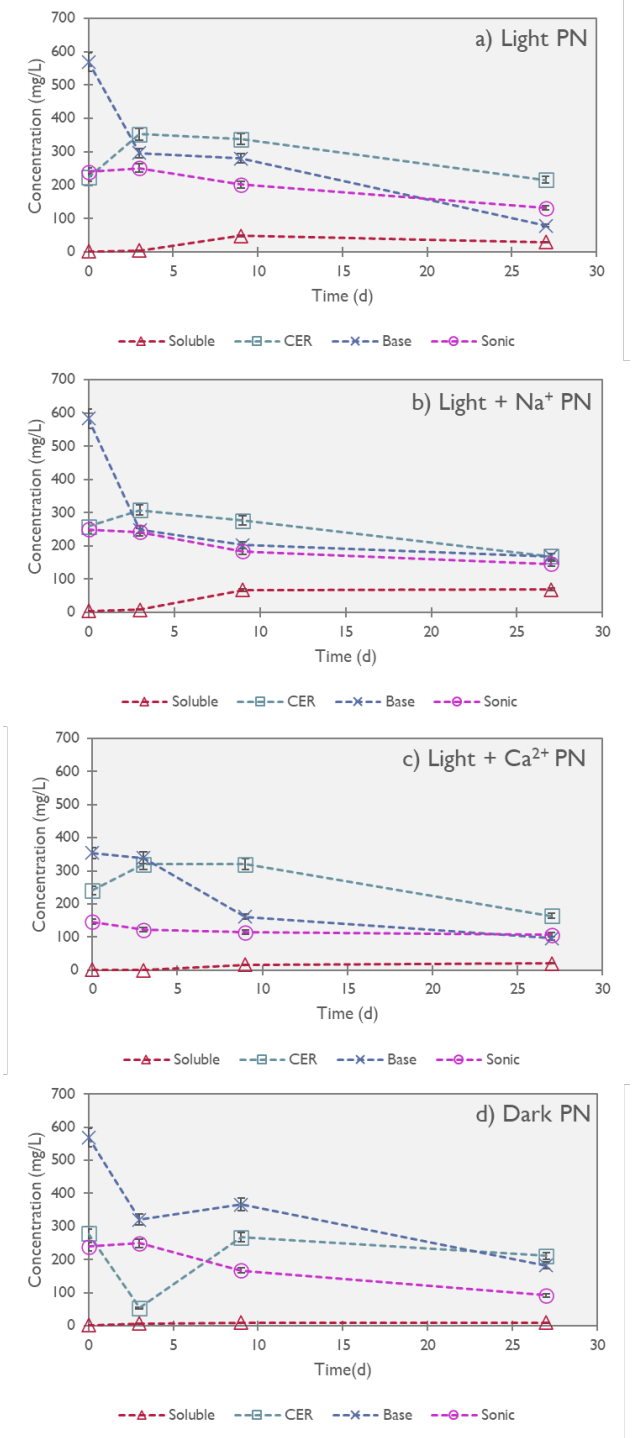

Figure 5.11: Changes in Soluble and Biomass-bound EPS Proteins (PN) During the Hydrostatic Cultivation of Photogranules. EPS are extracted by CER procedure, base and sonication treatments. Light control (a), light with the addition of Na^+ (b), light with the addition of Ca^{2+} (c), and dark control (d) are shown with concentration in mg/L on the y-axis and time in days on the x-axis. Error bars represent the standard deviation of triplicate samples.

Soluble EPS PS showed different trends between the light control and the two treatments (Na^+ and Ca^{2+}) (Figure 5.12). Light control shows an initial increase until day 9 followed by a slight decrease at the end of the cultivation. Both light+Na^+ and light+Ca^{2+} treatments show an increasing trend in soluble EPS polysaccharides until the end of the cultivation; however, the day 27 concentration is 2.7 times higher for the light+Na^+ in comparison to the light+Ca^{2+} treatment indicating a higher degree of polysaccharides solubilization from the biomass in light+Na^+ treatment. Bound base extractable polysaccharides for the light control shows a slight increase until day 3 followed by a 46% decrease until day 9, then an increase again until day 27. CER extractable polysaccharides shows a 50% increase until day 3 and remains relatively constant until day 27. Sonication extractable polysaccharides increases by 1.1 times by day 9 and remains constant until day 27. For light+Na^+ treatment, CER extracted EPS polysaccharides follows similar trend to the light control with an initial 50% increase at day 3, followed by a decrease until day 9, and then another increase by day 27 for an overall increase of 67% in polysaccharides concentration during photogranulation. Base extractable polysaccharides in the light+Na^+ treatment decreases by 56% until day 9, then remains constant until day 27. Sonication extractable polysaccharides showed similar trend to the light control, with an overall increase in concentration of 4.3 times from day 0 until day 27. Light+Ca^{2+} treatment shows increasing trends for all bound EPS polysaccharides. CER extractable polysaccharides has the highest increase at 2.3 times the initial concentration on day 27 in comparison to the other treatments. Base and sonication extractable EPS polysaccharides also increase by 8.8 and 2.0 times, respectively, in concentration from day 0 to day 27.

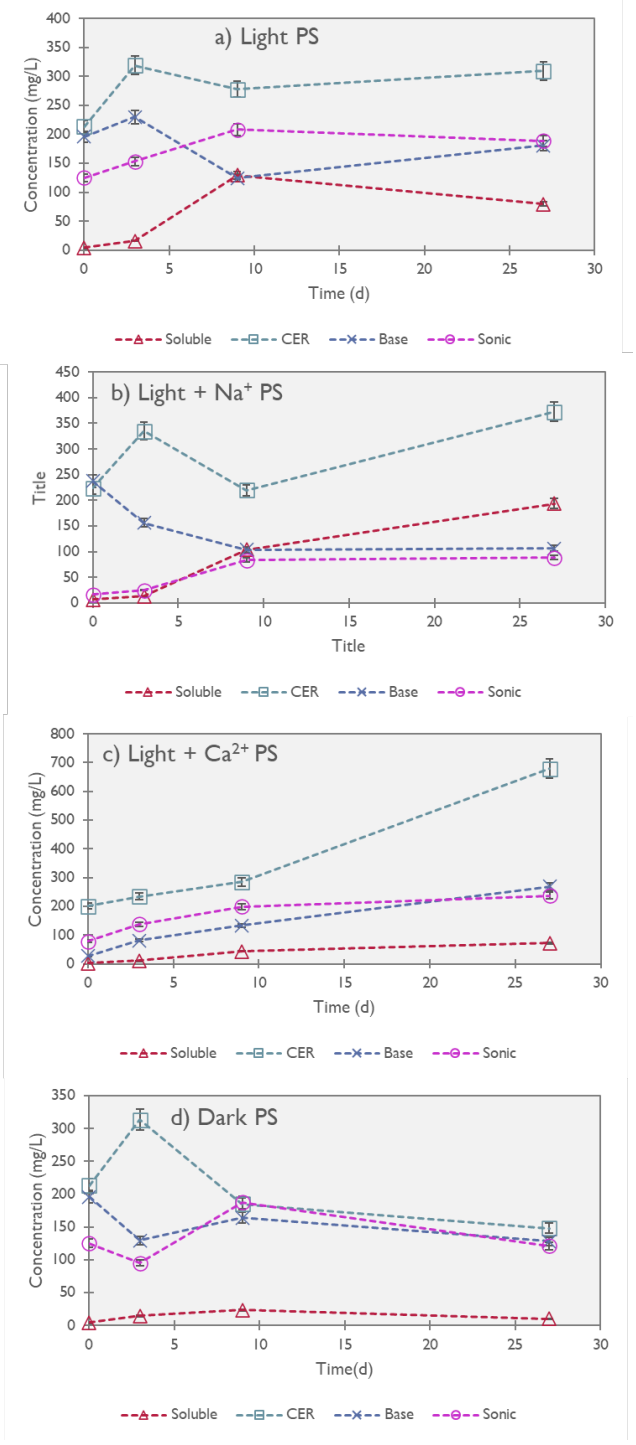

Figure 5.12: Changes in Soluble and Biomass-bound EPS PS During the Hydrostatic Cultivation of Photogranules. EPS are extracted by CER procedure, base and sonication treatments. Light control (a), light with the addition of Na^+ (b), light with the addition of Ca^{2+} (c), and dark control (d) are shown with concentration in mg/L on the y-axis and time in days on the x-axis. Error bars represent the standard deviation of triplicate samples.

All humic acid trends show very similar results between the different treatments except CER extracts, which still show a similar trend but different magnitude of intensity. On day 3, light and dark control show the greatest increases in humic acids, followed by the light+Na^{+} treatment, than light+Ca^{2+} treatment. After day 3, the trends decreased and remained relatively constant until the end of photogranulation (Figure 5.13). The EPS trends in this study for the different extraction methods all corroborate results shown in Chapter 4 for humic acids.

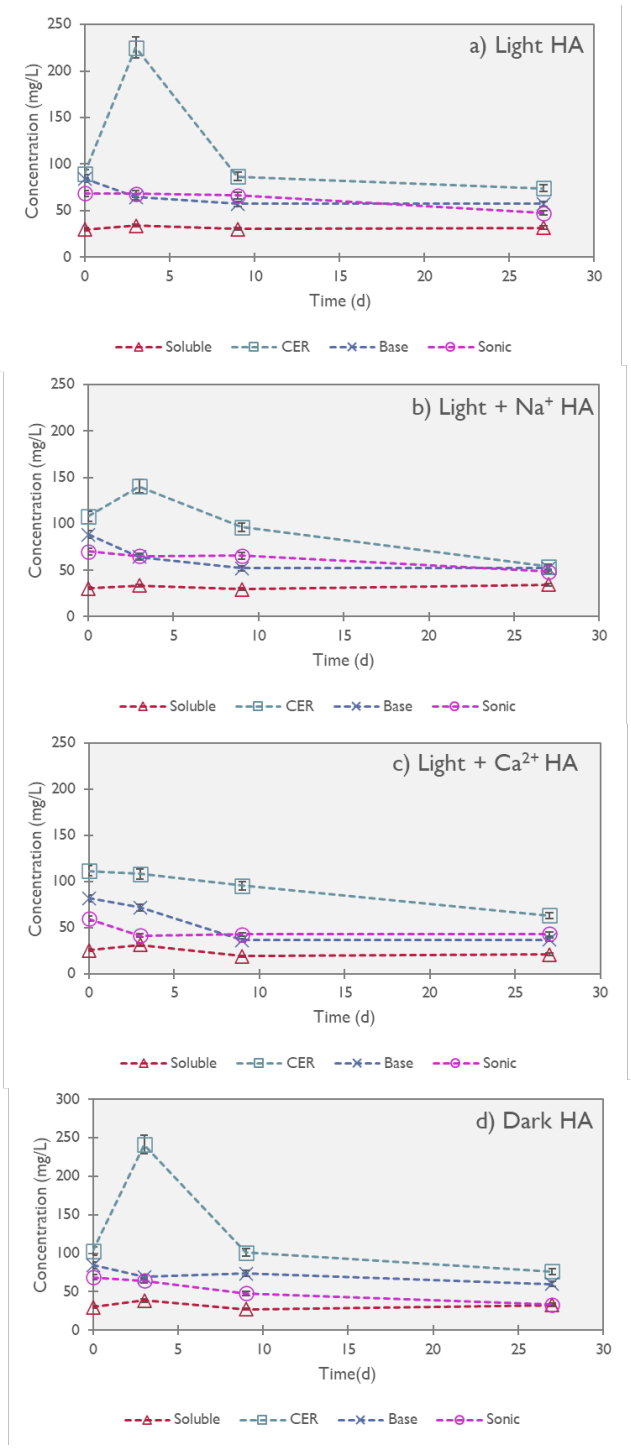

Figure 5.13: Changes in Soluble and Biomass-Bound EPS HA During the Hydrostatic Cultivation of Photogranules. EPS are extracted by CER procedure, base and sonication treatments. Light control (a), light with the addition of Na^+ (b), light with the addition of Ca^{2+} (c), and dark control (d) are shown with concentration in mg/L on the y-axis and time in days on the x-axis. Error bars represent the standard deviation of triplicate samples.

Pearson correlation analysis between extraction methods, controls and different treatments (addition of Na^+ and Ca^{2+}) was conducted. Pearson correlation coefficients are presented in Figure 5.14 to Figure 5.17. The strongest significant positive correlations shown between light control and light+Na^+ treatment were soluble proteins (r=0.93), base proteins (r=0.93), sonication proteins (r=0.96), sonication polysaccharides (r=0.94), and sonication humic acids (r=0.98). Two significant positive correlations were shown between light control and light+Ca^{2+} treatment for CER proteins (r=0.92) and sonication polysaccharides (r=0.90). These correlations were also observed in Chapter 4 and suggest that these trends are signatures of hydrostatic photogranulation that persist even with cation addition.

On the other hand, results also show that addition of divalent cation Ca^{2+} has a significant effect on the CER protein and sonication extractable polysaccharides. There is a significant increase in bound CER proteins suggesting that the addition of Ca^{2+} may increase the quantity of proteins in this fraction, potentially by physically binding more proteins in comparison to the light control. The overall concentration of polysaccharides in soluble fraction polysaccharides in the light+Ca^{2+} treatment is less than the light control, while bound polysaccharides in the sonication fraction increases in the light+Ca^{2+} treatment in comparison to the light control, suggesting that Ca^{2+} addition could also bind more polysaccharides in the sonication fraction when added during hydrostatic photogranulation. A strong significant positive correlation between soluble polysaccharides is also observed between the two treatments (Na^+ and Ca^{2+}) (r=0.99) suggesting that these are affected by cation addition, as no significant correlation was observed with light control for these two treatments. The other EPS fractions (Figure 5.14 to Figure 5.17) for light+Na^+ and light+Ca^{2+} show correlation with light control but not on a significant level (p-values= 1.0).

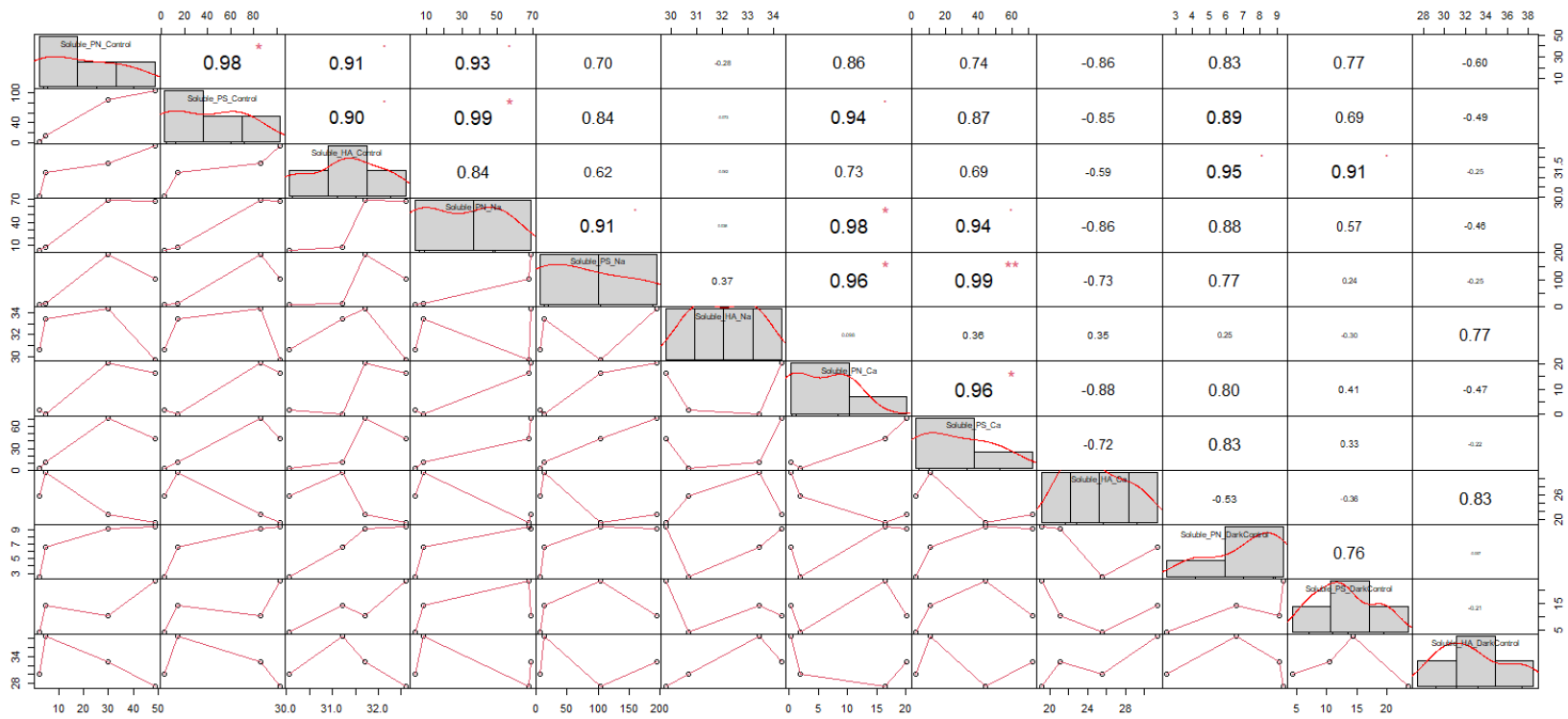

Figure 5.14: The correlation of soluble EPS between different treatments for Hadley sludge. The distribution of each variable (soluble proteins (PN), soluble polysaccharides (PS), and soluble humic acids (HA)) for light control, light+Na^{+}, light+Ca^{2+} and dark control is shown on the diagonal. On the bottom of the diagonal: the bivariate scatter plots with a fitted line are displayed. On the top of the diagonal: the value of the correlation plus the significance level as stars. Each significance level is associated to a symbol: p-values (0.001, 0.01, 0.05, 0.1, 1) <=> symbols (“*”, “**”, “*”, “.”, " “).**

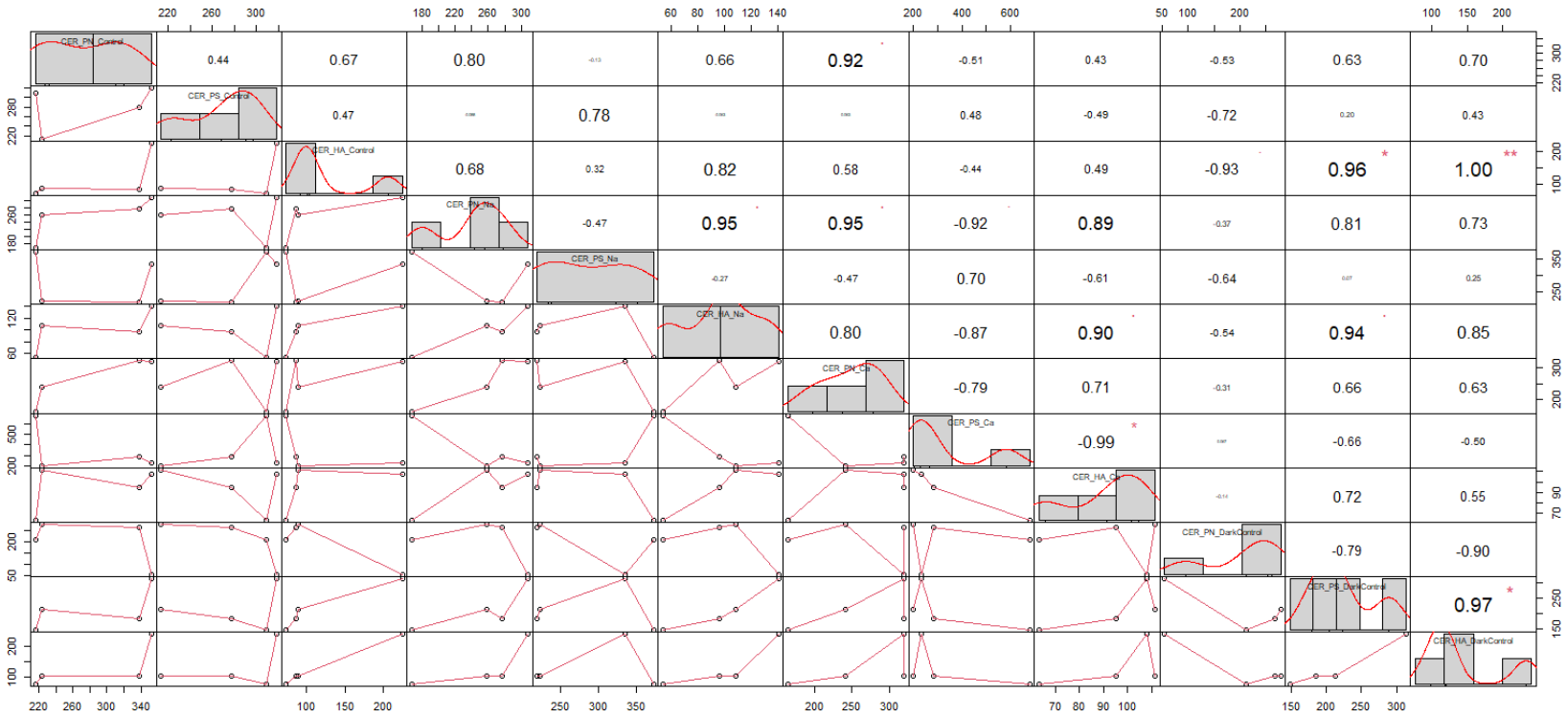

Figure 5.15: The correlation of soluble EPS between different treatments for Hadley sludge. The distribution of each variable (CER proteins (PN), CER polysaccharides (PS), and CER humic acids (HA)) for light control, light+Na^{+}, light+Ca^{2+} and dark control is shown on the diagonal. On the bottom of the diagonal: the bivariate scatter plots with a fitted line are displayed. On the top of the diagonal: the value of the correlation plus the significance level as stars. Each significance level is associated to a symbol: p-values (0.001, 0.01, 0.05, 0.1, 1) <=> symbols (“*”, “**”, “*”, “.”, " “).**

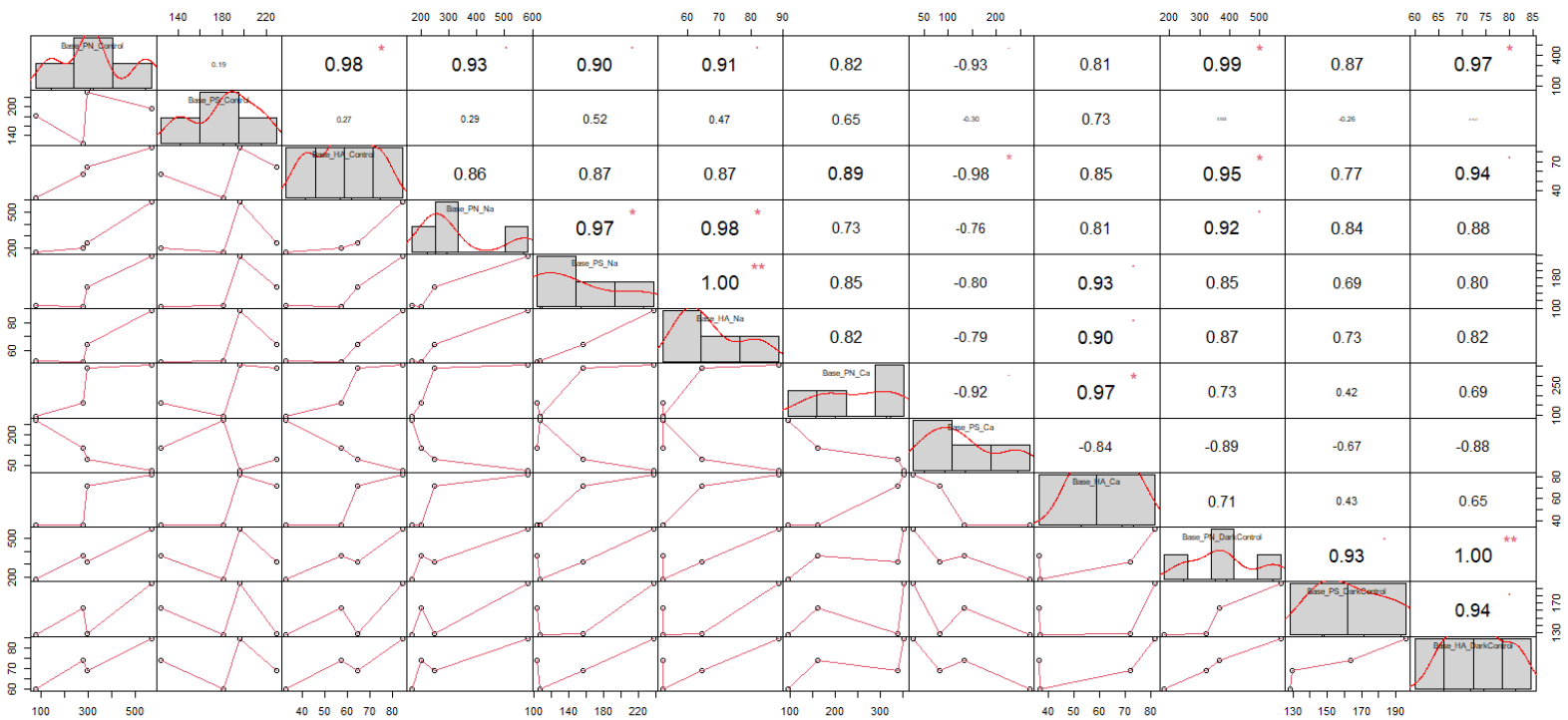

Figure 5.16: The correlation of base extractable EPS between different treatments for Hadley sludge. The distribution of each variable (base proteins (PN), base polysaccharides (PS), and base humic acids (HA)) for light control, light+Na^{+}, light+Ca^{2+} and dark control is shown on the diagonal. On the bottom of the diagonal: the bivariate scatter plots with a fitted line are displayed. On the top of the diagonal: the value of the correlation plus the significance level as stars. Each significance level is associated to a symbol: p-values (0.001, 0.01, 0.05, 0.1, 1) <=> symbols (“*”, “**”, “*”, “.”, " “).**

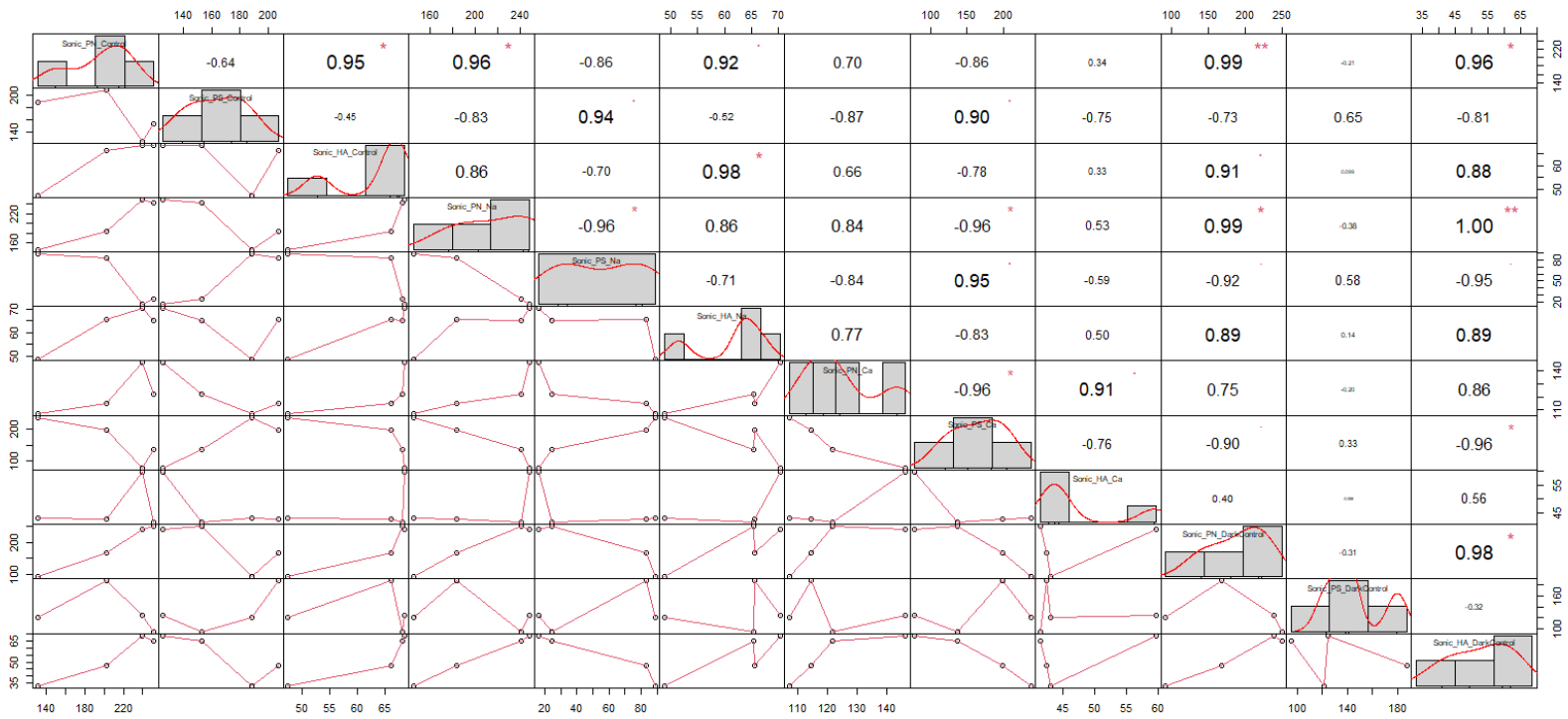

Figure 5.17: The correlation of sonication extractable EPS between different treatments for Hadley sludge. The distribution of each variable (sonication proteins (PN), sonication polysaccharides (PS), and sonication humic acids (HA)) for light control, light+Na^{+}, light+Ca^{2+} and dark control is shown on the diagonal. On the bottom of the diagonal: the bivariate scatter plots with a fitted line are displayed. On the top of the diagonal: the value of the correlation plus the significance level as stars. Each significance level is associated to a symbol: p-values (0.001, 0.01, 0.05, 0.1, 1) <=> symbols (“*”, “**”, “*”, “.”, " “).**

5.3.6 Isolation and Analysis of EPS Protein Pools During Photogranulation

5.3.6.1 Ammonium Sulfate Precipitation of Protein

Crude EPS extract, from each extraction method, was subjected to $(NH_4)_2SO_4$ precipitation. Only light control, light+Ca^{2+} treatment, and dark control crude EPS extract was selected for ASP and subsequent SDS-PAGE analysis. The protein concentrations for CER, base, and sonication EPS extracts after ASP and the percentage recovery for each extract, during photogranulation, are shown in Figure 5.18. Recovered proteins versus non-recovered proteins are also shown in Figure 5.19.

The total percent protein recovered for activated sludge inoculum (day 0), in the light control cultivation, is the highest for CER, followed by sonication, then base treatment. These results are similar to and support results published by Park et al. (2008b) for activated sludge. Park et al. found that CER protein recovery is approximately 10-30% higher in comparison to recovery of proteins by base extraction. This suggests that CER and sonication extracted protein are more hydrophobic and/or larger in mass than base-extracted protein, while base-extracted are more hydrophilic in the activated sludge inoculum (Figure 5.18).

During photogranulation, the concentration of base extractable protein after ASP decreases from day 0 to day 27 for the light control set. The percentage of protein recovered after ASP is relatively low, approximately 20-40% for the first 9 days of the cultivation and increases to about 100% by day 27(Figure 5.18; Figure 5.19). Additionally, the fraction of protein not-recovered decreases with photogranulation. This suggests that the base extractable protein portion that is degraded and utilized for phototrophic growth may be hydrophilic protein. In contrast, CER extractable protein concentration after ASP increases until day 3, followed by a decrease until day 27. The

percentage of protein recovered is relatively constant at 60% for the first 9 days and decreases to approximately 30% by day 27 (Figure 5.18; Figure 5.19). This shows that the hydrophilic portion of CER protein increases with photogranulation. The concentration of recovered protein from sonication closely follows the base extract trend, decreasing over the cultivation period. The protein recovery after ASP decreases from day 0 to 3, but then remains constant at approximately 35-40% decreases while the concentration not-recovered increases after the first 3 days (Figure 5.18; Figure 5.19). This shows that the hydrophilic portion of sonication protein also increases with photogranulation.

The total percent of protein recovered for the activated sludge inoculum treated with the addition of Ca^{2+} is highest for sonication, followed by CER than base treatments. These results are also in accordance with previous studies on activated sludge inoculum, and both CER and sonication recovered 10-40% more protein than base extraction. In the light+Ca^{2+} treatment cultivation, the concentration of base and CER extractable protein closely follows the overall trends observed for the light control set (Figure 18). However, the percentage of protein recovered after ASP differs slightly at each sample point. The percentage of protein recovered by base extraction decreases slightly until day 3, then increases significantly from approximately 30% to 100% by day 27. The fraction not-recovered also decreases significantly (Figure 5.19). Like the light control, the CER extracted protein concentration and percent recovery after ASP increases from day 0 to day 3, followed by a decrease from day 3 to 27 (Figure 5.18). Initially, sonication has the highest recovery at day 0, then decreases to 40% at day 3, and increases to approximately 50-65% for the remainder of the cultivation period.

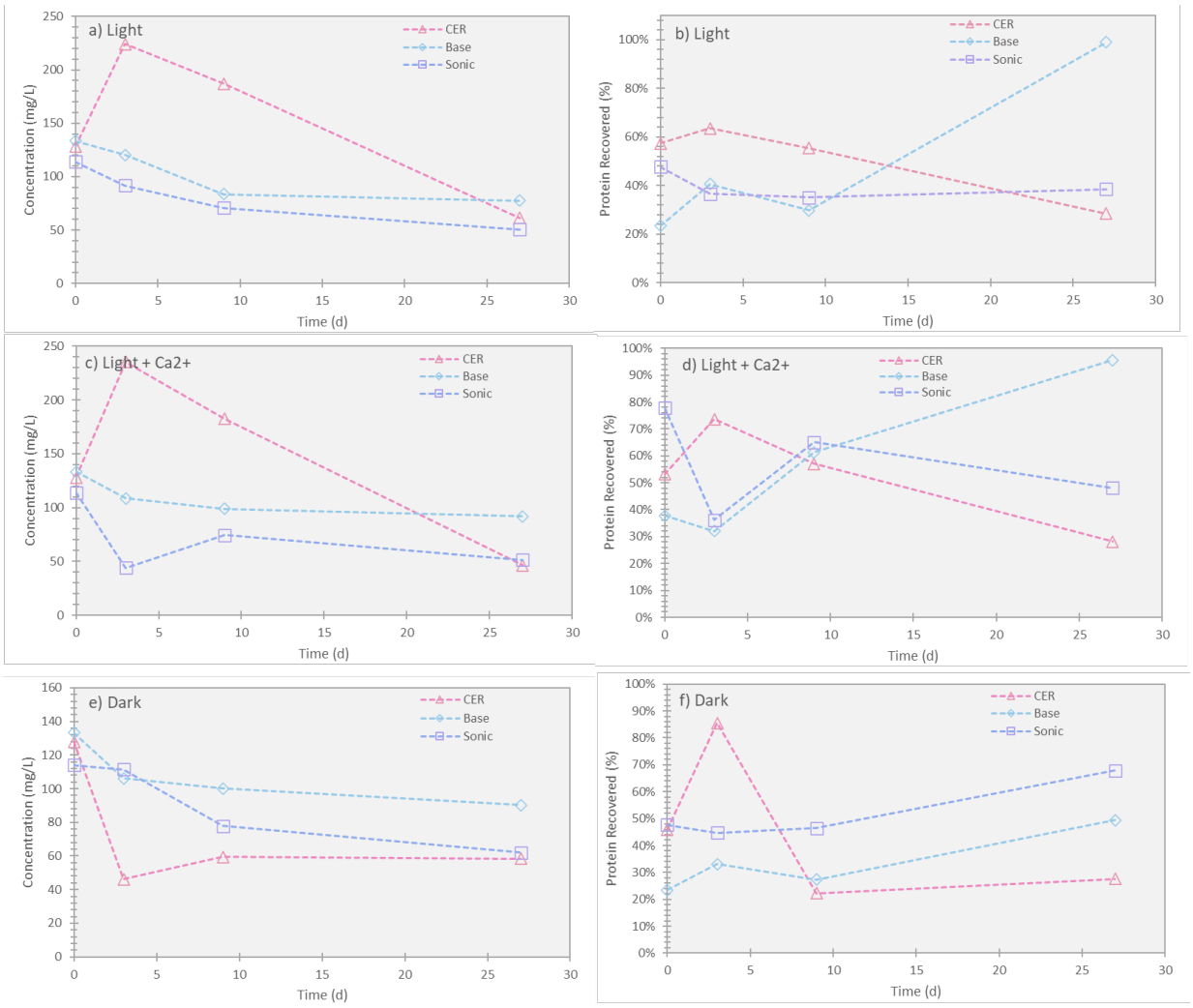

Figure 5.18: Changes in (a) Protein Concentration (as mg/L BSA) and (b) Protein Recovery (as %) by Ammonium Sulfate $(NH_4)_2SO_4$ Precipitation During Photogranulation for CER, Base, and Sonication Treatments from Crude EPS Extracts, for Each Treatment

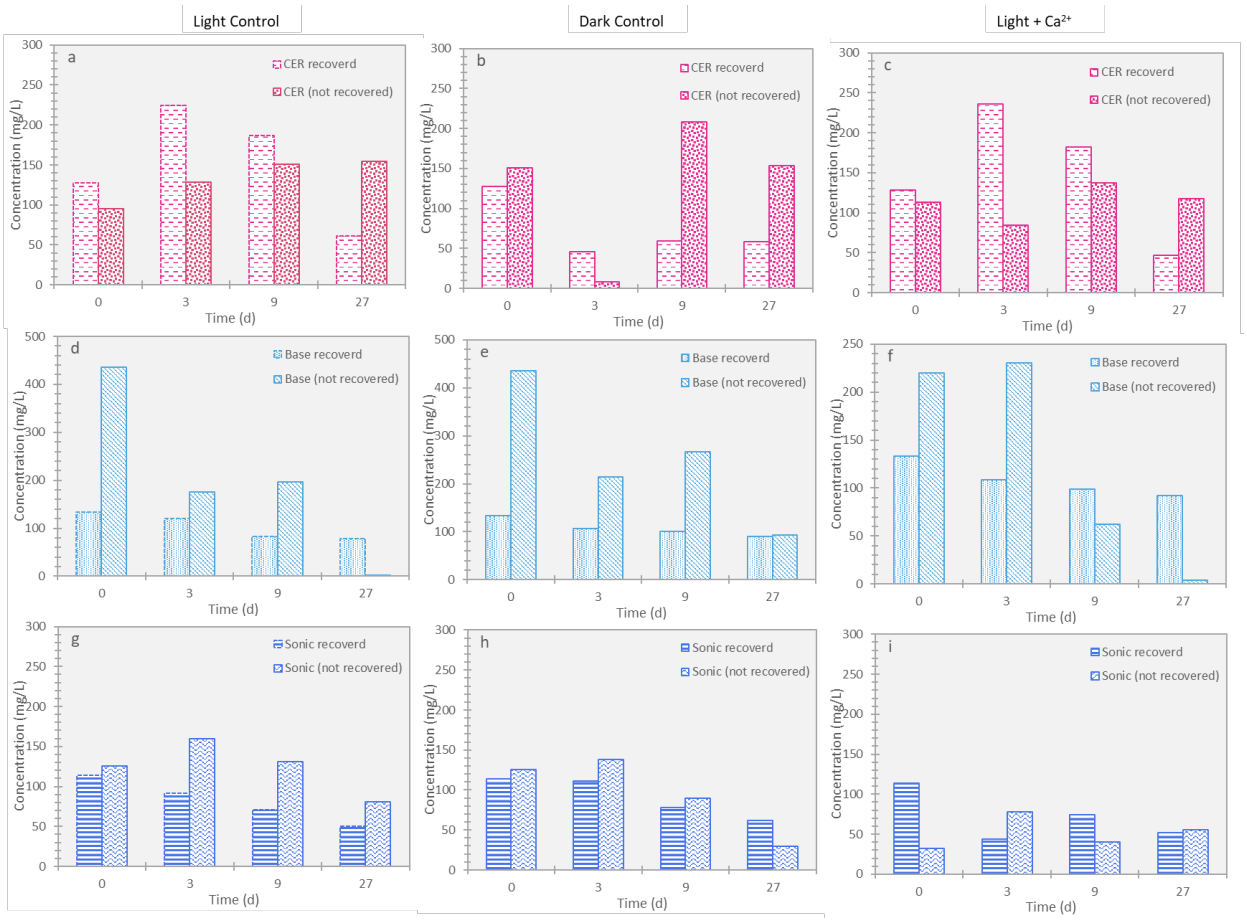

Figure 5.19: Changes in the Concentration (mg/L BSA) of Protein Recovered and Not Recovered for CER (a) Light Control, (b) Dark Control and (c) light+Ca^{2+}, Base (d) Light Control, (e) Dark Control, and (f) light+Ca^{2+}, and Sonication (g) Light Control, (h) Dark Control, and (i) light+Ca^{2+}

5.3.6.2 SDS-PAGE Banding Profile During Photogranulation

Chapter 4 revealed that EPS extraction procedures isolated unique protein groups so the understand the full relationship between cation augmentation and protein niches, three protein isolations methods were analyzed with SDS-PAGE. EPS proteins based on molecular mass, for the two controls (light and dark) and the light+Ca^{2+} treatment, extracts were subjected to separation by SDS-PAGE. SDS-PAGE was not utilized for soluble EPS proteins because concentrations were too low to perform the analysis. SDS-PAGE was utilized to reduce the complexity of the extracts, separate out

different molecular mass proteins, and to generate a “fingerprint” for each sample. The presence of different molecular mass proteins in environmental samples can potentially be a reliable indicator of microbial function. The SDS-PAGE profile of EPS protein during hydrostatic photogranulation are shown in Figure 5.20. Several distinct protein bands were present, predominantly in the molecular mass region 10 -75 kDa for base and CER extracts, and region 10-37 kDa for sonication extracts (Figure 5.20) for all treatments (light control, light+Ca^{2+}, and dark control). For all three treatments, although similar bands were present in multiple lanes, each extraction method contained different profiles, indicating that different fractions of protein were released from different EPS extraction methods, which corroborates results from Chapter 4. The diffuse “smearing” pattern in low molecular mass ranges, especially by base and sonication extraction, is potentially due to hydrolyzed/degraded protein or low molecular mass substances that bind silver, such as free carbohydrates. The SDS-PAGE banding patterns were also different with respect to each extraction method, and the level of smearing in the low molecular mass range, over the course of photogranulation.

Figure 5.20 and Table 5.3 to Table 5.5 show the results of the SDS-PAGE banding pattern for the three different extraction methods (base, CER and sonication) and three different treatments (light control, light+Ca^{2+}, and dark control). Interestingly, on a molecular level, the banding pattern between the three treatments show fairly similar results for each extraction method, with differences of only one or two bands or the time point/sample point when a specific band appears or disappears on the SDS-PAGE profile.

Base extraction shows six distinct bands at day 0- bands a1-a6 (Figure 5.20;Table 5.3 to Table 5.5) for all treatments with their respective molecular masses. All of these bands are seen in day 3 samples for all treatments with the addition of two other bands, a7 and a8. By day 9, due to heavy “smearing” on the lower region of the lane, we

are unable to identify any protein bands below 37 kDa. In the light control treatment, band a9 appears in the light control on day 9 but disappears or is too faint to be identified by day 27. Band a10 appears on day 27 but is rather faint. In contrast, for the light+Ca^{2+} treatment, new bands a9 and a 10 only appear on day 27 with much higher molecular masses at approximately 150 and 250 kDa, respectively. Dark control shows no new bands, only changes in the intensity of specific bands over the 27-day period.

CER extraction shows seven distinct bands at day 0- bands b1-b7 (Figure 5.20;Table 5.3 to Table 5.5) for all treatments. Day 3 shows similar results for all three treatments with bands b1-b4 remaining, and while b5-b7 disappear almost entirely from the profile. For light control, band b1 remains through day 27 and b2 until day 9 while all other bands lose intensity or completely disappear from the profile. For light+Ca^{2+} similar pattern is observed for bands b1 and b2, while bands b3 and b4 also remain on day 9 but with a higher level of smearing. By day 27, the SDS-PAGE profile is the same as light control. Dark control shows a different profile with bands b1-b5 remaining until day 9, and bands b1-b4 until day 27.

Sonication extraction shows only three distinct bands that are visible for all treatments (Figure 5.20;Table 5.3 to Table 5.5). For light treatment, these bands remain through day 9 and disappear by day 27. There is an appearance of a new band, c4, on day 27 for light treatment. Light+Ca^{2+} treatment shows a similar banding pattern to light control, but without the appearance of a new band on the last day. Dark control banding pattern is like the other treatments, but more smears are observed on day 9 and 27 making it difficult to clearly identify any bands.

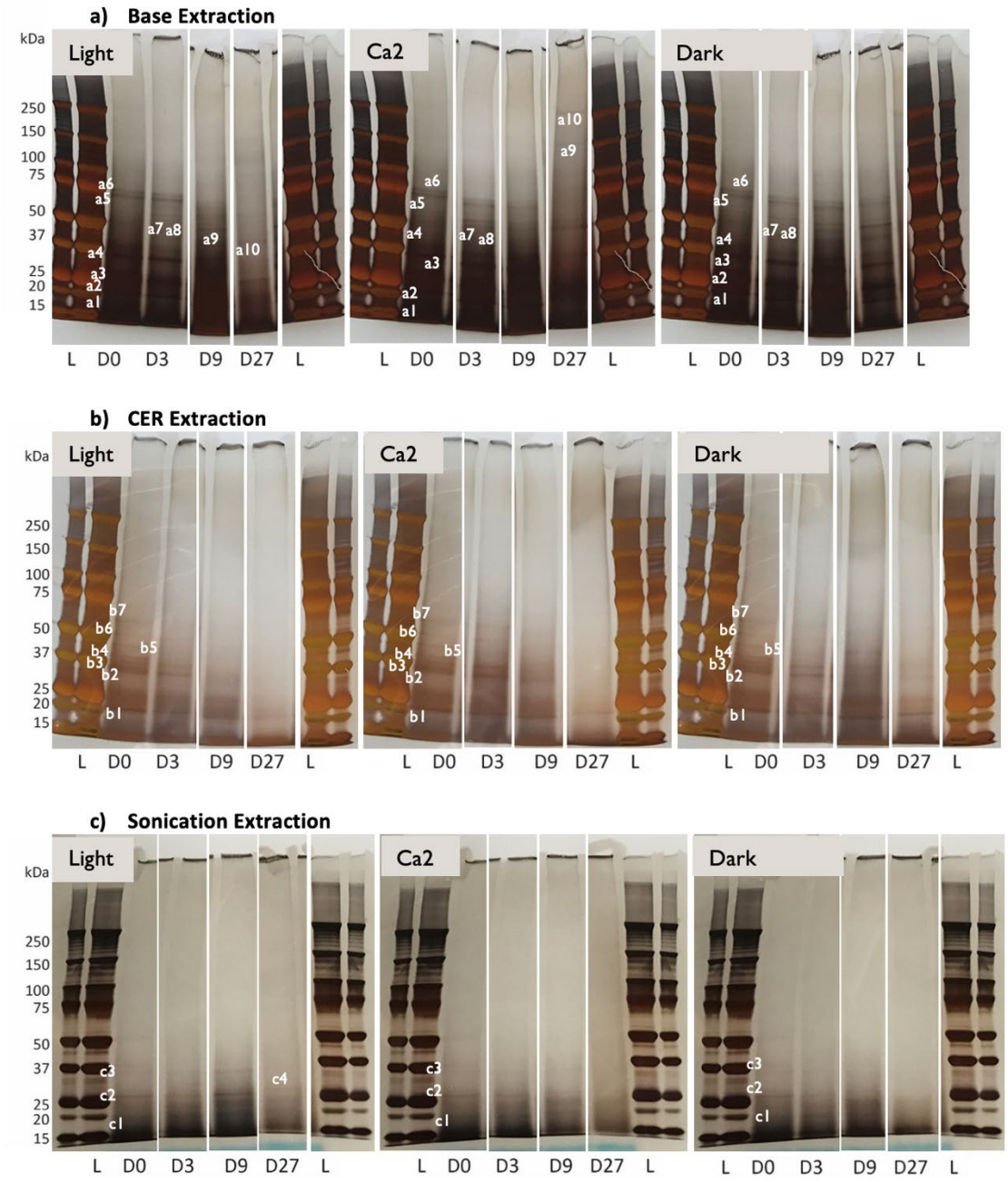

Figure 5.20: SDS-PAGE of Extracellular PN During Progression of Photogranulation Extracted by (a) Base (Alkaline) Treatment, (b) the CER Procedure and (c) Sonication Procedure, Subsequently Fractionated by an $(NH_4)_2SO_4$ Precipitation. Lanes: L, molecular mass ladder; lanes D0 thru D27, PN separated with 90% $(NH_4)_2SO_4$ saturation from samples, indicated by the day (i.e., D3 is day 3), during photogranulation. PN sample loading is 8 µg per lane.

Table 5.3 Appearance of SDS-PAGE Bands for and Corresponding Approximate Molecular Mass During Photogranulation of Light Control Cultivation

		Light Control			
Band	**MW**	**Day**			
	(kDa)	**D0**	**D3**	**D9**	**D27**
a1	~18	X	X	*	*
a2	~20	X	X	*	*
a3	~37	X	X	*	X
a4	~40	X	X	*	*
a5	~72	X	X	-	-
a6	~75	X	X	-	-
a7	~52	-	X	X	-
a8	~54	-	X	X	-
a9	~50	-	-	X	-
a10	~42	-	-	-	X
b1	~20	X	X	X	X
b2	~35	X	X	X	-
b3	~37	X	X	-	-
b4	~39	X	-	-	-
b5	~48	X	-	-	-
b6	~52	X	-	-	-
b7	~60	X	-	-	-
c1	~20	X	X	X	X
c2	~25	X	X	X	-
c3	~37	X	X	X	-
c4	~27	-	-	-	X

Note. Sizes were approximated by using the standard ladder. “X” signifies band is present, “-“ signifies band is not present, and “*” signifies band may be present but is not clearly visible due to smearing.

Table 5.4. Appearance of SDS-PAGE Bands for and Corresponding Approximate Molecular Mass During Photogranulation of Light + Ca^{2+} Cultivation

		Light + Ca^{2+}			
Band	MW	Day			
	(kDa)	D0	D3	D9	D27
a1	~18	X	X	*	*
a2	~20	X	X	*	*
a3	~37	X	X	X	*
a4	~40	X	X	X	X
a5	~72	X	X	X	-
a6	~75	X	X	X	-
a7	~52	-	X	X	X
a8	~54	-	X	X	X
a9	~150	-	-	-	X
a10	~250	-	-	-	X
b1	~20	X	X	X	X
b2	~35	X	X	X	-
b3	~37	X	X	*	-
b4	~39	X	X	*	-
b5	~48	X	*	-	-
b6	~52	X	X	-	-
b7	~60	X	X	-	-
c1	~20	X	X	X	*
c2	~25	X	X	X	*
c3	~37	X	-	-	*

Note. Sizes were approximated by using the standard ladder. “X” signifies band is present, “-“ signifies band is not present, and “*” signifies band may be present but is not clearly visible due to smearing.

Table 5.5. Appearance of SDS-PAGE Bands for and Corresponding Approximate Molecular Mass During Photogranulation of Dark Control Cultivation

		Dark Control			
Band	**MW**	**Day**			
	(kDa)	**D0**	**D3**	**D9**	**D27**
a1	~18	X	X	X	X
a2	~20	X	X	*	X
a3	~37	X	X	X	X
a4	~40	X	X	*	X
a5	~72	X	X	X	X
a6	~75	X	X	X	X
a7	~52	-	X	X	X
a8	~54	-	X	X	X
b1	~20	X	X	X	X
b2	~35	X	X	X	X
b3	~37	X	X	X	X
b4	~39	X	X	X	X
b5	~48	X	-	X	-
b6	~52	X	-	-	-
b7	~60	X	-	-	-
c1	~20	X	*	-	-
c2	~25	X	*	-	-
c3	~37	X	X	-	-

Note. Sizes were approximated by using the standard ladder. “X” signifies band is present, “-“ signifies band is not present, and “*” signifies band may be present but is not clearly visible due to smearing.

5.4 Discussion

The current study aimed to investigate the addition of monovalent (Na^+) and divalent cations (Ca^{2+} and Mg^{2+}) to enhance hydrostatic photogranulation of activated sludge inoculum. Initial results show that addition of cations (Na^+, Ca^{2+} and Mg^{2+}), at

specific concentrations, leads to a higher percentage of spherical granules in comparison to light control (no treatments) vials during hydrostatic cultivation and a dark control where no granules formed. Characterization of soluble constituents in a subset of the augmented sludges revealed correlated trends between different treatments and key trends previously reported as indicators of successful granulation phenomena. Chlorophylls, nitrogen species, anions, cations, and EPS are utilized to characterize photogranulation on four different treatments, 1) light control, 2) light with addition of 20 meq/L Na^+ (light+Na^+), 3) light with the addition of 40 meq/L Ca^{2+} (light+Ca^{2+}), and 4) dark control. EPS dynamics are studied using three different extraction methods, base, CER and sonication, followed by ASP and SDS-PAGE analysis.

The addition of Ca^{2+} enhanced percentage of total (n=100%) and spherical granules (n=100%) in comparison to the light (total: 90%; spherical: 25%) and dark control (total: 0%; spherical: 0%). The addition of Na^+ resulted in the same percentage of total granules (n=90%), but increased the percentage of spherical granules (n=35%), in comparison to the light and dark controls. These results show that Ca^{2+} has a greater positive effect on total and spherical granules, in comparison to Na^+ addition. Previous studies report that cations have been shown to have a significant effect on the bulk properties of activated sludge aggregations from loosely bound floc to dense granules (Sheng et al., 2010). OPG initially start as activated sludge floc and over photogranulation became dense granules (Milferstedt et al., 2017; Stauch-White et al., 2017). As activated sludge floc is the initial starting material, previous research on the bioaggregation of activated sludge floc may provide insight on the initial stages of biofilm formation during photogranulation.

Activated sludge floc and granules both contain high amounts of EPS (Kuo-Dahab et al., 2018; Milferstedt et al., 2017; Park et al., 2008s, 2008b). One concept that pertains to EPS in both flocs and granules is the divalent cation bridging theory. The first

researchers to propose divalent cation bridging included McKinney and Horswood (1952) and Tezuka (1969) (McKinney & Horwood, 1952; Tezuka, 1969). According to this theory, divalent cations bridge negatively charged functional ions within the EPS and this bridge helps to aggregate and stabilize the EPS matrix and microbes, thereby promoting bioflocculation and aggregation. The divalent cation bridging theory has been supported by findings from several studies that divalent cations, specially Ca^{2+} and Mg^{2+}, helps bioflocculation. Higgins and Novak (1997b) reported that when the sum of monovalent cation concentration (Na^{+}, NH_4^{+}, and K^{+}) divided by the sum of the divalent cations (Ca^{2+} and Mg^{2+}) was greater than 2, then this could cause floc property deterioration. Results here show that without the addition of Ca^{2+}, ratio of monovalent to divalent cations is much greater than 2. This could partially account for the higher percentage of total granules and spherical granules seen with the addition of Ca^{2+} and Mg^{2+}, which brings the ratio of monovalent to divalent cations to <2. On the other hand, this still does not explain why the addition of Na^{+} also had a positive effect on the percentage of spherical granules. As we observed no change in Na^{+} in the bulk liquid, this could suggest that the addition of Na^{+} may have altered the water chemistry in a way that had a positive impact on photogranulation.

Additionally, Higgins and Novak (1997b) observed that the addition of Ca^{2+} and Mg^{2+} to activated sludge systems, increased the bound protein content which was observed with an improvement in settling. Addition of monovalent cations above 10 meq/L resulted in a decrease in the bound protein concentration, which was related to a deterioration in settling properties. High concentrations of monovalent cations can displace the divalent cations due to an ion-exchange mechanism and cause deflocculation due to release of biopolymer fraction that appears to be a lectin suggests the bound protein fraction is involved in the binding of sugar residues on polysaccharides (Higgins & Novak, 1997b). Higgins and Novak (1997b) proposed a new

model where cross-linking of polysaccharides and cation bridges act to stabilize the EPS network, and divalent cations may also be involved in the structural stability and binding activity of the lectin-like proteins. Here, we added 20 meq/L of Na^+ and observed an increase in spherical granules. Kuo-Dahab et al. (2018) showed that activated sludge degradation and recycle of base extractable proteins occurs, suggesting that potentially the addition of Na^+ possibly displaced divalent cations as both an increase in Ca^{2+} and Mg^{2+} concentration in the bulk liquid was observed for light+Na^+ sets during the first few days of photogranulation. In addition, EPS soluble and CER polysaccharides increased in light+Na^+ while CER extractable proteins decreased. CER is known to extract for EPS that is bound with divalent cations, and therefore, these results suggest that addition of Na^+ treatment follows the model proposed by Higgins and Novak (1997b) and possibly displaces divalent cations and decreases bound proteins in the CER fraction.

In contrast to the aforementioned model, Zita and Hermansson (1994) described the role of cations in floc formation in terms of the Derjaugin, Landau, Verwey and Overbeek (DLVO) theory. Using this theory, the presence of cations reduces the separation distance between negatively charged bacteria promoting flocculation. They found that both monovalent and divalent cations had the same capacity to enhance flocculation and no ion exchange was observed. Higgins and Novak (1997b) also maintained that according to the DLVO theory, settling and dewatering should be improved with Na^+ at any concentration. This was experimentally shown not to be the case (as described above). The cationic bridging model was also proposed by Eriksson and Alm (1991) and Kakii et al. (1985) who found the removal of Ca^{2+} from sludge with a chelating agent (ethylenediaminetetraacetic acid (EDTA)), resulted in reduced settling and dewatering characteristics. This was also observed in this study as addition of 1mM EDTA showed negative impacts on photogranulation with no disc or spherical granules, only floccular biomass.

Additionally, Cousin and Ganczarczyk (1999) investigated the effect of Ca^{2+} on specific floc properties such as size and density. It was found that the addition of calcium (> 4 meq/L) resulted in an increase in floc size and a decrease in porosity. A minimum addition of 4 meq/L was thought to be necessary to overcome the ion exchange between competing ions, such as Na^{+}. The increase in floc size was then speculated to be due to the formation of Ca^{2+} bridges among microbial aggregates and particles. Here, we observed that the light+Ca^{2+} treatment produced a higher percentage of spherical granules in comparison to the light control and light+Na^{+} treatment. This suggests that ion competition may be why the addition of Na^{+} still produced a high percentage of spherical granules but less than the Ca^{2+} added set.

In contrast to physical aggregation and bioflocculation through divalent cation bridging, cyanobacteria research has suggested that Ca^{2+} is a signaling molecule and is modulated by EPS. The prevalence of Ca^{2+}-binding protein identified by Vilhauer et al. (2014) and the known role of Ca^{2+} in cyanobacterial phenotypic state suggest that the control of Ca^{2+} levels is modulated to some degree by EPS. The diversity of protein and metabolites found indicate that the EPS matrix outside the cyanobacterial cell is an important contributor to cell fate decisions. The authors proposed that minor changes in EPS protein sequences can dramatically influence phenotypic outputs and these proteins are essentially the determinants of community organization. In this study, similar SDS-PAGE banding pattern across the treatments showed same EPS protein on a molecular level which did not change with the addition of Ca^{2+} (in comparison to control). This may further imply that enhancement is more likely due to Ca^{2+} cation bridging, as we also observe strong correlations between Mg^{2+} and base protein, versus changes on a molecular level influenced by cyanobacteria.

In addition, in the light+Ca^{2+} treatment, greater recovery of CER protein after ASP suggest that more hydrophobic protein is available thus addition of Ca^{2+} may

influence the hydrophobicity of proteins that are produced by cyanobacteria. In both conditions light control and light+Ca^{2+}, changes in ASP recovery occurred over photogranulation. Proteins with relatively few hydrophilic regions will aggregate and precipitate out at relatively low concentrations of AS. In contrast, proteins with more hydrophilic regions will remain in solution until the concentration of AS added is higher, hence, any proteins remaining in solution after 90% ASP are strongly hydrophilic. Thus, fraction that was not precipitated or not recovered could be hydrophilic glycoPN as these molecules are not expected to be precipitated during the salting out process (ASP). Additionally, a high recovery of proteins is indicative of high concentration of hydrophobic proteins in the solution before ASP.

5.5 Conclusion

The current study aimed to investigate the addition of monovalent (Na^+) and divalent cations (Ca^{2+} and Mg^{2+}) to enhance hydrostatic photogranulation of activated sludge inoculum. The results from our initial chemical addition study show that the addition of cations (Na^+, Ca^{2+} and Mg^{2+}), at specific concentrations, leads to a higher percentage of spherical granules in comparison to light control (no treatments) vials during hydrostatic cultivation and a dark control where no granules formed. An in-depth study was performed on the progression and characterization of 1) light control, 2) light with addition of 20 meq/L Na^+ (light+Na^+), 3) light with the addition of 40 meq/L Ca^{2+} (light+Ca^{2+}), and 4) dark control. The results from this study suggest the following:

- The addition of Ca^{2+} enhanced percentage of total (n=100%) and spherical granules (n=100%) in comparison to the light (total: 90%; spherical: 25%) and dark control (total: 0%; spherical: 0%).

- The addition of Na^+ resulted in the same percentage of total granules (n=90%), but increased the percentage of spherical granules (n=35%), in comparison to the light and dark controls. These results show that Ca^{2+} has a greater positive effect on total and spherical granules, in comparison to Na^+ addition.
- Results here show that without the addition of Ca^{2+}, ratio of monovalent to divalent cations is much greater than 2. This could partially account for the higher percentage of total granules and spherical granules seen with the addition of Ca^{2+} and Mg^{2+}, which brings the ratio of monovalent to divalent cations to <2.
- Results suggest that the addition of Na^+ may displace divalent cations as both an increase in Ca^{2+} and Mg^{2+} concentration in the bulk liquid was observed for light+Na^+ sets during the first few days of photogranulation. EPS soluble and CER polysaccharides increased in light+Na^+ while CER extractable proteins decreased.
- Similar SDS-PAGE banding pattern across the treatments showed same EPS protein on a molecular level which did not change with the addition of Ca^{2+} (in comparison to control). This may further imply that enhancement is more likely due to Ca^{2+} cation bridging, versus changes on a molecular level influenced by the microbial community.

Light+Ca^{2+} treatment showed greater recovery of CER protein after ASP, and different recovery patterns in comparison to light and dark control, suggesting that more hydrophobic protein is available. This further infers that the addition of Ca^{2+} may influence the hydrophobicity of EPS proteins during hydrostatic photogranulation.

CHAPTER 6

CONCLUSIONS

The purpose of this dissertation is to advance our understanding of photogranulation in a hydrostatic environment to better understand oxygenic photogranule (OPG) reactor operation for wastewater treatment and energy recovery. This dissertation focuses on and highlights the role of extracellular polymeric substances (EPS) in the formation of hydrostatic photogranules. The work presented has been divided into three separate sections:

In Chapter 3, the aim of this study was to investigate the fate and dynamics of EPS during photogranulation on activated sludge in a hydrostatic environment. The study shows that during the transformation of activated sludge into a photogranular biomass, sludge's base-extractable EPS proteins selectively degrade. Strong correlations between base-extracted proteins and the growth of chlorophyll *a* and chlorophyll *a/b* ratio suggest that the bioavailability of this organic nitrogen is linked with selection and enrichment of filamentous cyanobacteria under hydrostatic conditions. The results of soluble and sonication-extractable EPS and microscopy also show that the growth of filamentous cyanobacteria yielded large amounts of polysaccharide-based EPS, which it consistent with what is reported for their motility and maintenance. With findings on the progression of photogranulation, the fate and dynamics of EPS, and microscopy on microstructures associated with EPS, we discuss the potential mechanisms of photogranulation occurring under hydrostatic conditions.

In Chapter 4, the aim of the investigation is two-fold: First, to determine if multiple extraction methods are needed to fully characterize EPS fractions, and second, further describe the dynamics between EPS, carbon, and nitrogen, during hydrostatic photogranulation for OPG formation. The study shows that multiple EPS extraction methods are required in order to fully characterize EPS during the transformation of

activated sludge into a photogranule in a hydrostatic environment. While filamentous cyanobacteria, EPS and nitrogen are known to play key roles in photogranulation, the present study reveals why cyanobacteria are selected and how different fractions of EPS and their potential recycle leads to photogranulation in hydrostatic conditions. The different EPS extraction methods are required to capture different fractions of EPS with respect to protein, polysaccharide, and humic acid composition and organic carbon and nitrogen content. Though the fractions were different across methods, they were similar between cultivations from different sludge inoculums. EPS trends using five different extraction methods, centrifugation, CER, base, sonication, and heat, concentrations of EPS fractions were statistically similar, between sludge sources Amherst and Hadley treatment facilities despite variation in their initial sludge characteristics. EPS extraction methods for polysaccharides was found to be the most varied, followed by humic acids, then proteins. While overlap in the most likely abundant fractions exist, the different methods highlight that subgroups are only capture by certain methods whether because they are sensitive to degradation or omission by the extraction protocol.

All methods had statistically significant moderate to strong correlations with one or more constituents, chlorophylls, nitrogen-species, and select cations and anions, which have been previously established as strong indicators of successful granule formation. These results suggest that different EPS fractions are linked to multiple processes during hydrostatic photogranulation, including the enrichment of filamentous cyanobacteria, nitrogen metabolism and recycle of organic nitrogen, assimilation and biofilm incorporation of ammonium, and biofilm structure, further suggesting that the role of EPS is a complex process with multiple roles in photogranulation.

In Chapter 5, the aim of this study is to elucidate the addition of monovalent (Na^+) and divalent cations (Ca^{2+} and Mg^{2+}) to enhance hydrostatic photogranulation of activated sludge inoculum with respect to EPS fractions. The results from our initial

chemical addition study show that the addition of cations (Na^+, Ca^{2+} and Mg^{2+}), at specific concentrations, leads to a higher percentage of spherical granules in comparison to light control (no treatments) vials during hydrostatic cultivation and a dark control where no granules formed.

The EPS present during hydrostatic photogranulation of activated sludge were investigated using three different extraction methods: base treatment, cation exchange resin (CER) procedure, and sonication treatment. EPS protein, polysaccharide, and humic acid composition in crude EPS extracts was compared to chlorophylls and nutrients between the treatments (Na^+ and Ca^{2+}) and light and dark controls. The crude EPS extracted was subsequently precipitated by ammonium sulfate precipitation (ASP) and analyzed by sodium dodecyl sulfate polyacrylamide gel electrophoresis (SDS-PAGE). Key trends for successful granule formation were compared among different treatments.

An in-depth study was performed on the progression and characterization of 1) light control, 2) light with addition of 20 meq/L Na^+ (light+Na^+), 3) light with the addition of 40 meq/L Ca^{2+} (light+Ca^{2+}), and 4) dark control. The results from this study suggest the following: First, the addition of Ca^{2+} enhanced percentage of total (n=100%) and spherical granules (n=100%) in comparison to the light (total: 90%; spherical: 25%) and dark control (total: 0%; spherical: 0%). The addition of Na^+ resulted in the same percentage of total granules (n=90%), but increased the percentage of spherical granules (n=35%), in comparison to the light and dark controls. These results show that Ca^{2+} has a greater positive effect on total and spherical granules, in comparison to Na^+ addition.

Additionally, results show that initial activated sludge bulk liquid may have an imbalance between monovalent to divalent cations and without the addition of Ca^{2+}, ratio of monovalent to divalent cations is much greater than 2. This could partially account for

the higher percentage of total granules and spherical granules seen with the addition of Ca^{2+} and Mg^{2+}, which brings the ratio of monovalent to divalent cations to <2. These results corroborate findings by Higgins and Novak (1997a, 1997b), which suggest that the addition of Na^{+} may displace divalent cations as both an increase in Ca^{2+} and Mg^{2+} concentration in the bulk liquid was observed for light+Na^{+} sets during the first few days of photogranulation. Higgins and Novak also show that bound protein decreases which was observed here for CER extractable proteins, while EPS soluble and CER polysaccharides increased in light+Na^{+}.

Light+Ca^{2+} treatment showed greater recovery of CER protein after ASP, and different recovery patterns in comparison to light and dark control, suggesting that more hydrophobic protein is available. This further infers that the addition of Ca^{2+} may influence the hydrophobicity of EPS proteins during hydrostatic photogranulation. After ASP, SDS-PAGE was applied and banding pattern across the treatments showed same EPS protein on a molecular level which did not change with the addition of Ca^{2+} (in comparison to control). This may further imply that enhancement is more likely due to Ca^{2+} cation bridging, versus changes on a molecular level influenced by the microbial community.

EPS have significant impact on the structural development of granular biofilms (i.e., aerobic granules and anaerobic granules) and this work demonstrate this to be true for one specific type of granular biofilm OPGs. EPS are essential components that are required for microorganisms to aggregate, accounting for the compact and spherical structure of granules. Since the success of granule processes depends on the effectiveness of aggregation, compaction, and subsequent solid/liquid separation, the role of EPS in granule formation is clearly important. This work shows that different protocols, extract different fractions of EPS and these fractions are associated with a variety of processes. EPS extraction methods for polysaccharides was found to be the

most biased, followed by humic acids, then proteins. Results also show that there are common EPS trends associated with photogranulation, base extractable proteins are selectively degraded, and nitrogen derived from this fraction is linked to the selection and enrichment of filamentous cyanobacteria. In contrast, an increase of soluble and sonication extractable EPS and microscopy show that growth of filamentous cyanobacteria yielded large amounts of polysaccharide-based EPS which may be a result of their motility and maintenance. Further, an initial loss in bound humic acids and no corresponding increase in the bulk liquid may suggest that humic acids are substrate when reduced carbon is limited in the initial phase of granulation. Dynamics of EPS fractions during photogranulation also suggest that filamentous cyanobacteria may recycle organic C and N from different EPS fractions. This work also shows that the addition of Ca^{2+} increases the total percentage of successful granules and spherical granules during hydrostatic photogranulation, which may have an influence on the hydrophobicity of EPS proteins possibly leading to cation bridging and stabilization of negatively charged sites in the EPS matrix, thereby enhancing photogranulation.

The findings from this research are expected to enhance the fundamental knowledge on photogranulation in hydrostatic and hydrodynamic conditions. These results are also thought to be a significance to the current wastewater engineering community and contribute to developing scientifically sound engineering application of the OPG process for wastewater treatment.

APPENDIX A

INVESTIGATION OF THE FATE AND DYNAMICS OF EXTRACELLULAR POLYMERIC SUBSTANCES (EPS) DURING SLUDGE-BASED PHOTOGRANULATION UNDER HYDROSTATIC CONDITIONS

Investigation of the Fate and Dynamics of Extracellular Polymeric Substances (EPS) during Sludge-Based Photogranulation under Hydrostatic Conditions

Wenye Camilla Kuo-Dahab,[†,‡] Kristie Stauch-White,[†] Caitlyn S. Butler,[†] Gitau J. Gikonyo,[†] Blanca Carbajal-González,[§] Anastasia Ivanova,[∥] Sona Dolan,[†,⊥] and Chul Park*[,†]

[†]Department of Civil and Environmental Engineering, University of Massachusetts, Amherst, Massachusetts 01003 United States
[‡]Brown and Caldwell; One Tech Drive, Andover, Massachusetts 01810, United States
[§]Science Center Microscopy Facility, Mount Holyoke College, South Hadley, Massachusetts 01075, United States
[∥]Department of Biology, University of Massachusetts, Amherst, Massachusetts 01003, United States

Supporting Information

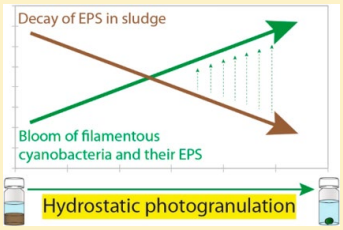

structure and microbial characteristics as HSP.[7,10,11] This suggests that hydrostatic cultivation of photogranules may provide an opportunity to study the photogranulation phenomenon that also occurs in bioreactor operation.

Like other granules, photogranules possess a high and complex network of extracellular polymeric substances (EPS).[7,10] It is well-known that EPS in bioaggregates have a significant influence on their physiochemical and physiological properties, including surface charge, dewaterability, settleability, structural stability, and rheology.[4,16−22] The function of EPS is governed by its composition.[23] At the macromolecular level, proteins and polysaccharides are the major components of EPS in bioaggregates.[24,25] This composition can be affected by many factors, including environmental signals, such as species and concentrations of nutrients, substrates, and growth conditions.[22,26,27] Generally, EPS are categorized by their association with the cell surface, i.e., soluble or biomass-bound EPS, which may lead to different functions for bioaggregation.[24,25] Soluble EPS can be generally obtained by centrifugation and/or filtration. Biomass-bound EPS can be obtained using various extraction methods, such as sonication, cation exchange resin (CER) extraction, base treatment, etc.

Numerous studies have been conducted to understand granulation with EPS. Tay et al.[16] reported that extraction using sequential base and heat treatment showed an increase of EPS polysaccharides to proteins (PS/PN) ratio with increased level of granulation for aerobic granule sludge. The same study concluded that an increase in aeration rate (thus, increased shear) resulted in the increase in PS/PN, which seemed to promote granulation. However, McSwain et al.,[17] using the same extraction methods as Tay et al.,[16] found that a high yield of proteins versus polysaccharides correlated with an increase in granulation. They also found that CER extraction showed a preferential isolation of proteins but with an overall lower extraction efficiency compared to the sequential base and heat treatment.[17] McSwain et al.[17] concluded that the aerobic granular sludge systems with constant aeration but shorter settling time promoted granulation with a decrease in PS/PN. These examples in literature suggest that there are different observations about EPS and granulation, which can be more complicated if different extraction methods are used. Nonetheless, it is well agreed that EPS plays a major role in granulation and studies about EPS in granulation have continued.[17,18,20,28−32] For photogranules, although Milferstedt et al.[10] showed an increasing trend of PS/PN during photogranulation under hydrostatic conditions, no further details about EPS as well as progressive changes in biomass that occur along with the changes in EPS have yet been reported. Thus, despite increasing interest about the photogranular process, EPS in photogranulation remains mainly undiscovered.

In this study, we present photogranulation of activated sludge under hydrostatic conditions with focus on different fractions of EPS and their associated microstructure development. Two different sludge sources were incubated in a closed, hydrostatic environment under light conditions to produce photogranules. We present changes in nutrients, phototrophic constituents of biomass, and the composition of EPS during the photogranulation process. Microscopy was conducted to study the structure of photogranules, including the distribution of filamentous cyanobacteria and EPS network in photogranules. The outcome of this study is expected to advance the understanding of photogranulation, which should be useful for the development of the OPG process for aeration-free wastewater treatment.

MATERIALS AND METHODS

Generation of HSP. Cultivation of photogranules followed the procedure shown by Milferstedt et al.[10] Briefly, activated sludge, the inoculum of photogranules, was collected from the aeration basin at two local wastewater treatment plants (WWTP): Amherst and Hadley, MA. Aliquots of 10 mL of activated sludge were pipetted into 20 mL glass vials and capped. Subsequently, all replicates were placed under unmixed, 24 h artificial-light illumination at 20 °C. Light irradiation was 20−55 and 160−200 μmol/m^2-s along the sides and the tops of the vials, respectively. Numerous replicates were prepared for destructive sampling. Sampling dates were chosen to reflect various phases of granulation through macroscopic and microscopic imaging.

Study of EPS during Photogranulation. We obtained and analyzed both soluble and biomass-bound EPS during the progression of photogranulation. For biomass-bound EPS, we employed two extraction methods, base extraction and sonication, since these two methods are known to target different fractions of EPS, which are linked with different metal contents in sludge. Earlier proteomics work investigated EPS proteins that were extracted when divalent cations, Fe^{3+} and Al^{3+} were targeted by CER procedure, sulfide treatment, and base treatment, respectively.[33] It was found that while proteins extracted from sulfide and base treatments were similar to each other, the composition and origin of the CER-extracted proteins were substantially different from the two other methods. CER-extracted proteins showed more bacterial proteins involved in aggregation while base and sulfide-extracted proteins showed more sewage-derived proteins that persisted in the activated sludge process. Studies have also shown that sonication has high tendency to select for EPS associated with divalent cations,[19,34,35] which we also confirmed with our preliminary sodium dodecyl sulfate polyacrylamide gel electrophoresis work showing that proteins released by sonication and the CER procedure are similar. In the current study, we chose sonication and base treatment to target EPS that are bound with divalent cations and trivalent cations (Fe^{3+} and Al^{3+}), respectively, and studied how these fractions of EPS change during photogranulation.

All EPS extractions were performed in triplicates. Sample from the cultivation vial was collected in a sterile tube and centrifuged at 9000 rpm for 20 min to separate supernatant and solid fractions. The supernatant was filtered with 0.45 μm filters, and EPS in these filtrates were classified as soluble EPS. The solids after centrifugation were resuspended in 20 mL of designated extraction solution and subjected to sonication or base treatment. Sonication and base treatment followed the procedures of Wang et al.[36] and Park and Novak[37] with slight modifications, respectively. The detailed procedures of sonication and base treatment for the extraction of biomass-bound EPS are shown in the Supporting Information (SI).

Analytical Measurements. Total and volatile suspended solids (TSS, VSS) of samples were measured following Standard Methods 2540D/E.[38] Extraction and quantification of chlorophyll followed Standard Methods 10200H.[38] Soluble fractions of samples, for total dissolved nitrogen (TDN), dissolved inorganic nitrogen (DIN) (ammonium, nitrate, nitrite), dissolved organic carbon (DOC), phosphate, calcium, and magnesium, were obtained by centrifuging samples at

DOI: 10.1021/acs.est.8b03033
Environ. Sci. Technol. 2018, 52, 10462−10471

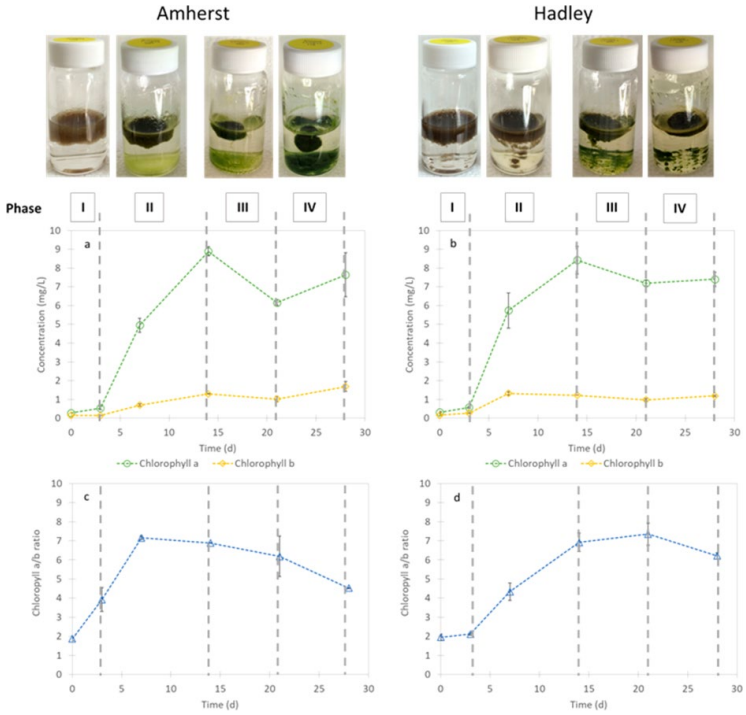

Figure 1. Transformation of activated sludge into a photogranule in a hydrostatic environment shown with the macroscopic progression and changes in the chlorophyll content. Sources of activated sludge are Amherst (left column) and Hadley (right column) WWTP. Macroscopic images of biomass at different photogranulation phases are shown above the label of each phase: Phase I, sludge compaction; Phase II, phototrophic bloom; Phase III, main granulation; and Phase IV, granule maturation. Concentrations of chlorophyll *a* and *b* for (a) Amherst and (b) Hadley cultivations. Chlorophyll *a*/*b* ratio for (c) Amherst and (d) Hadley cultivations. Error bars represent standard deviation of three replicates for chlorophylls.

12 000 rpm for 20 min and filtering the supernatant using 0.45 μm filters. TDN and DOC were measured using a Shimadzu TN/TOC analyzer (TOC-VCPH, Shimadzu, U.S.A). DIN species, phosphate, Ca^{2+} and Mg^{2+} were measured using a Metrohm 850 Professional Ion Chromatograph (IC) (Metrohm, Switzerland). Dissolved organic nitrogen (DON) was calculated by subtracting DIN species from TDN values. Quantification of EPS polysaccharides followed Dubois et al. (1956) using glucose as the standard.[39] EPS Proteins were determined using the Frølund modification of the Lowry method with bovine serum albumin as the standards.[40,41]

Microscopy. Light microscopy was conducted using light microscope EVOS FL Color AMEFC 4300. Scanning electron microscopy (SEM) of HSP was conducted using a FEI Quanta 200 SEM. Microscopy details are provided in the SI.

Statistical Analysis. Pearson correlation coefficient and regression analyses were conducted using the Pearson and Regression functions, respectively, in Microsoft Excel 2017 to compute correlations and significance between the variables.

RESULTS AND DISCUSSION

Characteristics of Activated Sludge as Photogranule Inoculum. Both Amherst and Hadley WWTPs employ the activated sludge process with mechanical aeration in open basins (Table S1). Amherst operates predenitrification and intermittent aeration, at 10–15 d solids retention time (SRT), to support biological nutrient removal for N removal.[42] Hadley operates conventional activated sludge with nitrification at 10 d SRT. Consequently, soluble phase of each activated sludge, which can be considered the secondary effluent of WWTPs, showed considerably different TDN and composition (Table

DOI: 10.1021/acs.est.8b03033
Environ. Sci. Technol. 2018, 52, 10462–10471

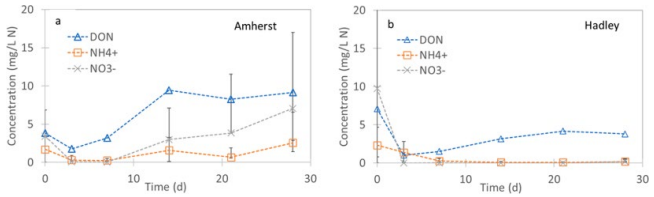

dissolved N. NO_2^- not shown as values were all <0.4 mg/L N.

S1). This also means that photogranulation from these sludge inoculums started with different levels of soluble N. While domestic wastewater is the primary source for both facilities, Hadley also receives storm runoff which contains high levels of agricultural runoff. The entry of agricultural wastewater could potentially account for high DON in Hadley activated sludge. VSS of Amherst and Hadley activated sludge was 1783 ± 12 and 2810 ± 20 mg/L, respectively. Both activated sludges contained very low but detectable levels of chlorophylls *a* and *b* (Table S1). Light microscopy also showed minor presence of phototrophic microorganisms, although sludge flocs were composed primarily of nonphototrophic bacterial aggregates (data not shown).

Transformation of Activated Sludge into Photogranules under Hydrostatic Conditions. Despite the different origins and initial parameters of Amherst and Hadley activated sludges, photogranulation of both sludges showed four common phases (Figure 1).

Phase I (the sludge compaction period) occurred during about the first 3 days of cultivation. During this stage, sludge first settled. Then, the majority of vials in this study showed sludge rising, an indication of denitrification. While floating, sludge compacted further, represented by shrinking sludge height. During this stage, chlorophylls remained low (Figure 1).

Phase II (the phototrophic bloom period) typically occurred between 3 and 14 days of the cultivation with a visual color change of the biomass from brown to green and an inward contraction of the biomass. A substantial increase in chlorophylls, especially chlorophyll *a*, was observed, indicating a phototrophic bloom period during Phase II (Figure 1a,b). The substantial increase in chlorophyll *a*/*b* ratio over Phase II (Figure 1c,d) also suggests cyanobacterial enrichment because chlorophyll *a* is present in both cyanobacteria and green algae while chlorophyll *b* is absent in cyanobacteria. In both cultivation sets, the peak chlorophyll *a*/*b* ratio reached about 7, much greater than the average chlorophyll *a*/*b* ratio, 2.2 ± 1.2, for planktonic algae.[43] This is also consistent with microscopic observation that typically green algae bloom occurred first but filamentous cyanobacteria became a dominant phototrophic group during phase II and for the remainder of cultivation. Using light microscopy, filamentous cyanobacteria were found to exhibit motility through gliding, which was also reported by earlier studies.[10,15]

Phase III (the main granulation period) was established between 14 and 21 days of cultivation, which took place along with emergence of a more spherical or granular structure. During this phase, the sides of the biomass began to contract more and became round. The extent of biomass contraction up to this point was faster for Amherst than Hadley. Even though chlorophyll levels showed a similar trend up to this point, differences in chlorophyll *a*/*b* ratio seem to reflect different rates of contraction between the Amherst and Hadley cultivations (Figure 1c,d).

Finally, granules were fully formed by Phase IV (the maturation period), 21−28 days after the start of the hydrostatic cultivation (Figures 1 and S1). Filamentous cyanobacteria in photogranules were observed with significantly decreased motility during this phase.

Despite substantial growth of phototrophic organisms, VSS and TSS did not change during cultivation (Figure S2), which was also observed by earlier studies.[10,15] Assuming that chlorophyll *a* accounts for 1% of VSS of phototrophic organisms,[44] increase in chlorophyll *a* from 0.3 to approximately 9 mg/L in both cultivation sets could have accounted for the growth of about 900 mg/L VSS. This new phototrophic growth, however, did not result in the increase in VSS during cultivation. This suggests that the original sludge organic matter was decayed and recycled for phototrophic growth. This notion can be supported by examining the level of dissolved carbon in sludge inoculum that might have been available for the growth of phototrophic microorganisms. The measured DOC in both Amherst and Hadley activated sludge sets showed, on average, 7.2 mg/L or 0.6 mM C (Table S1). The alkalinity of secondary effluent from these WWTPs has shown the values less than 150 mg/L $CaCO_3$, which can provide up to approximately 3 mM carbon (C). Hence, the theoretical total dissolved C that could have been available for phototrophic growth is less than 4 mM. This is substantially smaller than 40 mM C that may be necessary to produce 900 mg/L VSS, with an assumption that the chemical formula of phototrophic VSS is $C_{106}H_{181}O_{45}N_{16}P$ in which C represents about 52% of molecular weight.[45]

Literature shows that EPS accounts for a large fraction of organic matter in activated sludge.[37,41,46,47] Thus, knowing the fate of EPS from sludge inoculum could be important to understand the C recycle and photogranulation in hydrostatic cultivation. Furthermore, studying the dynamics of EPS generated during the phototrophic growth could reveal more about photogranulation and these will be presented and discussed in the later sections of the current study.

Fate of Dissolved Nitrogen during the Process of Photogranulation under Hydrostatic Conditions. In addition to C, nitrogen (N) also seems to be available from

DOI: 10.1021/acs.est.8b03033
Environ. Sci. Technol. 2018, 52, 10462−10471

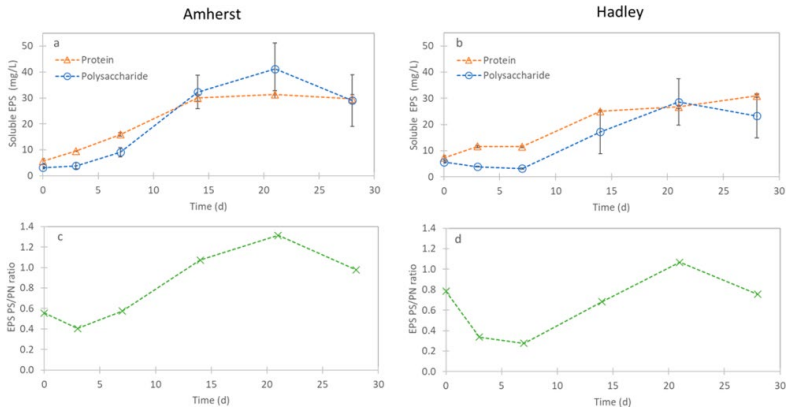

erst is top value, Hadley is bottom value.

inoculum biomass and recycled for phototrophic growth during hydrostatic cultivation of photogranules.

The changes in dissolved N in Amherst and Hadley cultivations are shown in Figure 2. Nitrate was depleted within the first 3 days of cultivation (Phase I). This removal appears to be linked with denitrification, as we observed the formation of gas bubbles and sludge rising during this period. In the Amherst set, nitrate was released during the later periods of cultivation, indicating the occurrence of nitrification along with the oxygenic photosynthesis. In the Hadley set, nitrate remained depleted, implying insignificant nitrification. Ammonia available from inoculum was also removed during the first 7 days of cultivation. In the Amherst set, some release of ammonia was observed during the later periods of cultivation. In contrast, ammonia in the Hadley set remained depleted until the end of cultivation. Finally, some or significant removal of DON occurred during the early period of cultivation. However, longer cultivation caused DON to be released back to the liquid phase.

These results show that both cultivation sets underwent a limitation of N, especially DIN, during the first two phases. Assuming that all TDN available in inoculum was used for phototrophic growth, this would mean 0.6 mM and 1.4 mM N from Amherst and Hadley, respectively (Table S1). It is unlikely that uptake of only these amounts of N can account for substantial increase of phototrophic biomass when considering the stoichiometric ratio of N to phototrophic biomass is about 0.1. Using the amounts and chemical formula of phototrophic VSS shown above, approximately 6 mM of N should have been needed, which is four to ten times greater than initial TDN. These differences could be even greater if initial nitrate was removed by denitrification, because denitrification was not considered in the above calculation. N fixation is unlikely to happen in this closed and substrate-limited environment because nitrogen fixation is energy

DOI: 10.1021/acs.est.8b03033
Environ. Sci. Technol. 2018, 52, 10462−10471

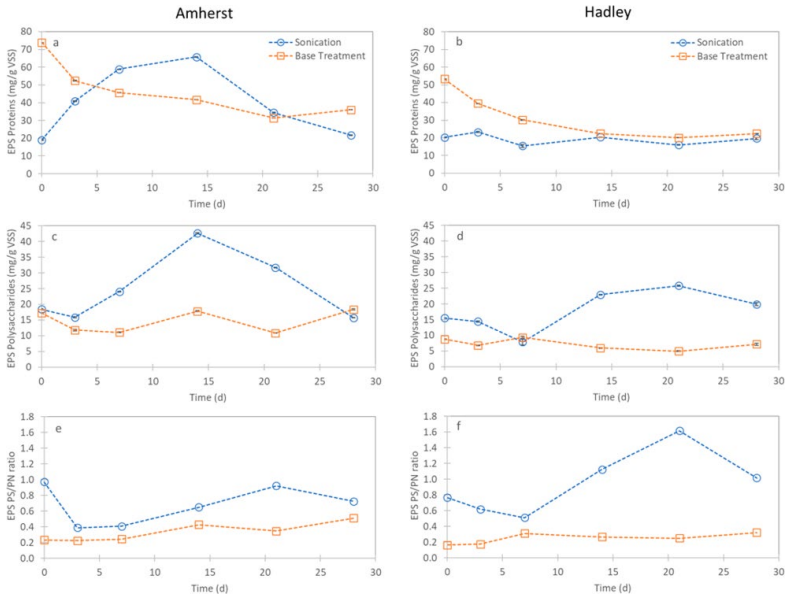

intensive process. Indeed, Stauch-White et al.[15] examined the presence of N fixation with qPCR but the results were negative. Consequently, to support phototrophic bloom (Phase II), more N than initial TDN should have been available and it is reasonable to assume that sludge VSS again became the source of N.

Depletion of DIN and degradation of sludge is thought to promote cyanobacteria, because these phototrophic organisms can utilize organic C and organic N from their extracellular environments.[18] Thus, when DIN becomes depleted organic N from the decay of sludge, such as nitrogenous EPS (i.e., proteins), could become the source of N for cyanobacteria, and this could give them the advantage to green algae. These points are partially supported by a moderate to strong Pearson correlation between chlorophyll *a*/*b* and the ratio of DOC/TDN for Amherst ($r = 0.87$) and Hadley ($r = 0.66$) during the first two phases of photogranulation.

Fate and Dynamics of EPS in the Progression of Photogranulation under Hydrostatic Conditions. The pattern of changes in soluble EPS, proteins, and polysaccharides, and even PS/PN ratio was very similar between the Amherst and Hadley cultivations (Figure 3), which suggests a common phenomenon in photogranulation under hydrostatic conditions. During the progression of photogranulation, a general increase for soluble proteins and polysaccharides was observed. As can be expected from the comparison of Figures 1 and 3, soluble EPS had positive correlations with chlorophyll *a*: proteins (Amherst, $r = 0.93$; Hadley, $r = 0.84$); polysaccharides (Amherst, $r = 0.84$; Hadley, $r = 0.72$) (Table 1). There were also correlations between soluble EPS and chlorophyll *b*, and this was particularly the case for Amherst as seen with proteins (Amherst, $r = 0.91$; Hadley, $r = 0.64$) and polysaccharides (Amherst, $r = 0.81$; Hadley, $r = 0.46$). The chlorophyll *a*/*b* also correlated moderately or strongly with soluble proteins (Amherst, $r = 0.64$; Hadley, $r = 0.90$) and polysaccharides (Amherst, $r = 0.54$; Hadley, $r = 0.87$).

It can also be seen that during Phase II and after, both cultivation sets showed more dramatic increase in soluble polysaccharides than proteins, which led to an evident increase of PS/PN in soluble EPS (Figure 3). These results imply an important role of EPS polysaccharides in the growth of filamentous cyanobacteria and photogranulation. Indeed, filamentous cyanobacteria are known to produce slime, a form of soluble polysaccharides or a mucilaginous substance that is loosely dispersed around the cell.[24,49] This slime is highly associated with gliding motility of filamentous cyanobacteria as it serves as lubricant or substratum for the movement of filamentous cyanobacteria.[49−52] According to literature, in new cultures of filamentous cyanobacteria, gliding motility was always accompanied by the presence of slime

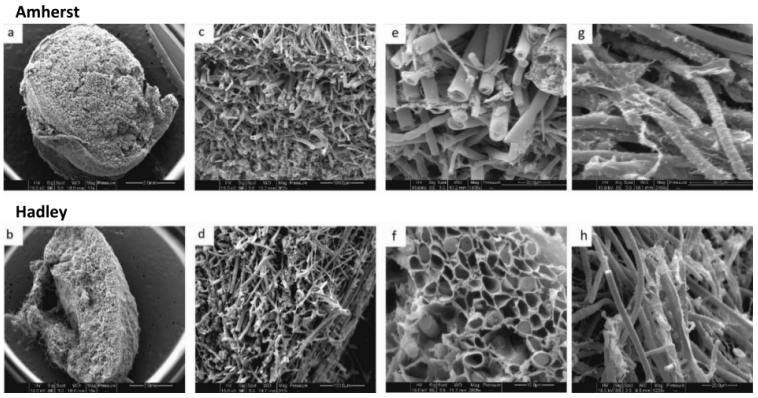

nd Hadley cultivation, respectively.

EPS.[49,50] In our study, gliding motility of filamentous cyanobacteria was also directly observed by light microscopy during the phototrophic bloom periods.

The dynamics of biomass-bound EPS were more complicated than those for soluble EPS due to different trends between extraction methods and both common and different phases existing between cultivations. Base-extracted proteins and polysaccharides showed very similar trends between Amherst and Hadley cultivations. Most notably, base-extracted proteins substantially decreased with the difference between day 0 (sludge inoculum) and day 28 (mature photogranules) by 51% and 58% for Amherst and Hadley, respectively (Figure 4a,b). Moreover, base-extracted proteins correlated negatively with chlorophyll *a* (Amherst, $r = -0.80$; Hadley, $r = -0.93$) and chlorophyll *a*/*b* (Amherst, $r = -0.75$; Hadley, $r = -0.93$) (Table 1). Significant reduction of base-extractable proteins over the cultivation and their strong correlations with chlorophylls suggest that this particular pool of EPS in sludge degraded and was available for phototrophic growth.

Base treatment can extract EPS proteins that are bound with Fe^{3+}.[33] It is a reasonable postulation that sludge in a closed vial undergoes anoxic decay before an oxic environment prevails with the bloom of phototrophs. Then, Fe^{3+} in the sludge is expected to be reduced to soluble Fe^{2+}, leading to the release of EPS proteins that are bound with Fe^{3+}. These released proteins then could become the source of C and N for phototrophic growth. As discussed earlier, the limitation of original DIN but the release of organic N could be advantageous to filamentous cyanobacteria because they can utilize organic N as a source of N.[48] Literature also shows that cyanobacteria can recycle extracellular organic C and N in mats where the typical turnover of EPS is 5−8% in 20−30 min.[48] These points, thus, could potentially explain the dominance of filamentous cyanobacteria after green algae in the progression of photogranulation.

While it might be possible that some of the reduced base-extracted proteins became soluble proteins (base-extracted proteins vs soluble proteins: Amherst, $r = -0.89$; Hadley, $r = -0.87$), base-extracted proteins also moderately correlated with soluble polysaccharides (Amherst, $r = -0.82$; Hadley, $r = -0.75$) (Table S2). Since only base-extracted proteins, not base-extracted polysaccharides, correlate with soluble EPS (Table S2), these observations suggest that the decreased base-extracted proteins were more likely utilized for the growth of phototrophs. In other words, soluble EPS is more likely associated with the growth of phototrophs rather than the residual of sludge decay, and strong correlations between soluble EPS and chlorophyll contents shown earlier support this statement.

In contrast to base-extracted proteins, sonication-extracted proteins showed different trends between the two sludge sources (Figure 4). Amherst cultivation showed substantial increase during the first two phases followed by a decrease, while Hadley one showed little change. Sonication extraction is known to select for EPS bound with divalent cations, which is also partially supported by this study showing a negative correlation between sonication-extracted proteins and soluble Ca^{2+} for Amherst ($r = -0.79$) and Hadley ($r = -0.71$) cultivations.

Different from proteins, sonication-extracted polysaccharides showed similar trends between the two cultivations (Figure 4c,d), like the common trends of base-extracted proteins or soluble EPS across the cultivations. An initial decrease of sonication-extracted polysaccharides during Phase I was followed by an increase for both sludge sources. Worth noting is that this fraction of polysaccharide showed stronger correlation with chlorophyll *a*/*b* (Amherst, $r = 0.68$; Hadley,

DOI: 10.1021/acs.est.8b03033
Environ. Sci. Technol. 2018, 52, 10462−10471

r = 0.71) than chlorophyll a (Amherst, r = 0.64; Hadley, r = 0.51). Furthermore, there was no correlation between sonication-extracted polysaccharides and chlorophyll b (Amherst, r = 0.37; Hadley, r = 0.16) (Table 1). These trends are comparable to what was seen with soluble polysaccharides, and indeed sonication-extracted polysaccharides were found to positively correlate with soluble polysaccharides (Amherst, r = 0.62; Hadley, r = 0.89) (Table S2) while no or negative correlation was found between base-extracted polysaccharides and soluble polysaccharides (Amherst, r = 0.11; Hadley, r = −0.76).

Similar to PS/PN in soluble EPS, a clear increase in PS/PN of sonication-extracted EPS was observed during Phase II and III (Figure 4e,f). The regression analysis on PS/PN of soluble EPS and sonication-extracted EPS from day 3 until the end of cultivation showed very strong correlations (Amherst, r = 0.96; Hadley, r = 0.98). These results again suggest that photogranulation under hydrostatic conditions occurs via enrichment of polysaccharides that are highly associated with the growth of filamentous cyanobacteria and their motility.

Morphology of EPS and Microstructures in Photogranules. Milferstedt et al.[10] showed an SEM image of a cross-section of an HSP. There, interwoven mat of cyanobacterial biomass constituted the outer layer of the photogranule and enclosed inner biomass. In the current study, we report more detailed morphology of photogranules by SEM, with focuses on EPS network and filamentous cyanobacteria in the outer layer.

First, SEM shows the overall cross sections of photogranules generated from Amherst and Hadley cultivations (Figures 5a,b). The interwoven nature of the outer layer of photogranules due to dense and complicated layering of filamentous cyanobacteria can also be seen (Figure 5c,d).

A larger magnification shows that EPS in sheath and tube structures encased filamentous cyanobacteria for both Amherst and Hadley photogranules (Figure 5e,f), which were observed and identified in comparison to literature.[50,53] Filamentous cyanobacteria were observed to occupy the interior of some sheath and tube structures, while others were empty. Particularly, Hadley granules show multiple tubes and sheaths that are meshed into a honeycomb-like structure (Figure 5f). It has been reported that these sheath and tube structures are of polysaccharide nature and mostly composed of glucose.[50] While these sheath and tubes EPS were abundantly present in the outer layer of photogranules, we could also find slime-like EPS coating the surface of filamentous cyanobacteria (Figure 5g,h).

While future research may help to gain more insight of these different types of EPS in photogranules, information shown in literature suggests that sheath/tube EPS reflect aging or maturation of granulation. With time in established, aged cultures of filamentous cyanobacteria, a change in the form of EPS (slime → sheath) was observed, with reduced motility.[54,55] One reason this can occur is due to unbalanced C to N metabolism.[56,57] Hoiczyk[54] also observed by light microscopy that in *Phormidium* sp., ensheathed filamentous cyanobacteria were never observed to move. On the basis of the methods from Hoiczyk to visualize motility, filamentous cyanobacteria in our mature photogranules showed much less motility compared to earlier phases of development.

Potential Mechanisms of Sludge-Based Photogranulation under Hydrostatic Conditions. The current study shows that both degradation and generation of EPS are closely involved in the transformation of activated sludge into a photogranule in a hydrostatic environment that is, based on conventional understanding, highly unlikely to produce granular biomass. While filamentous cyanobacteria are known to play a key role in photogranulation,[10,15] the present study starts to reveal why this group of phototrophs is selected and how the recycle of EPS leads to photogranulation under hydrostatic conditions.

On the basis of the results of EPS and basic characteristics of biomass, it seems clear that the decaying sludge inoculum, especially base-extractable proteins, is recycled for the growth of phototrophic biomass. Furthermore, on the basis of the results of SEM as well as correlations among soluble and sonication-extracted EPS with chlorophylls, significant amounts of C from photosynthesis seem to be invested toward the production of EPS polysaccharides.

Movement of filamentous cyanobacteria with their adhesive EPS covering entire trichomes[50,54] is thought to enhance aggregation of biomass during Phase II (the phototrophic, especially, cyanobacterial, bloom period). This motility occurs in the microscale, but filamentous cyanobacteria can glide as fast as 10 μm/s with a rate of elongation up to 3 μm/s.[49] Hence, this "movement" in "hydrostatic" environment may be somewhat analogous to hydrodynamic conditions in reactor operation, affecting granulation.

However, the motility of filamentous cyanobacteria itself seems to cause the limitation of their growth, because the motility becomes significantly restricted as they grow substantially. Literature shows that when filamentous cyanobacteria reach high densities, their motility creates collision and random movements, including flexing motions, leading to the formation of interwoven mat.[58−61] This point may also be supported by observations that chlorophylls and soluble/sonication EPS started leveling off (Phase III), despite the presence of substrates and nutrients, including light, DOC (as the source of CO_2), N (even DIN in the Amherst set), and phosphorus (Figures 1,2, and S3). The restricted growth of filamentous cyanobacteria from substantial entanglement then seemed to promote the granule formation, which might be enhanced by the production of sheath/tubes-like EPS.

The other possibility of the limited growth of filamentous cyanobacteria and the entry into the main granulation phase is that there might have been actually no more effective form of organic C to recycle as base-extracted proteins become depleted. This statement can be supported by a strong correlation between base-extracted proteins and chlorophylls so that the declination in chlorophyll a (phototrophic growth) as well as a/b (cyanobacterial growth) took place along with no further change in base-extracted proteins (Figures 1 and 4 and Table 1).

We expect that EPS in photogranules grown in reactors could be different from EPS in HSP due to the presence of shear. In other words, the key force(s) to push for photogranulation under hydrostatic and hydrodynamic conditions may be different. Future studies will require direct comparison on EPS between photogranules formed by hydrostatic cultivation and hydrodynamic reactor operation. Furthermore, the analysis of EPS would be useful to investigate the formation of photogranules under different conditions, such as different hydraulic and light conditions. Ultimately, these efforts will advance our understanding of photogranulation phenomenon and be helpful for developing the OPG process for aeration-free wastewater treatment.

DOI: 10.1021/acs.est.8b03033
Environ. Sci. Technol. 2018, 52, 10462−10471

■ ASSOCIATED CONTENT

Supporting Information

The Supporting Information is available free of charge on the ACS Publications website at DOI: 10.1021/acs.est.8b03033.

Detailed materials and methods; basic description of Amherst and Hadley WWTPs and properties of activated sludge inoculums (Table S1); Pearson correlation coefficients among different fractions of EPS in hydrostatic cultivation of photogranules (Table S2); mature photogranules produced by hydrostatic cultivation (Figure S1); and changes in the biomass concentrations for the duration of the hydrostatic cultivation of photogranules (Figure S2) (PDF)

■ AUTHOR INFORMATION

Corresponding Author

*E-mail: chulp@umass.edu (C.P.).

ORCID

Chul Park: 0000-0003-0695-8562

Notes

The authors declare no competing financial interest.

⊥Deceased.

■ ACKNOWLEDGMENTS

The authors thank Ahmed Abouhend, Adam McNair, Jérôme Hamelin, and Kim Milferstedt for valuable comments and discussion of the manuscript. This work was supported by the National Science Foundation [CBET1335816, CBET1605424] and 2013 Paul Busch Award by Water Environment Research Foundation.

■ REFERENCES

(1) Lettinga, G.; van Velsen, A. F. M.; Hobma, S. W.; de Zeeuw, W.; Klapwijk, A. Use of the Upflow Sludge Blanket (USB) Reactor Concept for Biological Wastewater Treatment, Especially for Anaerobic Treatment. *Biotechnol. Bioeng.* **1980**, *22*, 699−734.

(2) Morgenroth, E.; Sherden, T.; Van Loosdrecht, M. C. M.; Heijnen, J. J.; Wilderer, P. a. Aerobic Granular Sludge in a Sequencing Batch Reactor. *Water Res.* **1997**, *31* (12), 3191−3194.

(3) Beun, J. J.; Hendriks, A.; Van Loosdrecht, M. C. M.; Morgenroth, E.; Wilderer, P. A.; Heijnen, J. J. Aerobic Granulation in a Sequencing Batch Reactor. *Water Res.* **1999**, *33* (10), 2283−2290.

(4) Liu, Y.; Tay, J. H. State of the Art of Biogranulation Technology for Wastewater Treatment. *Biotechnol. Adv.* **2004**, *22* (7), 533−563.

(5) Liu, Y.; Tay, J. The Essential Role of Hydrodynamic Shear Force in the Formation of Biofilm and Granular Sludge. *Water Res.* **2002**, *36* (7), 1653−1665.

(6) Ding, Z.; Bourven, I.; Guibaud, G.; van Hullebusch, E. D.; Panico, A.; Pirozzi, F.; Esposito, G. Role of Extracellular Polymeric Substances (EPS) Production in Bioaggregation: Application to Wastewater Treatment. *Appl. Microbiol. Biotechnol.* **2015**, *99* (23), 9883−9905.

(7) Park, C.; Dolan, S. Algal-Sludge Granule for Wastewater Treatment and Bioenergy Feedstock Generation. WO2015112654 A2, 2015.

(8) Tiron, O.; Bumbac, C.; Patroescu, I. V.; Badescu, V. R.; Postolache, C. Granular Activated Algae for Wastewater Treatment. *Water Sci. Technol.* **2015**, *71* (6), 832−839.

(9) Tiron, O.; Bumbac, C.; Manea, E.; Stefanescu, M.; Lazar, M. N. Overcoming Microalgae Harvesting Barrier by Activated Algae Granules. *Sci. Rep.* **2017**, *7* (1), 1−11.

(10) Milferstedt, K.; Kuo-dahab, W. C.; Butler, C. S.; Hamelin, J.; Abouhend, A. S.; Stauch-White, K.; McNair, A.; Watt, C.; Carbajal-Gonzalez, B. I.; Dolan, S.; et al. The Importance of Filamentous Cyanobacteria in the Development of Unusual Oxygenic Photogranules. *Sci. Rep.* **2017**, *7* (1), 17944.

(11) Abouhend, A. S.; McNair, A.; Kuo-Dahab, W. C.; Watt, C.; Butler, C. S.; Milferstedt, K.; Hamelin, J.; Seo, J.; Gikonyo, G. J.; El-Moselhy, K. M.; et al. The Oxygenic Photogranule Process for Aeration-Free Wastewater Treatment. *Environ. Sci. Technol.* **2018**, *52* (6), 3503−3511.

(12) New York State Energy Research and Development Authority. *Statewide Assessment of Energy Use by the Municipal Water and Wastewater Sector*; Albany, NY, 2008.

(13) United States Environmental Protection Agency. *Energy Efficiency in Water and Wastewater Facilities*; 2013.

(14) United States Environmental Protection Agency. *Inventory of U. S. Greenhouse Gas Emissions and Sinks*; 2016, pp 1990−1998

(15) Stauch-White, K.; Srinivasan, V. N.; Kuo-Dahab, W. C.; Park, C.; Butler, C. S. The Role of Inorganic Nitrogen in Successful Formation of Granular Biofilms for Wastewater Treatment That Support Cyanobacteria and Bacteria. *AMB Express* **2017**, *7* (146), 1−10.

(16) Tay, J.-H.; Liu, Q.-S.; Liu, Y. The Effects of Shear Force on the Formation, Structure and Metabolism of Aerobic Granules. *Appl. Microbiol. Biotechnol.* **2001**, *57* (1−2), 227−233.

(17) McSwain, B. S.; Irvine, R. L.; Hausner, M.; Wilderer, P. A. Composition and Distribution of Extracellular Polymeric Substances in Aerobic Flocs and Granular Sludge. *Appl. Environ. Microbiol.* **2005**, *71* (2), 1051−1057.

(18) Adav, S. S.; Lee, D. J.; Tay, J. H. Extracellular Polymeric Substances and Structural Stability of Aerobic Granule. *Water Res.* **2008**, *42* (6−7), 1644−1650.

(19) Caudan, C.; Filali, A.; Spérandio, M.; Girbal-Neuhauser, E. Multiple EPS Interactions Involved in the Cohesion and Structure of Aerobic Granules. *Chemosphere* **2014**, *117* (1), 262−270.

(20) Sajjad, M.; Kim, K. S. Studies on the Interactions of Ca2+ and Mg2+ with EPS and Their Role in Determining the Physicochemical Characteristics of Granular Sludges in SBR System. *Process Biochem.* **2015**, *50* (6), 966−972.

(21) Deng, S.; Wang, L.; Su, H. Role and Influence of Extracellular Polymeric Substances on the Preparation of Aerobic Granular Sludge. *J. Environ. Manage.* **2016**, *173*, 49−54.

(22) Arcila, J. S.; Buitrón, G. Influence of Solar Irradiance Levels on the Formation of Microalgae-Bacteria Aggregates for Municipal Wastewater Treatment. *Algal Res.* **2017**, *27*, 190−197.

(23) Jiao, Y.; D'haeseleer, P.; Dill, B. D.; Shah, M.; Verberkmoes, N. C.; Hettich, R. L.; Banfield, J. F.; Thelen, M. P. Identification of Biofilm Matrix-Associated Proteins from an Acid Mine Drainage Microbial Community. *Appl. Environ. Microbiol.* **2011**, *77* (15), 5230−5237.

(24) *Microbial Extracellular Polymeric Substances: Characterization, Structure and Funciton*, 1st ed.; Wingender, J., Neu, T. R., Flemming, H.-C., Eds.; Springer-Verlag: Berlin Heidelberg, 1999.

(25) Flemming, H.-C.; Wingender, J. The Biofilm Matrix. *Nat. Rev. Microbiol.* **2010**, *8* (9), 623−633.

(26) Quijano, G.; Arcila, J. S.; Buitrón, G. Microalgal-Bacterial Aggregates: Applications and Perspectives for Wastewater Treatment. *Biotechnol. Adv.* **2017**, *35* (6), 772−781.

(27) Kragh, K. N.; Alhede, M.; Rybtke, M.; Stavnsberg, C.; Jensen, P. O.; Tolker-Nielsen, T.; Whiteley, M.; Bjarnsholt, T. The Inoculation Method Could Impact the Outcome of Microbiological Experiments. *Appl. Environ. Microbiol.* **2018**, *84* (5), 1−14.

(28) Seviour, T.; Pijuan, M.; Nicholson, T.; Keller, J.; Yuan, Z. Gel-Forming Exopolysaccharides Explain Basic Differences between Structures of Aerobic Sludge Granules and Floccular Sludges. *Water Res.* **2009**, *43* (18), 4469−4478.

(29) Sheng, G.-P.; Yu, H.-Q.; Li, X.-Y. Extracellular Polymeric Substances (EPS) of Microbial Aggregates in Biological Wastewater Treatment Systems: A Review. *Biotechnol. Adv.* **2010**, *28* (6), 882−894.

(30) Seviour, T.; Yuan, Z.; van Loosdrecht, M. C. M.; Lin, Y. Aerobic Sludge Granulation: A Tale of Two Polysaccharides? *Water Res.* **2012**, *46* (15), 4803−4813.
(31) Sheng, G. P.; Xu, J.; Li, W. H.; Yu, H. Q. Quantification of the Interactions between Ca2+, Hg2+and Extracellular Polymeric Substances (EPS) of Sludge. *Chemosphere* **2013**, *93* (7), 1436−1441.
(32) Caudan, C.; Filali, A.; Spérandio, M.; Girbal-Neuhauser, E. Multiple EPS Interactions Involved in the Cohesion and Structure of Aerobic Granules. *Chemosphere* **2014**, *117*, 262−270.
(33) Park, C.; Novak, J. T.; Helm, R. F.; Ahn, Y.-O.; Esen, A. Evaluation of the Extracellular Proteins in Full-Scale Activated Sludges. *Water Res.* **2008**, *42* (14), 3879−3889.
(34) Muller, C. D. *Shear Forces, Floc Structure and Their Impact on Anaerobic Digestion and Biosolids Stability Shear Forces, Floc Structure and Their Impact on Anaerobic Digestion and Biosolids Stability*; Virginia Polytechnic Insitute and State University, 2006.
(35) D'Abzac, P.; Bordas, F.; Van Hullebusch, E.; Lens, P. N. L.; Guibaud, G. Extraction of Extracellular Polymeric Substances (EPS) from Anaerobic Granular Sludges: Comparison of Chemical and Physical Extraction Protocols. *Appl. Microbiol. Biotechnol.* **2010**, *85* (5), 1589−1599.
(36) Wang, M. *Investigation of Microalgae Cultivation and Anaerobic Codigestion of Algae and Sewage Sludge for Wastewater Treatment Facilities*; University of Massachusetts: Amherst, 2013.
(37) Park, C.; Novak, J. T. Characterization of Activated Sludge Exocellular Polymers Using Several Cation-Associated Extraction Methods. *Water Res.* **2007**, *41* (8), 1679−1688.
(38) APHA. *Standard Methods of Water and Wastewater*, 20th ed.; American Public Health Association: Washington, DC, 1998.
(39) Dubois, M.; Gilles, K.; Hamilton, J.; Rebers, P.; Smith, S. Colorimetric Method for Determination of Sugars and Related Substances. *Anal. Chem.* **1956**, *28* (3), 350−356.
(40) Lowry, O. H.; Rosebrough, N. J.; Farr, A. L.; Randall, R. J. Protein Measurement with the Folin Phenol Reagent. *J. Biol. Chem.* **1951**, *193* (1), 265−275.
(41) Frølund, B.; Griebe, T.; Nielsen, P. H. Enzymatic Activity in the Activated-Sludge Floc Matrix. *Appl. Microbiol. Biotechnol.* **1995**, *43* (4), 755−761.
(42) Eom, H.; Borgatti, D.; Paerl, H. W.; Park, C. Formation of Low-Molecular-Weight Dissolved Organic Nitrogen in Predenitrification Biological Nutrient Removal Systems and Its Impact on Eutrophication in Coastal Waters. *Environ. Sci. Technol.* **2017**, *51* (7), 3776−3783.
(43) Wood, A. M. Chlorophyll a:B Ratios in Marine Planktonic Algae1. *J. Phycol.* **1979**, *15* (3), 330−332.
(44) Park, J. B. K.; Craggs, R. J. Effect of Algal Recycling Rate on the Performance of Pediastrum Boryanum Dominated Wastewater Treatment High Rate Algal Pond. *Water Sci. Technol.* **2014**, *70* (8), 1299−1306.
(45) Rittmann, B. E.; McCarty, P. L. *Environmental Biotechnology: Principles and Applications*; McGraw-Hill, International: New York, 2001.
(46) Frølund, B.; Palmgren, R.; Keiding, K.; Nielsen, P. H. Extraction of Extracellular Polymers from Activated Sludge Using a Cation Exchange Resin. *Water Res.* **1996**, *30* (8), 1749−1758.
(47) Park, C.; Novak, J. T. Characterization of Lectins and Bacterial Adhesins in Activated Sludge Flocs. *Water Environ. Res.* **2009**, *81* (8), 755−764.
(48) Stuart, R. K.; Mayali, X.; Lee, J. Z.; Craig Everroad, R.; Hwang, M.; Bebout, B. M.; Weber, P. K.; Pett-Ridge, J.; Thelen, M. P. Cyanobacterial Reuse of Extracellular Organic Carbon in Microbial Mats. *ISME J.* **2016**, *10* (5), 1240−1251.
(49) Hoiczyk, E. Gliding Motility in Cyanobacteria: Observations and Possible Explanations. *Arch. Microbiol.* **2000**, *174* (1−2), 11−17.
(50) Hoiczyk, E.; Baumeister, W. Envelope Structure of Four Gliding Filamentous Cyanobacteria. *J. Bacteriol.* **1995**, *177* (9), 2387−2395.
(51) *Ecology of Cyanobacteria II: Their Diversity in Space and Time*, 1st ed.; Whitton, B. A., Ed.; Springer: Netherlands, 2012.
(52) Park, C.; Muller, C. D.; Abu-orf, M. M.; Novak, J. T. The Effect of Eastewater Cations on Activated Sludge Characteristics: Effects of Aluminum and Iron in Floc. *Water Environ. Res.* **2006**, *78* (1), 31−40.
(53) Bellinger, E. G.; Sigee, D. C. *Freshwater Algae: Identification and Use as Bioindicators*, 1st ed.; Wiley-Blackwell: West Sussex, UK, 2010.
(54) Hoiczyk, E. Structural and Biochemical Analysis of the Sheath of Phormidium Uncinatum. *J. Bacteriol.* **1998**, *180* (15), 3923−3932.
(55) Finkel, S. E.; Kolter, R. Evolution of Microbial Diversity during Prolonged Starvation. *Proc. Natl. Acad. Sci. U. S. A.* **1999**, *96* (7), 4023−4027.
(56) Otero, A.; Vincenzini, M. Nostoc (Cyanopyceae) Goes Nude: Extracelular Polysachharides Serve as a Sink for Reducing Power under Unbalanced C/N Metabolism. *J. Phycol.* **2004**, *40* (1), 74−81.
(57) De Philippis, R.; Vincenzini, M. Exocellular Polysccharides from Cyanobacteria and Their Possible Applications. *FEMS Microbiol. Rev.* **1998**, *22*, 151−175.
(58) Castenholz, R. W. Aggregation in a thermophilic. *Nature* **1967**, *215*, 1285−1286.
(59) Malin, G.; Pearson, H. W. Aerobic Nitrogen Fixation in Aggregate-forming Cultures of the Nonheterocystous Cyanobacterium Microcoleus chthonoplustes. *Microbiology* **1988**, *134*, 1755−1763.
(60) Shepard, R. N.; Sumner, D. Y. Undirected Motility of Filamentous Cyanobacteria Produces Reticulate Mats. *Geobiology* **2010**, *8* (3), 179−190.
(61) Tamulonis, C.; Kaandorp, J. A Model of Filamentous Cyanobacteria Leading to Reticulate Pattern Formation. *Life* **2014**, *4* (3), 433−456.

DOI: 10.1021/acs.est.8b03033
Environ. Sci. Technol. 2018, 52, 10462−10471

BIBLIOGRAPHY

Abellovich, A. (1982). Site of Ca+2 action in Triggering Motility in the Cyanobacterium Spirulina subsalsa. *Cell Motility*, *4*, 393–403.

Abouhend, A. S. A. S., McNair, A., Kuo-Dahab, W. C. W. C., Watt, C., Butler, C. S. C. S., Milferstedt, K., Hamelin, J., Seo, J., Gikonyo, G. J. G. J., El-Moselhy, K. M. K. M., & Park, C. (2018). The Oxygenic Photogranule Process for Aeration-Free Wastewater Treatment. *Environmental Science & Technology*, *52*(6), 3503–3511. https://doi.org/10.1021/acs.est.8b00403

Abouhend, A. S., Milferstedt, K., Hamelin, J., Ansari, A. A., Butler, C., Carbajal-González, B. I., & Park, C. (2020). Growth Progression of Oxygenic Photogranules and Its Impact on Bioactivity for Aeration-Free Wastewater Treatment. *Environmental Science and Technology*. https://doi.org/10.1021/acs.est.9b04745

Adav, S. S., & Lee, D. J. (2008a). Extraction of extracellular polymeric substances from aerobic granule with compact interior structure. *Journal of Hazardous Materials*, *154*(1–3), 1120–1126. https://doi.org/10.1016/j.jhazmat.2007.11.058

Adav, S. S., Lee, D. J., Show, K. Y., & Tay, J. H. (2008b). Aerobic granular sludge: Recent advances. *Biotechnology Advances*, *26*(5), 411–423. https://doi.org/10.1016/j.biotechadv.2008.05.002

Adav, S. S., Lee, D. J., & Tay, J. H. (2008c). Extracellular polymeric substances and structural stability of aerobic granule. *Water Research*, *42*(6–7), 1644–1650. https://doi.org/10.1016/j.watres.2007.10.013

Adav, S. S., Lee, D. J., & Lai, J. Y. (2009). Proteolytic activity in stored aerobic granular sludge and structural integrity. *Bioresource Technology*, *100*(1), 68–73. https://doi.org/10.1016/j.biortech.2008.05.045

Andreadakis, A. D. (1993). Physical and chemical properties of activated sludge flocs. *Water Research*, *27*(12), 1707–1714.

Ansari, A. A., Abouhend, A. S., & Park, C. (2019). Effects of seeding density on photogranulation and the start-up of the oxygenic photogranule process for aeration-free wastewater treatment. *Algal Research*, *40*(April), 101495. https://doi.org/10.1016/j.algal.2019.101495

APHA. (1998). *Standard Methods of Water and Wastewater* (Twentieth). American Public Health Association.

Arcila, J. S., & Buitrón, G. (2016). Microalgae–bacteria aggregates: effect of the hydraulic retention time on the municipal wastewater treatment, biomass settleability and methane potential. *Journal of Chemical Technology and Biotechnology*, *91*(11), 2862–2870. https://doi.org/10.1002/jctb.4901

Barros, A., Guerra, L. T., Simões, M., Santos, E., Fonseca, D., Silva, J., Costa, L., & Navalho, J. (2017). Mass balance analysis of carbon and nitrogen in industrial scale mixotrophic microalgae cultures. *Algal Research*, *21*, 35–41. https://doi.org/10.1016/j.algal.2016.10.014

Baskin, T. I., Orr, T. J., Jercinovic, M., & Yoshida, M. (2014). Sample Preparation for Scanning Electron Microscopy: The Surprising Case of Freeze Drying from Tertiary Butanol. *Microscopy Today*, 1–4. https://doi.org/10.1017/S1551929514000522

Basuvaraj, M., Fein, J., & Liss, S. N. (2015). Protein and polysaccharide content of tightly and loosely bound extracellular polymeric substances and the development of a granular activated sludge floc. *Water Research*, *82*, 104–117. https://doi.org/10.1016/j.watres.2015.05.014

Benemann, J. R., Weissman, J. C., Koopman, B. L., & Oswald, W. J. (1977). Energy production by microbial photosynthesis. *NatureNature*, *268*(7), 19–23.

Beun, J. J., Hendriks, A., Van Loosdrecht, M. C. M., Morgenroth, E., Wilderer, P. A., & Heijnen, J. J. (1999). Aerobic granulation in a sequencing batch reactor. *Water Research*, *33*(10), 2283–2290. https://doi.org/10.1016/S0043-1354(98)00463-1

Beun, J. J., Van Loosdrecht, M. C. M., & Heijnen, J. J. (2002). Aerobic granulation in a sequencing batch airlift reactor. *Water Research*, *36*(3), 702–712. https://doi.org/10.1016/S0043-1354(01)00250-0

Borowitzka, M., Beardall, J., & Raven, J. (1998). *The physiology of microalgae*.

Branyikova, I., Prochazkova, G., Potocar, T., Jezkova, Z., & Branyik, T. (2018). Harvesting of microalgae by flocculation. *Fermentation*, *4*(4), 1–12. https://doi.org/10.3390/fermentation4040093

Briones, A., & Raskin, L. (2003). Diversity and dynamics of microbial communities in engineered environments and their implications for process stability. *Current Opinion in Biotechnology*, *14*(3), 270–276. https://doi.org/10.1016/S0958-1669(03)00065-X

Brockmann, D., Gérand, Y., Park, C., Milferstedt, K., Hélias, A., & Hamelin, J. (2021). Wastewater treatment using oxygenic photogranule-based process has lower environmental impact than conventional activated sludge process. *Bioresource Technology*, *319*(July 2020). https://doi.org/10.1016/j.biortech.2020.124204

Brown, M. J., & Lester, J. N. (1980). Comparison of bacterial extracellular polymer extraction methods. *Applied and Environmental Microbiology*, *40*(2), 179–185. https://doi.org/10.1128/aem.40.2.179-185.1980

Brüll, L. P., Huang, Z., Thomas-Oates, J. E., Paulsen, B. S., Cohen, E. H., & Michaelsen, T. E. (2000). Studies of polysaccharides from three edible species of Nostoc (cyanobacteria) with different colony morphologies: Structural characterization and effect on the complement system of polysaccharides from

Nostoc commune. *Journal of Phycology*, *36*(5), 871–881. https://doi.org/10.1046/j.1529-8817.2000.00038.x

Bruus, J. H., Nielsen, P. H., & Keiding, K. (1992). On the stability of activated sludge flocs with implications to dewatering. *Water Research*, *26*(12), 1597–1604. https://doi.org/https://doi.org/10.1016/0043-1354(92)90159-2

Castenholz, R. W. (1968). The Behavior of Oscillatoria Terebriformis in Hot Springs. *Journal of Phycology*, *4*(2), 132–139.

Caudan, C., Filali, A., Lefebvre, D., Spérandio, M., & Girbal-Neuhauser, E. (2012). Extracellular polymeric substances (EPS) from aerobic granular sludges: Extraction, fractionation, and anionic properties. *Applied Biochemistry and Biotechnology*, *166*(7), 1685–1702. https://doi.org/10.1007/s12010-012-9569-z

Chau, R. M. W., Ursell, T., Wang, S., Huang, K. C., & Bhaya, D. (2015). Maintenance of motility bias during cyanobacterial phototaxis. *Biophysical Journal*, *108*(7), 1623–1632. https://doi.org/10.1016/j.bpj.2015.01.042

Chen, M. Y., Lee, D. J., & Tay, J. H. (2007). Distribution of extracellular polymeric substances in aerobic granules. *Applied Microbiology and Biotechnology*, *73*(6), 1463–1469. https://doi.org/10.1007/s00253-006-0617-x

Christenson, L., & Sims, R. (2011). Production and harvesting of microalgae for wastewater treatment, biofuels, and bioproducts. *Biotechnology Advances*, *29*(6), 686–702. https://doi.org/10.1016/j.biotechadv.2011.05.015

Comte, S., Guibaud, G., & Baudu, M. (2006a). Relations between extraction protocols for activated sludge extracellular polymeric substances (EPS) and EPS complexation properties: Part I. Comparison of the efficiency of eight EPS extraction methods. *Enzyme and Microbial Technology*, *38*(1–2), 237–245. https://doi.org/10.1016/j.enzmictec.2005.06.016

Comte, S., Guibaud, G., & Baudu, M. (2006b). Biosorption properties of extracellular polymeric substances (EPS) resulting from activated sludge according to their type: Soluble or bound. *Process Biochemistry*, *41*(4), 815–823. https://doi.org/10.1016/j.procbio.2005.10.014

Cousin, C. P., & Ganczarczyk, J. J. (1999). The Effect of Cationic Salt Addition on the Settling and Dewatering Properties of an Industrial Activated Sludge. *Water Environment Research*, *71*(2), 251–254. http://www.jstor.org/stable/25045205

D'Abzac, P., Bordas, F., Van Hullebusch, E., Lens, P. N. L., & Guibaud, G. (2010a). Extraction of extracellular polymeric substances (EPS) from anaerobic granular sludges: Comparison of chemical and physical extraction protocols. *Applied Microbiology and Biotechnology*, *85*(5), 1589–1599. https://doi.org/10.1007/s00253-009-2288-x

D'Abzac, P., Bordas, F., van Hullebusch, E., Lens, P. N. L., & Guibaud, G. (2010b). Effects of extraction procedures on metal binding properties of extracellular

polymeric substances (EPS) from anaerobic granular sludges. *Colloids and Surfaces B: Biointerfaces*, *80*(2), 161–168. https://doi.org/10.1016/j.colsurfb.2010.05.043

Dartora, N., De Souza, L. M., Santana-Filho, A. P., Iacomini, M., Valduga, A. T., Gorin, P. A. J., & Sassaki, G. L. (2011). UPLC-PDA-MS evaluation of bioactive compounds from leaves of Ilex paraguariensis with different growth conditions, treatments and ageing. *Food Chemistry*, *129*(4), 1453–1461. https://doi.org/10.1016/j.foodchem.2011.05.112

de Godos, I., Vargas, V. A., Guzmán, H. O., Soto, R., García, B., García, P. A., & Muñoz, R. (2014). Assessing carbon and nitrogen removal in a novel anoxic-aerobic cyanobacterial-bacterial photobioreactor configuration with enhanced biomass sedimentation. *Water Research*, *61*, 77–85. https://doi.org/10.1016/j.watres.2014.04.050

De Kreuk, M. K., Kishida, N., Tsuneda, S., & van Loosdrecht, M. C. M. (2010). Behavior of polymeric substrates in an aerobic granular sludge system. *Water Research*, *44*(20), 5929–5938. https://doi.org/10.1016/j.watres.2010.07.033

de la Noüe, J., & Bassères, A. (1989). Biotreatment of anaerobically digested swine manure with microalgae. *Biological Wastes*, *29*(1), 17–31. https://doi.org/10.1016/0269-7483(89)90100-6

de los Rios, A., Ascaso, C., Wierzchos, J., Fernanandez-Valiente, E., & Quesada, A. (2004). Microstructural Characterization of Cyanobacterial Mats from the McMurdo Ice Shelf, Antarctica. *Applied and Environmental Microbiology*, *70*(1), 569–580. https://doi.org/10.1128/AEM.70.1.569

De Philippis, R., & Vincenzini, M. (1998). Exocellular polysccharides from cyanobacteria and their possible applications. *FEMS Microbiology Reviews*, *22*, 151–175. https://doi.org/10.1111/j.1574-6976.1998.tb00365.x

De Philippis, R., Sili, C., & Vincenzini, M. (1996). Response of an exopolysaccharide-producing heterocystous cyanobacterium to changes in metabolic carbon flux. *Journal of Applied Phycology*, *8*(4–5), 275–281.

Decho, A. W., Visscher, P. T., & Reid, R. P. (2005). Production and cycling of natural microbial exopolymers (EPS) within a marine stromatolite. *Palaeogeography, Palaeoclimatology, Palaeoecology*, *219*(1–2), 71–86. https://doi.org/10.1016/j.palaeo.2004.10.015

Delattre, C., Pierre, G., Laroche, C., & Michaud, P. (2016). Production, extraction and characterization of microalgal and cyanobacterial exopolysaccharides. *Biotechnology Advances*, *34*(7), 1159–1179. https://doi.org/10.1016/j.biotechadv.2016.08.001

Di Pippo, F., Ellwood, N. T. W., Gismondi, A., Bruno, L., Rossi, F., Magni, P., & de Philippis, R. (2013). Characterization of exopolysaccharides produced by seven

biofilm-forming cyanobacterial strains for biotechnological applications. *Journal of Applied Phycology*, *25*(6), 1697–1708. https://doi.org/10.1007/s10811-013-0028-1

Dignac, M. F., Urbain, V., Rybacki, D., Bruchet, A., Snidaro, D., & Scribe, P. (1998). Chemical description of extracellular polymers: Implication on activated sludge floc structure. *Water Science and Technology*, *38*(8-9–9 pt 7), 45–53. https://doi.org/10.1016/S0273-1223(98)00676-3

Dillon, J. G., & Castenholz, R. W. (2003). The synthesis of the UV-screening pigment, scytonemin, and photosynthetic performance in isolates from closely related natural populations of cyanobacteria (Calothrix sp.). *Environmental Microbiology*, *5*(6), 484–491. https://doi.org/10.1046/j.1462-2920.2003.00436.x

Ding, Z., Bourven, I., Guibaud, G., van Hullebusch, E. D., Panico, A., Pirozzi, F., & Esposito, G. (2015). Role of extracellular polymeric substances (EPS) production in bioaggregation: application to wastewater treatment. In *Applied Microbiology and Biotechnology* (Vol. 99, Issue 23, pp. 9883–9905). https://doi.org/10.1007/s00253-015-6964-8

Dubois, M., Gilles, K., Hamilton, J., Rebers, P., & Smith, S. (1956). Colorimetric method for determination of sugars and related substances. *Analytical Chemistry*, *28*(3), 350–356. https://doi.org/10.1021/ac60111a017

Dupraz, C., Reid, R. P., Braissant, O., Decho, A. W., Norman, R. S., & Visscher, P. T. (2009). Processes of carbonate precipitation in modern microbial mats. *Earth-Science Reviews*, *96*(3), 141–162. https://doi.org/10.1016/j.earscirev.2008.10.005

Durmaz, B., & Sanin, F. D. (2001). Effect of carbon to nitrogen on the composition of microbial extracellular polymers in activated sludge. *Water Science and Technology*, *44*(10), 221–229.

Eriksson, L., & Alm, B. (1991). Study of Flocculation Mechanisms by Observing Effects of a Complexing Agent on Activated Sludge Properties. *Water Science and Technology*, *24*(7), 21–28. https://doi.org/10.2166/wst.1991.0180

Flemming, H.-C., & Windgender, J. (2010). The biofilm matrix. *Nature Reviews. Microbiology*, *8*(623–633).

Flemming, H. C. (2011). The perfect slime. *Colloids and Surfaces B: Biointerfaces*, *86*(2), 251–259. https://doi.org/10.1016/j.colsurfb.2011.04.025

Flemming, H. C., Neu, T. R., & Wozniak, D. J. (2007). The EPS matrix: The “House of Biofilm Cells.” *Journal of Bacteriology*, *189*(22), 7945–7947. https://doi.org/10.1128/JB.00858-07

Casiano Flores, C., Bressers, H., Gutierrez, C., & de Boer, C. (2018). Towards circular economy – a wastewater treatment perspective, the Presa Guadalupe case. *Management Research Review*, *41*(5), 554–571. https://doi.org/10.1108/MRR-02-2018-0056

Frølund, B., Griebe, T., & Nielsen, P. H. (1995). Enzymatic activity in the activated-sludge floc matrix. *Applied Microbiology and Biotechnology*, *43*(4), 755–761. https://doi.org/10.1007/BF00164784

Frølund, B., Palmgren, R., Keiding, K., & Nielsen, P. H. (1996). Extraction of extracellular polymers from activated sludge using a cation exchange resin. *Water Research*, *30*(8), 1749–1758. https://doi.org/10.1016/0043-1354(95)00323-1

Gao, D., Liu, L., Liang, H., & Wu, W.-M. (2011). Aerobic granular sludge: characterization, mechanism of granulation and application to wastewater treatment. *Critical Reviews in Biotechnology*, *31*(2), 137–152.

Garcı, J., & Mujeriego, R. (1996). *Influence of Phytoplankton Composition on Biomass Removal from High-Rate Oxidation Lagoons by Means of Sedimentation and Spontaneous Flocculation*. *72*(2).

Garcia-Vaquero, M., Rajauria, G., O'Doherty, J. V., & Sweeney, T. (2017). Polysaccharides from macroalgae: Recent advances, innovative technologies and challenges in extraction and purification. *Food Research International*, *99*, 1011–1020. https://doi.org/10.1016/j.foodres.2016.11.016

Gikonyo, J. G., Ansari, A. A., Abouhend, A. S., Tobiason, J. E., & Park, C. (2021). Hydrodynamic granulation of oxygenic photogranules. *Environ. Sci.: Water Res. Technol.*, *7*(2), 427–440. https://doi.org/10.1039/D0EW00957A

Gong, A. S., Bolster, C. H., Benavides, M., & Walker, S. L. (2009). Extraction and analysis of extracellular polymeric substances: Comparison of methods and extracellular polymeric substance levels in salmonella pullorum sa 1685. *Environmental Engineering Science*, *26*(10), 1523–1532. https://doi.org/10.1089/ees.2008.0398

Goodwin, J. A. S., & Forster, C. F. (1985). A further examination into the composition of activated sludge surfaces in relation to their settlement characteristics. *Water Research*, *19*(4), 527–533. https://doi.org/https://doi.org/10.1016/0043-1354(85)90045-4

Guest, J. S., Skerlos, S. J., Barnard, J. L., Beck, M. B., Daigger, G. T., Hilger, H., Jackson, S. J., Karvazy, K., Kelly, L., Macpherson, L., Mihelcic, J. R., Pramanik, A., Raskin, L., Van Loosdrecht, M. C. M., Yeh, D., & Love, N. G. (2009). A New Planning and Design Paradigm to Achieve Sustainable Resource Recovery from Wastewater. *Environmental Science & Technology*, *43*(16), 6126–6130. https://doi.org/10.1021/es9010515

Guibaud, G., Comte, S., Bordas, F., Dupuy, S., & Baudu, M. (2005). Comparison of the complexation potential of extracellular polymeric substances (EPS), extracted from activated sludges and produced by pure bacteria strains, for cadmium, lead and nickel. *Chemosphere*, *59*(5), 629–638. https://doi.org/10.1016/j.chemosphere.2004.10.028

Guo, X., Wang, X., & Liu, J. (2016). Composition analysis of fractions of extracellular polymeric substances from an activated sludge culture and identification of dominant forces affecting microbial aggregation. *Scientific Reports*, *6*(February), 28391. https://doi.org/10.1038/srep28391

Gutzeit, G., Lorch, D., Weber, A., Engels, M., & Neis, U. (2005). Bioflocculant algal-bacterial biomass improves low-cost wastewater treatment. *Water Science and Technology*, *52*(12), 9–18.

Harmsen, H. J. M., Akkermans, A. D. L., Stams, A. J. M., & De Vos, W. M. (1996). Population dynamics of propionate-oxidizing bacteria under methanogenic and sulfidogenic conditions in anaerobic granular sludge. *Applied and Environmental Microbiology*, *62*(6), 2163–2168. https://doi.org/10.1128/aem.62.6.2163-2168.1996

Hermansson, M. (1999). The DLVO theory in microbial adhesion. *Colloids and Surfaces B: Biointerfaces*, *14*(1–4), 105–119. https://doi.org/10.1016/S0927-7765(99)00029-6

Herrero, A., & FLores, E. . (2008). *The Cyanobacteria: Molecular Biology, Genomics and Evolution*.

Herrero, A., Muro-pastor, A. M., & Flores, E. (2001). *MINIREVIEW Nitrogen Control in Cyanobacteria*. *183*(2), 411–425. https://doi.org/10.1128/JB.183.2.411

Higgins, M. J., & Novak, J. T. (1997a). Characterization of exocellular protein and its role in bioflocculation. *Journal of Environmental Engineering*, *May*, 479–485.

Higgins, M. J., & Novak, J. T. (1997b). The effect of cations on the settling and dewatering of activated sludges: laboratory results. *Water Environment Research*, *69*(2), 215–224.

Hodson, A., Cameron, K., Bøggild, C., Irvine-Fynn, T., Langford, H., Pearce, D., & Banwart, S. (2010). The structure, biological activity and biogeochemistry of cryoconite aggregates upon an arctic valley glacier: Longyearbreen, Svalbard. *Journal of Glaciology*, *56*(196), 349–362. https://doi.org/10.3189/002214310791968403

Hodson, A., Cameron, K., Bøggild, C., Irvine-Fynn, T., Langford, H., Pearce, D., & Banwart, S. (2010). The structure, biological activity and biogeochemistry of cryoconite aggregates upon an arctic valley glacier: Longyearbreen, Svalbard. *Journal of Glaciology*, *56*(196), 349–362. https://doi.org/10.3189/002214310791968403

Hoiczyk, E. (2000). Gliding motility in cyanobacteria: observations and possible explanations. *Archives of Microbiology*, *174*(1–2), 11–17. https://doi.org/10.1007/s002030000187

Hoiczyk, E. (2000). Gliding motility in cyanobacterial: observations and possible explanations. *Archives of Microbiology*, *174*(1–2), 11–17. https://doi.org/10.1007/s002030000187

Hoiczyk, E., & Baumeister, W. (1995). Envelope structure of four gliding filamentous cyanobacteria. *Journal of Bacteriology*, *177*(9), 2387–2395. https://doi.org/10.1128/jb.177.9.2387-2395.1995

Hoiczyk, E. (1998). Structural and biochemical analysis of the sheath of Phormidium uncinatum. *Journal of Bacteriology*, *180*(15), 3923–3932.

Hoiczyk, E., & Baumeister, W. (1997). Essential for the Gliding Motility of Cyanobacteria. *Molecular Microbiology*, *26*, 699–708.

Horan, N. J., & Eccles, C. R. (1986). Purification and characterization of extracellular polysaccharide from activated sludges. *Water Research*, *20*(11), 1427–1432. https://doi.org/https://doi.org/10.1016/0043-1354(86)90142-9

Hori, K., Ishii, S., Ikeda, G., Okamoto, J., Tanji, Y., Weeraphasphong, C., & Unno, H. (2002). Behavior of filamentous cyanobacterium Anabaena spp. in water column and its cellular characteristics. *Biochemical Engineering Journal*, *10*(3), 217–225. https://doi.org/https://doi.org/10.1016/S1369-703X(01)00185-1

Hou, X., Liu, S., & Zhang, Z. (2015). Role of extracellular polymeric substance in determining the high aggregation ability of anammox sludge. *Water Research*, *75*(5), 51–62. https://doi.org/10.1016/j.watres.2015.02.031

Hsieh, H. H., Wang, S. Y., Chen, T. L., Huang, Y. L., & Chen, M. J. (2012). Effects of cow's and goat's milk as fermentation media on the microbial ecology of sugary kefir grains. *International Journal of Food Microbiology*, *157*(1), 73–81. https://doi.org/10.1016/j.ijfoodmicro.2012.04.014

Hulshoff Pol, L. W., de Zeeuw, W. J., Velzeboer, C. T. M., & Lettinga, G. (1983). Granulation in UASB-Reactors. *Water Science and Technology*, *15*(8–9), 291–304. https://doi.org/10.2166/wst.1983.0172

Ingvorsen, K., Nielsen, M. Y., & Joulian, C. (2003). Kinetics of bacterial sulfate reduction in an activated sludge plant. *FEMS Microbiology Ecology*, *46*(2), 129–137. https://doi.org/10.1016/S0168-6496(03)00209-5

Jahn, A., & Nielsen, P. H. (1995). Extraction of extracellular polymeric substances (EPS) from biofilms using cation exchange resin. *Water Science and Technology*, *32*(8), 157–164.

Ji, B., Zhang, M., Gu, J., Ma, Y., & Liu, Y. (2020). A self-sustaining synergetic microalgal-bacterial granular sludge process towards energy-efficient and environmentally sustainable municipal wastewater treatment. *Water Research*, *179*, 115884. https://doi.org/10.1016/j.watres.2020.115884

Ji, X., Jiang, M., Zhang, J., Jiang, X., & Zheng, Z. (2018). The interactions of algae-bacteria symbiotic system and its effects on nutrients removal from synthetic wastewater. *Bioresource Technology*, *247*(July 2017), 44–50. https://doi.org/10.1016/j.biortech.2017.09.074

Jiang, B., & Liu, Y. (2012). Dependence of structure stability and integrity of aerobic granules on ATP and cell communication. *Applied Microbiology and Biotechnology*, *97*(11), 5105–5112. https://doi.org/10.1007/s00253-012-4315-6

Jorand, F., Boué-Bigne, F., Block, J. C., & Urbain, V. (1998). Hydrophobic/hydrophilic properties of activated sludge exopolymeric substances. *Water Science and Technology*, *37*(4–5), 307–315. https://doi.org/10.1016/S0273-1223(98)00123-1

Jorand, F., Zartarian, F., Thomas, F., Block, J. C., Bottero, J. Y., Villemin, G., Urbain, V., & Manem, J. (1995). Chemical and structural (2D) linkage between bacteria within activated sludge flocs. *Water Research*, *29*(7), 1639–1647. https://doi.org/10.1016/0043-1354(94)00350-G

Kakii, K., Kitamura, S., Shirakashi, T., & Kuriyama, M. (1985). Effect of Calcium Ion on Sludge Characteristics: *Journal of Fermentation Technology*, *63*(3), 263–270. https://ci.nii.ac.jp/naid/110002672931/en/

Kara, F., Gurakan, G. C., & Sanin, F. D. (2008). Monovalent cations and their influence on activated sludge floc chemistry, structure, and physical characteristics. *Biotechnology and Bioengineering*, *100*(2), 231–239. https://doi.org/10.1002/bit.21755

Kent, T. R., Bott, C. B., & Wang, Z.-W. (2018). State of the art of aerobic granulation in continuous flow bioreactors. *Biotechnology Advances*, *36*(4), 1139–1166. https://doi.org/https://doi.org/10.1016/j.biotechadv.2018.03.015

Kersters, K., & De Ley, J. (1975). Identification and grouping of bacteria by numerical analysis of their electrophoretic protein patterns. *Journal of General Microbiology*, *87*(2), 333–342. https://doi.org/10.1099/00221287-87-2-333

Kersters, K., & De Ley, J. (1980). Classification and identification of bacteria by electrophoresis of their proteins. *Society for Applied Bacteriology Symposium Series*, *8*, 273–297.

Klock, J. H., Wieland, A., Seifert, R., & Michaelis, W. (2007). Extracellular polymeric substances (EPS) from cyanobacterial mats: Characterisation and isolation method optimisation. *Marine Biology*, *152*(5), 1077–1085. https://doi.org/10.1007/s00227-007-0754-5

Kończak, B., Karcz, J., & Miksch, K. (2014). Influence of Calcium, Magnesium, and Iron Ions on Aerobic Granulation. *Applied Biochemistry and Biotechnology*, *174*(8), 2910–2918. https://doi.org/10.1007/s12010-014-1236-0

Kruschel, C., & Castenholz, R. W. (1998). The effect of solar UV and visible irradiance ont he vertical movements of cyanobacterial in microbial mats of hypersaline waters. *FEMS Microbiol Ecol.*, *27*, 53–72. https://doi.org/10.1111/j.1574-6941.1998.tb00525.x

Kuo-Dahab, W. C., Stauch-White, K., Butler, C. S., Gikonyo, G. J., Carbajal-González, B., Ivanova, A., Dolan, S., & Park, C. (2018). Investigation of the Fate and

Dynamics of Extracellular Polymeric Substances (EPS) during Sludge-Based Photogranulation under Hydrostatic Conditions. *Environmental Science and Technology*, *52*(18). https://doi.org/10.1021/acs.est.8b03033

Kuo-Dahab, W. C., Stauch-White, K., Butler, C. S., Carbajal-Gonzalez, B. I., Ivanova, A., & Park, C. (2017). Characterization and elucidation of oxygenic photogranule formation in a static environment. *Association of Environmental Engineering and Science Professors*.

Kuo-Dahab, W. C., Stauch-White, K., Butler, C. S., Milferstedt, K., Hamelin, J., Dolan, S., & Park, C. (2015). Photosynthetic sludge granule for wastewater treatment. *Water Environment Federation Annual Conference*.

Langford, H. J., Irvine-Fynn, T. D. L., Edwards, A., Banwart, S. A., & Hodson, A. J. (2014). A spatial investigation of the environmental controls over cryoconite aggregation on Longyearbreen glacier, Svalbard. *Biogeosciences*, *11*(19), 5365–5380. https://doi.org/10.5194/bg-11-5365-2014

Laspidou, C. S., & Rittmann, B. E. (2002). Non-steady state modeling of extracellular polymeric substances, soluble microbial products, and active and inert biomass. *Water Research*, *36*(8), 1983–1992. https://doi.org/10.1016/S0043-1354(01)00414-6

Lens, P. N. L., De Beer, D., Cronenberg, C. C. H., Houwen, F. P., Ottengraf, S. P. P., & Verstraete, W. H. (1993). Heterogeneous distribution of microbial activity in methanogenic aggregates: pH and glucose microprofiles. *Applied and Environmental Microbiology*, *59*(11), 3803–3815. https://doi.org/10.1128/aem.59.11.3803-3815.1993

Lettinga, G., Velsen, A. F. M. V. A. N., & Hobma, S. W. (1980). Use of the upflow sludge blanket (USB) reactor concept for biological wastewater treatment, especially for anaerobic treatment. *Biotechnology and Bioengineering*, *22*, 699–734.

Li, H., Wen, Y., Cao, A., Huang, J., Zhou, Q., & Somasundaran, P. (2012a). The influence of additives (Ca 2+, Al 3+, and Fe 3+) on the interaction energy and loosely bound extracellular polymeric substances (EPS) of activated sludge and their flocculation mechanisms. *Bioresource Technology*, *114*, 188–194. https://doi.org/10.1016/j.biortech.2012.03.043

Li, L., Gao, N., Deng, Y., Yao, J., & Zhang, K. (2012b). Characterization of intracellular & extracellular algae organic matters (AOM) of Microcystic aeruginosa and formation of AOM-associated disinfection byproducts and odor & taste compounds. *Water Research*, *46*(4), 1233–1240. https://doi.org/10.1016/j.watres.2011.12.026

Li, X. Y., & Yang, S. F. (2007). Influence of loosely bound extracellular polymeric substances (EPS) on the flocculation, sedimentation and dewaterability of activated sludge. *Water Research*, *41*(5), 1022–1030. https://doi.org/10.1016/j.watres.2006.06.037

Li, X.Y., Yang, S. F., Li, X. Y., & Yang, S. F. (2007). Influence of loosely bound extracellular polymeric substances (EPS) on the flocculation, sedimentation and dewaterability of activated sludge. *Water Research*, *41*, 1022–1030.

Li, Y. C., & Zhu, J. R. (2014). Role of N-acyl homoserine lactone (AHL)-based quorum sensing (QS) in aerobic sludge granulation. *Applied Microbiology and Biotechnology*, *98*(17), 7623–7632. https://doi.org/10.1007/s00253-014-5815-3

Limoli, D. H., Jones, C. J., Wozniak, D. J., & Cruz, S. (2015). Bacterial Extracellular Polysaccharides in Biofilm Formation and Function. *Microbiol Spectr.*, *3*(3), 1–30. https://doi.org/10.1128/microbiolspec.MB-0011-2014.Bacterial

Lin, Y., de Kreuk, M., van Loosdrecht, M. C. M., & Adin, A. (2010). Characterization of alginate-like exopolysaccharides isolated from aerobic granular sludge in pilot-plant. *Water Research*, *44*(11), 3355–3364. https://doi.org/10.1016/j.watres.2010.03.019

Liu, H., & Fang, H. H. P. (2002). Extraction of extracellular polymeric substances (EPS) of sludges. *Journal of Biotechnology*, *95*(3), 249–256. https://doi.org/10.1016/S0168-1656(02)00025-1

Liu, L., Gao, D. W., Zhang, M., & Fu, Y. (2010a). Comparison of Ca2+ and Mg2+ enhancing aerobic granulation in SBR. *Journal of Hazardous Materials*, *181*(1–3), 382–387. https://doi.org/10.1016/j.jhazmat.2010.05.021

Liu, L., Sheng, G. P., Liu, Z. F., Li, W. W., Zeng, R. J., Lee, D. J., Liu, J. X., & Yu, H. Q. (2010b). Characterization of multiporous structure and oxygen transfer inside aerobic granules with the percolation model. *Environmental Science and Technology*, *44*(22), 8535–8540. https://doi.org/10.1021/es102437a

Liu, L., Huang, Q., Qin, B., Zhu, G., Wu, P., & Wu, Y. (2016). Characterizing cell surface of blooming Microcystis in Lake Taihu, China. *Water Science and Technology*, *73*(11), 2731–2738. https://doi.org/10.2166/wst.2016.069

Liu, Y. Q., Liu, Y., & Tay, J. H. (2004). The effects of extracellular polymeric substances on the formation and stability of biogranules. *Applied Microbiology and Biotechnology*, *65*(2), 143–148. https://doi.org/10.1007/s00253-004-1657-8

Liu, Y., Wang, W., Zhang, M., Xing, P., & Yang, Z. (2010). PSII-efficiency, polysaccharide production, and phenotypic plasticity of Scenedesmus obliquus in response to changes in metabolic carbon flux. *Biochemical Systematics and Ecology*, *38*(3), 292–299. https://doi.org/10.1016/j.bse.2010.02.003

Liu, Y.-Q. Q., Tay, J.-H. H., & Moy, B. Y.-P. P. (2006). Characteristics of aerobic granular sludge in a sequencing batch reactor with variable aeration. *Applied Microbiology and Biotechnology*, *71*(5), 761–766. https://doi.org/10.1007/s00253-005-0209-1

Liu, Y., & Tay, J. H. (2004). State of the art of biogranulation technology for wastewater treatment. *Biotechnology Advances*, *22*(7), 533–563. https://doi.org/10.1016/j.biotechadv.2004.05.001

Liu, Y., & Tay, J. (2002). The essential role of hydrodynamic shear force in the formation of biofilm and granular sludge. *Water Research*, *36*(7), 1653–1665.

Liu, Y., Xu, H. Lou, Yang, S. F., & Tay, J. H. (2003). Mechanisms and models for anaerobic granulation in upflow anaerobic sludge blanket reactor. *Water Research*, *37*(3), 661–673. https://doi.org/10.1016/S0043-1354(02)00351-2

Lowry, O. H., Rosebrough, N. J., Farr, A. L., & Randall, R. J. (1951). Protein measurement with the Folin phenol reagent. *The Journal of Biological Chemistry*, *193*(1), 265–275. https://doi.org/10.1016/0304-3894(92)87011-4

Lü, F., Wang, J., Shao, L., & He, P. (2016). Enzyme disintegration with spatial resolution reveals different distributions of sludge extracellular polymer substances. *Biotechnology for Biofuels*, *9*(1), 29. https://doi.org/10.1186/s13068-016-0444-y

Lupi, F. M., Fernandes, H. M. ., Tome, M. M., Sa-Correia, I., & Novais, J. M. (1994). Influence of nitrogen source and photoperiod on exopolysaccharide synthesis by the microalga Botryococcus braunii UC 58. *Enzyme and Microbial Technology*, *16*(7), 546–550.

Lv, Y., Wan, C., Lee, D. J., Liu, X., & Tay, J. H. (2014). Microbial communities of aerobic granules: Granulation mechanisms. *Bioresource Technology*, *169*, 344–351. https://doi.org/10.1016/j.biortech.2014.07.005

Lv, Y., Wan, C., Lee, D. J., Liu, X., & Tay, J. H. (2014). Microbial communities of aerobic granules: Granulation mechanisms. *Bioresource Technology*, *169*, 344–351. https://doi.org/10.1016/j.biortech.2014.07.005

Mata, T. M., Martins, A. A., & Caetano, N. S. (2010). Microalgae for biodiesel production and other applications: A review. *Renewable and Sustainable Energy Reviews*, *14*(1), 217–232. https://doi.org/https://doi.org/10.1016/j.rser.2009.07.020

Mata-Alvarez, J., Dosta, J., Macé, S., & Astals, S. (2011). Codigestion of solid wastes: A review of its uses and perspectives including modeling. *Critical Reviews in Biotechnology*, *31*(2), 99–111. https://doi.org/10.3109/07388551.2010.525496

McKinney, R. E., & Horwood, M. P. (1952). Fundamental Approach to the Activated Sludge Process: I. Floc-Producing Bacteria. *Sewage and Industrial Wastes*, *24*(2), 117–123. http://www.jstor.org/stable/25031814

Meisen, S., Wingender, J., & Telgheder, U. (2008). Analysis of microbial extracellular polysaccharides in biofilms by HPLC. Part I: Development of the analytical method using two complementary stationary phases. *Analytical and Bioanalytical Chemistry*, *391*(3), 993–1002. https://doi.org/10.1007/s00216-008-2068-y

Milferstedt, K., Kuo-dahab, W. C., Butler, C. S., Hamelin, J., Abouhend, A. S., Stauch-White, K., McNair, A., Watt, C., Carbajal-Gonzalez, B. I., Dolan, S., & Park, C. (2017). The importance of filamentous cyanobacteria in the development of oxygenic photogranules. *Scientific Reports*, *7*(17944), 1–15. https://doi.org/10.1038/s41598-017-16614-9

Molina Grima, E., Belarbi, E.-H., Acién Fernández, F. G., Robles Medina, A., & Chisti, Y. (2003). Recovery of microalgal biomass and metabolites: process options and economics. *Biotechnology Advances*, *20*(7–8), 491–515. http://www.ncbi.nlm.nih.gov/pubmed/14550018

Monique, R., Elisabeth, G.-N., Etienne, P., & Dominique, L. (2008). A high yield multi-method extraction protocol for protein quantification in activated sludge. *Bioresource Technology*, *99*(16), 7464–7471. https://doi.org/10.1016/j.biortech.2008.02.025

Moreno, J., Vargas, M. A., Madiedo, J. M., Munoz, J., Rivas, J., & Guerrero, M. G. (2000). Chemical and rheological properties of an extracellular polysaccharide produced by the cyanobacterium Anabaena sp. ATCC 33047. *Biotechnology and Bioengineering*, *67*(3), 283–290.

Moreno, J., Vargas, M. A., Olivares, H., Rivas, J., & Guerrero, M. G. (1998). Exopolysaccharide production by the cyanobacterium *Anabaena* sp. ATCC 33047 in batch and continuous culture. *Journal of Biotechnology*, *60*(3), 175–182. https://doi.org/10.1016/S0168-1656(98)00003-0

Morgenroth, E., Sherden, T., van Loosdrecht, M. C. M. C. ., Heijnen, J. J. J., & Wilderer, P. a. A. (1997). Aerobic granular sludge in a sequencing batch reactor. *Water Research*, *31*(12), 3191–3194. https://doi.org/10.1016/S0043-1354(97)00216-9

Mota, R., Guimarães, R., Büttel, Z., Rossi, F., Colica, G., Silva, C. J., Santos, C., Gales, L., Zille, A., De Philippis, R., Pereira, S. B., & Tamagnini, P. (2013). Production and characterization of extracellular carbohydrate polymer from Cyanothece sp. CCY 0110. *Carbohydrate Polymers*, *92*(2), 1408–1415. https://doi.org/10.1016/j.carbpol.2012.10.070

Muller, C. D. (2006). *Shear Forces , Floc Structure and their Impact on Anaerobic Digestion and Biosolids Stability Shear Forces , Floc Structure and Their Impact on Anaerobic Digestion and Biosolids Stability*. Virginia Polytechnic Insitute and State University.

Muro-Pastor, M. I., & Florencio, F. J. (2003). Regulation of ammonium assimilation in cyanobacteria. *Plant Physiology and Biochemistry*, *41*(6–7), 595–603. https://doi.org/10.1016/S0981-9428(03)00066-4

New York State Energy Research and Development Authority. (2008). *Statewide assessment of energy use by the municipal water and wastewater sector*.

Ni, B. J., Xie, W. M., Liu, S. G., Yu, H. Q., Wang, Y. Z., Wang, G., & Dai, X. L. (2009). Granulation of activated sludge in a pilot-scale sequencing batch reactor for the treatment of low-strength municipal wastewater. *Water Research*, *43*(3), 751–761. https://doi.org/10.1016/j.watres.2008.11.009

Nielsen, P. H., Frølund, B., & Keiding, K. (1996). Changes in the composition of extracellular polymeric substances in activated sludge during anaerobic storage.

Applied Microbiology and Biotechnology, *44*(6), 823–830. https://doi.org/10.1007/BF00178625

Nielsen, P. H., & Jahn, A. (1999). Extraction of EPS. In J. Wingender, T. R. Neu, & H. C. Flemming (Eds.), *Microbial Extracellular Polymeric Substances* (pp. 50–69).

Novak, J. T., Love, N. G., Smith, M. L., & Wheeler, E. R. (1998). The effect of cationic salt addition on the settling and dewatering properties of an industrial activated sludge. *Water Environment Research*, *70*(5), 984–996. https://doi.org/10.2175/106143098x123318

Novak, J., & Haugan, B. (1981). Polymer Extraction from Activated Sludge. *Journal (Water Pollution Control Federation), 53*(9), 1420-1424. Retrieved June 14, 2021, from http://www.jstor.org/stable/25041506.

Oswald, J., & Ludwig, F. (1952). Algae symbiosis in oxidation ponds. *25th Annual Meeting Federation of Sewage and Industrial Wastes Associat*, *25*(6), 692–705.

Otero, A., & Vincenzini, M. (2004). Nostoc (Cyanopyceae) goes nude: Extracelular polysachharides serve as a sink for reducing power under unbalanced C/N metabolism. *Journal of Phycology*, *81*, 74–81. https://doi.org/10.1046/j.1529-8817.2004.03067.x

Ouazaite, H., Milferstedt, K., Hamelin, J., & Desmond-Le Quéméner, E. (2021). Mapping the biological activities of filamentous oxygenic photogranules. *Biotechnology and Bioengineering*, *118*(2), 601–611. https://doi.org/10.1002/bit.27585

Ozturk, S., & Aslim, B. (2010). Modification of exopolysaccharide composition and production by three cyanobacterial isolates under salt stress. *Environmental Science and Pollution Research*, *17*(3), 595–602. https://doi.org/10.1007/s11356-009-0233-2

Paes Leme, A. F., Koo, H., Bellato, C. M., Bedi, G., & Cury, J. A. (2006). The role of sucrose in cariogenic dental biofilm formation--new insight. *Journal of Dental Research*, *85*(10), 878–887. https://doi.org/10.1177/154405910608501002

Park, C., Abu-Orf, M. M., & Novak, J. T. (2006). The Digestibility of Waste Activated Sludges. *Water Environment Research*, *78*(1), 59–68. https://doi.org/10.2175/106143005x84521

Park, C., & Novak, J. T. (2007). Characterization of activated sludge exocellular polymers using several cation-associated extraction methods. *Water Research*, *41*(8), 1679–1688. https://doi.org/10.1016/j.watres.2007.01.031

Park, C., & Helm, R. F. (2008). Application of metaproteomic analysis for studying extracellular polymeric substances (EPS) in activated sludge flocs and their fate in sludge digestion. *Water Science and Technology*, *57*(12), 2009–2015. https://doi.org/10.2166/wst.2008.620

Park, C., Helm, R. F., & Novak, J. T. (2008a). Investigating the Fate of Activated Sludge Extracellular Proteins in Sludge Digestion Using Sodium Dodecyl Sulfate Polyacrylamide Gel Electrophoresis. *Water Environment Research*, *80*(12), 2219–2227. https://doi.org/10.2175/106143008x325791

Park, C., Novak, J. T., Helm, R. F., Ahn, Y.-O., & Esen, A. (2008b). Evaluation of the extracellular proteins in full-scale activated sludges. *Water Research*, *42*(14), 3879–3889. https://doi.org/10.1016/j.watres.2008.05.014

Park, C., & Novak, J. T. (2009). Characterization of Lectins and Bacterial Adhesins in Activated Sludge Flocs. *Water Environment Research*, *81*(8), 755–764. https://doi.org/10.2175/106143008X370421

Park, J. B. K., Craggs, R. J., & Shilton, a N. (2011). Recycling algae to improve species control and harvest efficiency from a high rate algal pond. *Water Research*, *45*(20), 6637–6649. https://doi.org/10.1016/j.watres.2011.09.042

Park, J. B. K., & Craggs, R. J. (2014). Effect of algal recycling rate on the performance of Pediastrum boryanum dominated wastewater treatment high rate algal pond. *Water Science and Technology*, *70*(8), 1299–1306. https://doi.org/10.2166/wst.2014.369

Pellicer-Nàcher, C., Domingo-Félez, C., Mutlu, A. G., & Smets, B. F. (2013). Critical assessment of extracellular polymeric substances extraction methods from mixed culture biomass. *Water Research*, *47*(15), 5564–5574. https://doi.org/10.1016/j.watres.2013.06.026

Pereira, S. B., Mota, R., Vieira, C. P., Vieira, J., & Tamagnini, P. (2015). Phylum-wide analysis of genes/proteins related to the last steps of assembly and export of extracellular polymeric substances (EPS) in cyanobacteria. *Scientific Reports*, *5*(September), 1–16. https://doi.org/10.1038/srep14835

Pereira, S., Zille, A., Micheletti, E., Moradas-Ferreira, P., De Philippis, R., & Tamagnini, P. (2009). Complexity of cyanobacterial exopolysaccharides: Composition, structures, inducing factors and putative genes involved in their biosynthesis and assembly. *FEMS Microbiology Reviews*, *33*(5), 917–941. https://doi.org/10.1111/j.1574-6976.2009.00183.x

Philippis, R. De, Sili, C., Vincenzini, M., De Philippis, R., Sili, C., & Vincenzini, M. (1996). Response of an exopolysaccharide-producing heterocystous cyanobacterium to changes in metabolic carbon flux. *Journal of Applied Phycology*, *8*(4–5), 275–281.

Pittman, J. K., Dean, A. P., & Osundeko, O. (2011). The potential of sustainable algal biofuel production using wastewater resources. *Bioresource Technology*, *102*(1), 17–25. https://doi.org/10.1016/j.biortech.2010.06.035

Ras, M., Girbal-Neuhauser, E., Paul, E., Spérandio, M., & Lefebvre, D. (2008). Protein extraction from activated sludge: An analytical approach. *Water Research*, *42*(8–9), 1867–1878. https://doi.org/10.1016/j.watres.2007.11.011

Rastogi, R. P., & Incharoensakdi, A. (2014). Characterization of UV-screening compounds, mycosporine-like amino acids, and scytonemin in the cyanobacterium Lyngbya sp. CU2555. *FEMS Microbiology Ecology*, *87*(1), 244–256. https://doi.org/10.1111/1574-6941.12220

Rittmann, B. E., & McCarty, P. L. (2001). *Environmental biotechnology: principles and applications* (Internatio). McGraw-Hill Book Co.

Rossi, F., & De Philippis, R. (2015). Role of Cyanobacterial Exopolysaccharides in Phototrophic Biofilms and in Complex Microbial Mats. *Life*, *5*, 1218–1238. https://doi.org/10.3390/life5021218

Sajjad, M., & Kim, K. S. (2015). Studies on the interactions of Ca2+ and Mg2+ with EPS and their role in determining the physicochemical characteristics of granular sludges in SBR system. *Process Biochemistry*, *50*(6), 966–972. https://doi.org/10.1016/j.procbio.2015.02.020

Schink, B. (1997). Energetics of syntrophic cooperation in methanogenic degradation. *Microbiology and Molecular Biology Reviews : MMBR*, *61*(2), 262–280. https://doi.org/10.1128/.61.2.262-280.1997

Seviour, Thomas, Yuan, Zhigu, van Loosdrecht, Mark C.M., Lin, Y. (2012). Aerobic sludge granulation: A tale of two polysaccharides? *Water Research*, *46*, 4803–4813.

Seviour, T., Derlon, N., Dueholm, M. S., Flemming, H. C., Girbal-Neuhauser, E., Horn, H., Kjelleberg, S., van Loosdrecht, M. C. M., Lotti, T., Malpei, M. F., Nerenberg, R., Neu, T. R., Paul, E., Yu, H., & Lin, Y. (2019). Extracellular polymeric substances of biofilms: Suffering from an identity crisis. *Water Research*, *151*, 1–7. https://doi.org/10.1016/j.watres.2018.11.020

Seviour, T., Pijuan, M., Nicholson, T., Keller, J., & Yuan, Z. (2009). Gel-forming exopolysaccharides explain basic differences between structures of aerobic sludge granules and floccular sludges. *Water Research*, *43*(18), 4469–4478. https://doi.org/10.1016/j.watres.2009.07.018

Seviour, T., Yuan, Z., van Loosdrecht, M. C. M., Lin, Y., Seviour, Thomas, Yuan, Zhigu, van Loosdrecht, Mark C.M., Lin, Y., Seviour, T., Yuan, Z., van Loosdrecht, M. C. M., & Lin, Y. (2012). Aerobic sludge granulation: A tale of two polysaccharides? *Water Research*, *46*(15), 4803–4813. https://doi.org/10.1016/j.watres.2012.06.018

Shammi, M., Pan, X., Mostofa, K. M. G., Zhang, D., & Liu, C. Q. (2017). Photo-flocculation of microbial mat extracellular polymeric substances and their transformation into transparent exopolymer particles: Chemical and spectroscopic evidences. *Scientific Reports*, *7*(1), 1–12. https://doi.org/10.1038/s41598-017-09066-8

Shapiro, L., Mcadams, H. H., & Losick, R. (2002). Generating and Exploiting Polarity in Bacteria. *Science*, *298*(December), 1942–1946. https://doi.org/10.1126/science.1072163

Sheehan John, Terri, D., John, B., & Paul, R. (1998). A Look Back at the U.S. Department of Energy's Aquatic Species. *The European Physical Journal C*, *72*(6), 14. http://www.springerlink.com/index/10.1140/epjc/s10052-012-2043-9%5Cnhttp://arxiv.org/abs/1203.5015

Sheng, G. P., & Yu, H. Q. (2006). Characterization of extracellular polymeric substances of aerobic and anaerobic sludge using three-dimensional excitation and emission matrix fluorescence spectroscopy. *Water Research*, *40*(6), 1233–1239. https://doi.org/10.1016/j.watres.2006.01.023

Sheng, G.-P. P., Yu, H.-Q. Q., & Li, X.-Y. Y. (2010). Extracellular polymeric substances (EPS) of microbial aggregates in biological wastewater treatment systems: A review. *Biotechnology Advances*, *28*(6), 882–894. https://doi.org/10.1016/j.biotechadv.2010.08.001

Stal, L. J. (1995). Physiological ecology of cyanobacteria in microbial mats and other communities. In *New Phytologist* (Vol. 131, Issue 1, pp. 1–32). https://doi.org/10.1111/j.1469-8137.1995.tb03051.x

Stauch-White, K., Srinivasan, V. N., Camilla Kuo-Dahab, W., Park, C., Butler, C. S., Kuo-Dahab, W. C., Park, C., & Butler, C. S. (2017). The role of inorganic nitrogen in successful formation of granular biofilms for wastewater treatment that support cyanobacteria and bacteria. *AMB Express*, *7*(146), 1–10. https://doi.org/10.1186/s13568-017-0444-8

Steiner, A. E., McLaren, D. A., & Forster, C. F. (1976). The nature of activated sludge flocs. *Water Research*, *10*(25–30).

Stibal, M., Šabacká, M., & Kaštovská, K. (2006). Microbial communities on glacier surfaces in Svalbard: Impact of physical and chemical properties on abundance and structure of cyanobacteria and algae. *Microbial Ecology*, *52*(4), 644–654. https://doi.org/10.1007/s00248-006-9083-3

Stuart, R. K., Mayali, X., Boaro, A. A., Zemla, A., Everroad, R. C., Nilson, D., Weber, P. K., Lipton, M., Bebout, B. M., Pett-Ridge, J., & Thelen, M. P. (2016). Light regimes shape utilization of extracellular organic C and N in a cyanobacterial biofilm. *MBio*, *7*(3), 1–14. https://doi.org/10.1128/mBio.00650-16

Stuart, R. K., Mayali, X., Lee, J. Z., Craig Everroad, R., Hwang, M., Bebout, B. M., Weber, P. K., Pett-Ridge, J., & Thelen, M. P. (2016). Cyanobacterial reuse of extracellular organic carbon in microbial mats. *ISME Journal*, *10*(5), 1240–1251. https://doi.org/10.1038/ismej.2015.180

Sturm, B. S. M., & Lamer, S. L. (2011). An energy evaluation of coupling nutrient removal from wastewater with algal biomass production. *Applied Energy*, *88*(10), 3499–3506. https://doi.org/10.1016/j.apenergy.2010.12.056

Takahashi, E., Ledauphin, J., Goux, D., & Orvain, F. (2009). Optimising extraction of extracellular polymeric substances (EPS) from benthic diatoms: Comparison of the

efficiency of six EPS extraction methods. *Marine and Freshwater Research*, *60*(12), 1201–1210. https://doi.org/10.1071/MF08258

Takeuchi, N., Kohshima, S., & Seko, K. (2001). Structure, formation, and darkening process of albedo-reducing material (cryoconite) on a Himalayan glacier: A granular algal mat growing on the glacier. *Arctic, Antarctic, and Alpine Research*, *33*(2), 115–122. https://doi.org/10.2307/1552211

Takeuchi, N., Nishiyama, H., & Li, Z. (2010). Structure and formation process of cryoconite granules on Urumqi glacier No. 1, Tien Shan, China. *Annals of Glaciology*, *51*(56), 9–14.

Tan, C. H., Koh, K. S., Xie, C., Tay, M., Zhou, Y., Williams, R., Ng, W. J., Rice, S. a, & Kjelleberg, S. (2014). The role of quorum sensing signalling in EPS production and the assembly of a sludge community into aerobic granules. *The ISME Journal*, *8*(6), 1186–1197. https://doi.org/10.1038/ismej.2013.240

Tay, J. H., Yang, S. F., & Liu, Y. (2002). Hydraulic selection pressure-induced nitrifying granulation in sequencing batch reactors. *Applied Microbiology and Biotechnology*, *59*(2–3), 332–337. https://doi.org/10.1007/s00253-002-0996-6

Tay, J.-H., Liu, Q.-S., & Liu, Y. (2001). The effects of shear force on the formation, structure and metabolism of aerobic granules. *Applied Microbiology and Biotechnology*, *57*(1–2), 227–233. https://doi.org/10.1007/s002530100766

Tease, B. E., & Walker, R. W. (1987). Comparative composition of the sheath of the cyanobacterium Gloeothece ATCC 27152 cultured with and without combined nitrogen. *Journal of General Microbiology*, *133*(1987), 3331–3339. https://doi.org/10.1099/00221287-133-12-3331

Tenore, A., Mattei, M. R., & Frunzo, L. (2021). *Multiscale modelling of oxygenic photogranules*. http://arxiv.org/abs/2104.12273

Tezuka, Y. (1969). Cation-dependent flocculation in a Flavobacterium species predominant in activated sludge. *Applied Microbiology*, *17*(2), 222–226. https://doi.org/10.1128/am.17.2.222-226.1969

Thomsen, T. R., Kjellerup, B. V., Nielsen, J. L., Hugenholtz, P., & Nielsen, P. H. (2002). In situ studies of the phylogeny and physiology of filamentous bacteria with attached growth. *Environmental Microbiology*, *4*(7), 383–391. https://doi.org/10.1046/j.1462-2920.2002.00316.x

Tiron, O., Bumbac, C., Patroescu, I. V., Badescu, V. R., & Postolache, C. (2015). Granular activated algae for wastewater treatment. *Water Science and Technology*, *71*(6), 832–839. https://doi.org/10.2166/wst.2015.010

Tiron, O., Bumbac, C., Manea, E., Stefanescu, M., & Lazar, M. N. (2017). Overcoming Microalgae Harvesting Barrier by Activated Algae Granules. *Scientific Reports*, *7*(1), 1–11. https://doi.org/10.1038/s41598-017-05027-3

Torres, C. A. V., Antunes, S., Ricardo, A. R., Grandfils, C., Alves, V. D., Freitas, F., & Reis, M. A. M. (2012). Study of the interactive effect of temperature and pH on exopolysaccharide production by Enterobacter A47 using multivariate statistical analysis. *Bioresource Technology*, *119*, 148–156. https://doi.org/10.1016/j.biortech.2012.05.106

Toyofuku, M., Roschitzki, B., Riedel, K., & Eberl, L. (2012). Identification of proteins associated with the pseudomonas aeruginosa biofilm extracellular matrix. *Journal of Proteome Research*, *11*(10), 4906–4915. https://doi.org/10.1021/pr300395j

Trabelsi, L., Ben Ouada, H., Bacha, H., & Ghoul, M. (2008). Combined effect of temperature and light intensity on growth and extracellular polymeric substance production by the cyanobacterium Arthrospira platensis. *Journal of Applied Phycology*, *21*(4), 405–412. https://doi.org/10.1007/s10811-008-9383-8

Tuomainen, J. M., Hietanen, S., Kuparinen, J., Martikainen, P. J., & Servomaa, K. (2003). Baltic Sea cyanobacterial bloom contains denitrification and nitrification genes, but has negligible denitrification activity. *FEMS Microbiology Ecology*, *45*(2), 83–96. https://doi.org/10.1016/S0168-6496(03)00131-4

United States Environmental Protection Agency. (2010). *Evaluation of energy conservation measures for wastewater treatment facilities*.

United States Environmental Protection Agency. (2013). *Energy Efficiency in Water and Wastewater Facilities*.

Urbain, V., Block, J. C., & Manem, J. (1993). Bioflocculation in activated sludge: an analytic approach. *Water Research*, *27*(5), 829–838. https://doi.org/https://doi.org/10.1016/0043-1354(93)90147-A

Van Rijssel, M., Janse, I., Noordkamp, D. J. B., & Gieskes, W. W. C. (2000). An inventory of factors that affect polysaccharide production by Phaeocystis globosa. *Journal of Sea Research*, *43*, 297–306.

Verawaty, M., Pijuan, M., Yuan, Z., & Bond, P. L. (2012). Determining the mechanisms for aerobic granulation from mixed seed of floccular and crushed granules in activated sludge wastewater treatment. *Water Research*, *46*(3), 761–771. https://doi.org/10.1016/j.watres.2011.11.054

Vivanco, E., Puñal, A., & Chamy, R. (2006). Effect of addition of an exogenous exopolymeric substance in UASB and EGSB reactors. *Water Science and Technology : A Journal of the International Association on Water Pollution Research*, *54*(2), 25–31. https://doi.org/10.2166/wst.2006.482

Vlaeminck, S. E., Terada, A., Smets, B. F., De Clippeleir, H., Schaubroeck, T., Bolea, S., Demeestere, L., Mast, J., Boon, N., Carballa, M., & Verstraete, W. (2010). Aggregate size and architecture determine microbial activity balance for one-stage partial nitritation and anammox. *Applied and Environmental Microbiology*, *76*(3), 900–909. https://doi.org/10.1128/AEM.02337-09

Wang, B. Bin, Liu, X. T., Chen, J. M., Peng, D. C., & He, F. (2018). Composition and functional group characterization of extracellular polymeric substances (EPS) in activated sludge: the impacts of polymerization degree of proteinaceous substrates. *Water Research*, *129*, 133–142. https://doi.org/10.1016/j.watres.2017.11.008

Wang, M. (2013). *Investigation of microalgae cultivation and anaerobic codigestion of algae and sewage sludge for wastewater treatment facilities*. University of Massachusetts, Amherst.

Wang, Z. W., Liu, Y., & Tay, J. H. (2006). The role of SBR mixed liquor volume exchange ratio in aerobic granulation. *Chemosphere*, *62*(5), 767–771.

Weber, S. D., Ludwig, W., Schleifer, K. H., & Fried, J. (2007). Microbial composition and structure of aerobic granular sewage biofilms. *Applied and Environmental Microbiology*, *73*(19), 6233–6240. https://doi.org/10.1128/AEM.01002-07

White, D., Drummond, J., & Fuqua, C. (2012). *The physiology and biochemistry of prokayotes* (Fourth edi). Oxford University Press.

Ecology of cyanobacteria II: Their diversity in space and time. (2012). In B. A. Whitton (Ed.), *Ecology of Cyanobacteria II: Their Diversity in Space and Time* (1st ed.). Springer Netherlands. https://doi.org/10.1007/978-94-007-3855-3

WHO/UNICEF. (2015). 2015 Update and MDG Assessment. *World Health Organization*, 90. https://doi.org/10.1007/s13398-014-0173-7.2

Wilde, A., & Mullineaux, C. W. (2015). Motility in cyanobacteria: Polysaccharide tracks and Type IV pilus motors. *Molecular Microbiology*, *98*(6), 998–1001. https://doi.org/10.1111/mmi.13242

Wingender, J., Neu, T. R., & Flemming, H.-C. (Eds.). (1999). *Microbial extracellular polymeric substances: characterization, structure and funciton* (1st ed.). Springer-Verlag Berlin Heidelberg. https://doi.org/10.1007/978-3-642-60147-7

Wu, A. M. (2003). Carbohydrate Structural Units in Glycoproteins and Polysaccharides as Important Ligands for Gal and GalNAc Reactive Lectins. *Journal of Biomedical Science*, *10*(6), 676–688. https://doi.org/10.1159/000073954

Wu, J., & Xi, C. (2009). Evaluation of different methods for extracting extracellular DNA from the biofilm matrix. *Applied and Environmental Microbiology*, *75*(16), 5390–5395. https://doi.org/10.1128/AEM.00400-09

Xue, C., Wang, L., Wu, T., Zhang, S., Tang, T., Wang, L., Zhao, Q., & Sun, Y. (2017). Characterization of Co-Cultivation of Cyanobacteria on Growth, Productions of Polysaccharides and Extracellular Proteins, Nitrogenase Activity, and Photosynthetic Activity. *Applied Biochemistry and Biotechnology*, *181*(1), 340–349. https://doi.org/10.1007/s12010-016-2215-4

Ye, F., Peng, G., & Li, Y. (2011). Influences of influent carbon source on extracellular polymeric substances (EPS) and physicochemical properties of activated sludge. *Chemosphere*, *84*(9), 1250–1255. https://doi.org/10.1016/j.chemosphere.2011.05.004

Ye, F., Ye, Y., & Li, Y. (2011). Effect of C/N ratio on extracellular polymeric substances (EPS) and physicochemical properties of activated sludge flocs. *Journal of Hazardous Materials*, *188*(1–3), 37–43. https://doi.org/10.1016/j.jhazmat.2011.01.043

Yoon-Jung Moon, Young Mok Park, Young-Ho Chung, J.-S. C. (2004). Calcium Is Involved in Photomovement of Cyanobacterium Synechocystis sp. PCC 6803. *Photochemistry and Photobiology*, *79*(1).

Yu, G.-H., He, P.-J., Shao, L.-M., & Zhu, Y.-S. (2008). Extracellular proteins, polysaccharides and enzymes impact on sludge aerobic digestion after ultrasonic pretreatment. *Water Research*, *42*(8–9), 1925–1934. https://doi.org/10.1016/j.watres.2007.11.022

Zayas, J. (1996). Functionality of Proteins in Food. In *Functionality of Proteins in Food*.

Zhang, L. L., Fen, X. X., Zhu, N. ., & Chen, J. M. (2007). Role of extracellular protein in the formation and stability of aerobic granules. *Enzyme Microbioloy Technology*, *41*(5), 551–557.

Zhang, M., Ji, B., & Liu, Y. (2021). Microalgal-bacterial granular sludge process: A game changer of future municipal wastewater treatment? *Science of the Total Environment*, *752*, 141957. https://doi.org/10.1016/j.scitotenv.2020.141957

Zhang, X., & Bishop, P. L. (2003). Biodegradability of biofilm extracellular polymeric substances. *Chemosphere*, *50*(1), 63–69. https://doi.org/10.1016/S0045-6535(02)00319-3

Zhang, X., Bishop, P. L., & Kinkle, B. K. (1999). Comparison of extraction methods for quantifying extracellular polymers in biofilms. *Water Science and Technology*, *39*(7), 211–218. https://doi.org/10.1016/S0273-1223(99)00170-5

Zheng, D., Angenent, L., & Raskin, L. (2006). Monitoring granule formation in anaerobic upflow bioreactors using oligonucleotide hybrdization probes. *Wiley InterScience*.

Zhou, D., Niu, S., Xiong, Y., Yang, Y., & Dong, S. (2014). Microbial selection pressure is not a prerequisite for granulation: Dynamic granulation and microbial community study in a complete mixing bioreactor. *Bioresource Technology*, *161*, 102–108. https://doi.org/10.1016/j.biortech.2014.03.001

Zhu, Liang , Zhou, Jiaheng , Lv, Meile, Yu, Haitian, Zhao, Hang, Xu, X., Zhu, L., Zhou, J., Lv, M., Yu, H., Zhao, H., & Xu, X. (2015). Specific component comparison of extracellular polymeric substances (EPS) in flocs and granular sludge using EEM and SDS-PAGE. *Chemosphere*, *121*, 26–32. https://doi.org/10.1016/j.chemosphere.2014.10.053

Zita, A., & Hermansson, M. (1994). Effects of ionic strength on bacterial adhesion and stability of flocs in a wastewater activated sludge system. *Applied and Environmental Microbiology*, *60*(9), 3041–3048. https://doi.org/10.1128/aem.60.9.3041-3048.1994